UNIVERSITEIT VAN PRETORIA
UNIVERSITY OF PRETORIA
YUNIBESITHI YA PRETORIA

Interpolation in stationary spatial and spatial-temporal datasets

by

ANSIE SMIT

Submitted in partial fulfilment of the requirements for the degree

MSc (Course Work) Mathematical Statistics

In the Faculty of Natural & Agricultural Sciences

University of Pretoria

Pretoria

July 2010

UNIVERSITEIT VAN PRETORIA
UNIVERSITY OF PRETORIA
YUNIBESITHI YA PRETORIA

DECLARATION

I, Ansie Smit declare that the thesis/dissertation, which I hereby submit for the degree MSc (Course Work) Mathematical Statistics at the University of Pretoria, is my own work and has not previously been submitted by me for a degree at this or any other tertiary institution.

SIGNATURE: ..……..

DATE: …….

ACKNOWLEDGEMENT

I would like to express my sincere appreciation to my supervisor, Dr. Hermi Boraine, for her constructive guidance and support during the course of my study. I would also like to thank Loina Bodenstein, May van Rooyen, Danie Barnardo and Adri van Heerden who helped improve the grammar and format of the dissertation. My family was by far my biggest supporters. I would like to thank my parents, Arnold and Susanne Smit as well as my sisters Retha and Christa for their endless supply of encouragement, interest and cups of tea.

DECICATION

I dedicate this thesis to my parents Arnold and Susanne Smit**.**

CONTENTS

CHAPTER 1

INTRODUCTION

1.1 INTRODUCTION AND BACKGROUND

Modern technology has provided tools that significantly increased the efficiency with which information can be gathered as well as the number of measurements and attributes available for analysis. Most analytical tools that have been developed over the years, depend on complete datasets, and often on measurements made at regular intervals. The question that arises is what to do when technology fails and the researcher is left with an incomplete dataset.

Over the years, several techniques have been developed in fields such as mathematics, statistics, engineering and actuarial and natural sciences to provide for incompleteness of data. Governments, universities, institutes and businesses have invested significant resources into building models or developing field-specific techniques that will either work around the incompleteness, or interpolate the missing values.

This dissertation focuses on incomplete datasets in the geosciences. The term 'geoscience' represents the broad spectrum of physical earth sciences, such as the geological, meteorological, planetary, hydrological and environmental sciences. The types of data investigated, using geostatistical tools, are either spatially (location) or spatial-temporal (location-time) dependent.

1.2 WHAT IS GEOSTATISTICS?

Geostatistics is commonly defined as the study of natural phenomena that are spatially or spatial-temporal correlated by means of numerical tools (*Deutsch, 2002; Isaaks and Srivastava, 1989*). Instead of assuming that data are independently and identically distributed, and follows a particular population distribution (*Krige, 1951*), in geostatistics the data are considered as a vector of spatial or spatial-temporal

correlated measurements. The main goal of geostatistics is to combine the quantifiable uncertainty structure with the existing data in order to interpolate or simulate the spatial distribution of the phenomena being studied (*Zhang, 2007*).

A South African mining engineer, D.G. Krige, (*Krige, 1951*) first introduced the above concepts for the process of determining true ore-grade distributions from sample-based ore grades. However, it was G. Matheron (*Matheron, 1963*) who provided the first mathematical formulation of geostatistics and kriging. Matheron was also the first person to use the term kriging, which refers to the optimal interpolation or simulation of measurements at unsampled locations, in honour of Krige's contribution. Other researchers who made the first significant contributions to the field of spatial variation were B. Matern (*Matern, 1986 – English version)* in the early 1960s and A.N. Kolmogorov in 1941 (*Kolmogorov, 1941*).

Geostatistics was initially only applied in the mining and petroleum industries, but were found to be a strong interpolation and simulation tool in several additional environmental fields, such a geohydrology, hydrology, meteorology and climatology.

1.3 LAYOUT OF THE STUDY

The aim of this dissertation is to demonstrate the application, advantages and disadvantages of the most commonly used interpolation technique on a simulated dataset that exhibits spatial and temporal dependencies using geostatistics. This includes defining the descriptive statistics, moments and the interpolation methodology for stationary univariate and multivariate spatial and spatial-temporal data.

Chapter 2 provides insight into the spatial descriptive statistics, which describes any possible correlation that may exist between the different locations where measurements were made. These techniques rely heavily on mapping tools that can highlight any outliers or anomalies. The spatial variation in the data is represented visually and numerically through the spatial and spatial-temporal moments. Additional data dependencies that are investigated include stationarity of the data,

possible anisotropic behaviour, ergodicity and procedures for irregularly spaced measurements.

In Chapter 3 the variation in the data is defined by means of fitting models to the moments (variogram and covariance) of the data. Since the fitted models must adhere to pre-defined conditions, specific models are defined. Attention is given to the difficulties surrounding spatial-temporal modelling and the techniques to overcome them. These models are subsequently used in the interpolation and simulation processes to represent the inherent variation in the data.

Chapters 4 to 7 discuss the most commonly used interpolation technique in geostatistics, namely kriging. The four chapters respectively provide the background, methodology and examples of the spatial univariate, spatial multivariate, spatial-temporal univariate and spatial-temporal multivariate cases. Chapter 8 applies the methodologies defined in Chapters 4 to 7 to a practical dataset, and Chapter 9 concludes with a short discussion on the advantages and disadvantages of the different interpolation tools discussed, as well as suggestions for future research.

Supplementary information provided in the appendices is categorized according to theory and programs. Appendix A contains the supplementary theory. Appendix B contains the programs used in the examples.

CHAPTER 2

SPATIAL DESCRIPTIVE STATISTICS

2.1 INTRODUCTION

The first step in geostatistical analysis is the investigation of the distributional properties of the data which enables the researcher to make an informed decision on which analytical tools will best suit the data and render the required output. Chapter 2 will provide a brief overview of the organizing, graphical and summary tools, as well as additional tools that are used to describe the spatial characteristics.

Textbooks by *Cressie* (*1993*), *Journel and Huijbregts* (*1978*), *Isaaks and Srivastava* (*1989*), and the more recent publication of *Webster and Oliver* (*2007*) are excellent reference material on spatial descriptive statistics. These measures are designed to provide the researcher with an understanding of what influence the additional spatial dependency has on the data.

In Section 2.2, a theoretical univariate and multivariate spatial and spatial-temporal variable set and interpolation models are defined, according to which a bivariate spatial-temporal dataset was simulated (Section 2.3). The data were allocated to the four categories of univariate spatial, bivariate spatial, univariate spatial-temporal and bivariate spatial-temporal dependent data. The simulated dataset was subjected to a series of descriptive statistics in Section 2.4 in order to assess the location, spread, shape and dependencies of the underlying probability distributions. The moments (variance, covariance and correlation) form the foundation for optimal interpolation and stochastic simulation in geostatistics. These moments are defined in Section 2.5. Spatial properties that influence how the moments are modelled in Chapter 3 are introduced in Section 2.6. Chapter 2 concludes in Section 2.7 with a brief description of the available computer software, resources and journals that can be utilized for both the descriptive statistics and modelling techniques.

2.2 GENERAL NOTATION

A broad spectrum of interpolation methods exist that can be utilized for statistical interpolation. Over the years, several techniques have been developed to cater for the different types of missing structures in data. In earth studies, such as hydrology, one or more attributes are typically observed over a period of time at a number of locations. Data can be missing for a number of reasons, e.g. equipment failure. The applicability and availability of methods for the statistical analysis of this information are restricted by discontinuities in the sequence of measurements.

The different missing data structures are (a) missing completely at random (MCAR), (b) missing at random (MAR), and (c) data that have a non-random missing structure (MANR). Normally the structure plays a crucial role in determining the interpolation technique to be used. Several of the interpolation methodologies defined in geostatistics do not depend on this structure, which makes it ideally suited to univariate and multivariate, spatial and spatial-temporal data.

To define the methodology of the identified interpolation techniques a general stochastic variable set is defined, based on spatial data as well as spatial-temporal data. The main purpose of the model is to utilize the behaviour of the observed data to estimate unobserved measurements.

It is important to note that there is a fundamental difference between the co-ordinate axes of spatial and spatial-temporal data (*Weyl, 1952; Reichenbach, 1958; Journel, 1986; Kyriakidis and Journel, 1999*). The spatial axis is characterized by the state of co-existence, which often contains several dimensions and directions. The order in which the measurements appear at each location plays no significant role. The temporal axis is, however, characterized as a state of successive existence where the non-reversible ordering of data into past, present and future measurements in one dimension is of great significance (*Kyriakidis and Journal, 1999*). For this reason two general models are defined for univariate and multivariate analysis.

Suppose the spatial co-ordinate is defined as the x (latitude) and y (longitude) co-ordinates of the α^{th} spatial location $\underline{u}_\alpha = (x_\alpha, y_\alpha)$. The set of n locations available for analysis is then defined as

$$\{\underline{u}_\alpha \mid \underline{u}_\alpha \in D \subseteq \Re^d, \quad \alpha = 1,2,...,n\} \tag{2.1}$$

where D is a subset of the d- dimensional real Euclidean space. The two-dimensional case is investigated in this study.

The four main problem types that will be reviewed in this study are the combinations between univariate and multivariate data that do or do not take possible time dependency into account. Table 2-1 indicates which method will be discussed with each combination.

Table 2-1: Possible combinations of spatial and spatial-temporal analysis.

	Univariate data	**Multivariate data**
Time dependencies not taken into account	I. Spatial ordinary kriging. (Chapter 4)	II. Spatial ordinary co-kriging. (Chapter 5)
Utilize time dependencies	III. Spatial-temporal ordinary kriging. (Chapter 6)	IV. Spatial-temporal ordinary co-kriging. (Chapter 7)

Basic notation used in this dissertation for the univariate and multivariate cases with and without time dependencies is introduced below.

Univariate Spatial Case

Let random variable $Z(\underline{u}_\alpha)$ represent the single measurement of an attribute at location $\underline{u}_\alpha$. Then

$$Z(\underline{u}_1), Z(\underline{u}_2),..., Z(\underline{u}_n) \tag{2.2}$$

is the set of dependent stochastic variables measured at n locations.

Multivariate Spatial Case

Most environmental datasets consist of several measured attributes, such as the copper, lead and zinc contents in soil-analysis measurements. The stochastic spatial case defined in (2.2) is expanded to allow an attribute correlation structure to increase the prediction capability of the model.

Suppose that a total of K attributes are measured and that the primary attribute of interest is always represented by $k=1$ while the remaining $K-1$ attributes are secondary.

Let

$$\underline{Z}(\underline{u}_\alpha)=(Z_1(\underline{u}_\alpha),Z_2(\underline{u}_\alpha),...,Z_K(\underline{u}_\alpha)) \tag{2.3}$$

represent the random vector of K attributes measured at the location $\underline{u}_\alpha$, $\alpha=1,2,...,n.$ It follows that the set of the primary random stochastic attribute is expressed as

$$Z_1(\underline{u}_1),Z_1(\underline{u}_2),...,Z_1(\underline{u}_n) \tag{2.4}$$

and the set of the secondary random stochastic attribute is expressed as

$$Z_2(\underline{u}_1),Z_2(\underline{u}_2),...,Z_2(\underline{u}_n)\,. \tag{2.5}$$

By definition, the methodology of co-kriging (Chapter 6) allows for the possibility that not all the attributes were measured at each of the locations as seen in Figure 2-1. Both attributes are available at locations $\underline{u}_1$ and $\underline{u}_2$, but the primary attribute is missing at location $\underline{u}_3$.

The multivariate spatial model is commonly used to predict the missing attribute with the help of the information contained in the primary and secondary attributes at neighbouring locations.

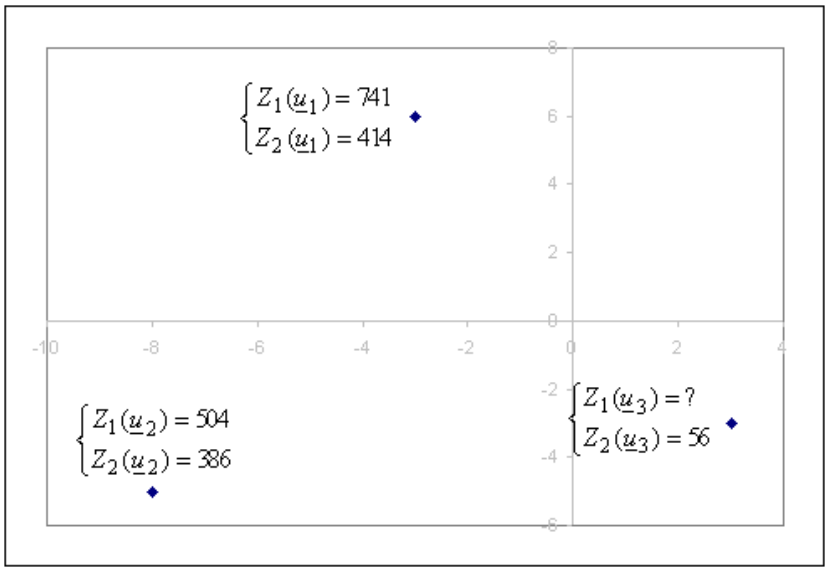

Figure 2-1: Example of attribute sampling.

Univariate Spatial-Temporal Case

In the case of the spatial-temporal stochastic process, the finite time domain $\Im \subseteq \Re^1$ is introduced to interact with the spatial domain $D \subseteq \Re^d$ (*Kyriakidis and Journel, 1999*). The spatial-temporal random variable is defined from (2.2) to include the instant in time when the measurement was made. Let $Z(\underline{u}_\alpha,1), Z(\underline{u}_\alpha,2),..., Z(\underline{u}_\alpha,T)$ represent a discrete, equally spaced time series of observations of an attribute Z observed at location $\underline{u}_\alpha$. The set of stochastic random variables measured at n locations and time instant t is given as

$$Z(\underline{u}_1,t), Z(\underline{u}_2,t),..., Z(\underline{u}_n,t) \tag{2.6}$$

where $t = 1,2,...,T$. Time can be expressed in any unit, e.g. years, months, days, minutes or seconds. This variable can therefore take any series of outcomes at any spatial location $\underline{u} \in D$ and any time point $t \in \Im$. In a complete dataset, the total number of measurements is nT.

Multivariate Spatial-Temporal Case

Suppose that K attributes are measured at n locations at time points $t = 1,2,...,T$. Let

$$\underline{Z}(\underline{u}_\alpha, t) = (Z_1(\underline{u}_\alpha, t), Z_2(\underline{u}_\alpha, t), \cdots, Z_K(\underline{u}_\alpha, t)) \tag{2.7}$$

be the observation vector of the K attributes at location $\underline{u}_\alpha$ and the time point t.

Interpolation Estimates

A typical univariate spatial interpolation function that interpolates the single missing measurement at location $\underline{u}_0$ is defined as

$$\hat{Z}(\underline{u}_0) = f(Z(\underline{u}_1), Z(\underline{u}_2), ..., Z(\underline{u}_n)) \tag{2.8a}$$

and the multivariate spatial interpolation function is defined as

$$\hat{\underline{Z}}(\underline{u}_0) = f(\underline{Z}(\underline{u}_1), \underline{Z}(\underline{u}_2), ..., \underline{Z}(\underline{u}_n)) \tag{2.8b}$$

The univariate spatial-temporal interpolation function is defined as the function that interpolates the single missing measurement at location $\underline{u}_0$ and time point t_0

$$\hat{Z}(\underline{u}_0, t_0) = f(Z(\underline{u}_1,1), ...Z(\underline{u}_1,T), Z(\underline{u}_2,1), ..., Z(\underline{u}_2,T), ..., Z(\underline{u}_n,1), ..., Z(\underline{u}_n,T)) \tag{2.8c}$$

and the multivariate equivalent of (2.8c) is expressed as

$$\hat{\underline{Z}}(\underline{u}_0, t_0) = f(\underline{Z}(\underline{u}_1,1), ...\underline{Z}(\underline{u}_1,T), \underline{Z}(\underline{u}_2,1), ..., \underline{Z}(\underline{u}_2,T), ..., \underline{Z}(\underline{u}_n,1), ..., \underline{Z}(\underline{u}_n,T)) \tag{2.8d}$$

2.3 SIMULATION OF BIVARIATE SPATIAL-TEMPORAL DATA

For illustration and concept clarification purposes a bivariate spatial-temporal dataset was simulated using the statistical tool SAS 9.2. A total of 100 spatially dependent 2-dimensional $VMA(4)$ time series of 30 observations each were generated from the multivariate normal distribution with mean

$$\underset{(6000\times1)}{\underline{\mu}'} = [100 \quad ... \quad 100]$$

and covariance matrix Σ

$$\underset{(6000\times6000)}{\Sigma} = R \otimes \Sigma_{AT} \tag{2.9}$$

where

$$[\underset{100\times100}{R}]_{ij} = e^{-\delta\|\underline{u}_i - \underline{u}_j\|} \tag{2.10}$$

is the ij^{th} element of a correlation matrix where the strength of the correlation is directly related to the proximity of the location with $\delta = -\frac{1}{50}$ and

$$\|\underline{u}_i - \underline{u}_j\| = \sqrt{(x_i - x_j)^2 + (y_i - y_j)^2}$$

It is assumed that the bivariate time series are generated by a vector moving average model of order 4:

$$\underline{y}(t) = \underline{\mu} + \underline{a}_t + \underline{\theta}_1\underline{a}_{t-1} + \underline{\theta}_2\underline{a}_{t-2} + \underline{\theta}_3\underline{a}_{t-3} + \underline{\theta}_4 a_{t-4} \tag{2.11}$$

with error terms $\underline{a}_t$, $t = 1,2,...$ as independent $N(\underline{0}, \Sigma_a)$ vectors with

$$\Sigma_A = \begin{bmatrix} 1.0 & 0.5 \\ 0.5 & 0.9 \end{bmatrix}$$

The bivariate covariance matrix of the $VMA(4)$ time series is defined as

$$\Sigma_{AT} = \begin{bmatrix} \Gamma(0) & \Gamma(1)' & \Gamma(2)' & ... & \Gamma(30)' \\ \Gamma(1) & \Gamma(0) & \Gamma(2)' & ... & \\ \Gamma(2) & \Gamma(1) & \Gamma(0) & ... & \\ ... & & & ... & \\ \Gamma(30) & & & & \Gamma(0) \end{bmatrix} \tag{2.12}$$

which is a Toeplitz matrix with the auto- and cross-covariances defined as

$$\begin{aligned} \Gamma(0) &= \Sigma_\alpha + \theta_1\textstyle\sum_\alpha\theta_1' + \theta_2\sum_\alpha\theta_2' + \theta_3\sum_\alpha\theta_3' + \theta_4\sum_\alpha\theta_4' \\ \Gamma(1) &= \theta_1\textstyle\sum_\alpha + \theta_2\sum_\alpha\theta_1' + \theta_3\sum_\alpha\theta_2' + \theta_4\sum_\alpha\theta_3' \\ \Gamma(2) &= \theta_2\Sigma_\alpha + \theta_3\textstyle\sum_\alpha\theta_1' + \theta_4\sum_\alpha\theta_2' \\ \Gamma(3) &= \theta_3\Sigma_\alpha + \theta_4\textstyle\sum_\alpha\theta_1' \\ \Gamma(4) &= \theta_4\Sigma_\alpha \end{aligned} \tag{2.13}$$

$$\Gamma(5) = \Gamma(6) = ... = \Gamma(30) = \underline{0}$$

The covariance matrix is assumed to be constant over the grid, with the spatial correlation dependent on the distance between the locations. The locations are defined as a fixed grid as depicted in Figure 2-2.

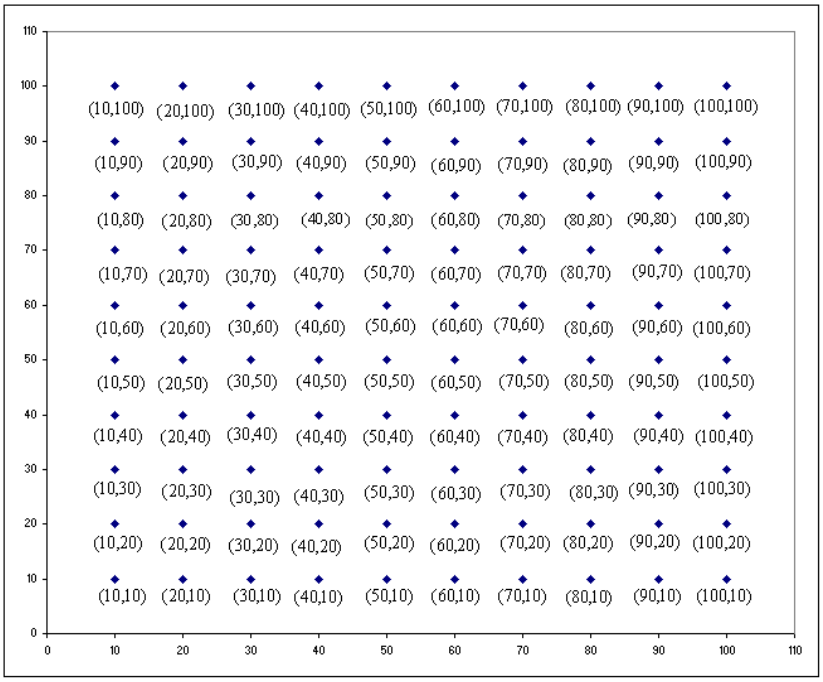

Figure 2-2: Grid of selected sampling locations.

A single vector, generated from the 6000-dimensional $N(\underline{\mu}, \Sigma)$ distribution, defined the complete bivariate spatial-temporal database. The final complete bivariate, spatial-temporal dataset ($ST - COM$) and the complete bivariate spatial dataset named ($S - COM$) are used to illustrate the different concepts of geostatistics and kriging. The dataset $S - COM$ is a subset of $ST - COM$ and was derived by taking the first time measurements from all attributes and locations. This subset is used to illustrate the spatial descriptive statistics discussed in Sections 2.4 and 2.5. The simulation program is available in *Appendix B.1*.

Figure 2-3a depicts the 30 time measurements of the two attributes for location $\underline{u}_1 = (10,10)$ in a time series format. Figure 2-3b provides the surface plot of the primary attribute over all the locations.

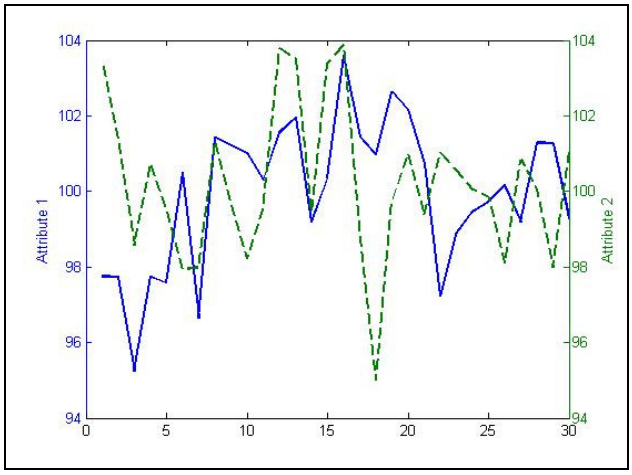

Figure 2-3a: Estimated time series data at location $\underline{u}_1 = (10,10)$ for Z_1 $(-)$ and Z_2 $(--)$

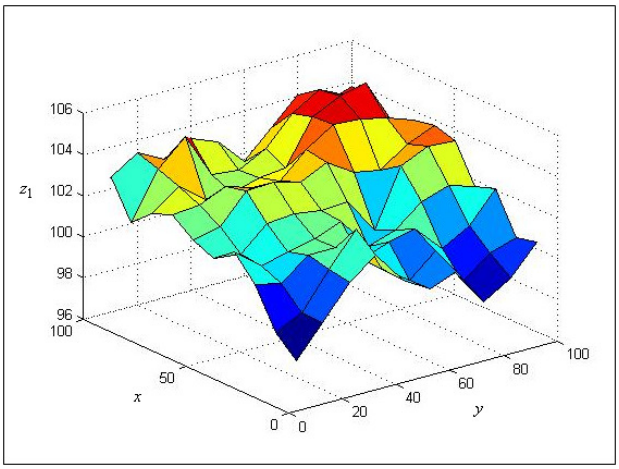

Figure 2-3b: Surface plot of the primary attribute generated

Since the purpose of this study is to demonstrate the efficiency of kriging as an interpolation technique, the datasets used for Chapters 4 to 7 will be subsets of $S-COM$ and $ST-COM$, with a percentage of missing observations in the primary attribute.

The rest of Chapter 2 is devoted to the understanding of the distribution and variation of spatial data, as well as computer software and resources that can be utilized in geostatistics.

2.4 DATA EXPLORATION

The aim of the data exploration is to develop a comprehensive understanding of the data and all possible underlying structures that may influence the behaviour of the given dataset. Descriptive statistics in geostatistics can be classified into non-spatial and spatial data exploration, each developed to best illustrate certain aspects of the data.

Non-Spatial Exploratory Methods

Non-spatial exploration organizes and visually represents univariate data, ignoring spatial dependencies. Frequency tables, histograms and cumulative histograms allow the researcher to visually inspect portions of the data above and below certain thresholds, and some preliminary conclusions on the location, spread and shape of the distributions can be made.

Non-spatial univariate and multivariate descriptive statistics that measure the location, spread and shape are assumed to be known and will therefore only be mentioned in Example 2-1. For more in-depth discussion, the reader may refer to *Cressie* (*1993*), *Isaaks and Srivastava* (*1989*), or any introductory literature on statistics.

Example 2-1

Example 2-1 provides an illustration of plotting and calculating non-spatial descriptive statistics for the attribute sets Z_1 and Z_2 as provided by $S-COM$. The SAS program for this example is provided in *Appendix B.2*. The graphs were plotted using Matlab and Excel.

The histogram and normal probability plots (Figure 2-4) indicate that the measurements for both attributes are approximately normally distributed. This is supported by an analysis provided in Tables 2-2 and 2-3.

Table 2-2: Descriptive statistics of the primary variable Z_1.

Statistic	Value	Statistic	Value
Min	97.75	P10	99.77
Max	105.21	P90	104.00
Mean	101.87	P95	104.29
Median	101.91	P99	105.07
Variance	2.58	Range	7.47
Standard deviation	1.61	Inter-quartile range	2.32
Coefficient of variation	1.58	Skewness	-0.24
Q1	100.70	Kurtosis	-0.37
Q3	103.02		

Table 2-3: Descriptive statistics of the secondary variable Z_2.

Statistic	Value	Statistic	Value
Min	95.56	P10	97.78
Max	103.75	P90	102.52
Mean	99.90	P95	103.34
Median	99.76	P99	103.65
Variance	3.30	Range	8.19
Standard deviation	1.82	Inter-quartile range	2.26
Coefficient of variation	1.82	Skewness	0.21
Q1	98.80	Kurtosis	-0.30
Q3	101.06		

The correlation between Z_1 and Z_2 was determined by the Pearson correlation formula as -0.39 and the negative relationship is confirmed by Figure 2-5.

The Q-Q-plot of the two attributes indicates that the underlying distributions are fairly similar, but there is a difference between the location and spread, as seen from Table 2-2 and Table 2-3.

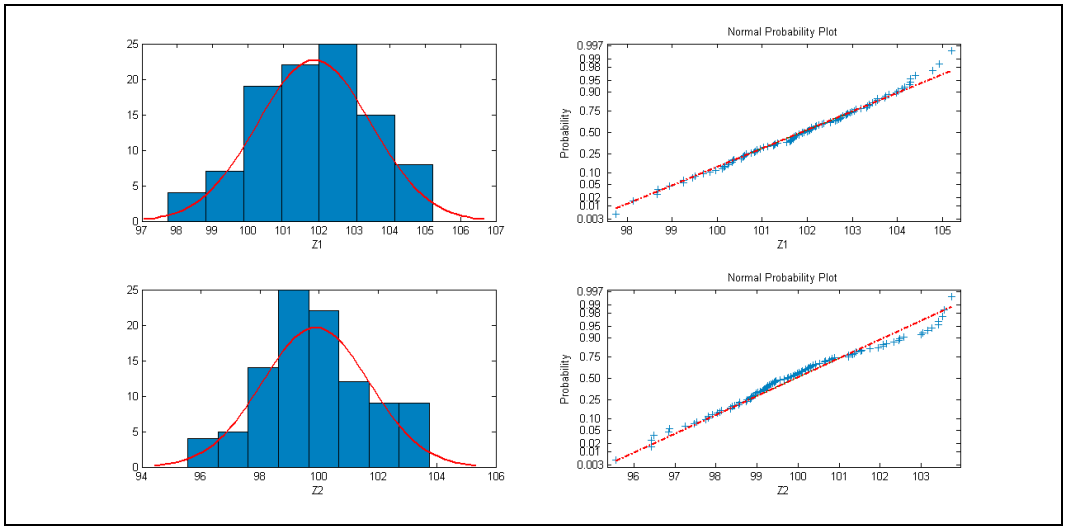

Figure 2-4: Histogram and normality plots for Z_1 (top) and Z_2 (bottom).

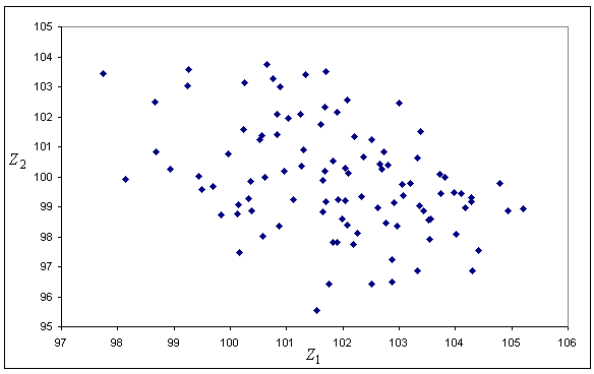

Figure 2-5: Scatter plot representing the correlation between the two attributes.

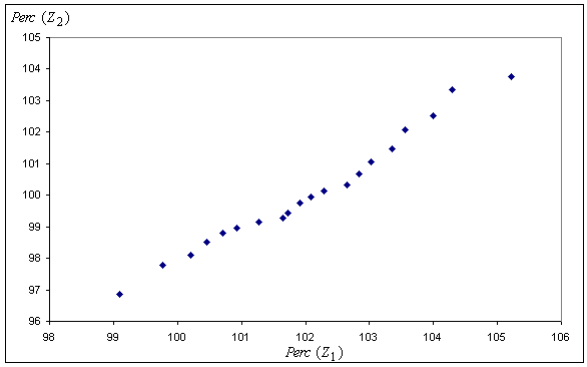

Figure 2-6: Q-Q plot of the primary variable Z_1 and secondary variable Z_2.

As described in Chapter 1, it is necessary to take into account the fact that, in certain study fields, data belong to and depends on a specific location in space. Spatial

features, such as the location of extreme measurements, overall trend and degree of continuity are often of considerable interest and are being taken into account by the spatial methods.

Spatial Exploratory Methods

Spatial data exploration does not consist of a fixed set of techniques used to inspect data, as in the case of non-spatial exploration. In the past, basic analysis was done mainly in terms of the distribution (location, spread and shape) and variation (moments) of the data (*Cressie*, *1991*; *Journel and Huijbregts*, *1978*). *Isaaks and Srivastava* (*1989*) attempted to identify a set of existing spatial visualization techniques which will afford the researcher the opportunity to visualize spatial dependence and to identify possible anomalies.

The different spatial exploration techniques discussed by *Isaaks and Srivastava* (*1989*) were chosen to help identify different aspects of the simulated data. Extreme values (outliers) and measurement mistakes can be detected using data postings and symbol maps. Possible patterns in spatial dependencies are illustrated using contour maps, proportional effect graphs and the *h*-scatter and cross *h*-scatter plots. Moving window statistics and spatial continuity graphs are techniques to illustrate the spatial continuity of the data.

The rest of the section discusses each of these techniques in terms of the univariate and bivariate (where applicable) data structures, utilizing the bivariate dataset simulated in Section 2.3.

Data Postings

A visual technique, named data postings, is a very simplistic tool to identify obvious trends and errors in specific locations (*Isaaks and Srivastava, 1989, p40*). Erroneous measurements are also often revealed in these data postings maps. Each location is plotted along with the corresponding measurement on a map. Figure 2.8 depicts the primary measurements (above the dot) and the secondary measurements (below the

dot). A single high measurement surrounded by low measurements and vice versa warrants re-checking of the data.

One disadvantage of the data postings map is that it is only effective for a small number of locations and, at most, two attributes. Data postings maps for larger datasets are impractical and difficult to interpret. The map can also only effectively demonstrate spatially dependency, effectively ignoring any potential time dependencies that may exist.

Example 2-2

Data postings maps for the simulated dataset $S-COM$ were created to illustrate the univariate (Figure 2-7) and the bivariate (Figure 2-8) simulated data. The data postings maps were done in Excel.

Closer inspection of the primary attribute in Figure 2-7 illustrates that the lower measurements are associated with the smaller x-co-ordinate. Closer inspection also does not reveal any combinations of lower and higher variables or any other discrepancies in the data.

Although not considered an anomaly, in the bivariate case it seems that the the lower y- co-ordinates for $x=60$ and $x=80$ have primary and secondary attribute measurements that are relatively small compared with the rest of the combinations in the dataset. Subsequent analysis will illustrate if this will have a measurable effect on the data.

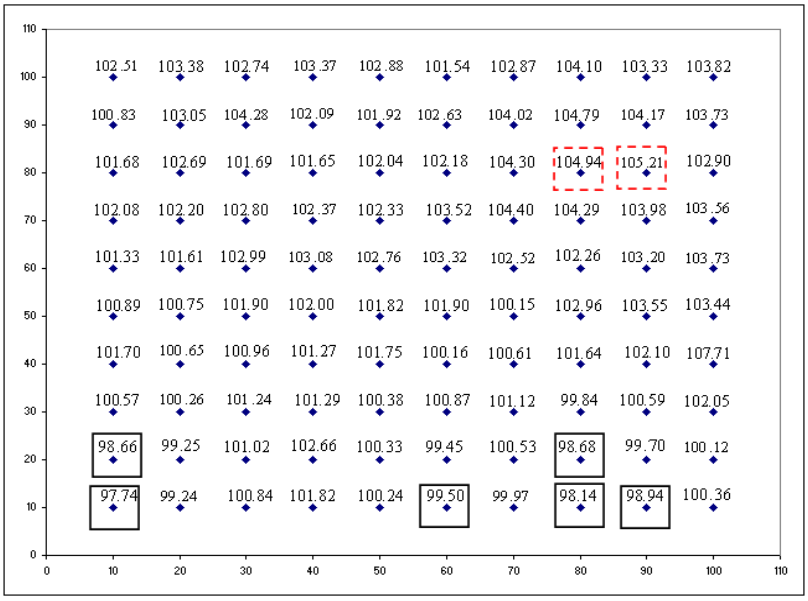

Figure 2-7: Location of the lowest primary measurements in black (solid line) and the highest measurements in red (dashed line).

Figure 2-8: Data postings map of the primary (above the dot) and the secondary measurements (below the dot) at each of the 100 measured locations.

Contour Maps

Contour maps are used to identify overall trends and to become familiar with two-dimensional univariate data (*Isaaks and Srivastava, 1989, p41*). These maps demonstrate the relationships between three variables on a two-dimensional plane. An attribute (Z_1 or Z_2) is plotted against the two dimensional location co-ordinates (x and y) by using a pattern of coloured contour lines. These lines connect locations with the same attribute at regular intervals and are either coloured or labelled with the associated measurements. Since the maps are used to identify trends, care should be taken not to include too many (over-crowded) or too few (loss of information) intervals.

The interpretation of contour maps consists of viewing the levels in the map (*Diablo Valley College*). Measurements directly on either side of the contour line are respectively higher and lower than the measurements on the contour line itself. This effectively divides the map into different regions. The measurements along the contour lines do not vary across the line.

The rate of variation is the highest in a direction perpendicular to a specific contour line (*Diablo Valley College*). The gradient is defined as the amount by which these measurements vary across each unit of distance in a direction perpendicular to the contour line. That is, the gradient measures how rapidly measurements vary from place –to place (spatial location). If more contour lines are packed in one unit of distance, the differences in measurements are larger and so is the gradient.

One disadvantage is that a regular sampled grid is needed for accurate contour maps, although most statistical tools can build contour maps by automatically interpolating the missing grid measurements using simplistic methods, such as spline interpolation.

In Example 2-3 the contour maps for the primary and secondary variables are constructed using the GCONTOUR procedure from SAS (Figures 2-9 and 2-10).

Example 2-3

The contour plots for the primary (Z_1) and secondary variables (Z_2) were created by using the SAS procedure GCONTOUR on the measurements in $S-COM$.

The contour maps do not provide conclusive proof of possible trends in the data. This is indicative of a fixed mean and variance across the grid, according to which the data were simulated. The program is available in *Appendix B.3*.

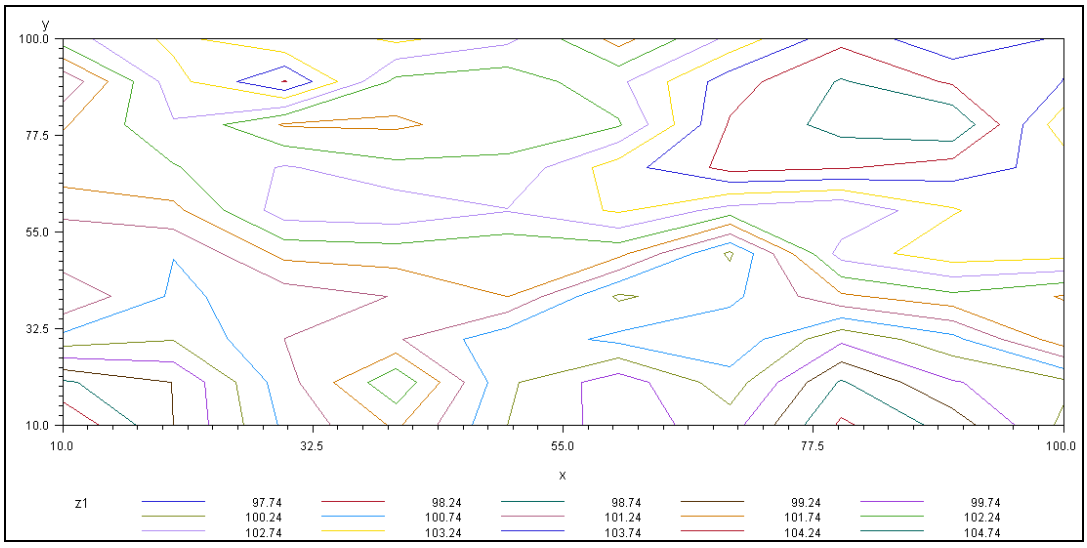

Figure 2-9: Contour map representing the primary attribute Z_1.

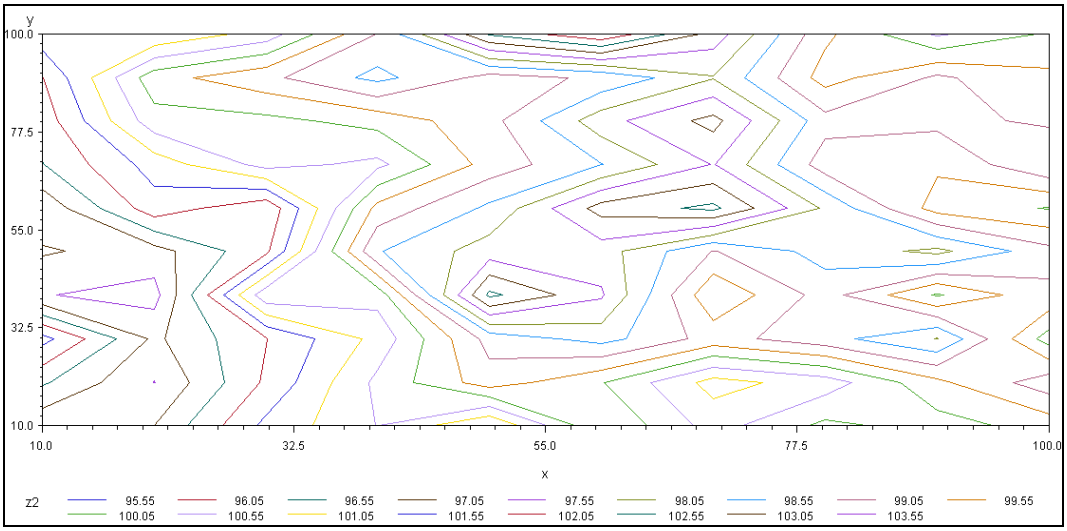

Figure 2-10: Contour maps representing the primary attribute Z_2.

Symbol Maps

Symbol maps are useful when the number of locations to plot become too large for data postings and contour maps, since the sheer number of measurements may mask interesting local details in the univariate datasets (*Isaaks and Srivastava, 1989, p43 – 46*). These maps are similar to data postings maps, with each location replaced by a symbol that denotes the class to which the measurement belongs. These symbols are chosen to convey the relative ordering by their visual density (Figure 2-11).

Greyscale- and indicator maps are by-products of symbol maps (*Isaaks and Srivastava, 1989, p44*). Instead of using symbols, blocks are used for greyscale maps. Black and white blocks are used in the indicator maps to represent the number of measurements on the grid that are above and below a certain threshold. A series of indicator maps provides a good view of the spatial features in the data, but is computationally more intensive and ignores possible temporal dependencies.

Example 2-4

The symbol, greyscale and indicator maps were created for the generated primary variable in the dataset $S-COM$. Some visible trends are that the data follow a natural trend from low to high values in both a vertical and diagonal directions.

y										
100	7	7	6	7	6	4	6	8	7	7
90	6	6	8	5	5	6	8	9	8	7
80	6	6	5	6	5	5	8	9	9	6
70	5	5	6	6	5	7	8	8	8	7
60	5	5	6	6	6	7	6	5	7	7
50	3	3	5	5	5	5	3	6	7	7
40	3	3	4	4	4	3	3	5	5	5
30	3	3	4	5	3	4	4	2	3	5
20	1	1	2	6	3	0	3	1	2	3
10	1	1	3	5	3	2	2	0	1	3
x	10	20	30	40	50	60	70	80	90	100

0	97.74	98.50
1	98.51	99.27
2	99.28	100.04
3	100.05	100.81
4	100.82	101.58
5	101.59	102.35
6	102.36	103.12
7	103.13	103.89
8	103.90	104.66
9	104.67	105.43

Figure 2-11: Symbol map of the primary attribute (Z_1).

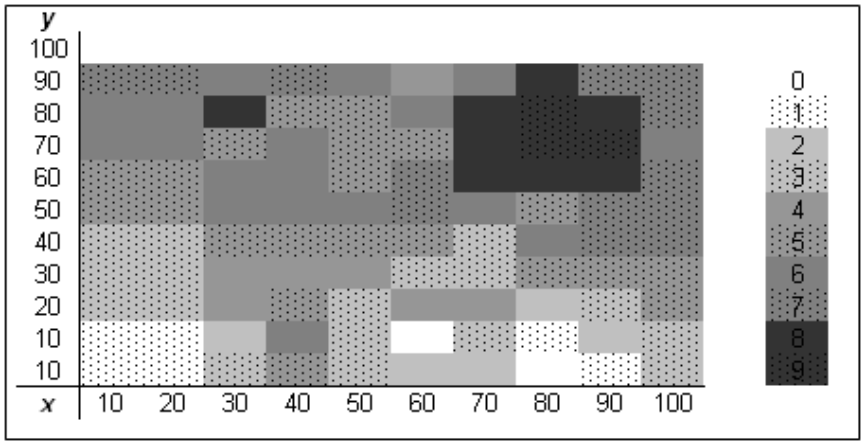

Figure 2-12: Greyscale map of the primary attribute (Z_1).

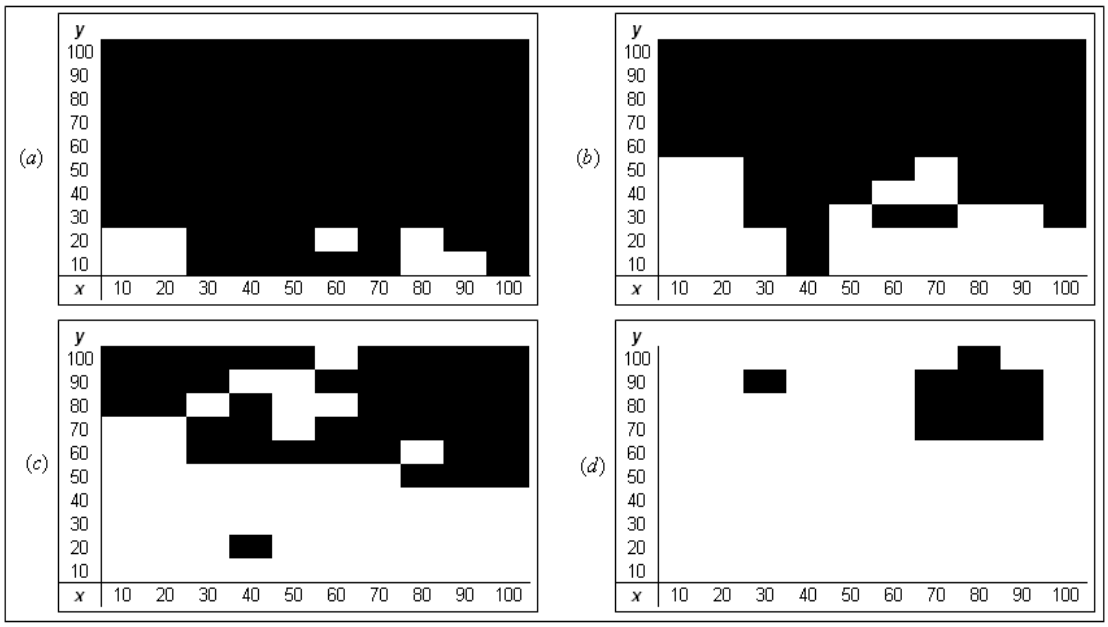

Figure 2-13: Series of indicator maps for Z_1. The black blocks indicate all measurements that are >98.50 (a), >100.81 (b), >102.35 (c) and >103.89 (d).

These maps proved to be more effective and convenient to use than data postings and contour maps in extracting high-level information. Approximate constant variability over the grid, including the maximum and minimum values, are clearly visible in the greyscale map. All maps were created in Excel.

Moving Window Statistics

Additional anomalies in a cleaned, univariate spatial dataset can be of great interest as they may have significant practical implications (*Isaaks and Srivastava, 1989, p46; Goovaerts, 1997*). These anomalies could, for example, be the unexpected increase or dropping-off in high-grade gold deposits along a certain sampling line, which will have a serious effect on the cost –to company of a gold mine.

Data postings, contour and symbol maps are useful tools to identify areas where the average value of the variability appears to be anomalous (non-stationary in space). Moving window statistics are applied to investigate these anomalies (heteroscedasticity) in the average and variance when comparing smaller regions within the grid.

The first step in moving window statistics is to divide the entire region into several local neighbourhoods that are of equal size. Rectangular windows are computationally efficient and therefore most popular. The average spacing between the locations, as well as the overall dimensions of the data determine the size of the window. Each window must ideally contain enough information to calculate accurate summary statistics, including the local mean, standard deviation, correlation and tests for normality for each window. These statistics are used to identify local anomalies.

To avoid difficulties that may arise from determining a window size that is neither too small nor too large, the literature *(Isaaks and Srivastava, 1989, p47)* suggests overlapping windows of adjacent neighbourhoods. This practice is especially useful for small or irregularly-spaced grids. The reliability of the results of the moving window statistics depends on the number of locations in each window.

Example 2-5

For the moving window analysis, two separate analyses were carried out on the same data. The first analysis was based on 9 windows, which were identified by creating 4×4 overlapping blocks, as seen in Figure 2-14. The next window was identified by moving the window three grid points to the right, or up. The second analysis was

performed on four equal non-overlapping windows of size 5×5.

The statistics for each window of the two groups were calculated by using the UNIVARIATE procedure from SAS and are provided in Table 2-4 and Table 2.5.

No definite trend is visible for the standard deviation. The distributions for all the windows are normal, except in window 1 for Z_1 in the first analysis and window 4 for Z_2. As expected, the windows with more observations have more stable means and standard deviations than those with fewer observations.

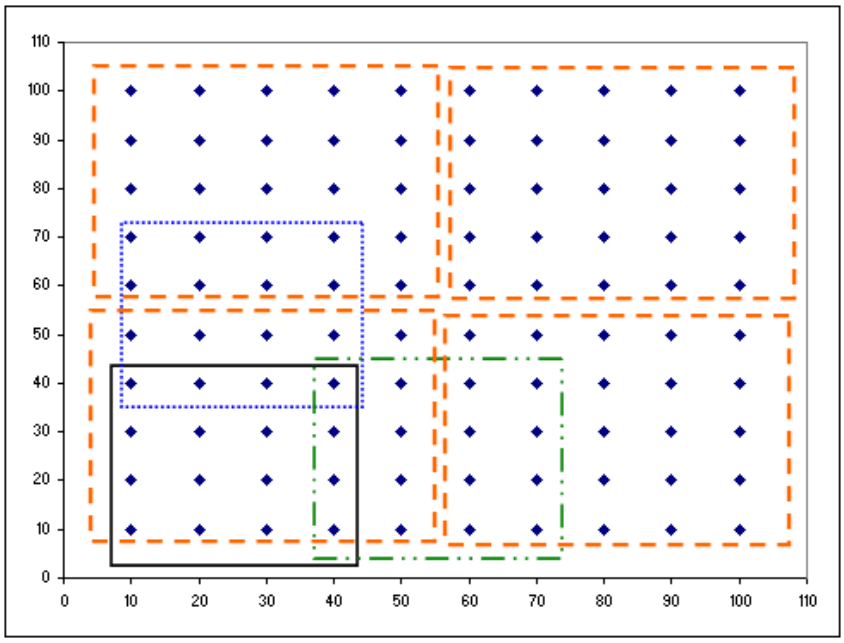

Figure 2-14: The moving window group 1 is represented by the black $(-)$, blue $(\cdots)$ and green $(\cdots - \cdots)$ blocks and group by orange $(—)$ windows.

There is a noticeable difference between the global mean and standard deviations for Z_1 and Z_2, as calculated in Example 2-1. These discrepancies and the positive correlation of the fourth non-overlapping window can be attributed to unreliable window statistics since only 100 locations are available.

The Kolmogorov-Smirnov statistic for each window is also calculated here to determine if any of the windows deviate from the general normal character of the complete dataset. In Table 2-4 and 2-5, the first windows of the primary attribute are

not normally distributed. This is, however, attributed to the small number of observations available for calculation.

The code for this example is available in *Appendix B.4*.

Table 2-4: Summary statistics of the 9 overlapping windows.

Window	MEAN		STD DEV		Kolmogorov-Smirnoff p-value		Corr
	Z_1	Z_2	Z_1	Z_2	Z_1	Z_2	
1	100.57	102.01	1.27	1.29	0.147	>0.150	-0.60
2	101.79	101.67	0.78	1.59	>0.150	>0.150	-0.46
3	102.46	100.60	0.83	1.20	>0.150	>0.150	-0.44
4	100.75	99.68	0.87	1.38	>0.150	>0.150	-0.05
5	102.12	98.42	1.19	1.33	>0.150	>0.150	-0.22
6	102.76	98.30	0.92	1.33	>0.150	>0.150	-0.24
7	100.38	99.73	1.17	0.88	>0.150	>0.150	-0.22
8	102.76	98.85	1.26	1.01	>0.150	>0.150	-0.18
9	104.03	98.89	0.66	1.02	>0.150	>0.150	-0.01

Table 2-5: Summary statistics of the 4 non-overlapping windows.

Window	MEAN		STD DEV		Kolmogorov-Smirnoff p-value		Corr
	Z_1	Z_2	Z_1	Z_2	Z_1	Z_2	
1	100.77	101.32	1.13	1.98	0.097	>0.150	-0.48
2	102.41	100.37	0.76	1.60	>0.150	>0.150	-0.40
3	100.72	99.33	1.42	1.01	>0.150	>0.150	-0.43
4	103.57	98.57	0.91	1.27	>0.150	0.144	0.44

Proportional Effect Graph

Anomalies may be of interest, as indicated above, but widely fluctuating measurements can have a detrimental effect on the accuracy of any derived estimates. However, they do not have any influence on which interpolation method is to be used. Fluctuations can be described by the following four different relationships that could exist between the local average and local variability, as defined by the moving window statistics (*Isaaks and Srivastava, 1989, p49; Stein* et al*., 1999)*.

- Both local mean and variability are constant
- A trend exists in local mean but the variability remains constant
- Local mean remains constant but a trend exists in variability
- Both the local trend and variability exhibit a trend.

Constant variability is preferred since the estimates in each window are equally good or bad. Since this is unfortunately rarely the case, the next preferred relationship is where a trend exists in both the local mean and variability. If a relationship exists between these trends, the data becomes more predictable. A scatter plot between the local means for the select windows, overlaid by the standard deviations for the same window selection will illustrate any relationship that may exist. This relationship is referred to as the proportional effect (*Isaaks and Srivastava, 1989*).

Univariate and multivariate normally distributed data usually have no proportional effect as the variances are roughly constant. The lognormal distribution, however, presents a linear relationship, since the local variances increases with the local mean in positively skewed distributions (*Goovaerts, 1997*).

Example 2-6

The proportional effect of the windows identified in the first group of Example 2-5 can be seen in Figure 2-15 and Figure 2-16.

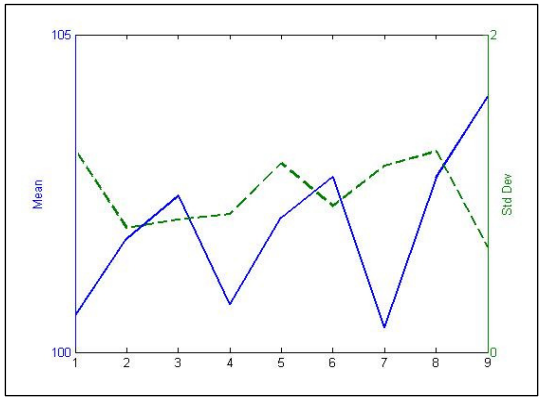

Figure 2-15: Proportional effect of Z_1.

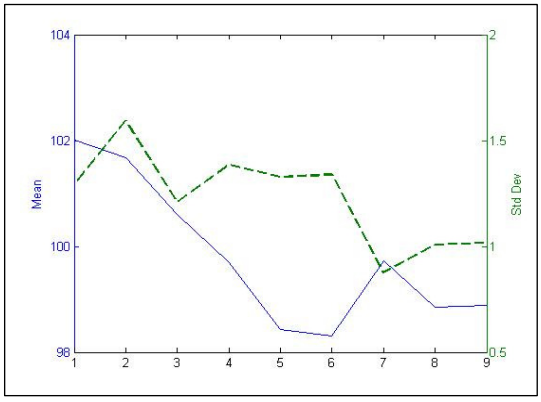

Figure 2-16: Proportional effect of Z_2.

Table 2-6: Variability interval of mean and standard deviation of Z_1 and Z_2.

(*Max-Min*)	Z_1	Z_2
Mean	3.65	3.71
Standard deviation	0.61	0.71

Even though these figures give the appearance of great variability, Table 2-4 and Table 2.6 confirm that the ranges of the means and standard deviations are not large. It will therefore be assumed that they are fairly constant.

Spatial Continuity Graph

Univariate spatial continuity is present in the data when the measurements from neighbouring locations are similar (*Isaaks and Srivastava, 1989, p50*). The closer the locations are to one another, the more similar the values of the measurements are and *vice versa*. Data postings and contour maps are particularly effective in exhibiting this property. If the maps indicate that low measurements are associated in space with other low measurements, and high measurements are associated with high measurements, spatial continuity is confirmed. Anomalies are presented by the combination of high and low measurements.

Example 2-7

Figure 2-17 depicts the spatial continuity of the primary (Z_1) and secondary (Z_2) attributes, based on the 9 windows group. The mean-standard deviation scatter plots for Z_1 and Z_2 seem to have no specific trend, therefore no assumptions can be made on the type of discontinuity.

When taking into consideration the information provided by the moving window statistics, proportional effect and spatial continuity, it appears that there is a lot of unexpected variability in the data. It is important to keep in mind that only 100 locations were sampled, leaving the researcher with a limited number of windows to select. The number of measurements in each window can be considered too small,

therefore unstable results.

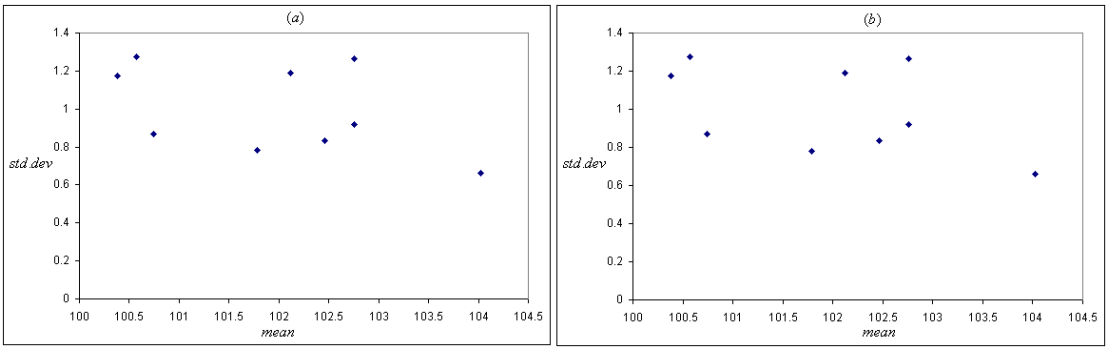

Figure 2-17: Scatter plot mean against the standard deviation of the primary (a) and the secondary attributes (b).

Additional tools that describe the spatial continuity are the *h*-scatter plot for univariate data and the cross h-scatter plot for multivariate data.

h-Scatter Plot

The *h*-scatter plot, where all the possible pairs (N) of measurements, for which locations are separated by a certain lag distance ($\| \underline{h}_s \|$) in a particular direction, is presented on a scatter plot (*Isaaks and Srivastava, 1989, p52; Goovaerts, 1997, p25*). The *h*-scatter plot is represented by plotting the $Z(\underline{u}_\alpha)$ measurements on the x-axis and the $Z(\underline{u}_\alpha + \underline{h}_s)$ measurements on the y-axis, for all pairs of locations located in a specific direction and separated by a specific distance. The shape of the cloud in the scatter plot provides insight into the spatial continuity over a particular distance and direction. The closer the points lie to the 45º line, the more similar the neighbouring measurements are. Several *h*-scatter plots for different lag distances and directions are needed to provide a comprehensive view of the data and aid the researcher in identifing possible anisotropic (Section 2.6) behaviour in the data. An example of the *h*-scatterplots for the simulated data is provided in Example 2-8.

Example 2-8

Figure 2-18 presents three possible combinations in which data can be paired for the *h*-scatter plot for the simulated data. The pairings can be done in any direction and for any distance. If there are measurements missing, then any pairing that contains the missing point is disregarded, as seen in Figure 2-19.

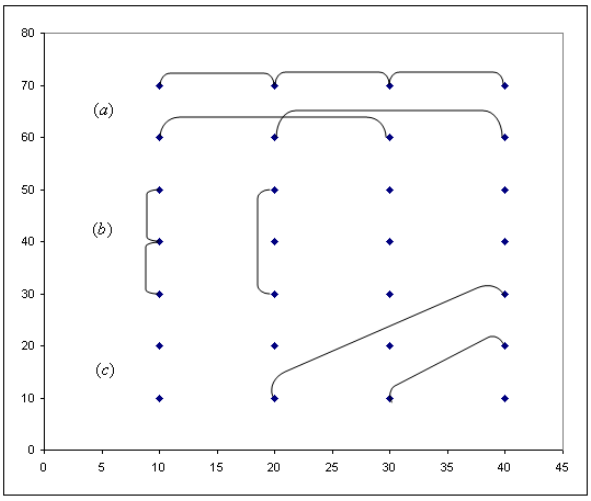

Figure 2-18: Graphical representation of the different directions and lag distances that can be of interest. Horizontal (a), vertical (b) and diagonal (c) are three possible options (*Clark, 1979*).

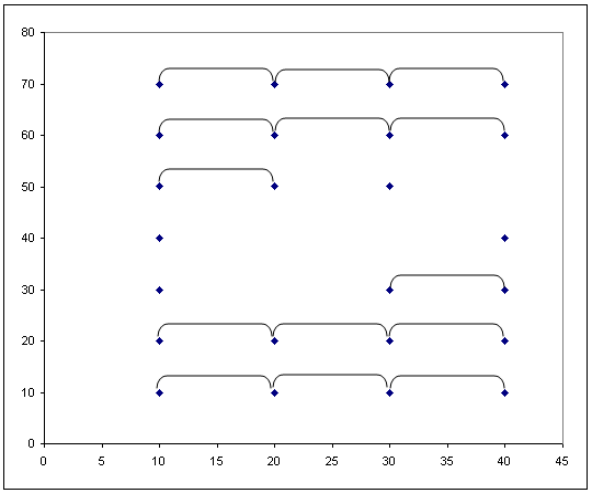

Figure 2-19: Horizontal pairing of locations at $10m$ when locations are missing.

The *h*-scatter plots for the simulated dataset $S-COM$ were created for the horizontal direction (left to right) and vertical (bottom to top) at $10m$ to $50m$ apart in intervals

of $10m$. The third group consists of diagonal pairings (bottom left to top right) at $14.14m$ to $70.71m$ apart in intervals of $14.14m$.

The *h*-scatter plots for Z_1, direction horizontal left to right at intervals of $10m$ is presented in Figures 2-20a to 2-20c. As expected, a strong relationship exists at distance $10m$, with the relationship decreasing as the lag distance increases. The *h*-scatter plots for vertical and diagonal measurements exhibit a similar pattern. A similar trend was observed for the secondary attribute Z_2. The simulated data (as expected) are therefore not sensitive to direction (isotropic), as seen in Figure 2-20d.

The SAS code is available in *Appendix B.5.*

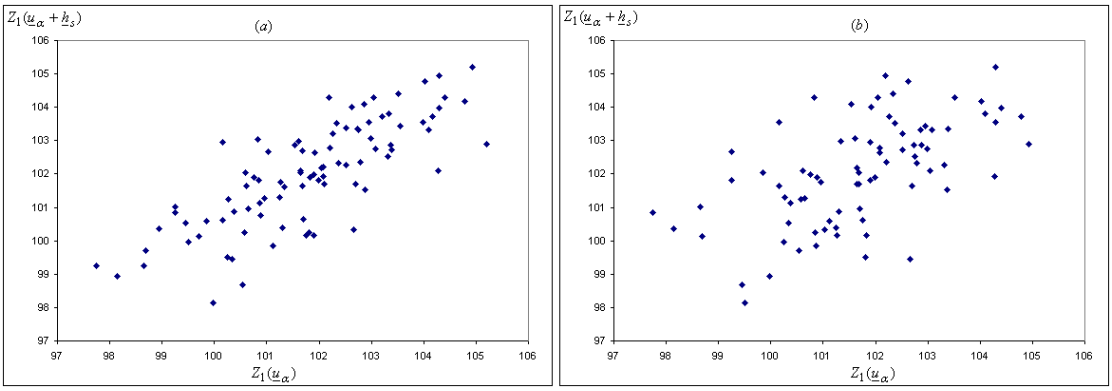

Figure 2-20a: Horizontal, left to right, $10m$ (a) and $20m$ (b) apart for Z_1.

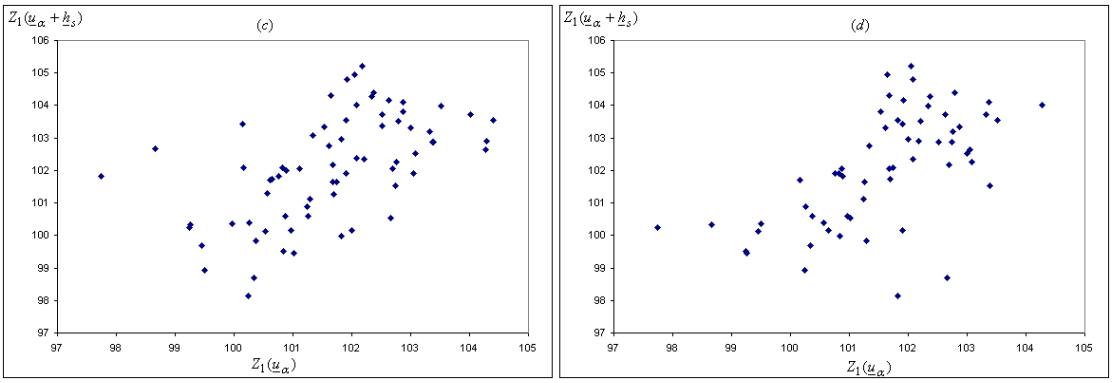

Figure 2-20b: Horizontal, left to right, $30m$ (c) and $40m$ (d) apart for Z_1.

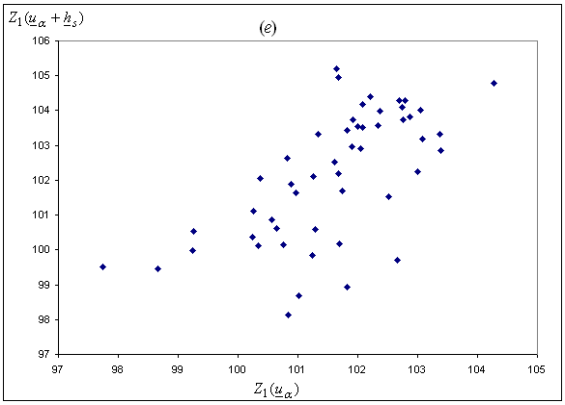

Figure 2-20c: Horizontal, left to right, $50m$ (e) apart for Z_1.

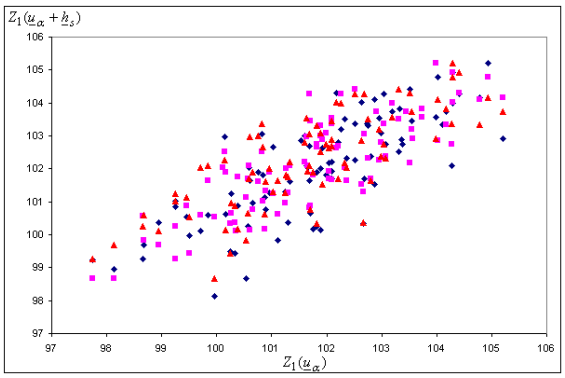

Figure 2-20d: *h*-scatterplot of Z_1 for $10m$ in the horizontal (blue diamond), vertical (pink square) and diagonal (red triangle) directions.

Cross *h*-Scatter Plot

The cross *h*-scatter plot is an extension of the *h*-scatter plot described above. Instead of pairing the measurements from one attribute, the pairs between two attributes are used (*Isaaks and Srivastava, 1989, p60*). The x-axis is represented by $Z_1(\underline{u}_\alpha)$, which are the measurements of the primary attribute, and the y-axis by $Z_2(\underline{u}_\alpha + \underline{h}_s)$, which are the measurements of the secondary attributes. The cross *h*-scatter plot is used to describe the relationship between multivariate data, based on the distance between the locations of the measured values.

Example 2-9

The horizontal cross *h*-scatter plot between the primary and secondary attributes at distances of $0m$ and $10m$ is depicted in Figure 2-21a and 2-21b. The negative correlation between the primary and secondary attributes within each location is visible in Figure 2-21a, and the same as the correlation plot (Figure 2-5) from Example 2-1.

As with the *h*-scatter plots, the relationship decreases as the distance between the points increases. The vertical and diagonal plots, as well as the secondary attribute follow the same trend.

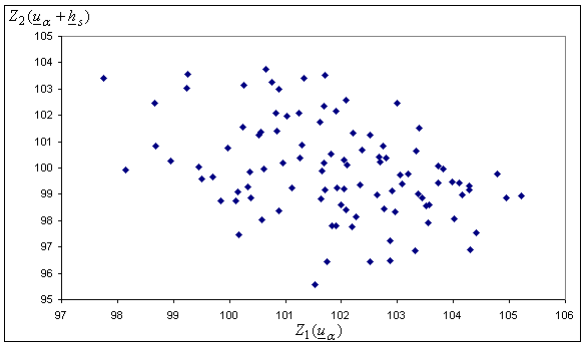

Figure 2-21a: In location, $0m$ apart for Z_1 and Z_2.

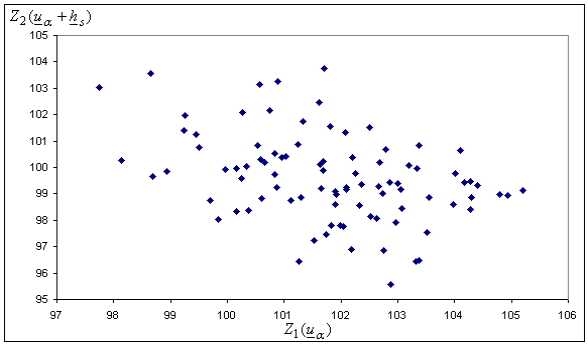

Figure 2-21b: Horizontal, left-right $10m$ apart for Z_1 and Z_2.

The SAS code is available in *Appendix B.6.*

Once the researcher has a better understanding of the data, the univariate (variogram, covariance and correlation) and multivariate (cross-variogram, cross-covariance and cross-correlation) moments can be investigated.

2.5 MOMENTS IN GEOSTATISTICS

In geostatistics, the variance, covariance and correlation structure of the data are presented in terms of variograms. The kriging methodology uses these structures by means of building a variogram, covariance or correlation model that graphically describes the structures and correlation. All three tools are used to numerically characterize the relationship between the measurements in terms of the distance and direction between all the locations. In multivariate analysis the cross-variogram, cross-covariance and cross-correlation models are used to describe the underlying spatial dependencies between several attributes.

Since the variogram and covariance are the functions that are primarily utilized, these two will be discussed alongside each other to better illustrate the relationship between them. The section begins with a comprehensive description of the spatial univariate and multivariate variograms, covariance and correlation functions. These definitions are then used to derive the spatial-temporal univariate and multivariate moments.

Spatial Moments

The spatial moments are defined in terms of the variogram, cross-variogram, covariance, cross-covariance, correlation and the cross-correlation. These moments are used to describe the dissimilarity between measurements that are separated by a lag distance.

Univariate Spatial Variogram

The variogram can be defined as the graphical representation of the variance of the data. It is a function of the distance between measurements that describe the spatial continuity and structure of the data, as well as the direction. (*Journel and Huijbreghts,*

1978; Isaaks and Srivastava, 1989; Cressie, 1993; Goovaerts, 1997; Clark and Harper, 2000; Webster and Oliver, 2007).

If $E[Z(\underline{u}_\alpha)]$ is constant for all $\underline{u}_\alpha \in D$, the theoretical variogram model is defined as

$$\begin{aligned} 2\gamma(\underline{h}_s) &= \text{var}[Z(\underline{u}_\alpha) - Z(\underline{u}_\alpha + \underline{h}_s)] \\ &= E[(Z(\underline{u}_\alpha) - Z(\underline{u}_\alpha + \underline{h}_s))^2]. \end{aligned} \tag{2.14}$$

The theoretical variogram was defined by the "intrinsic hypothesis" of Matheron (*Matheron, 1962; Gilgen, 2006*), which is defined by (2.40) and (2.14). This hypothesis allows for the calculation of a variogram without having several realizations of the same data pair (*Deutsch and Journel, 1998 p13*). A single, experimental variogram estimate $2\hat{\gamma}(\underline{h}_s)$ is defined as the mean-square of the difference between the attribute at all grid points that are separated by a vector $\underline{h}_s$.

The experimental variogram estimates over all locations and lag distances are expressed as (*Matheron, 1962*)

$$2\hat{\gamma}(\underline{h}_s) = \frac{1}{N_A}\sum_A [Z(\underline{u}_\alpha) - Z(\underline{u}_\alpha + \underline{h}_s)]^2 \tag{2.15}$$

where $A = \{(\underline{u}_\alpha, \underline{u}_\beta) \mid \underline{u}_\alpha - \underline{u}_\beta = \underline{h}_s\}$ and N_A is the number of elements in A. For a total of n locations there exist $N = \frac{n(n-1)}{2}$ pairs of locations. For the rest of the study, the *experimental semi-variogram* $\hat{\gamma}$ will be referred to only as the *semi-variogram*.

Once the scatter plot of estimates is obtained, it is necessary to select a semi-variogram model. Mathematical models are used to describe the semi-variograms; experimental semi-variograms are used to estimate these models. The relationship between the variogram model and the experimental variogram is the same as the relationship between a probability function and a histogram.

Example 2-10

The individual semi-variograms for Z_1 and Z_2 were developed to follow the same structure as that of the *h*-scatter plots defined in Section 2.4. Because of the small number of locations, only 5 point semi-variograms in each direction (horizontal, vertical and diagonal) were calculated.

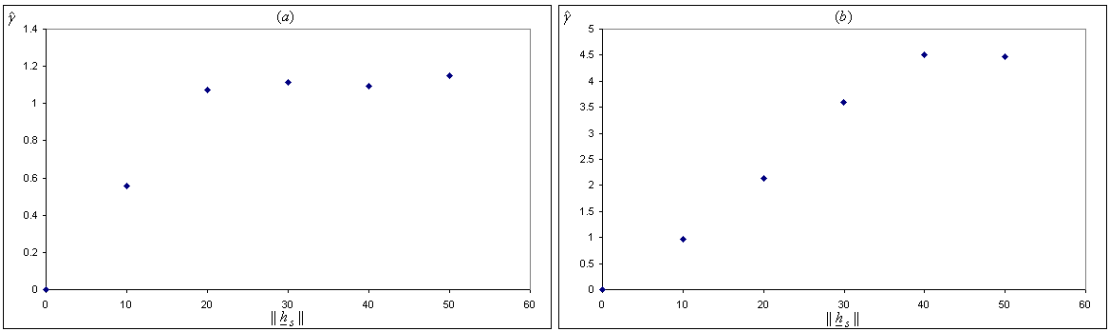

Figure 2-22a: Horizontal semi-variogram $\hat{\gamma}(\underline{h}_s)$ for Z_1 in (a) and Z_2 in (b).

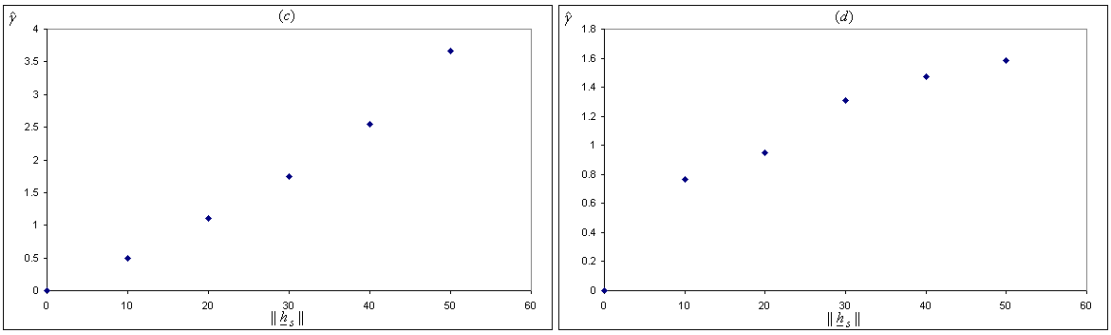

Figure 2-22b: Vertical semi-variogram $\hat{\gamma}(\underline{h}_s)$ for Z_1 in (c) and Z_2 in (d).

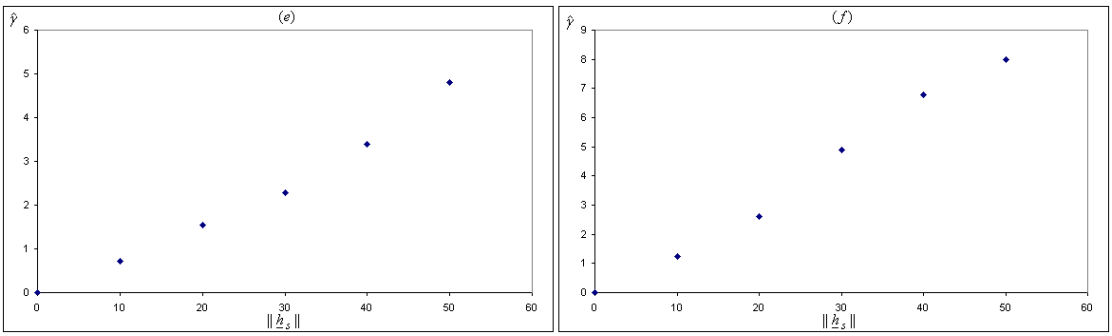

Figure 2-22c: Diagonal semi-variogram $\hat{\gamma}(\underline{h}_s)$ for Z_1 in (e) and Z_2 in (f). The lag distance is measured as multiples of $14.14m$.

The horizontal semi-variogram scatter plots, for both attributes, increase to a specific asymptote. The vertical and diagonal variogram scatter plots increase monotonically.

These variograms exhibit anisotropic (Section 2.6) behaviour, since the semi-variograms do not follow the same trend. The SAS code is available in *Appendix B.7*.

Typically, the semi-variogram scatter plot and, ultimately, the model takes on a monotonically increasing shape as the distance increases. This shape can be characterized by specific parameters, namely the range, sill and the nugget effect, as seen in Figure 2-23 (*Cressie, 1993*; *Webster and Olivier 2007; Goovaerts, 1997*).

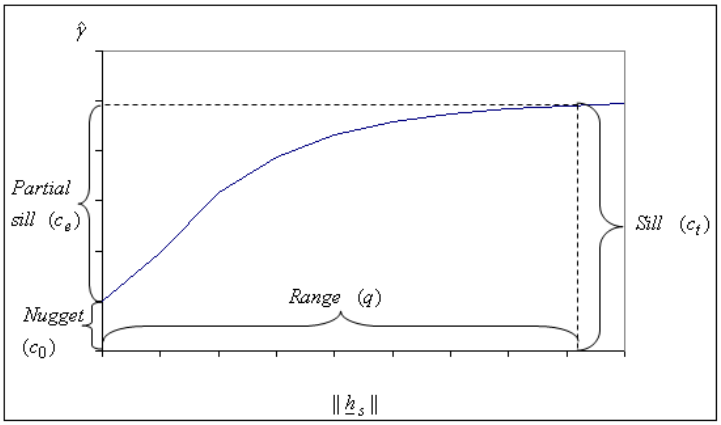

Figure 2-23: Graphical view of the different data dependencies that can be present in the variogram.

The range (q) indicates the maximum distance, within which data pairs are still significantly correlated and therefore significant in the estimation processes. The sill (c_t) is the value of the semi-variogram at its asymptote. The sill represents the distance at which the inclusion of information beyond this point adds little or no additional information to the semi-variogram. It is thus the upper bound value attained by the variogram.

The nugget effect represents the randomness at very small lag distances in the data. It could be the result of using a limited dataset and is that part of the variance that is unusable for interpolation purposes.

The partial sill is defined as c_e and is the difference between the total sill (c_t) and the nugget effect (c_0).

The characteristics of the semi-variogram plots and models can provide the following additional information, as indicated by *Christakos* (*1992*).

- The investigation of the semi-variogram variation in different directions provides information about the anisotropy structure of the random process (Section 2.6)
- The semi-variogram also indicates the neighbourhoods of influence from any given location
- The behaviour of the semi-variogram at large distances provides information about the stationarity (Section 2.6) of the data. Asymptotic behaviour is a strong indication of stationarity
- The behaviour of the semi-variogram close to and at the origin indicates the degree of short-scale variability in the process. Three types of behaviour can be observed at the origin, namely the nugget effect, linear or parabolic tendencies. The nugget effect represents the discontinuity that is a result of erratic behaviour or noise in the data. A linear form is indicative of no discontinuity at the origin. The semi-variogram does not present erratic behaviour, but can abruptly change at small distances. Parabolic behaviour is indicative of very regular and smooth spatial variation as it is twice differentiable at the origin (*Gómez-Hernández, 1996*).
- Potential periodicities or anomalies in the spatial process can also be identified by the behaviour of the range of the semi-variogram.

Univariate Spatial Covariance

The population covariance (*Isaaks and Srivastava, 1989; Cressie, 1993*; *Webster and Olivier, 2007; Goovaerts, 1997*) is defined as

$$\begin{aligned} C(\underline{h}_s) &= \mathrm{cov}(Z(\underline{u}_\alpha), Z(\underline{u}_\alpha + \underline{h}_s)) \\ &= E[(Z(\underline{u}_\alpha) - E(Z(\underline{u}_\alpha))(Z(\underline{u}_\alpha + \underline{h}_s) - E(Z(\underline{u}_\alpha + \underline{h}_s))] \end{aligned} \tag{2.16}$$

and the sample covariance function as

$$c(\underline{h}_s) = \frac{1}{N_A} \sum_A [z(\underline{u}_\alpha) - m_{+1}][z(\underline{u}_\alpha + \underline{h}_s) - m_{-1}] \tag{2.17}$$

with

$$m_{+1} = \frac{1}{N_A} \sum_A z(\underline{u}_\alpha) \tag{2.17a}$$

and

$$m_{-1} = \frac{1}{N_A} \sum_A z(\underline{u}_\alpha + \underline{h}_s) \cdot \tag{2.17b}$$

with $A = \{(\underline{u}_\alpha, \underline{u}_\beta) \,|\, \underline{u}_\alpha - \underline{u}_\beta = \underline{h}_s\}$. The ordered set of covariances calculated at different lags is known as the experimental covariance (or co-variogram) function. The scatter plots for the covariance and correlation are plotted in the same fashion as the univariate variogram.

Univariate Spatial Correlation

The population correlation (*Isaaks and Srivastava, 1989; Cressie, 1993*; *Webster and Olivier, 2007; Goovaerts, 1997*) is defined as

$$\begin{aligned} \rho(\underline{h}_s) &= \frac{\text{cov}(Z(\underline{u}_\alpha), Z(\underline{u}_\alpha + \underline{h}_s))}{\sqrt{\text{var}(Z(\underline{u}_\alpha))\,\text{var}(Z(\underline{u}_\alpha + \underline{h}_s)}} \\ &= \frac{E[(Z(\underline{u}_\alpha) - E(Z(\underline{u}_\alpha))(Z(\underline{u}_\alpha + \underline{h}_s) - E(Z(\underline{u}_\alpha + \underline{h}_s))]}{\sqrt{\text{var}(Z(\underline{u}_\alpha))\,\text{var}(Z(\underline{u}_\alpha + \underline{h}_s)}} \end{aligned} \tag{2.18}$$

The experimental correlation (correlogram) defined as the ordered set of correlation coefficients calculated at different lags, is expressed as

$$r(\underline{h}_s) = \frac{c(\underline{h}_s)}{\sqrt{s^2_{+1} s^2_{-1}}} \quad \in [-1,1] \tag{2.19}$$

with

$$s^2_{+1} = \frac{1}{N_A} \sum_A [z(\underline{u}_\alpha) - m_{+1}]^2 \tag{2.19a}$$

and

$$s_{-1}^2 = \frac{1}{N_A}\sum_A [z(\underline{u}_\alpha + \underline{h}_s) - m_{-1}]^2 \,. \tag{2.19b}$$

with $A = \{(\underline{u}_\alpha, \underline{u}_\beta) \mid \underline{u}_\alpha - \underline{u}_\beta = \underline{h}_s\}$.

Multivariate Spatial Cross -Variogram

The cross-variogram (*Isaaks and Srivastava, 1989; Cressie, 1993*; *Webster and Olivier, 2007; Goovaerts, 1997*) is based on the same methodology as the variogram defined in the univariate case. The cross-variogram presents the correlation between the primary and secondary attributes at different lag distances. The cross-variogram model is also described by the nugget, range and sill parameters.

The theoretical cross-variogram function between the attributes k and k' in $\underline{h}_s$ is defined as the element in row k and k' of the covariance matrix.

$$\begin{aligned} 2\gamma_{kk'}(\underline{h}_s) &= \mathrm{cov}[(Z_k(\underline{u}_\alpha) - Z_k(\underline{u}_\alpha + \underline{h}_s)), (Z_{k'}(\underline{u}_\alpha) - Z_{k'}(\underline{u}_\alpha + \underline{h}_s))] \\ &= E[(Z_k(\underline{u}_\alpha) - Z_k(\underline{u}_\alpha + \underline{h}_s))(Z_{k'}(\underline{u}_\alpha) - Z_{k'}(\underline{u}_\alpha + \underline{h}_s))] \end{aligned} \tag{2.20}$$

since $E[Z_k(\underline{u}_\alpha) - Z_k(\underline{u}_\alpha + \underline{h}_s)] = 0$ in the isotropic case. The experimental cross variogram is defined as

$$2\hat{\gamma}_{kk'}(\underline{h}_s) = \frac{1}{N_A}\sum_A [z_k(\underline{u}_\alpha) - z_k(\underline{u}_\alpha + \underline{h}_s)][z_{k'}(\underline{u}_\alpha) - z_{k'}(\underline{u}_\alpha + \underline{h}_s)] \tag{2.21}$$

where A is defined as $A = \{(\underline{u}_\alpha, \underline{u}_\beta) \mid \underline{u}_\alpha - \underline{u}_\beta = \underline{h}_s\}$. The cross semi-variogram (cross variogram) can be expressed in terms of the matrix where the diagonal elements of the matrix represent the univariate semi-variograms and the off-diagonal elements represent the cross semi-variograms.

$$\underset{K\times K}{\hat{\gamma}(\underline{h}_s)} = \begin{bmatrix} \hat{\gamma}_{11}(\underline{h}_s) & \hat{\gamma}_{12}(\underline{h}_s) & \cdots & \hat{\gamma}_{1K}(\underline{h}_s) \\ \hat{\gamma}_{21}(\underline{h}_s) & \hat{\gamma}_{22}(\underline{h}_s) & \cdots & \cdots \\ \cdot\cdot & \cdot\cdot & \cdot\cdot & \cdots \\ \hat{\gamma}_{K1}(\underline{h}_s) & \cdots & \cdots & \hat{\gamma}_{KK}(\underline{h}_s) \end{bmatrix}$$

For illustration purposes, (2.21) is expressed in terms of the bivariate case ($K = 2$).

$$2\hat{\gamma}_{12}(\underline{h}_s) = \frac{1}{N_A}\sum_{A}[z_1(\underline{u}_\alpha) - z_1(\underline{u}_\alpha + \underline{h}_s)][z_2(\underline{u}_\alpha) - z_2(\underline{u}_\alpha + \underline{h}_s)] = 2\hat{\gamma}_{21}(\underline{h}_s) \quad (2.21a)$$

Example 2-11

The cross semi-variograms (Figures 2-24a-c) are determined using the simulated bivariate spatial dataset $S-COM$ and (2.21a). The SAS code is available in *Appendix B.8*.

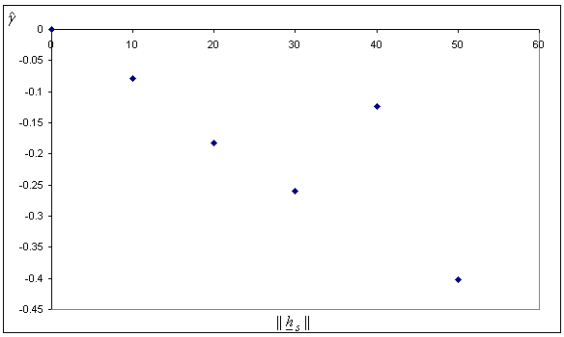

Figure 2-24a: Cross semi-variogram in the horizontal direction $\hat{\gamma}$ for Z_1 and Z_2.

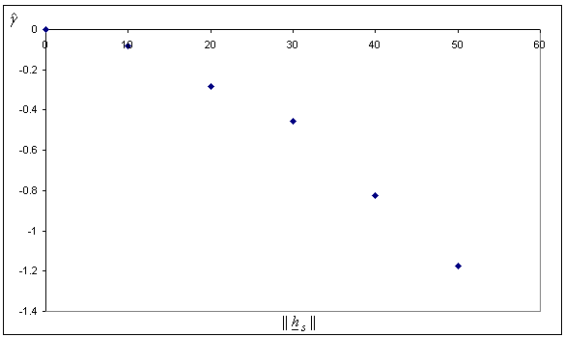

Figure 2-24b: Cross semi-variogram in the vertical direction $\hat{\gamma}$ for Z_1 and Z_2.

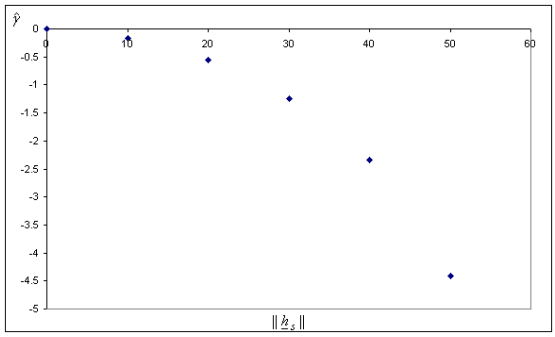

Figure 2-24c: Cross semi-variogram in the diagonal direction $\hat{\gamma}$ for Z_1 and Z_2.

All three of the cross semi-variograms decrease monotonically, reflecting the negative correlation in the data. However, in the horizontal direction an anomaly at the lag distance $40m$ is identified. Closer inspection indicated a reverse in the sign of the correlation between the primary and secondary attributes when moving in a horizontal direction for the locations in the bottom right corner of the grid. This tendency was also identified during the moving windows statistics (Table 2.5). Given that the value at lag distance $50m$ follows the general decreasing trend, it was not regarded as an anomaly in the data.

Multivariate Spatial Cross-Covariance

The cross-covariance (2.23) and cross-correlation (2.25) measure the statistical tendency, as well as the direction- and location-dependent correlation between attributes. The population cross-covariance (*Isaaks and Srivastava, 1989; Cressie, 1993*; *Webster and Olivier, 2007; Goovaerts, 1997*) between attributes k and k' in $\underline{h}_s$ is expressed as

$$C_{kk'}(\underline{h}_s) = \text{cov}\left(Z_k(\underline{u}_\alpha), Z_{k'}(\underline{u}_\alpha + \underline{h}_s)\right) \tag{2.22}$$

resulting in a sample cross-covariance of

$$c_{kk'}(\underline{h}_s) = \frac{1}{N_A}\sum_A [z_k(\underline{u}_\alpha) - \underline{m}_{+1}][z_{k'}(\underline{u}_\alpha + \underline{h}_s) - \underline{m}_{-1})] \tag{2.23}$$

where A is defined as $A = \{(\underline{u}_\alpha, \underline{u}_\beta) \,|\, \underline{u}_\alpha - \underline{u}_\beta = \underline{h}_s\}$ and the cross-covariance as

$$\underset{K\times K}{\boldsymbol{c}}(\underline{h}_s) = \begin{bmatrix} c_{11}(\underline{h}_s) & c_{12}(\underline{h}_s) & \ldots & c_{1K}(\underline{h}_s) \\ c_{21}(\underline{h}_s) & c_{22}(\underline{h}_s) & \ldots & \ldots \\ .. & .. & .. & \ldots \\ c_{K1}(\underline{h}_s) & \ldots & \ldots & c_{KK}(\underline{h}_s) \end{bmatrix}$$

The means are defined as

$$\underline{m}_{+1} = \frac{1}{N_A}\sum_A z_k(\underline{u}_\alpha) \tag{2.23a}$$

and

$$\underline{m}_{-1} = \frac{1}{N_A}\sum_{A} z_{k'}(\underline{u}_\alpha + \underline{h}_s) \tag{2.23b}$$

for all combinations of k and k' and $A = \{(\underline{u}_\alpha, \underline{u}_\beta) \mid \underline{u}_\alpha - \underline{u}_\beta = \underline{h}_s\}$.

The cross-covariances in the bivariate case is defined as

$$c_{12}(\underline{h}_s) = \frac{1}{N_A}\sum_{A}[z_1(\underline{u}_\alpha) - \underline{m}_{+1}][z_2(\underline{u}_\alpha + \underline{h}_s) - \underline{m}_{-1}] \tag{2.23c}$$

and

$$c_{21}(\underline{h}_s) = \frac{1}{N_A}\sum_{A}[z_2(\underline{u}_\alpha) - \underline{m}_{+1}][z_1(\underline{u}_\alpha + \underline{h}_s) - \underline{m}_{-1}]. \tag{2.23d}$$

A new characteristic introduced by the cross-covariance is that of asymmetry, where

$$E\left[\{Z_1(\underline{u}_\alpha) - \underline{m}_{+1}\}\{Z_2(\underline{u}_\alpha + \underline{h}_s) - \underline{m}_{-1}\}\right] \neq E\left[\{Z_2(\underline{u}_\alpha) - \underline{m}_{+1}\}\{Z_1(\underline{u}_\alpha + \underline{h}_s) - \underline{m}_{-1}\}\right] \tag{2.23d}$$

such that $c_{12}(\underline{h}_s) \neq c_{12}(-\underline{h}_s)$ and $c_{12}(\underline{h}_s) \neq c_{21}(\underline{h}_s)$ but $c_{12}(\underline{h}_s) = c_{21}(-\underline{h}_s)$.

It cannot be assumed that the value of the second attribute lagging the primary attribute is the same as the values of the primary attribute lagging the second attribute. For example, if irrigation flooding is always from the same end of a field, the salts in the soil might be distributed differently according to the direction of the water flow (*Webster and Oliver, 2007*).

Multivariate Spatial Cross-Correlation

The population cross-correlation (*Isaaks and Srivastava, 1989; Cressie, 1993*; *Webster and Olivier, 2007; Goovaerts, 1997*) between attributes k and k' in $\underline{h}_s$ is defined as

$$\rho_{kk'}(\underline{h}_s) = \frac{C_{kk'}(\underline{h}_s)}{\sqrt{C_{kk}(\underline{0})C_{k'k'}(\underline{0})}} \quad \in [-1,+1] \tag{2.24}$$

and sample cross-correlation as

$$r_{kk'}(\underline{h}_s) = \frac{c_{kk'}(\underline{h}_s)}{\sqrt{c_{kk}(\underline{0})c_{k'k'}(\underline{0})}} \in [-1,+1] \tag{2.25}$$

The bivariate function is expressed as

$$r_{12}(\underline{h}_s) = \frac{c_{12}(\underline{h}_s)}{\sqrt{c_{11}(\underline{0})c_{22}(\underline{0})}} \in [-1,+1]. \tag{2.25a}$$

and

$$r_{21}(\underline{h}_s) = \frac{c_{21}(\underline{h}_s)}{\sqrt{c_{11}(\underline{0})c_{22}(\underline{0})}} \in [-1,+1]. \tag{2.25b}$$

The cross-correlation matrix for k attributes is defined as

$$\underset{K\times K}{\boldsymbol{r}}(\underline{h}_s) = \begin{bmatrix} r_{11}(\underline{h}_s) & r_{12}(\underline{h}_s) & \ldots & r_{1K}(\underline{h}_s) \\ r_{21}(\underline{h}_s) & r_{22}(\underline{h}_s) & \ldots & \ldots \\ .. & .. & .. & \ldots \\ r_{K1}(\underline{h}_s) & \ldots & \ldots & r_{KK}(\underline{h}_s) \end{bmatrix}$$

Spatial-Temporal Moments

The spatial-temporal moments are based on a similar underlying structure as the spatial moments, except that the time component must be taken into account. As mentioned in Section 2.2, the order in which measurements are observed in time plays an important role in optimal interpolation and simulation. To graphically represent these moments is fairly easy; however, the modelling proves to be complicated and is discussed in detail in Chapter 3.

Univariate Spatial-Temporal Variogram

The univariate spatial-temporal variogram, covariance and correlogram are based on the same structures as their spatial counterparts when the temporal factor is included. The variance in the data is described by the graphical representation of the variogram as a function of the spatial lag distances ($\underline{h}_s$) and the temporal lag distances (h_t). The spatial and temporal distances respectively describe the spatial and temporal

continuity between the measurements (*Rouhani and Wackernagel, 1990; De Cesare* et al*., 1996; Kyriakidis and Journel, 1999*).

The theoretical variogram is defined as

$$\begin{aligned} 2\gamma(\underline{h}_s, h_t) &= \text{var}[Z(\underline{u}_\alpha, t_\tau) - Z(\underline{u}_\alpha + \underline{h}_s, t_\tau + h_t)] \\ &= E[(Z(\underline{u}_\alpha, t_\tau) - Z(\underline{u}_\alpha + \underline{h}_s, t_\tau + h_t))^2] \end{aligned} \tag{2.26}$$

with the variogram estimate at lag distance $\underline{h}_s$ and time lag h_t as

$$2\hat{\gamma}(\underline{h}_s, h_t) = \frac{1}{N_B}\sum_B [z(\underline{u}_\alpha, t_\tau) - z(\underline{u}_\alpha + \underline{h}_s, t_\tau + h_t)]^2 \quad \forall \quad \alpha = 1,..,n, \tau = 1,...T \tag{2.27}$$

where $B = \{[(\underline{u}_\alpha, t_\tau), (\underline{u}_\beta, t_s)] | \underline{u}_\alpha - \underline{u}_\beta = \underline{h}_s \quad and \quad | t_s - t_\tau | = h_t\}$ and N_B is the number of elements in the set B.

The graphical representation of the semi-variogram will now be in terms of $(\underline{h}_s, h_t)$, and not only $\underline{h}_s$ and is therefore a three-dimensional plot. The definitions of the range, sills and nugget effect as defined in Figure 2-23 remain unchanged.

Example 2-12

The spatial-temporal semi-variograms for the simulated dataset $ST - COM$ were calculated per attribute in the three directions utilized in the previous examples. The addition of the temporal lag to the variogram renders a three-dimensional plot that clearly illustrates its effects.

The temporal lag effect has a substantial effect on the variogram and can therefore not be ignored in case studies where time information is available. The complexity that will be encountered to determine an empirical model is also evident from Figures 2-25a to 2-25c.

The isotropic behaviour of the data is apparent, as Figures 2-25a to 2-25c indicate that the spatial-temporal data follow that same trend in all three directions.

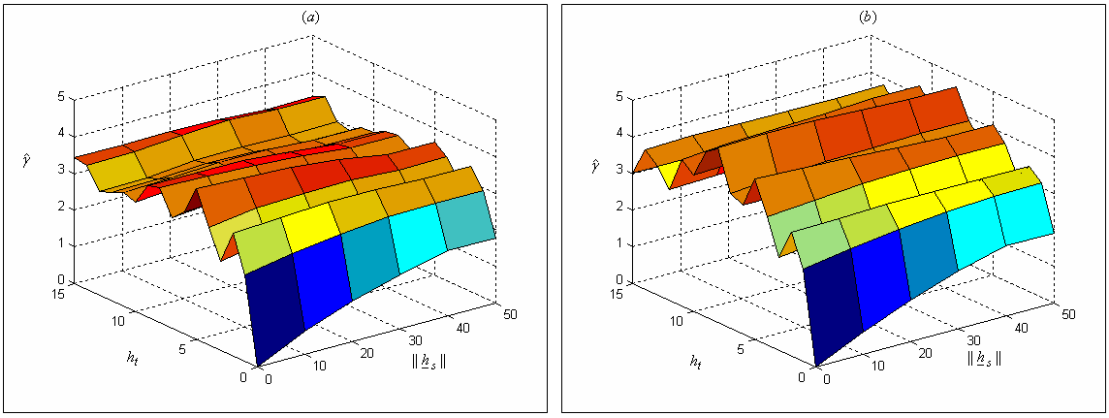

Figure 2-25a: Spatial-temporal semi-variogram in the horizontal direction for Z_1 in (a) and for Z_2 in (b).

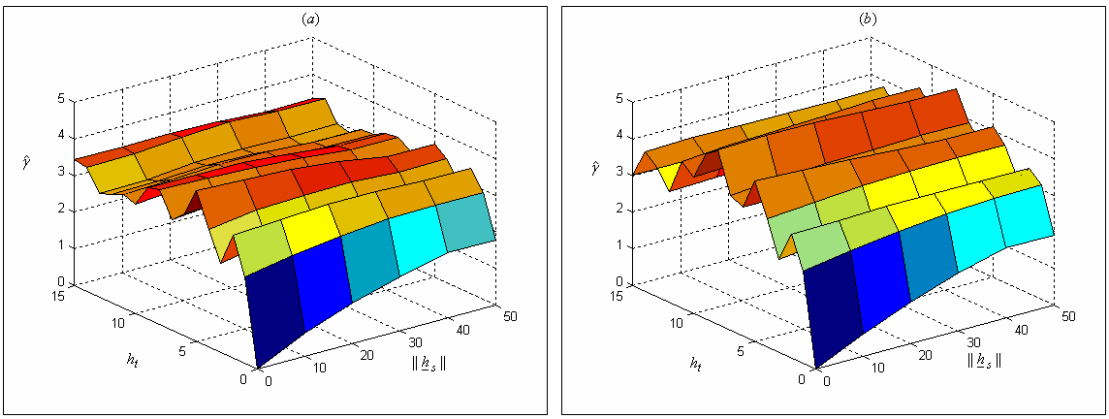

Figure 2-25b: Spatial-temporal semi-variogram in the vertical direction for Z_1 in (a) and for Z_2 in (b).

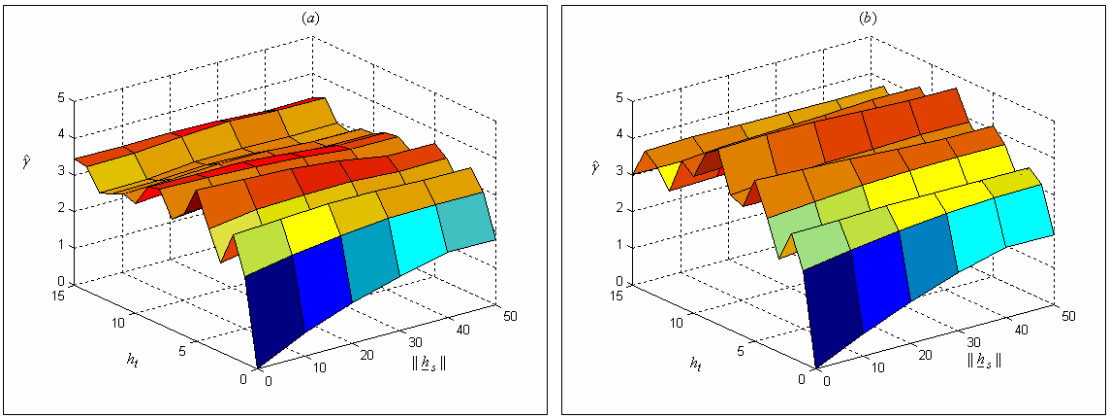

Figure 2-25c: Spatial-temporal semi-variogram in the diagonal direction for Z_1 in (a) and for Z_2 in (b).

Normally the semi-variograms are plotted using scatter points. It is, however, difficult to accurately assess a three-dimensional semi-variogram by using only scatter points. The spatial-temporal semi-variogram and cross semi-variogram (Example 2-13) are visually represented by a surface plot. The SAS code to determine the directional spatial-temporal semi-variograms is available in *Appendix B.9*.

Univariate Spatial-Temporal Covariance

The spatial-temporal population covariance (*Rouhani and Wackernagel, 1990; De Cesare* et al., *1996; Kyriakidis and Journel, 1999*) is expressed as

$$\begin{aligned} & C(\underline{h}_s, h_t) \\ & = \operatorname{cov}(Z(\underline{u}_\alpha, t_\tau), Z(\underline{u}_\alpha + \underline{h}_s, t_\tau + h_t)) \\ & = E[(Z(\underline{u}_\alpha, t_\tau) - E(Z(\underline{u}_\alpha, t_\tau))(Z(\underline{u}_\alpha + \underline{h}_s, t_\tau + h_t) - E(Z(\underline{u}_\alpha + \underline{h}_s, t_\tau + h_t))] \end{aligned} \tag{2.28}$$

with the sample spatial-temporal covariance function is defined as

$$c(\underline{h}_s, h_t) = \frac{1}{N_B} \sum_B [z(\underline{u}_\alpha, t_\tau) - m_{+1}][z(\underline{u}_\alpha + \underline{h}_s, t_\tau + h_t) - m_{-1}] \tag{2.29}$$

with

$$m_{+1} = \frac{1}{N_B} \sum_B z(\underline{u}_\alpha, t_\tau) \tag{2.29a}$$

and

$$m_{-1} = \frac{1}{N_B} \sum_B z(\underline{u}_\alpha + \underline{h}_s, t_\tau + h_t). \tag{2.29b}$$

where B is defined as $B = \{[(\underline{u}_\alpha, t_\tau), (\underline{u}_\beta, t_s)] \mid \underline{u}_\alpha - \underline{u}_\beta = \underline{h}_s \text{ and } \mid t_s - t_\tau \mid = h_t\}$.

Univariate Spatial-Temporal Correlation

The population spatial-temporal correlation coefficient is given as

$$\rho(\underline{h}_s, \underline{h}_t) = \frac{\text{cov}(Z(\underline{u}_\alpha, t_\tau), Z(\underline{u}_\alpha + \underline{h}_s, t_\tau + h_t))}{\sqrt{\text{var}(Z(\underline{u}_\alpha, t_\tau))\,\text{var}(Z(\underline{u}_\alpha + \underline{h}_s, t_\tau + h_t))}} \tag{2.30}$$

The correlogram is defined as

$$r(\underline{h}_s, h_t) = \frac{c(\underline{h}_s, h_t)}{\sqrt{s_{+1}^2 s_{-1}^2}} \in [-1,1] \tag{2.31}$$

with

$$s_{+1}^2 = \frac{1}{N_B} \sum_B [z(\underline{u}_\alpha, t_\tau) - m_{+1}]^2 \tag{2.31a}$$

and

$$s_{-1}^2 = \frac{1}{N_B} \sum_B [z(\underline{u}_\alpha + \underline{h}_s, t_\tau + h_t) - m_{-1}]^2 \tag{2.31b}$$

where B is defined as $B = \{[(\underline{u}_\alpha, t_\tau), (\underline{u}_\beta, t_s)] \mid \underline{u}_\alpha - \underline{u}_\beta = \underline{h}_s \text{ and } \mid t_s - t_\tau \mid = h_t\}$.

Multivariate Spatial-Temporal Cross-Variogram

The spatial-temporal cross-variogram (*Rouhani and Wackernagel 1990; De Cesare* et al., *1996; Kyriakidis and Journel, 1999*) combines the spatial cross-variogram (2.21) with the spatial-temporal structure.

The theoretical cross variogram for the space-time structure for all locations and time points is defined as

$$\begin{aligned} &2\gamma_{kk'}(\underline{h}_s, h_t) \\ &= E\left[\{(Z_k(\underline{u}_\alpha, t_\tau) - Z_k(\underline{u}_\alpha + \underline{h}_s, t_\tau + h_t)\}\{(Z_{k'}(\underline{u}_\alpha, t_\tau) - Z_{k'}(\underline{u}_\alpha + \underline{h}_s, t_\tau + h_t)\}\right] \end{aligned} \tag{2.32}$$

and the experimental cross semi-variogram as

$$\begin{aligned} &\hat{\gamma}_{kk'}(\underline{h}_s, h_t) \\ &= \frac{1}{2N_B} \sum_B [z_k(\underline{u}_\alpha, t_\tau) - z_k(\underline{u}_\alpha + \underline{h}_s, t_\tau + h_t)][z_{k'}(\underline{u}_\alpha, t_\tau) - z_{k'}(\underline{u}_\alpha + \underline{h}_s, t_\tau + h_t)] \end{aligned} \tag{2.33}$$

where B is defined as $B = \{[(\underline{u}_\alpha, t_\tau), (\underline{u}_\beta, t_s)] \mid \underline{u}_\alpha - \underline{u}_\beta = \underline{h}_s \text{ and } \mid t_s - t_\tau \mid = h_t\}$.

Example 2-13

The spatial-temporal cross semi-variograms for Z_1 and Z_2 were calculated in the same manner as the spatial-temporal semi-variograms (Example 2-12).

Similar to semi-variograms in Example 2-12, the cross semi-variograms are similar in all three directions.

Appendix B.10 provides the SAS code for the directional spatial-temporal cross semi-variograms.

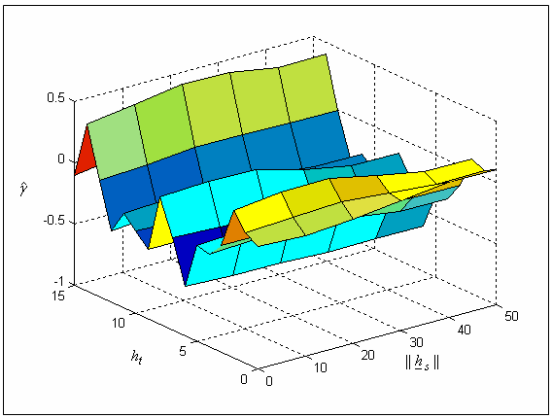

Figure 2-26: Horizontal spatial-temporal cross semi-variogram for $Z_1 Z_2$ and $Z_2 Z_1$.

Multivariate Spatial-Temporal Cross-Covariance

The population cross-covariance is defined as

$$C_{kk'}(\underline{h}_s, h_t) = \text{cov}\left(Z_k(\underline{u}_\alpha, t_\tau), Z_{k'}(\underline{u}_\alpha + \underline{h}_s, t_\tau + h_t)\right)$$
$$= E\left[\{(Z_k(\underline{u}_\alpha, t_\tau) - E(Z_k(\underline{u}_\alpha, t_\tau)\}\{(Z_{k'}(\underline{u}_\alpha + \underline{h}_s, t_\tau + h_t) - E(Z_k(\underline{u}_\alpha + \underline{h}_s, t_\tau + h_t))\}\right] \quad (2.34)$$

with the sample cross-covariance defined as

$$c(\underline{h}_s, h_t) = \frac{1}{N_B} \sum_B [z_k(\underline{u}_\alpha, t_\tau) - \underline{m}_{+1}][z_{k'}(\underline{u}_\alpha + \underline{h}_s, t_\tau + h_t) - \underline{m}_{-1}] \tag{2.35}$$

with

$$\underline{m}_{+1} = \frac{1}{N_B} \sum_B z(\underline{u}_\alpha, t_\tau) \tag{2.35a}$$

and

$$\underline{m}_{-1} = \frac{1}{N_B} \sum_B z(\underline{u}_\alpha + \underline{h}_s, t_\tau + \underline{h}_t) \tag{2.35b}$$

where B is defined as $B = \{[(\underline{u}_\alpha, t_\tau), (\underline{u}_\beta, t_s)] \mid \underline{u}_\alpha - \underline{u}_\beta = \underline{h}_s \ \ and \mid t_s - t_\tau \mid = h_t\}$.

For the two attributes, (2.35) reduces to

$$\begin{aligned} & c_{12}(\underline{h}_s, h_t) \\ & = \frac{1}{N_B} \sum_B [z_1(\underline{u}_\alpha, t_\tau - \underline{m}_{+1})][z_2(\underline{u}_\alpha + \underline{h}_s, t_\tau + h_t) - \underline{m}_{-1})] \end{aligned} \tag{2.35c}$$

A new characteristic introduced by the cross-covariance is that of asymmetry.

$$\begin{aligned} & E[\{Z_1(\underline{u}_\alpha, t_\tau) - \underline{m}_{+1}\}\{Z_2(\underline{u}_\alpha + \underline{h}_s, t_\tau + h_t) - \underline{m}_{-1}\}] \\ & \qquad \neq \\ & E\left[\{Z_2(\underline{u}_\alpha, t_\tau) - m_{+1}\}\{Z_1(\underline{u}_\alpha + \underline{h}_s, t_\tau + h_t) - \underline{m}_{-1}\}\right] \end{aligned} \tag{2.36}$$

and therefore $C_{12}(\underline{h}_s, h_t) \neq C_{12}(-\underline{h}_s, -h_t)$ and $C_{12}(\underline{h}_s, h_t) \neq C_{21}(\underline{h}_s, h_t)$.

Multivariate Spatial-Temporal Cross-Correlation

The correlogram between attributes k and k' is defined as

$$\rho_{kk'}(\underline{h}_s, h_t) = \frac{C_{kk'}(\underline{h}_s, h_t)}{\sqrt{C_{kk}(\underline{0},0) C_{k'k'}(\underline{0},0)}} \quad \in [-1,1] \tag{2.37}$$

with the notation for the sample correlation as

$$r_{kk'}(\underline{h}_s, h_t) = \frac{c_{kk'}(\underline{h}_s, h_t)}{\sqrt{c_{kk}(\underline{0},0)c_{k'k'}(\underline{0},0)}} \quad \in [-1,1] \tag{2.38}$$

The spatial-temporal cross-correlation for two attributes is represented as

$$r_{12}(\underline{h}_s, h_t) = \frac{c_{12}(\underline{h}_s, h_t)}{\sqrt{c_{11}(\underline{0},0)c_{22}(\underline{0},0)}} \quad \in [-1,1] \tag{2.38a}$$

and

$$r_{21}(\underline{h}_s, h_t) = \frac{c_{21}(\underline{h}_s, h_t)}{\sqrt{c_{11}(\underline{0},0)c_{22}(\underline{0},0)}} \quad \in [-1,1]. \tag{2.38b}$$

where B is defined as $B = \{[(\underline{u}_\alpha, t_\tau), (\underline{u}_\beta, t_s)] \mid \underline{u}_\alpha - \underline{u}_\beta = \underline{h}_s \text{ and } \mid t_s - t_\tau \mid = h_t\}$.

The next step in the interpolation process is to fit an empirical model to the scatter plot of the variogram. To fit a model that will adhere to the requirements of the kriging models, certain spatial and spatial-temporal data properties must be defined and tested for. Section 2.6 describes these properties and their connection with the interpolation methodology.

2.6 DATA PROPERTIES

The main data properties that require consideration in the modelling of the statistics described in Section 2.5 are stationarity, anisotropy, ergodicity and irregularly spaced measurements. These properties allow the researcher to select appropriate models that accurately describe the spatial and spatial-temporal dependence structure in such a way that a best linear unbiased estimate (*BLUE*) of the missing data is achieved.

Stationarity

Stationarity is a set of assumptions based on the distribution of the data, which allows the researcher to estimate model parameters according to a standard set of properties (*Cressie, 1991; Goovaerts, 1997; Isaaks and Srivastava, 1989*). In kriging,

stationarity is one of the primary factors required to determine a unique set of kriging parameters.

The three types of spatial stationarity that are identified in the kriging methodology are strict, second-order and intrinsic stationarity. A random function is considered *strictly stationary* if the distribution's spatial law is invariant under translation. The joint distributions of the random variables $Z(\underline{u}_1),...,Z(\underline{u}_n)$ are identical to the joint distributions of $Z(\underline{u}_1+\underline{h}_s),...,Z(\underline{u}_n+\underline{h}_s)$ for all $\underline{h}_s$.

Second-order stationarity is applicable if only the first two moments, the mean and covariance, are invariant to the spatial position of the data. The mean is required to be constant regardless of the position of $\underline{u}_\alpha$

$$\begin{aligned} E[Z(\underline{u}_\alpha)] &= \mu(\underline{u}_\alpha) \\ &= \mu \qquad \forall \ \underline{u}_\alpha \end{aligned} \tag{2.39a}$$

and the covariance between observations at two locations $\underline{u}_\alpha$ and $\underline{u}_\alpha+\underline{h}_s$ should only depend on the length of lag and not on the position $\underline{u}_\alpha$.

$$\begin{aligned} \text{cov}(Z(\underline{u}_\alpha), Z(\underline{u}_\alpha+\underline{h}_s)) &= E\left[\left(Z(\underline{u}_\alpha)-\mu(\underline{u}_\alpha)\right)\left(Z(\underline{u}_\alpha+\underline{h}_s)-\mu(\underline{u}_\alpha+\underline{h}_s)\right)\right] \\ &= E\left[\left(Z(\underline{u}_\alpha)-\mu\right)\left(Z(\underline{u}_\alpha+\underline{h}_s)-\mu\right)\right] \\ &= C(\underline{h}_s) \end{aligned} \tag{2.39b}$$

Intrinsic stationarity is considered when the variance may be unlimited and it follows from the 'intrinsic hypothesis' of *Matheron* (*1962*) that the two conditions for intrinsic stationarity to be valid are

$$E[Z(\underline{u}_\alpha)-Z(\underline{u}_\alpha+\underline{h}_s)]=0 \qquad \forall \ \underline{u}_\alpha \in D \tag{2.40}$$

and

$$\text{var}\left[Z(\underline{u}_\alpha+\underline{h}_s)-Z(\underline{u}_\alpha)\right]=E\left[\left(Z(\underline{u}_\alpha+\underline{h}_s)-Z(\underline{u}_\alpha)\right)^2\right]=2\gamma(\underline{h}_s) \quad \forall \underline{u}_\alpha \in D \tag{2.14}$$

and is only dependent on the spatial lag. This hypothesis releases the researcher from the strict conditions of second-order stationarity. Data where the variance increases as

the spatial lag increases until the population variance is reached, can now also be analyzed. Second-order stationarity implicitly implies intrinsic stationary, but the reverse is not true.

The relationship between the variogram and the covariance functions, based on intrinsic stationarity, is depicted in Figure 2-27 and defined by (2.41).

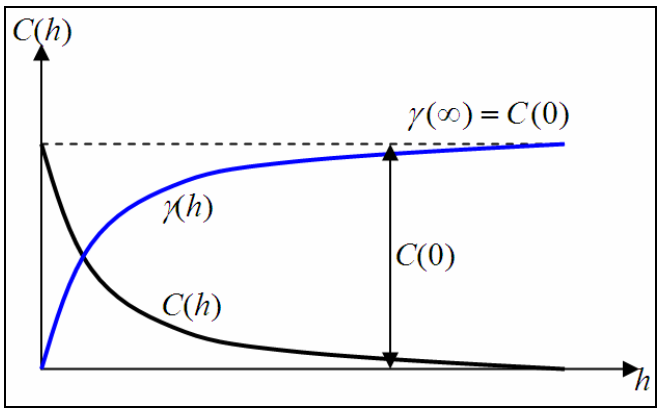

Figure 2-27: Relationship between covariance and semi-variogram.

$$\gamma(\underline{h}_s) = C(\underline{0}) - C(\underline{h}_s) \tag{2.41}$$

Equation (2.41) is derived as follows (*Banerjee* et al., *2004*):

$$2\gamma(\underline{h}_s) = \text{var}\left[Z(\underline{u}_\alpha + \underline{h}_s) - Z(\underline{u}_\alpha)\right]$$

$$= \text{var}\left[Z(\underline{u}_\alpha + \underline{h}_s)\right] + \text{var}\left[Z(\underline{u}_\alpha)\right] - 2\,\text{cov}\left[Z(\underline{u}_\alpha + \underline{h}_s), Z(\underline{u}_\alpha)\right]$$

$$= C(\underline{0}) + C(\underline{0}) - 2C(\underline{h}_s)$$

$$\gamma(\underline{h}_s) = C(\underline{0}) - C(\underline{h}_s).$$

Some properties of the covariance function in the second-order stationary field are (*Schabenberger and Gotway, 2000*)

- $C(\underline{0}) \geq 0$
- $C(\underline{h}_s) = C(-\underline{h}_s)$ i.e. the covariance is an even function

- $|C(\underline{h}_s)| \leq C(\underline{0})$
- $C(\underline{h}_s) \to (0)$ as $\underline{h}_s \to +\infty$
- $C(\underline{h}_s) = \text{cov}[Z(\underline{u}_\alpha), Z(\underline{u}_\alpha + \underline{h}_s)] = \text{cov}[Z(\underline{u}_\beta), Z(\underline{u}_\beta + \underline{h}_s)]$

Similarly, the following properties hold for the variogram (*Schabenberger and Gotway, ,2000*)

- $\gamma(\underline{0}) = 0$
- $\gamma(\underline{h}_s) = \gamma(-\underline{h}_s) \geq 0$
- $\gamma(\underline{h}_s) \to C(\underline{0})$ as $\underline{h}_s \to +\infty$.

The main difference between the variogram, covariance and correlogram is that the variogram and covariance standardize the local means, and the correlogram standardizes both the local mean and variation of the data. The covariance and correlogram are less likely to be influenced by erratic measurements. If there is a significant difference between the three models, it may indicate that the data are not stationary.

Spatial-temporal stationarity is defined in a similar fashion in terms of strict, second-order and intrinsic stationarity. Strict stationarity within $D \times \Im$ is defined as the random variables having the same multivariate cumulative distribution function regardless $(\underline{h}_s, h_t) \in D \times \Im$ (*Kyriakidis and Journel, 1999*).

$$F(\underline{u}_1, t_1, \underline{u}_2, t_2 ..., \underline{u}_n, t_T) =$$

$$F(\underline{u}_1 + \underline{h}_s, t_1 + \underline{h}_t, \underline{u}_2 + \underline{h}_s, t_2 + \underline{h}_t, ..., \underline{u}_n + \underline{h}_s, t_T + h_t) \qquad (2.42)$$

$$\forall \ \ \underline{u}_1, ..., \underline{u}_n \in D \text{ and } t \in \Im .$$

Second-order stationarity is then defined in terms of the $D \times \Im$ with dependence only on the spatial and temporal lags

$$E(Z(\underline{u}_\alpha, t_\tau)) = \mu \quad \forall \quad (\underline{u}_\alpha, t_\tau) \in D \times \Im \qquad (2.43a)$$

and

$$C(\underline{u}_\alpha, t_\tau; \underline{u}_\alpha + \underline{h}_s, t_\tau + h_t) = E[(Z(\underline{u}_\alpha, t_\tau) - \mu)(Z(\underline{u}_\alpha + \underline{h}_s, t_\tau + h_t) - \mu)] \\ = C(\underline{h}_s, h_t) \quad \forall \quad (\underline{u}_\alpha, t_\tau) \in D \times \Im \tag{2.43b}$$

Intrinsic stationary as defined through (2.40) and (2.14) is re-defined as

$$E[Z(\underline{u}_\alpha, t_\tau) - Z(\underline{u}_\alpha + \underline{h}_s, t_\tau + h_t)] = 0 \\ \forall \quad \underline{u}_\alpha, \underline{t}_\tau, \underline{h}_s, \; h_t \quad \ni \quad \underline{u}_\alpha + \underline{h}_s \in D \text{ and } t_\tau + h_t \in \Im \tag{2.44a}$$

The second condition that must be satisfied is

$$2\gamma(\underline{h}_s, h_t) = \text{var}\left[Z(\underline{u}_\alpha + \underline{h}_s, t_\tau + h_t) - Z(\underline{u}_\alpha, t_\tau)\right] \\ = E\left[\left(Z(\underline{u}_\alpha + \underline{h}_s, t_\tau + h_t) - Z(\underline{u}_\alpha, t_\tau)\right)^2\right] \tag{2.44b}$$

Example 2-14

Compared with time series analysis, there is no universally applied test that can be used to determine whether the spatial dataset is stationary or not. The most commonly used method is the non-mathematical inspection of the data and the variograms.

Another method is to plot the attributes on the grid and visually inspect for trends. As seen from Figure 2-3b, it seems that a decreasing trend exists for the primary attribute. To err on the side of caution, it will be assumed that the data are not stationary. The nature of non-stationarity will determine the method to be used to obtain stationary residuals. In this case, the data were found to be trend-stationary in the spatial dimension. The trend was obtained by fitting a regression model and the residuals by subtracting the trend.

One of the primary constraints for the application of interpolation and simulation is the stationarity of the datasets. For both intrinsic and second-order stationarity, the mean of the data should be constant. As most real-time measurements do not comply with the stationarity conditions, several transformation methods were introduced.

Webster and Oliver (*2007, p61–63*) defined a support as the volume of a "particular size, shape and orientation". Measurements are to be taken out of these finite volumes. The variogram is therefore a function of the support, in that the "larger the support is the more variation each measurement encompasses, and the less there is in the intervening space to appear in the variogram". This eventually has a decreasing effect on the sill, resulting in a smooth, decreasing, and upward-concave line close to the origin, which represents the drift or trend. If the trend is removed, the data consist of second-order stationary residuals to which interpolation techniques can be applied. This is also known as quasi-stationarity.

In practice non-stationary data is a common occurrence. To overcome this hurdle, a trend is extracted, resulting in stationary or non-stationary residuals (*Journel and Huijbregts, 1978*). For the rest of this study, the residuals will be assumed as stationary.

Let $Z(\underline{u}_\alpha)$ be the random variable that can be split into a trend and residual components (*Goovaerts, 1997*)

$$Z(\underline{u}_\alpha) = m(\underline{u}_\alpha) + R(\underline{u}_\alpha)\,. \tag{2.45a}$$

where $m(\underline{u}_\alpha)$ is the trend and $R(\underline{u}_\alpha)$ is the residual component. The residual component is, by definition, modelled as a stationary random variable with a mean of zero

$$E[R(\underline{u}_\alpha)] = 0 \quad \forall \quad \underline{u}_\alpha \in D$$

and a covariance $C_R(\underline{h}_s)$

$$\begin{aligned}\operatorname{cov}(R(\underline{u}_\alpha), R(\underline{u}_\alpha + \underline{h}_s)) &= E\left[\{R(\underline{u}_\alpha) - E(R(\underline{u}_\alpha)\}\{R(\underline{u}_\alpha + \underline{h}_s) - E(R(\underline{u}_\alpha + \underline{h}_s)\right] \\ &= E[\{R(\underline{u}_\alpha) - 0\}\{R(\underline{u}_\alpha + \underline{h}_s) - 0\}] \\ &= E[(R(\underline{u}_\alpha)R(\underline{u}_\alpha + \underline{h}_s)] \\ &= C_R(\underline{h}_s)\end{aligned}$$

The trend represents the constant variation in the data and the residual component is the small-scale fluctuations around that trend.

When considering spatial residual kriging, the assumption of intrinsic stationarity describes the spatial dependence given by the variogram as

$$2\hat{\gamma}_R(\underline{h}_s) = E[\{R(\underline{u}_\alpha + \underline{h}_s) - R(\underline{u}_\alpha)\}^2] \tag{2.45b}$$

which is equivalent to (2.14) for a constant mean. It is therefore possible to replace the original data series with the residual values in each of the variogram equations discussed in the preceding sections without any loss of generality.

Several methods have been developed to de-trend a dataset. Regression analysis is often used in the spatial case, using the linear and quadratic models. The most basic trend models for spatial-temporal measurements is to utilize deterministic functions (*Kyriakidis and Journel, 1999*), which includes the polynomial Fourier and mixed forms as provided by *Dimitrakopoulos and Luo* (*1997*). Another, much simpler method is the moving-average estimation method (*Brockwell and Davies, 1987*), where both a deterministic and seasonal component can be identified and removed.

One disadvantage of using residuals is that they are dependent on the identified trend and can therefore introduce additional bias to the data.

Example 2-15

The spatial-temporal dataset ($ST-COM$) is stationary compared with the spatial dataset $S-COM$ (Example 2.14).

Table 2.7: Regression output for using Z_1 and Z_2.

Attribute		β_j	SSE	Pr>F	R^2
Z_1	Intercept	98.76752	0.28277	<0.0001	0.6351
	x	0.01453	0.00341	<0.0001	
	y	0.04187	0.00341	<0.0001	
Z_2	Intercept	102.96153	0.39934	<0.0001	0.4324
	x	-0.03689	0.00482	<0.0001	
	y	-0.01880	0.00482	<0.0001	

The spatial dataset was de-trended by fitting a regression line, using the REG procedure in SAS (*Appendix B.11*). The sum of squared residuals (SSE) for each of the coefficients is small and the $H_0 : \beta_j = 0$ is rejected for all the coefficients. The coefficient of determination R^2 is also acceptable.

The semi-variograms for the different directions were plotted (Figures 2-30a to 2-30c in Example 2-16) using the residual values. An asymptote is now reached in all directions for the primary and secondary semi-variograms. These residuals are stationary and will be used in any additional interpolation or simulation analysis.

Anisotropy

The second spatial data property to be considered is that of anisotropy (*Cressie 1991; Isaaks and Srivastava, 1989*). If the variance of $Z(\underline{u}_\alpha)$ depends on the spatial direction, the data are anisotropic. The measurements along a specific spatial direction may be highly correlated, while other directions have little or no correlation. If the spatial data are isotropic, where only the distances plays a role, the variograms in the different directions are reduced to a single variogram. If the observed measurements are defined as a second-order stationary series, then the covariance function $C(\underline{u}_\alpha)$ is defined isotropic if $C[Z(\underline{u}_\alpha) - Z(\underline{u}_\alpha + \underline{h}_s)]$ is only a function of $\| Z(\underline{u}_\alpha) - Z(\underline{u}_\alpha + \underline{h}_s) \|$ (*Gaetan and Guyon, 2009*).

Several forms of anisotropy exist. Geometric anisotropy is defined in terms of a variogram (Figure 2-23) that have different ranges (q) for different spatial directions. If the sill c_t depends on the spatial direction, the anisotropy is classified as zonal. Either geometric- or zonal anisotropy, or both types can be present.

To accurately assess whether anisotropy is present in a dataset, variograms in different directions should be calculated. *Goovaerts (1997)* suggests that at least $d+1$ directional semi-variograms be calculated for a dataset in $\Re^d$. If the semi-variograms exhibit the same characteristics, it can be safely assumed that the data are isotropic;

data are homogeneous in all possible directions. The isotropic variogram depends only on the length of the spatial lag.

For geometric anisotropic data, the ranges (q) of the different directional variograms can be plotted according to the respective directions by means of a rose diagram. This provides a graphical representation of the major and minor axes that influence the data. Figure 2-28 is an example of a rose diagram (*Isaaks and Srivastava, 1989*).

For two-dimensional datasets, only one major and one minor axis are expected. The major axis is identified by the directional semi-variogram with the maximum range. The largest sill, as a measure of variability, is perpendicular to the major axis. Conversely, the directional semi-variogram with the minimum range represents the minor axis.

Geometric anisotropy is included in the semi-variogram by means of a simple linear transformation of the rectangular co-ordinates and is best illustrated with a Spherical variogram in Figure 2-29 (*Webster and Oliver, 2007*) and the range that describes an ellipse in the plane of the spatial lag. From Figure 2-29**,** A is the range of the major axis (maximum diameter of the ellipse) and B the range of the minor axis and is perpendicular to the first. If it is assumed that θ is the angle of the direction of the major axis and ϑ is the direction of the lag, the equation for transformation is expressed as

$$\Omega(\vartheta) = \left\{A^2 \cos^2(\vartheta - \theta) + B^2 \sin^2(\vartheta - \theta)\right\}^{1/2} \tag{2.46}$$

with Ω defined as the anisotropy and ϑ the direction of the spatial lag. The function $\Omega(\vartheta)$ will replace q in the basic semi-variogram models defined later in Section 3.3.

A large range in a specific direction indicates strong covariance, even at large lag distances, whereas the converse is true for small values of q. If this occurs, the same model cannot be used for all directions.

Zonal anisotropy is present in a dataset when the sill (c_t) differs in different directions. Nested variograms (Section 3.3) and geometric anisotropy are used to

approximate zonal anisotropy as no direct transformations exist (*Goovaerts, 1997, p93*). A nested variogram is defined as a variogram model that consists of two or more basic variogram models that are valid for specific intervals of the lag distances.

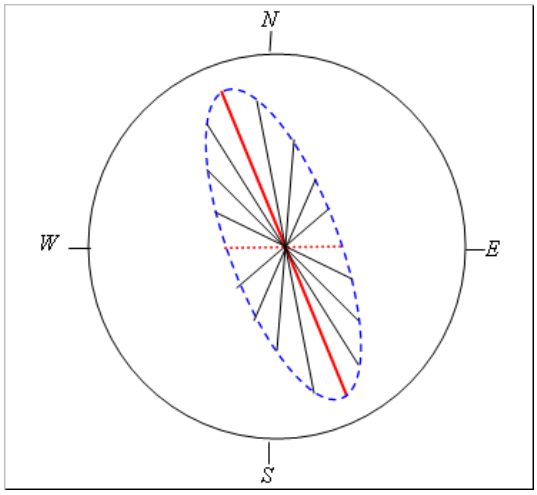

Figure 2-28: The ranges of 9 directional semi-variograms were plotted in their respective directions. An ellipse (——) can be fitted, and highlights the major (–) and the minor (···) geometric anisotropic axes.

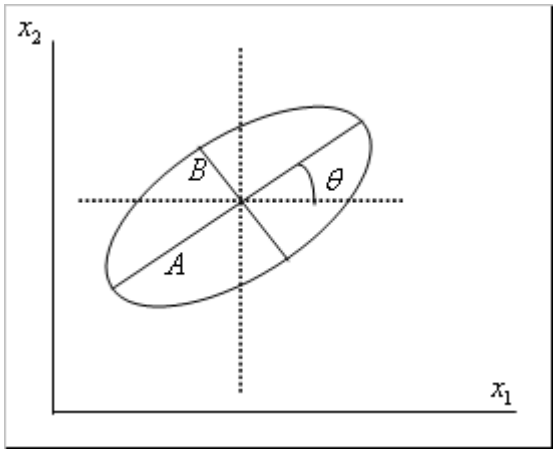

Figure 2-29: A representation of geometric anisotropy. The ellipse describes the ranges of the Spherical variogram in $\Re^2$.

Anisotropy for spatial-temporal models is best explained in terms of zonal anisotropy. Owing to the complexity surrounding the fitting of a spatial-temporal variogram model, anisotropy will be discussed under the heading of permissible models in Chapter 3.

Example 2-16

In this example, the residuals of the simulated dataset $S-COM$ are tested for anisotropy by inspecting the three directions of 0° (horizontal), 90° (vertical) and 45° (diagonally), as investigated in Example 2-10.

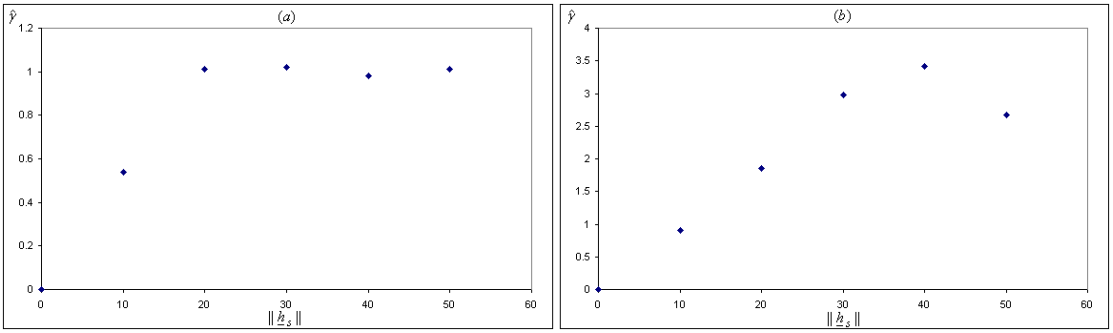

Figure 2-30a: Horizontal de-trended semi-variogram for Z_1 and Z_2.

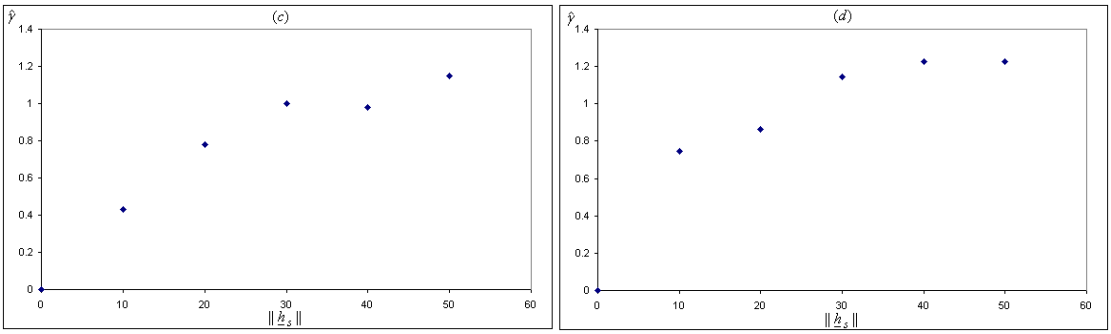

Figure 2-30b: Vertical de-trended semi-variogram for Z_1 and Z_2.

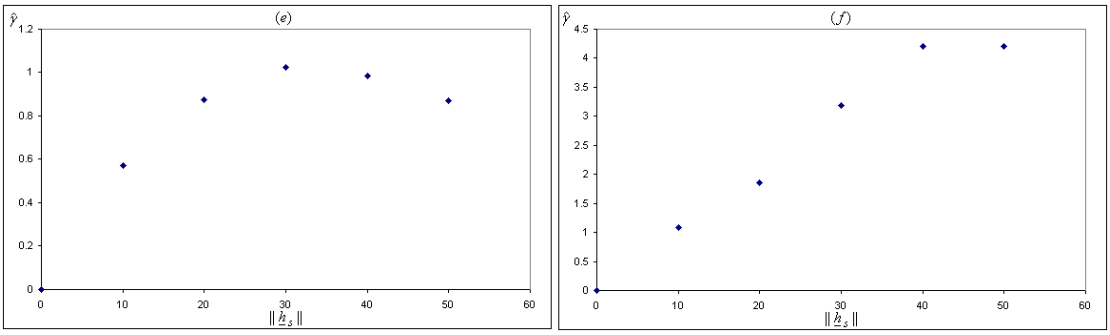

Figure 2-30c: Diagonal de-trended semi-variogram for Z_1 and Z_2.

The variograms depicted in Figures 2-22a to 2-22c indicated that the raw data are anisotropic. The residuals determined in Example 2-15 were used to calculated the

residual semi-variogram estimates and were plotted in Figures 2-30a to 2-30c.

The ranges for Z_1 is $20m$ in the horizontal direction and $30m$ in both the vertical and diagonal directions. The second attribute Z_2 exhibits isotropic behaviour, with ranges of $40m$ in all three directions. The first attribute is assumed to be isotropic since the difference in the ranges is only $10m$. One omnidirectional variogram will be calculated for both Z_1 and Z_2 in Example 2-17. It appears that the anisotropic behaviour is connected to the trend of the data.

Ergodicity

Ergodicity flows from the stationarity assumptions. Along with the constant mean and the assumption of intrinsic stationarity, ergodicity is needed to estimate the semi-variogram. Simply put, if you have a random variable $Z(\underline{u}_\alpha)$ with a constant sample mean of $\overline{Z}$, the hypothesis of ergodicity assumes that $\overline{Z} = E[Z(\underline{u}_\alpha)]$. This allows spatial averages to be used as the expectation in the total space of data and is applicable to the second-order stationary subset (*Cressie, 1991*).

The assumption of ergodicity provides the platform from which the joint probability law of several subsets can be utilized. Prediction equations, based on the estimated covariance and mean squared errors of prediction can proceed on a consistent basis that provides a prediction algorithm with statistically optimal properties.

Spatial-temporal ergodicity is extended for the random variable $Z(\underline{u}_\alpha, t_\tau)$, with a constant sample mean of $\overline{Z}$. Assume that the constant sample mean can be expressed as $\overline{Z} = E[Z(\underline{u}_\alpha, t_\tau)]$. This allows spatial-temporal averages to be used as the expectation in the total spatial-temporal structure and is applicable to the second-order stationary subset. As with spatial ergodicity, spatial-temporal ergodicity provides the platform from which the joint probability law of several subsets can be utilized.

Irregular Spaced Measurements

In practise, measurements are rarely made at exactly equidistant locations similar to the simulated data in this study. If the researcher strictly adheres to the formulae for variogram and covariances, the number of pairs available for computation is minimal.

To overcome these obstacles, tolerances in both distance and direction can be built into the variogram and covariance functions (*Goovaerts, 1997; Isaaks and Srivastava, 1989*). Figure 2-31 represents how a tolerance of $\pm 1m$ in distance and $\pm 20^{\circ}$ in direction is added. Any pair that falls into the shaded area will be included in the calculation of the semi-variogram of $\underline{h}_s = 5m$.

An omnidirectional variogram is defined when the directional tolerance is large enough that the direction becomes unimportant. This variogram provides the researcher with a basis on which he can concentrate when choosing the distance parameters that produce the clearest structure.

The directional variogram is created by calculating the semi-variogram estimates at all the different distances and directions identified by the angle and distance tolerance process. All the estimates are then plotted in a single graph and modelled accordingly.

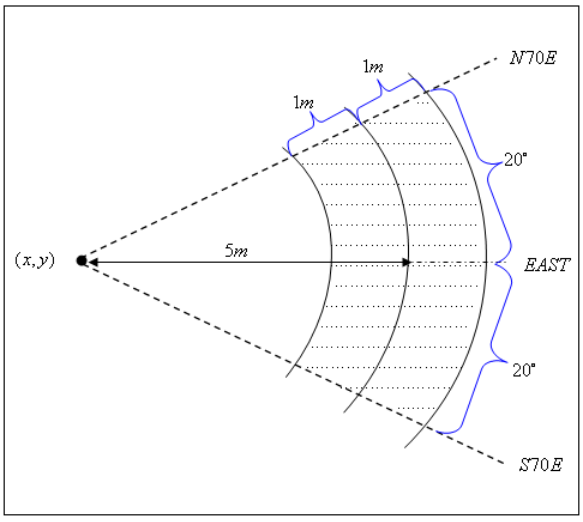

Figure 2-31: Graphical representation of how magnitude and directional tolerance can be included in the semi-variogram model (*Isaaks and Srivastava, 1989*).

Messy omnidirectional variograms can also indicate an underlying structural problem that should be addressed before continuing with the analysis. Once this variogram is well-behaved, investigations in terms of anisotropy can continue.

Example 2-17

Figures 2-32 (a-c) represent the omnidirectional residual semi-variograms for the primary and secondary datasets, as well as the cross of primary with the secondary and *vice versa*. The cross semi-variograms of Z_1Z_2 and Z_2Z_1 are identical, but it appears that the some of the strength of the correlation between the variables were lost in the de-trending of the data. The fact that the cross semi-variogram value at $50m$ does not follow the general trend is attributed to the positive correlation between the primary and secondary attribute as discussed in Example 2-11. Since the data were sampled on a regular grid, no tolerances for distance were built into the semi-variogram estimates.

The code is available in *Appendix B.12*.

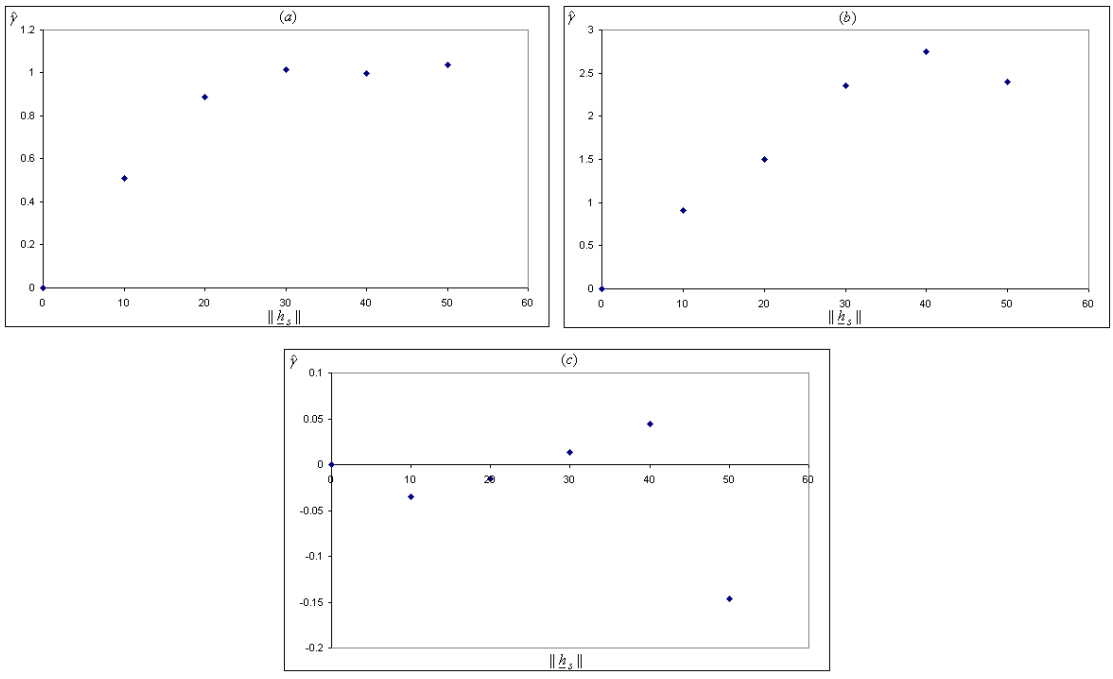

Figure 2-32: Residual omnidirectional spatial semi-variograms for Z_1 in (a), Z_2 in (b), Z_1Z_2 and Z_2Z_1 in (c).

2.7 SOFTWARE AND RESOURCES

Over the years several scientists have developed commercial and open-source programs and graphical user interface (GUI) applications to aid researchers with spatial and spatial-temporal analysis.

The most commonly used open-source software for building variograms and interpolation through kriging are the FORTRAN-based programs, such as the comprehensive GSLIB toolbox (Geostatistical Software Library) and the FORTRAN 77 code, developed by *De Cesare* et al. (*2002*) for univariate spatial-temporal kriging.

Other open-source programs are the DOS-based GEO-EAS (http://igwmc.mines.edu/zipfiles/geo-eas.htm) and the R language programs (https://stat.ethz.ch/pipermail/ r-help/2003-January/028762.html). Gstat (http://www.gstat.org/) was code developed for multivariable geostatistical modelling, prediction and simulation that can interface with other open-source programs, such as R or the S-Plus library.
Well-known commercial statistical software that can be used includes Matlab and SAS. The official toolbox that is available from Matlab was developed by Caroline Lafleur and Yves Gratton from the INRS-Ocanologiea of the Universit du Qubec Rimouski. Another toolbox that also runs in Matlab is EasyKrig, which was developed by Dezhang Chu and is available at ftp://globec.whoi.edu/pub/software/kriging/easy_krig.

GEOSTATS is a GUI application in Matlab developed by Luke Spadavecchia, from the School of Geosciences at the University of Edinburgh. This application caters for the two-dimensional Inverse Distance Weighting function, space-time statistics that utilize the product-sum covariance model and the option of space-time simulation.

SAS procedures which can be used are the VARIOGRAM and KRIG2D procedures. The VARIOGRAM procedure is used to calculate the spatial continuity two-dimensional functions, and KRIG2D performs the spatial ordinary kriging.

Some of the other geostatistical software tools that are available from Rockware, are the ArcGIS Geostatistical Analyst Tool (http://www.rockware.com/product/featureCa

tegories.php?id=193), GS+ (http://www.rockware.com/product/overview.php?Id= 98) and Surfer (http://www.rockware.com/product/featureCategories.php?id=129& parent =592).

Compared with the commercial applications, open-source programs are freely available from the Internet and are used at the researcher's own risk, without any technical support.

For the purposes of this study, existing SAS procedures were used and IML routines were developed to cater for all four options. The code were written to best explain the theory and are not for commercial use.

Websites such as *Matlab newsgroup, Math Forum*, *ai-geostats* and *R-sig-geo* are four of the more commonly used platforms for communications partaining geostatistics between people working in different fields. Questions regarding theory and open-source software can be posted and answered on this platform.
Several academic institutions have research institutions dedicated to the development of theoretical methodologies, focusing specifically on space and time distributions of the earth sciences. In 1968 Georges Matheron, who is known as the founder of geostatistics, established the Centre de Geóstatistique et de Morphologie Mathématique. This centre was integrated into the Centre de Geósciences Mines Paris Tech, which is a "research organization which deals specifically with earth sciences and the environment". Another well-known centre is the GFZ German Research Centre for Geosciences, with the primary goal of research on all aspects of the earth system. The Geostatistics/Geomathematics programme at the University of Stanford consists of several departments dedicated to "the development and statistical validation of numerical models to characterize the distribution in time and space of earth science phenomena". Students at the centre were thanked by C. Deutsch and A. Journel for their insight into the book GSLIB Geostatistical Software Library and User's Guide (*Deutsch and Journel, 1998*).

Since geostatistics is applied to a wide range of study fields, related publications are spread between the leading journals in each of these fields. Two journals primarily referenced are Mathematical Geosciences (formerly Mathematical Geology), which

"publishes original, high-quality, interdisciplinary papers focusing on quantitative methods and studies of the Earth, its natural resources and the environment". This journal is the official, international journal of the International Association for Mathematical Geology (IAMG) and is published on a quarterly basis by Springer Verlag. The second journal is Geoderma by Elsevier and is "a global journal of soil science" which "welcomes interdisciplinary work focussing on dynamic soil processes and their occurrence in space and time".

CHAPTER 3

MOMENT MODELLING

3.1 INTRODUCTION

Chapter 2 provided an overview of the moments that could be utilized to provide additional information on the relationships between data that were measured in space and time.

To proceed to the next level of interpolation and stochastic simulation, an empirical model is fitted to the variogram. Methods of modelling of the spatial moments defined in Section 2.5 are available in textbooks by *Cressie* (*1993*), *Journel and Huijbregts* (*1978*), *Isaaks and Srivastava* (*1989*), *Goovaerts* (*1997*), and the more recent publication of *Webster and Oliver* (*2007*). Articles by *Rodriguez-Iturbe and Meija* (*1974*), *De Cesare* et al. (*1996*), *Dimitrakopoulos and Luo (1993*), *Rouhani and Hall* (*1989*), *Kyriakidis and Journal* (*1999*), *De Cesare* et al. (*2001a, 2001b, 2002*) and *De Iaco* et al. (*2001*) are reference material for the more complicated procedures necessary for modelling the spatial-temporal moments.

The functional form selected is critical in the estimation of the model parameters and the creation of a permissible model. Stationarity, anisotropy and ergodicity, as defined in Section 2.6, play an integral role to ensure that the fitted models faithfully adhere to the underlying data structures. Two additional model conditions required are the semi-positive and conditionally semi-negative definite conditions for the covariance and variograms respectively, as defined in Section 3.2.

Chapter 3 consists of defining the necessary model conditions to ensure best linear unbiased estimators (Section 3.2), permissible spatial models (Section 3.3) and permissible spatial-temporal models (Section 3.4).

3.2 MODEL CONDITION

The principle concern of the model condition is to ensure that the model chosen is permissible (valid). The variogram must adhere to the requirement of conditionally negative semi-definiteness, and the covariance to the positive semi-definite condition.

If the data are stationary, the variogram and the covariance models are interchangeable, as illustrated by the relationship between the variogram and the covariance function (Figure 2-27 and (2.41)). The model fitting procedures, which are primarily discussed in terms of the semi-variogram, can therefore also be followed when working with the covariance function.

Positive Semi-Definite Condition for Covariance Functions

A function can only be used as a covariance model under the second-order stationarity assumption if the function complies with the positive semi-definite condition (*Wackernagel, 1995*). A function is positive semi-definite if the inequality (3.2) holds for any data set of $Z(\underline{u}_1), Z(\underline{u}_2)..., Z(\underline{u}_n)$ where $\underline{\lambda}$ is any vector of weights $(\lambda_1, \lambda_2, ..., \lambda_n)$. The proof is available in the *Appendix A.1*.

$$\sum_{\alpha=1}^{n}\sum_{\alpha'=1}^{n}\lambda_\alpha\lambda_{\alpha'}C(\underline{u}_\alpha - \underline{u}_{\alpha'}) \geq 0 \tag{3.2}$$

Conditional Negative Definite Condition for Variogram Functions

The variogram is defined only under intrinsic stationarity, where the stationarity of the variance is not required. This allows the fitting of variogram models that comply with the conditionally negative definite condition (*Wackernagel, 1995*) of

$$-\sum_{\alpha=1}^{n}\sum_{\alpha'=1}^{n}\lambda_\alpha\lambda_{\alpha'}\gamma(\underline{u}_\alpha - \underline{u}_{\alpha'}) \geq 0 \tag{3.3}$$

for all $\lambda_\alpha(\alpha = 1,2,\cdots,n) \in \Re$ and

$$\sum_{\alpha=1}^{n} \lambda_\alpha = 0 . \tag{3.3a}$$

Under the intrinsic stationarity definition, the covariance function does not exist as the variance isn't restricted to be invariant under translation. The only linear combinations of $Z(\underline{u}_\alpha)$ that have a finite variance, is when the sum of the weights are equal to zero. The derivation of (3.3) is available in *Appendix A.2*.

The easiest method to model a variogram or covariance function is to refer to the graphical representation of the calculated $\gamma(\underline{h}_s)$ or $C(\underline{h}_s)$ values. The stationarity, anisotropy, ergodicity, definite conditions, sill, range and nugget effects should be taken into account when deciding which model to fit to the data.

Spatial-Temporal Model Condition

Similar to the spatial case, the spatial-temporal variogram must adhere to the requirement of conditionally negative semi-definiteness, and the covariance to the positive definite condition (*Wackernagel, 1995; Ma, 2003*).

That is, the chosen covariance model must satisfy

$$\sum_{\alpha=1}^{nT} \sum_{\alpha'=1}^{nT} \lambda_\alpha \lambda_{\alpha'} C(\underline{u}_\alpha - \underline{u}_{\alpha'}, t_\alpha - t_{\alpha'}) \geq 0 \tag{3.4a}$$

where nT represents the total number of spatial-temporal combinations.

The semi-variogram as (*Ma, 2003*)

$$\sum_{\alpha=1}^{nT} \sum_{\alpha'=1}^{nT} \lambda_\alpha \lambda_{\alpha'} \gamma(\underline{u}_\alpha - \underline{u}_{\alpha'}, t_\alpha - t_{\alpha'}) \leq 0 . \tag{3.4b}$$

The proof of (3.4a) and (3.4b) is similar to the proof for (3.2) and (3.3).

3.3 SPATIAL PERMISSIBLE MODELS

In the literature, models are primarily defined for isotropic data (*Cressie, 1993; Goovaerts, 1997; Isaaks and Srivastava, 1989; Webster and Oliver, 2007*). An additional factor (2.46) can be introduced to the isotropic models to accurately describe anisotropic data.

Isotropic Models

Several functional forms (basic semi-variogram models) to model the semi-variogram estimates have been proposed and classified into two distinct groups. The range (q), sill (c_t), partial sill (c_e) and the nugget effect (c_0), as defined in Figure 2-23, are used to define the permissible models. All the models must also be valid for $\Re^d$ where $d \geq 1$, as defined in Section 2.2. Figure 3-1 represents a few of the most commonly used isotropic models defined in Table 3-1 and Table 3-2.

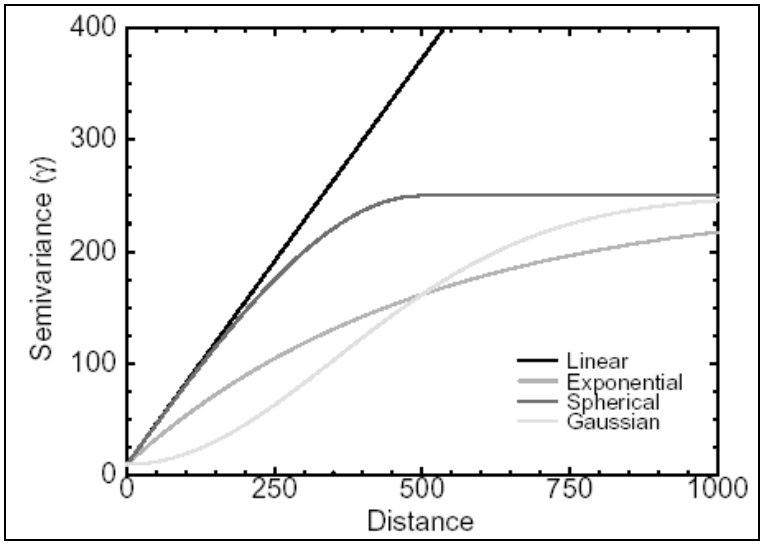

Figure 3-1: Graphical representation of models without nugget effects.

The Exponential (3.5a), Spherical (3.5b), Linear (3.5c) and the Rational quadratic (3.5d) models are examples of bounded models that have a linear behaviour at the origin and a sill c_e. Table 3-1 provides the empirical formulas of these models, as well as the formula of the Gaussian model (3.5e), which exhibits parabolic behaviour at the origin.

The isotropic permissible models are expressed as a function of $\| \underline{h}_s \| = \| \underline{u}_\alpha - \underline{u}_{\alpha'} \|$.

Table 3-1: Bounded isotropic models with a linear behaviour at the origin.

Exponential	$\gamma(\underline{h}_s) = c_0 + \begin{cases} c_e\left[1-\exp\left(-\dfrac{\| \underline{h}_s \|}{q}\right)\right] & \| \underline{h}_s \| \neq 0 \\ 0 & \| \underline{h}_s \| = 0 \end{cases}$	(3.5a)
Spherical Valid for $\Re^d$ where $d \in \{1.2.3\}$	$\gamma(\underline{h}_s) = c_0 + \begin{cases} c_e\left[\dfrac{3\| \underline{h}_s \|}{2q} - 0.5\left(\dfrac{\| \underline{h}_s \|}{q}\right)^3\right] & 0 \leq \| \underline{h}_s \| \leq q \\ c_e & \| \underline{h}_s \| > q \\ 0 & \| \underline{h}_s \| = 0 \end{cases}$	(3.5b)
Linear model that is valid for $b_l \geq 0$	$\gamma(\underline{h}_s) = c_0 + \begin{cases} b_l \| \underline{h}_s \| & 0 \leq \| \underline{h}_s \| \leq q \\ c_e & \| \underline{h}_s \| > q \\ 0 & \| \underline{h}_s \| = 0 \end{cases}$	(3.5c)
Rational quadratic	$\gamma(\underline{h}_s) = c_0 + \begin{cases} c_e\left[\dfrac{\| \underline{h}_s \|}{q}\right] \Big/ \left[1+\left(\dfrac{\| \underline{h}_s \|}{q}\right)^2\right] & \| \underline{h}_s \| \neq 0 \\ 0 & \| \underline{h}_s \| = 0 \end{cases}$	(3.5d)
Gaussian	$\gamma(\underline{h}_s) = c_0 + \begin{cases} c_e\left[1-\exp\left(-\dfrac{\| \underline{h}_s \|^2}{q^2}\right)\right] & \| \underline{h}_s \| > 0 \\ 0 & \| \underline{h}_s \| = 0 \end{cases}$	(3.5e)

The second group of isotropic models that have been developed in the literature are the unbounded models; in other words, models without a sill (Table 3-2). In these cases the random function is intrinsic without a covariance or a finite *a-priori* variance.

Table 3-2: Unbounded isotropic models.

Models in $\|h\|^{\theta}$	$\gamma(\underline{h}_s) = \|\underline{h}_s\|^{\theta}$ with $\theta \in (0,2)$	(3.5f)
Linear	$\gamma(\underline{h}_s) = \omega\|\underline{h}_s\|$ with ω the slope at the origin and $\|\underline{h}_s\| > 0$.	(3.5g)
Logarithmic	$\gamma(\underline{h}_s) = \log(\|\underline{h}_s\|)$	(3.5h)
Power	$\gamma(\underline{h}_s) = \omega\|\underline{h}_s\|^{\beta}$ were $\|\underline{h}_s\| \geq 0;\ 1 < \beta < 2$	(3.5i)

The last group of models is those that exhibit specific properties (Table 3-3). Two examples of these models are the hole-effect and the nugget-effect models. The hole-effect models are non-monotonic increasing that usually displays periodic tendencies. When an apparent discontinuity is visible at the origin, it can be interpreted as a transition structure reaching its sill at c_0 for a very small range. This transition structure is built into the nugget-effect models.

Table 3-3: Special models.

Hole-effect	$\gamma(\underline{h}_s) = \begin{cases} c_e\left\{1 - q\left(\dfrac{\sin(\|\underline{h}_s\|/q)}{\|\underline{h}_s\|}\right)\right\} & \|\underline{h}_s\| > 0 \\ 0 & \|\underline{h}_s\| = 0 \end{cases}$ with h_s in radians.	(3.5j)
Pure nugget-effect	$\gamma(\underline{h}_s) = \begin{cases} 0 & \|\underline{h}_s\| = 0 \\ C & \|\underline{h}_s\| > 0 \end{cases}$	(3.5k)

Figure 3-2 illustrates how certain models fit better to the data than others. Given the $\hat{\gamma}$ estimates, either the Spherical or Exponential model can be fitted. The model selected depends on which model provides the best linear unbiased estimates during the interpolation or simulation process of kriging (Chapters 4 to 7).

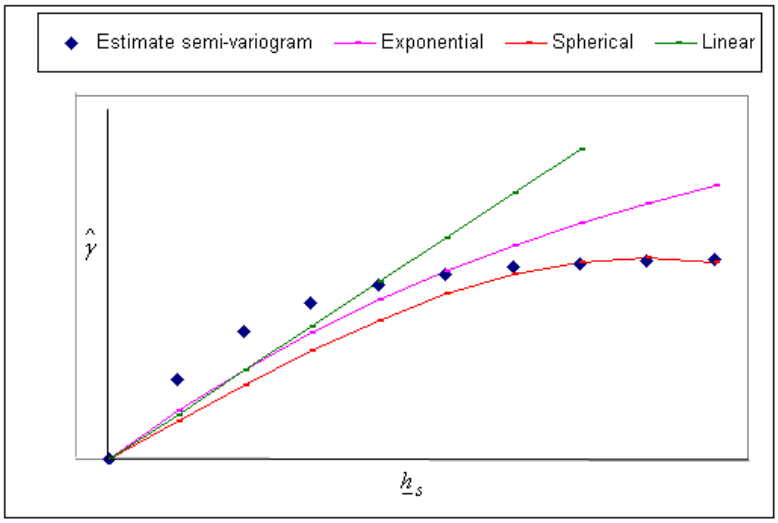

Figure 3-2: Graphical representation of how the Exponential (middle, pink line), Spherical (bottom, red line) and the Linear (top, green line) models were fitted to arbitrary semi-variogram values.

The semi-variogram models defined by (3.5a-k) are developed by means of the covariance functions and equation (2.41). If, for example, the covariance function is defined as

$$C(\underline{h}_s) = c_e \exp\left(-\frac{\| \underline{h}_s \|}{q}\right)$$

and substituted into equation (2.41), the Exponential semi-variogram is defined as

$$\gamma(\underline{h}_s) = c_e\left(1 - \exp\left(-\frac{\| \underline{h}_s \|}{q}\right)\right).$$

This function adheres to the four main requirements ($\gamma(\underline{0}) = 0$, $\gamma(\underline{h}_s) = \gamma(-\underline{h}_s)$, $\gamma(h_s) \geq 0$ and conditional negative semi-definiteness) for a variogram to be permissible.

Model Fitting

The determination of an empirical model to represent the variance or covariance structure of a given dataset, is a critical step in the kriging process. In geostatistics, the visual fitting of a semi-variogram model by trail-and-error is the most commonly used

method; providing the researcher with the freedom to include his/her field-specific knowledge. The disadvantages of this method are that the process can be time consuming, and statistically developed models - that may provide a better fit - is ignored.

The fitting of a model by means of automatic procedures, such as maximum likelihood or least squares methods, is preferred by some statisticians for a number of different reasons: (a) provides statistically sound model-fitting procedures for the selection of parameters and models, (b) provides a more objective modelling procedure where different researchers can obtain the same results, and (c) when numerous variograms are to be modelled on a regular basis (*Pardo-Igúzquiza, 1999; Jian* et al*., 1996*). Complications in automatic modelling include: (a) not all the models selected are permissible, which is required for the unique solution of kriging systems, (b) the sum of numerous permissible models (nested models) can be fitted-creating numerous models to select from, (c) models that are non-linear with respect to the parameters, and (d) correlated errors that may not be normally distributed.

The least squares methods are preferred over the maximum likelihood techniques since these methods rely heavily on the Gaussian distributional assumption, provides biased estimates and calculates the parameters directly from the raw data (*Cressie, 1991, Jian* et al*., 1996*). From the three different weighting schemes in the least squares family (ordinary, weighted and general), the weighted least squares method is more commonly used, as it is an instantaneous, iterative and transparent fitting method that automatically assigns more weight to those lags closer to the interpolation location, as well as smaller weights to lag distances with a smaller number of pairs available for calculation (*Cressie, 1985*).

The recommended method of semi-variogram model fitting is a combination of the visual (initial guess of parameters and possible models) and the automatic fitting (weighted least squares), providing a statistically sound model which can incorporate field-specific knowledge.

Anisotropic models

For the isotropic models defined above, it was assumed that the direction in which the data are distributed was of no significance. When this direction becomes significant, it must be incorporated into the lag vector and semi-variogram estimation.

Geometric anisotropic behaviour, as discussed in Section 2.6, can be incorporated into the empirical formulas defined in (3.5a-k) by replacing the range q with the transformation function $\Omega(\vartheta)$ (2.46) in the basic semi-variogram models (*Webster and Oliver*, *2007*).

For example, if the Spherical model must be adjusted for anisotropy then $\Omega(\vartheta)$ is substituted into the isotropic formula resulting in the anisotropic model

$$\gamma(\underline{h}_s,\vartheta)=\begin{cases} c_e\left[\dfrac{3\|\underline{h}_s\|}{2\Omega(\vartheta)}-0.5\left(\dfrac{\|\underline{h}_s\|}{\Omega(\vartheta)}\right)^3\right] & 0\le\|\underline{h}_s\|\le\Omega(\vartheta) \\ c_e & \|\underline{h}_s\|>\Omega(\vartheta) \\ 0 & \|\underline{h}_s\|<0 \end{cases}$$

Nested models

Real-time measurements can rarely be completely described by the smooth and simplistic models described above. Rather, a mixture of these models (nested) will provide a more realistic model to estimate the variance of differences. The models consist of additional parameters that render them more flexible.

Care should be taken with nested models to ensure that the new model is truly permissible. Linear models of regionalization and co-regionalization (co-kriging), as discussed by *Goovaerts* (*1993*), consist of splitting the random function of the attribute into several uncorrelated random functions. Each of the new random functions has a different variogram of covariance function and is combined into a permissible linear semi-variogram or covariance model (*Wackernagel, 1995*).

Example 3-1

Example 3-1 describes how a model can be fitted to the semi-variograms $(\hat{\gamma})$ derived. All the spatial models will be fitted visually on the omnidirectional semi-variograms of the residuals, as discussed in Example 2-17. This was done due to the small number of data points available for model fitting in this example. It is, however, recommended that a combination of visual and least squares fitting be used with larger datasets.

The forms of the residual omnidirectional semi-variogram are depicted in Figure 3-3. The model fitting was done by hand, using the equations from Table 3-1. Other methods of model fitting include regionalization (*Goovaerts, 1993*). Table 3-4 and Figures 3-4a and 3-4b represent the final models fitted to the semi-variogram.

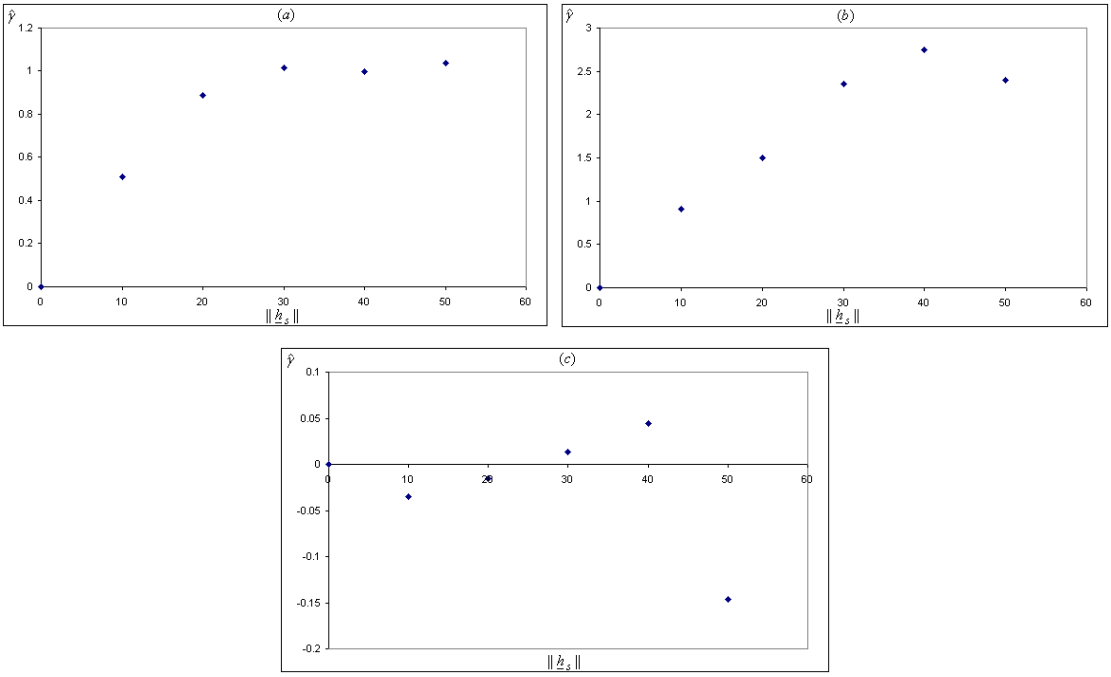

Figure 3-3: Omnidirectional residual semi-variograms for the Z_1 in (a), Z_2 in (b) and $Z_1Z_2 = Z_2Z_1$ in (c).

A nested model was fitted to the cross semi-variogram of Z_1Z_2 and Z_2Z_1 (which are identical) and consists of a Spherical model for lag distances less or equal to $10m$ and a linear model for larger distances. This model was tested and proven to fulfil

condition (3.4b). The last cross semi-variogram estimate was ignored, as it does not correspond to the general trend.

As seen from Figure 3-4b, the Spherical model was fitted to the second attribute. However, because of the definition of model (3.5b), the model does not follow the scatter plot for distances larger than the range. This can have a negative influence on the results of the co-kriging system in Chapter 5 (Example 5-1).

Table 3-4: Fitted omnidirectional semi-variogram models.

	Z_1	Z_2	$Z_1Z_2 = Z_2Z_1$	
Total sill (c_t)	1.00	2.40	0.04	
Partial sill (c_e)	1.00	2.40	0.04	0.002649
Nugget effect (c_0)	0.00	0.00	0.00	-0.06
Range (q)	30	50	10	
Type of model	Spherical	Spherical	Nested: Spherical($q \leq 10$) and Unbounded linear ($q > 10$)	

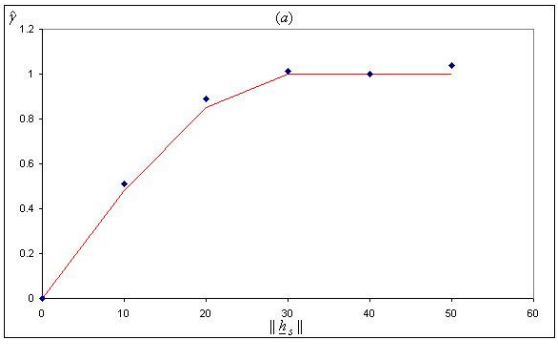

Figure 3-4a: The spherical model was fitted on the omnidirectional residuals for Z_1.

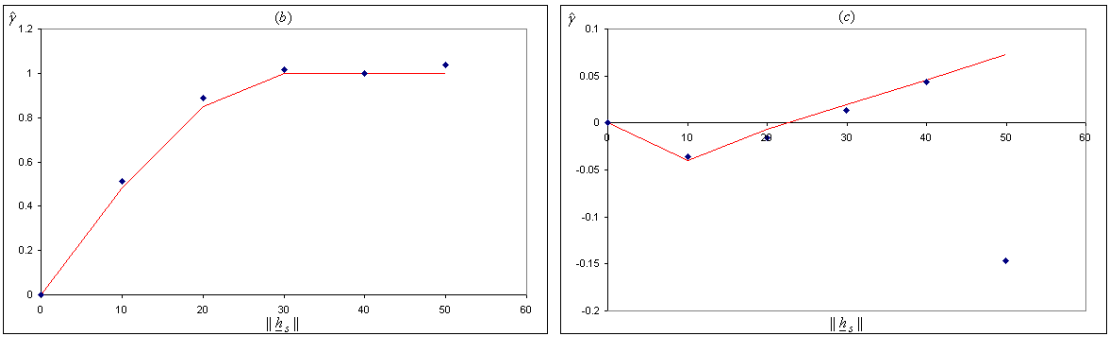

Figure 3-4b: Models fitted on the omnidirectional residuals for Z_2 in (b), Z_1Z_2 and Z_2Z_1 in (c).

The program that develops the semi-variogram estimate is provided in *Appendix B.12*, and the program that proves that the nested mode for the cross semi-variogram fulfils condition (3.4b) is available in *Appendix B.13*.

Notes

- In the case of multivariate interpolation and stochastic modelling, the two additional conditions that co-kriging must satisfy are that permissible models should be available for all the primary and secondary attributes, and that a permissible model exits between the primary and secondary attributes
- The basic variogram models defined in this section can also be fitted to the cross-variogram estimates. Alternatively, the linear model of co-regionalization method can be applied (*Goovaerts, 1993*).

3.4 SPATIAL-TEMPORAL PERMISSIBLE MODELS

Because of the complexity surrounding spatial-temporal data, the spatial models cannot be applied directly to the data. The variogram definition (2.27) and the model conditions give the appearance of straight-forward calculation that is misleading. Theoretical and practical problems exist that must be addressed before a permissible spatial-temporal model can be fitted. The problems are:

a. Qualitative differences between space and time.
b. Possible presence of spatial non-stationarity and temporal periodicity.
c. Spatial and temporal scales that are physically non-comparable.
d. Space-time datasets usually consist of a few spatial locations, each with a long time series.
e. Data must be second-order stationary to fit the existing permissible spatial-temporal models.

Several techniques have been introduced to take these structural problems into account and can be classified into two groups; separable and non-separable models, each with its advantages and disadvantages.

To illustrate existing permissible spatial-temporal models, assume that $Z(\underline{u}_\alpha, t_\tau)$ is a second-order stationary, spatial-temporal random variable with an expected value, covariance and variogram expressed as in (3.6a) to (3.6c) respectively.

$$E\left[Z(\underline{u}_\alpha, t_\tau)\right] = 0 \tag{3.6a}$$

$$C_{st}(\underline{h}_s, h_t) = \text{cov}\left[Z(\underline{u}_\alpha + \underline{h}_s, t_\tau + h_t), Z(\underline{u}_\alpha, t_\tau)\right] \tag{3.6b}$$

$$\gamma_{st}(\underline{h}_s, h_t) = \frac{1}{2}\text{var}\left[Z(\underline{u}_\alpha + \underline{h}_s, t_\tau + h_t) - Z(\underline{u}_\alpha, t_\tau)\right] \tag{3.6c}$$

Because of the second-order stationarity, all three statistics depend on the lag vector $(\underline{h}_s, h_t)$ and not on the location or time point. The covariance function (3.6b) also adheres to the semi-positive definite condition of (3.4a) (*Christakos, 1984*).

Separable Models

Separable models are characterized by the decomposition of the second-order stationary variable into its pure spatial $(C_s(\underline{h}_s))$ and pure temporal $(C_t(h_t))$ components (*Rodriguez-Iturbe and Meija, 1974; De Cesare* et al., *1996*). These components are reassembled in different combinations. The spatial and temporal zonal anisotropic factors are thus respectively included in the pure spatial and pure temporal covariances.

Some of the models introduced are the metric, linear, product and product-sum model.

1. The ***metric model*** (*Dimitrakopoulos and Luo, 1993*)

$$C_{st}(\underline{h}_s, h_t) = C(a^2 \| \underline{h}_s \|^2 + b^2 h_t^2) \tag{3.7}$$

where the coefficients $a, b \in \Re$. The disadvantage of this model is that it is assumed that the spatial and temporal covariance structures are described by the same covariance model. A second disadvantage is that the covariance model is only defined in terms of distance and anisotropic factors. Only the ranges have an influence on the final covariance structure.

2. The ***linear model*** (*Rouhani and Hall, 1989*)

The linear combination of the pure spatial and temporal covariances is referred to as the linear model.

$$C_{st}(\underline{h}_s, h_t) = C_s(\underline{h}_s) + C_t(h_t) \tag{3.8}$$

where

$$C_s(\underline{h}_s) = \text{cov}(Z(\underline{u}_\alpha), Z(\underline{u}_\alpha + \underline{h}_s)) \tag{3.9a}$$

and

$$C_t(h_t) = \text{cov}(Z(t_\tau), Z(t_\tau + h_t)) \tag{3.9b}$$

The linear model is prone to singularity, which hinders optimal prediction (*Myers and Journel, 1990*). If this method is used, additional tests should be performed to ensure that the model yields the required non-singular dataset.

3. The **product model** (*Rodriguez-Iturbe and Mejia, 1974*)

The product-model is defined in terms of the pure spatial (3.9a) and pure temporal (3.9b) covariances as

$$C_{st}(\underline{h}_s, h_t) = \kappa C_s(\underline{h}_s) C_t(h_t) \tag{3.10a}$$

The spatial-temporal variogram $\gamma_{st}(\underline{h}_s, h_t)$ is written in terms of the pure spatial ($\gamma_s(\underline{h}_s)$) and pure temporal ($\gamma_t(h_t)$) semi-variograms as

$$\gamma_{st}(\underline{h}_s, h_t) = \kappa\left[C_t(0)\gamma_s(\underline{h}_s) + C_s(\underline{0})\gamma_t(h_t) - \gamma_s(\underline{h}_s)\gamma_t(h_t)\right] \tag{3.10b}$$

where

- γ_{st} is the spatial-temporal variogram
- γ_t is the temporal variogram
- γ_s is the spatial variogram
- C_t is the temporal covariance
- C_s is the spatial covariance.

The parameter κ is determined as

$$\kappa = \frac{C_{st}(\underline{0},0)}{C_s(\underline{0})C_t(0)} \tag{3.10c}$$

where $C_{st}(\underline{0},0)$ is defined as the spatial-temporal sill. The product spatial-temporal semi-variogram (3.10b) is derived by expanding (2.41) in terms of spatial-temporal, pure spatial and pure temporal components.

$$\gamma_{st}(\underline{h}_s, h_t) = C_{st}(\underline{0},0) - C_{st}(\underline{h}_s, h_t) \tag{3.11a}$$

$$\gamma_s(\underline{h}_s) = C_s(\underline{0}) - C_s(\underline{h}_s) \tag{3.11b}$$

$$\gamma_t(h_t) = C_t(\underline{0}) - C_t(h_t) \tag{3.11c}$$

The metric, linear and product model assume that the spatial and temporal covariance structures always have the same shape. No allowance is made for the possibility that the structures may change over time. Another disadvantage is that no provision is made for interaction between the variability in space and time.

Non-Separable Models

Non-separable models are specifically constructed to take into the account the interaction between the spatial and temporal characteristics of the data. Statistical methods, such as Fourier transform pairs in $\Re^d$ are used (*Cressie and Huang, 1999*). The models are then restricted to a small class of functions for which the closed form solution to the d-variate Fourier integral is known.

The non-separable models proposed by *Cressie and Huang* (*1999*) and *Gneiting* (*2001*) are complex and difficult to implement compared with the separable models. The separable models are, in turn, too simplistic to correctly capture the relationship between the spatial and temporal dependencies. A generalized straight-forward non-separable model was introduced by *De Cesare* et al., (*2001a, 2001b*) and is known as the product-sum model.

The **product-sum model** (*De Cesare* et al., *2001a, 2001b, 2002, De Iaco* et al., *2001*) is the linear combination of arbitrarily complex and interacting covariance structures (including anisotropy) in the space-time structure. This model is considered non-separable (*De Iaco* et al., *2001*) and is most popular since a set of more flexible models are available and an arbitrary space-time metric is not required.

The product-sum model is defined as

$$C_{st}(\underline{h}_s, h_t) = k_1 C_s(\underline{h}_s) C_t(h_t) + k_2 C_s(\underline{h}_s) + k_3 C_t(h_t) \tag{3.12a}$$

or equivalently

$$\gamma_{st}(\underline{h}_s, h_t) = [k_2 + k_1 C_t(0)]\gamma_s(\underline{h}_s) + [k_3 + k_1 C_s(\underline{0})]\gamma_t(h_t) - k_1 \gamma_s(\underline{h}_s)\gamma_t(h_t) \tag{3.12b}$$

where C_s and C_t are the pure spatial and temporal covariance functions and γ_s and γ_t are the pure spatial and temporal semi-variograms. The function $C_{st}(\underline{0},0)$ is the global sill of γ_{st}, $C_s(\underline{0})$ is the sill of γ_s and $C_t(0)$ is the sill of γ_t. By definition

$$\gamma_{st}(\underline{0},0) = \gamma_s(\underline{0}) = \gamma_t(0) = 0 \tag{3.13}$$

is true as the second-order stationarity assumption is sufficient to ensure that the semi-variograms are asymptotically bounded and therefore have sills (*De Cesare* et al., *2001a, 2001b, De Iaco* et al., *2001*). It is sufficient that $k_1 > 0$, $k_2 \geq 0$ and $k_3 \geq 0$ to ensure positive definiteness (*Appendix A.4, Theorem 1*).

It follows that

$$\gamma_{st}(\underline{h}_s, 0) = (k_2 + k_1 C_t(0))\gamma_s(\underline{h}_s) = k_s \gamma_s(\underline{h}_s) \tag{3.13a}$$

and

$$\gamma_{st}(\underline{0}, h_t) = (k_3 + k_1 C_s(\underline{0}))\gamma_t(h_t) = k_t \gamma_t(h_t) \tag{3.13b}$$

where k_s and k_t are respectively perceived as the coefficients of proportionality between the spatial-temporal semi-variograms ($\gamma_{st}(\underline{h}_s,0)$ and $\gamma_{st}(\underline{0},h_t)$) and the pure spatial and pure temporal semi-variogram models (*De Iaco* et al., *2001*). The coefficients are defined as

$$k_s = k_2 + k_1 C_t(0) \tag{3.14a}$$

and

$$k_t = k_3 + k_1 C_s(\underline{0}) \tag{3.14b}$$

The coefficients of k_1, k_2 and k_3 are derived in *Appendix A.3* and are defined as

$$k_1 = \frac{k_s C_s(\underline{0}) + k_t C_t(0) - C_{st}(\underline{0},0)}{C_s(\underline{0}) C_t(0)} \tag{3.15a}$$

$$k_2 = \frac{C_{st}(\underline{0},0) - k_t C_t(0)}{C_s(\underline{0})} \tag{3.15b}$$

$$k_3 = \frac{C_{st}(\underline{0},0) - k_s C_s(\underline{0})}{C_t(0)} \tag{3.15c}$$

If $k_1 > 0$, $k_2 \geq 0$ and $k_3 \geq 0$ (*Theorem1, Corollary 1 and 2 in Appendix A.4*), the positive-definiteness is assured for any class of covariance models as it is related to the sill values.

A single coefficient k can be defined (*Appendix A.3*) by combining (3.13a) and (3.13b), (3.14a) and (3.14b) and the global sill

$$C_{st}(\underline{0},0) = k_1 C_s(\underline{0}) C_t(0) + k_2 C_s(\underline{0}) + k_3 C_t(0) \tag{3.16}$$

as

$$k = \frac{k_1}{k_s k_t} \tag{3.17}$$

The spatial-temporal semi-variogram can be re-defined (*Appendix A.4, Theorem 2*) in terms of the newly defined coefficient k as

$$\gamma_{st}(\underline{h}_s, h_t) = \gamma_{st}(\underline{h}_s,0) + \gamma_{st}(\underline{0}, h_t) - k\gamma_{st}(\underline{h}_s,0)\gamma_{st}(\underline{0}, h_t) \tag{3.18}$$

Some interesting results exhibited by the product-sum model are that the semi-variograms do not have the same sill.

$$\gamma_{st}(\underline{h}_s, h_t) = C_{st}(\underline{0},0) - C_{st}(\underline{h}_s, h_t) \tag{3.19a}$$

$$\gamma_{st}(\underline{h}_s, 0) = C_{st}(\underline{0},0) - C_{st}(\underline{h}_s, 0) \tag{3.19b}$$

$$\gamma_{st}(\underline{0}, h_t) = C_{st}(\underline{0},0) - C_{st}(\underline{0}, h_t) \tag{3.19c}$$

Theorem 2 (*Appendix A.4*) shows that the asymptotic behaviour of $\gamma_{st}(\underline{h}_s, h_t)$, $\gamma_{st}(\underline{h}_s, 0)$ and $\gamma_{st}(\underline{0}, h_t)$ as defined in *Appendix A.3*, does not allow the semi-variograms to reach the same sill. For the practical application of the product-sum model , refer to *De Iaco* et al. (*2001*).

The product-sum model is preferred to the separable and non-separable models because of the simplicity of the calculations and that a measure of the spatial-temporal interaction is included.

De Iaco et al.,. (*2003*) introduced the linear model of co-regionalization for spatial-temporal data. Similar to the linear models of regionalization and co-regionalization, this method is an alternative for fitting permissible models and can be applied to the univariate and multivariate datasets.

The product-sum model will be used to illustrate the model fitting process for the residuals of the simulated dataset ST_COM .

Example 3-2

Example 3-2 follows the process of fitting product-sum spatial-temporal models to the primary, secondary and cross omnidirectional semi-variograms, using (3.12b).

The first step in creating the semi-variogram scatterplots for $\gamma_{st}(\underline{h}_s, 0)$ and $\gamma_{st}(\underline{0}, h_t)$, as depicted in Figure 3.5 and Figure 3-6, is to de-trend the data according to Example

2-14. The isotropic bounded models defined in Table 3-1 were fitted to the semi-variogram scatterplot and the parameters of the selected models are defined in Table 3-5. Figures 3-5 and 3-6 represent the fitted models in Table 3-5. The whole program (excluding the graphs) is available in *Appendix B.14*.

Figures 3-5 to 3-7 were used to determine $k_s C_s(\underline{0})$, $k_t C_t(0)$ and $C_{st}(\underline{0},0)$ respectively, and subsequently the coefficient k (3.17) as provided in Table 3-6.

In this example the parameter values were visually identified and manually adjusted to obtain a relatively good fit. This method was followed due to the small number of data points available for modelling. It is, however, recommended to use the combination of visual and least squares model fitting as described in Section 3.3.

Table 3-5: Chosen bounded isotropic models for $\gamma_{st}(\underline{h}_s,0)$ and $\gamma_{st}(\underline{0},h_t)$.

		c_t	c_e	q	Model
$\gamma_{st}(\underline{h}_s,0)$	Z_1	1.00	1.00	50	Spherical
	Z_2	1.00	1.00	50	Spherical
	$Z_1Z_2 = Z_2Z_1$	-0.20	-0.20	41	Gaussian
$\gamma_{st}(\underline{0},\underline{h}_t)$	Z_1	1.27	1.27	5	Exponential
	Z_2	1.70	1.70	8	Spherical
	$Z_1Z_2 = Z_2Z_1$	-0.17	-0.17	10	Spherical

Table 3-6: Values of $C_{st}(\underline{0},0)$ and the coefficient k.

	Z_1	Z_2	Z_1Z_2	Z_2Z_1
$k_s C_s(\underline{0})$	1.00	1.00	-0.20	-0.20
$k_t C_t(0)$	1.27	1.70	-0.17	-0.17
$C_{st}(\underline{0},0)$	1.32	1.85	-0.37	-0.37
k	0.74	0.50	0.03	0.03

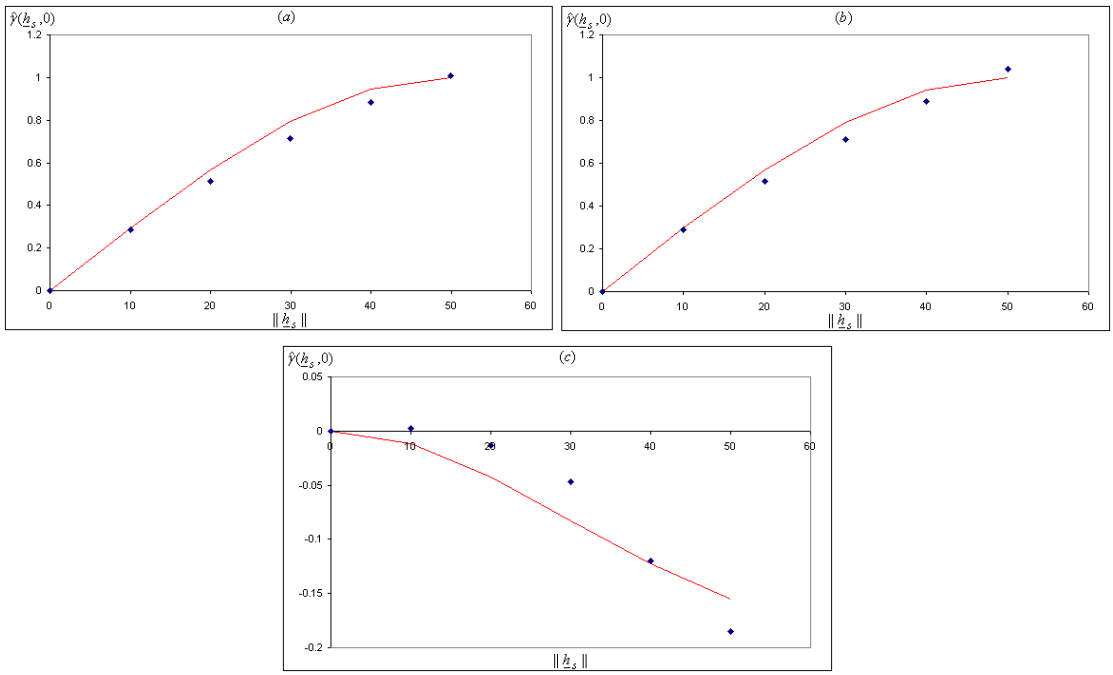

Figure 3-5: Omnidirectional semi-variograms for Z_1 in (a), Z_2 in (b), Z_1Z_2 and Z_2Z_1 in (c) for $\gamma(\underline{h}_s,0)$.

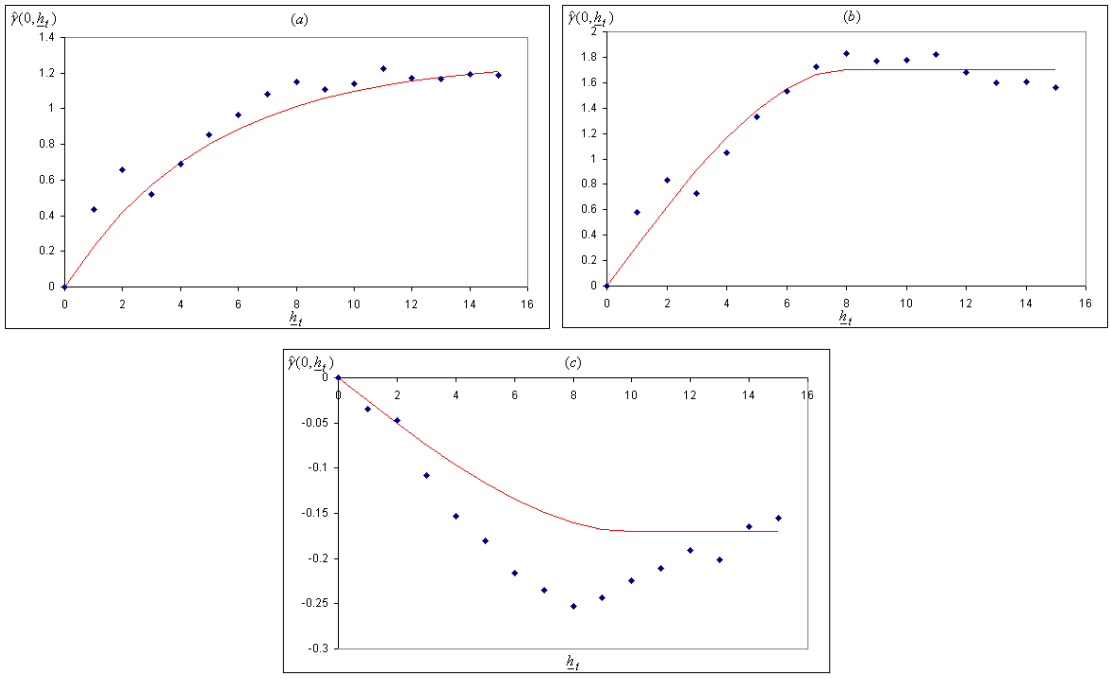

Figure 3-6: Omnidirectional semi-variograms for Z_1 in (a), Z_2 in (b) and Z_1Z_2 and Z_2Z_1 in (c) for $\gamma(\underline{0},h_t)$.

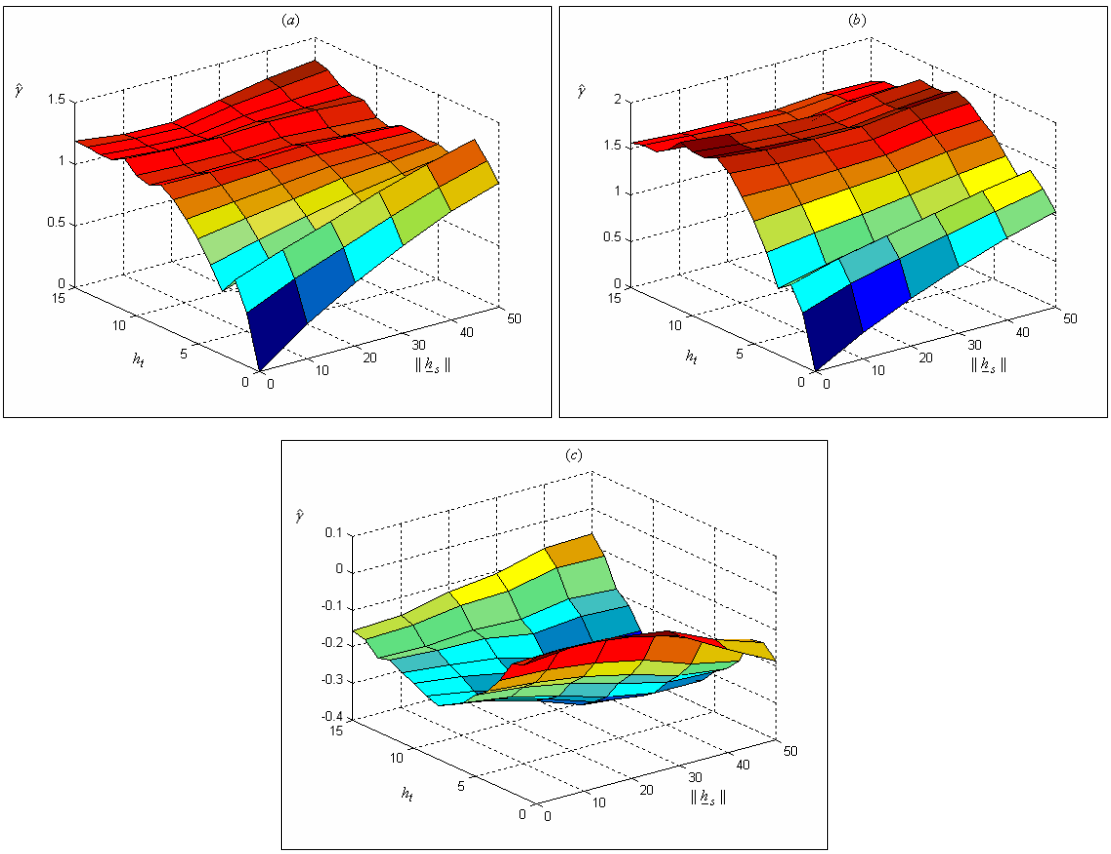

Figure 3-7: Omnidirectional spatial-temporal semi-variograms for Z_1 in (a), Z_2 in (b) and $Z_1 Z_2 = Z_2 Z_1$ (c) for $\gamma(\underline{h}_s, h_t)$.

The final product-sum model as per (3.18) for the primary attribute is

$$\gamma_{1,st}(\underline{h}_s, h_t) = \begin{cases} 1(\frac{3\| \underline{h}_s \|}{100} - 0.5\left(\frac{\| \underline{h}_s \|^3}{125000}\right)) + 1.27(1 - \exp\left(-\frac{h_t}{5}\right)) \\ -0.75(\frac{3\| \underline{h}_s \|}{100} - 0.5\left(\frac{\| \underline{h}_s \|^3}{125000}\right))(1.27(1 - \exp\left(-\frac{h_t}{5}\right)) & \| \underline{h}_s \| \leq 50 \\ 1 + 1.27(1 - \exp\left(-\frac{h_t}{5}\right)) \\ -0.75(1)(1.27(1 - \exp\left(-\frac{h_t}{5}\right)) & \| \underline{h}_s \| > 50 \end{cases}$$

The product-sum model for the secondary attribute assumes four possible options depending on the distance in space and time and is represented as $\gamma_{2,st}(\underline{h}_s, h_t) = (a)$

or (b) or (c) or (d) where

$$(a)\quad \begin{cases} 1(\frac{3\|\underline{h}_s\|}{100}-0.5\left(\frac{\|\underline{h}_s\|^3}{125000}\right))+1.70(\frac{3h_t}{16}-0.5\left(\frac{h_t^{\,3}}{512}\right)) \\ -0.50(\frac{3\|\underline{h}_s\|}{100}-0.5\left(\frac{\|\underline{h}_s\|^3}{125000}\right))*(1.70(\frac{3h_t}{10}-0.5\left(\frac{h_t^{\,3}}{512}\right))) \quad \|\underline{h}_s\|\le 50, h_t \le 5 \end{cases}$$

$$(b)\quad \begin{cases} 1+1.70(\frac{3h_t\|}{10}-0.5\left(\frac{h_t^{\,3}}{512}\right)) \\ -0.50(1)*(1.70(\frac{3h_t}{10}-0.5\left(\frac{h_t^{\,3}}{512}\right))) \quad \|\underline{h}_s\|> 50, h_t \le 5 \end{cases}$$

$$(c)\quad \begin{cases} (\frac{3\|\underline{h}_s\|}{100}-0.5\left(\frac{\|\underline{h}_s\|^3}{125000}\right))+1.7-0.50(\frac{3\|\underline{h}_s\|}{100}-0.5\left(\frac{\|\underline{h}_s\|^3}{125000}\right))*1.7 \\ \|\underline{h}_s\|\le 50, h_t > 5 \end{cases}$$

$$(d)\quad \{1+1.70-0.50(1)*(1.70) \quad \|\underline{h}_s\|> 50, h_t > 5\,.$$

Finally, the product-sum model for the cross semi-variogram is expressed as

$\gamma_{12,st}(\underline{h}_s, h_t) = \gamma_{21,st}(\underline{h}_s, h_t) = (a)$ or (b)

$$(a)\quad \begin{cases} -0.20(1-\exp\left(-\frac{\|\underline{h}_s\|^2}{1681}\right))-0.17(\frac{3h_t}{20}-0.5\left(\frac{h_t^{\,3}}{1000}\right)) \\ -0.03(0.20(1-\exp\left(-\frac{\|\underline{h}_s\|^2}{1681}\right))*(1.70(\frac{3h_t}{10}-0.5\left(\frac{h_t^{\,3}}{512}\right))) \quad h_t \le 10 \end{cases}$$

$$(b)\quad \begin{cases} -0.20(1-\exp\left(-\frac{\|\underline{h}_s\|^2}{1681}\right))-0.17 \\ -0.03(0.20(1-\exp\left(-\frac{\|\underline{h}_s\|^2}{1681}\right))*1.70 \quad h_t > 10 \end{cases}$$

CHAPTER 4

UNIVARIATE SPATIAL INTERPOLATION

The first methodology investigated for pure univariate spatial interpolation (CASE I in Table 2-1) is spatial ordinary kriging $(S-OK)$. This chapter provides background information (Section 4.1) and defines the general ordinary kriging methodology (Section 4.2).

4.1 INTRODUCTION

In geostatistics, kriging is one of the tools that best capitalize on the underlying spatial correlation structure resulting from the distance between neighbouring locations. Kriging can be applied to univariate, as well as multivariate spatial data to estimate measurements at unsampled locations. The underlying mechanism is similar to that of the Inverse Distance Weighting (IDW) function (*Shephard, 1968*) in that data points in closer proximity to missing values will be assigned a larger weight than those of the data points farther away. The main difference between the two techniques is that IDW primarily makes use of the Euclidean distance between the neighbouring locations to determine the weights, whereas kriging uses spatial dependent weights to describe the modelled degree and type of spatial dependence between the neighbouring locations.

The geostatistical algorithms defined as 'kriging' are based on empirical techniques developed by a South African mining engineer, D.G Krige, for the process of determining true ore-grade distributions from sample-based ore grades (*Krige, 1951*)**.** Over the years, several scientists, with the help of previously developed optimal linear prediction techniques, have expanded and refined those formulas into the kriging techniques used today.

The development of spatial statistics through kriging is mainly accredited to Georges Matheron and the "Centre de Géostatistique et de Morphologie Mathématique" established by him. Other key literature sources of kriging techniques are those of

Journel and Huijbregts (*1978*), *Cressie* (*1991*), *Goovaerts* (*1997*), *Clark and Harper* (*2000*), and *Nielsen and Wendroth* (*2003*). *Webster and Oliver* (*2007, p6*) provide a brief history on the development of variance analysis, as early as 1911, into the functional form of kriging used today.

Kriging forms part of the least square error family in that the method minimizes the mean squared error of a continuous model that was fitted to the stochastic spatial variation. The variation is used to generate a set of weighting factors that minimizes the error and provides a best linear unbiased estimate (*BLUE*).

Even though most texts refer to kriging as a non-parametric method, the underlying connection with the least square error family can result in unstable kriging estimates when a serious departure from normality exists in the data (*Webster and Oliver, 2007*). Subsequent inference and interpretation become less reliable. It is therefore recommended that normal or normalized data be used when using kriging for interpolation or simulation of data.

Spatial kriging utilizes the general spatial notation as defined by (2.2). Several different types of kriging methods, based on different model assumptions and available information, are defined and classified into linear and non-linear models. Table 4-1 distinguishes between the linear and non-linear methodologies and provides the core assumptions for each of the kriging techniques defined.

Kriging methodology primarily utilizes the variogram and covariance functions interchangeably. This chapter provides the tools necessary to build a successful kriging system, as defined in Section 4.2. The fitted variogram models from Chapter 3 will be used in the kriging process to create a set of weights that will be used to determine a best linear unbiased estimator (*BLUE*) for the missing values.

Table 4-1: Main kriging methodologies

Group	Type	Assumption
Linear Kriging	Simple	Least complex, but with strict model assumptions. Assumes a known constant trend: $E(Z(\underline{u})) = 0$
	Ordinary	Most robust and commonly used. Assumes a known constant trend: $E(Z(\underline{u})) = \mu$
	Universal	Kriging on a linear model with variable mean. Also known as kriging with external drift.
	Factorial	Useful when several scales of variation exist (nested variation).
	Lognormal	Ordinary kriging of the logarithmic transformations of non-normal and distinctly positively skewed data.
	Co-kriging	Ordinary kriging of data consisting of more than one attribute.
Non-linear Kriging	Indicator	Kriging of binary data.
	Disjunctive	Used in the determination of the likelihood or probability of true values exceeding a specified threshold.
	Probability	Similar to indicator kriging, but utilizes co-kriging methodology.
	Bayesian	Prior drift information used in universal kriging.

4.2 SPATIAL ORDINARY KRIGING $(S-OK)$

Kriging is the inference on missing values widely known as 'optimal prediction' or 'optimal interpolation'. The aim is to provide a solution for the problem of interpolating missing values that is based on a continuous model of the stochastic spatial variation.

Ordinary kriging is the most robust and the most frequently used kriging method. It uses a single attribute, which can be distributed in one, two or three dimensions. The

kriging methodology for this study will be defined in two dimensions by using the stochastic model definitions (2.2) and (2.8a).

Chapters 2 and 3 provided methods to describe the statistical variation of the data by means of descriptive statistics and the modelling of the moments. Kriging incorporates the models of the moments to generate a set of weighting factors that provides a minimum interpolation error (*Journel and Huijbreghts, 1978; Isaaks and Srivastava, 1989; Cressie, 1993*). This set of weighting factors depends on the distance between locations, the spatial dependency between the data and the accuracy of the developed permissible variogram (covariance). A *BLUE* system is achieved when the estimation variance is minimized.

The ordinary kriging methodology is based on the following assumptions:

- Mean is unknown and constant $E(Z(\underline{u})) = \mu(\underline{u}) = \mu$
- Variogram is known
- Covariance is known
- Weights are conditioned to sum to one to ensure unbiased estimators
- Intrinsic stationarity of the data are required.

If these requirements are met the spatial ordinary kriging estimator is given as

$$\hat{Z}(\underline{u}_0) = \sum_{\alpha=1}^{n} \lambda_\alpha Z(\underline{u}_\alpha) \tag{4.1}$$

where

$$\sum_{\alpha=1}^{n} \lambda_\alpha = 1 \tag{4.2}$$

with n as the number of locations sampled. To ensure that (4.1) is a best linear unbiased estimate, the weights λ_α must sum to one (*Appendix A.5*). The spatial ordinary kriging estimate $\hat{Z}(\underline{u}_0)$ is a linear weighted average of all the available measurements.

To ensure that (4.1) is a best linear unbiased estimator the expected error (4.4a) must be equal to zero and the estimation variance (4.4c) must be minimized.

Suppose that the data is second-order stationary. Let the estimation error be

$$\hat{Z}(\underline{u}_0) - Z(\underline{u}_0) \tag{4.3}$$

$\hat{Z}(\underline{u}_0)$ is an unbiased linear estimate if

$$E[\hat{Z}(\underline{u}_0) - Z(\underline{u}_0)] = 0 \tag{4.4a}$$

and

$$\begin{aligned}\sigma^2(\underline{u}_0) &= \text{var}[\hat{Z}(\underline{u}_0) - Z(\underline{u}_0)] \\ &= \text{var}[\hat{Z}(\underline{u}_0)] - 2\,\text{cov}[\hat{Z}(\underline{u}_0), Z(\underline{u}_0)] + \text{var}[Z(\underline{u}_0)] \\ &= \sum_{\alpha=1}^{n}\sum_{\alpha'=1}^{n}\lambda_\alpha\lambda_{\alpha'}C(\underline{u}_\alpha - \underline{u}_{\alpha'}) - 2\sum_{\alpha=1}^{n}\lambda_\alpha C(\underline{u}_\alpha - \underline{u}_0) + C(\underline{u}_0 - \underline{u}_0)\end{aligned} \tag{4.4b}$$

is minimized subjected to (4.2) (*Gilgen, 2006*). The estimation variance is written using the semi-variogram notation by utilizing (2.41)

$$\begin{aligned}\sigma^2(\underline{u}_0) &= \sum_{\alpha=1}^{n}\sum_{\alpha'=1}^{n}\lambda_\alpha\lambda_{\alpha'}[C(\underline{u}_0 - \underline{u}_0) - \gamma(\underline{u}_\alpha - \underline{u}_{\alpha'})] \\ &\quad - 2\sum_{\alpha=1}^{n}\lambda_\alpha[C(\underline{u}_0 - \underline{u}_0) - \gamma(\underline{u}_\alpha - \underline{u}_0)] + C(\underline{u}_0 - \underline{u}_0) \\ &= -\sum_{\alpha=1}^{n}\sum_{\alpha'=1}^{n}\lambda_\alpha\lambda_{\alpha'}\gamma(\underline{u}_\alpha - \underline{u}_{\alpha'}) + 2\sum_{\alpha=1}^{n}\lambda_\alpha\gamma(\underline{u}_\alpha - \underline{u}_0)\end{aligned} \tag{4.4c}$$

To minimize (4.4c) for the model (4.1), the weights are subjected to the condition (4.2), hold true for the variogram as defined in (2.15) and utilize Lagrange multipliers (*Appendix A.6*). At the location $\underline{u}_0$, the variance to be minimized is

$$E\left[\sum_{\alpha=1}^{n}\lambda_\alpha Z(\underline{u}_\alpha) - Z(\underline{u}_0)\right]^2 - 2\varphi\left[\sum_{\alpha=1}^{n}\lambda_\alpha - 1\right] \tag{4.5}$$

where φ is the Lagrange multiplier to ensure the condition (4.2) is met and results in

$$-\sum_{\alpha=1}^{n}\sum_{\alpha'=1}^{n}\lambda_{\alpha}\lambda_{\alpha'}\gamma(\underline{u}_{\alpha}-\underline{u}_{\alpha'})+2\sum_{\alpha=1}^{n}\lambda_{\alpha}\gamma(\underline{u}_{0}-\underline{u}_{\alpha})-2\varphi\left(\sum_{\alpha=1}^{n}\lambda_{\alpha}-1\right). \tag{4.6}$$

To adhere to the minimizing condition, (4.6) is differentiated with regard to λ_{α} and φ, and set equal to zero. This yields (4.7)

$$-\sum_{\alpha'=1}^{n}\lambda_{\alpha'}\gamma(\underline{u}_{\alpha}-\underline{u}_{\alpha'})+\gamma(\underline{u}_{0}-\underline{u}_{\alpha})-\varphi=0 \tag{4.7}$$

The spatial ordinary kriging system (*Goovaerts, 1997*) in terms of the variogram is expressed from (4.7) as

$$\begin{cases}\sum_{\alpha'=1}^{n}\lambda_{\alpha'}\gamma(\underline{u}_{\alpha}-\underline{u}_{\alpha'})-\varphi=\gamma(\underline{u}_{\alpha}-\underline{u}_{0}) & \alpha=1,2,\cdots n\\ \sum_{\alpha'=1}^{n}\lambda_{\alpha'}=1\end{cases} \tag{4.8}$$

The weights $\lambda_{\alpha'}$ are substituted back into equation (4.1) and the spatial ordinary kriging estimate for location $\underline{u}_{0}$ is calculated.

Equation (4.8) can be rewritten into the matrix format

$$\begin{bmatrix}\gamma_{11} & \cdots & \gamma_{1n} & 1\\ \cdots & \cdots & \cdots & 1\\ \gamma_{n1} & \cdots & \gamma_{nn} & 1\\ 1 & 1 & 1 & 0\end{bmatrix}\cdot\begin{bmatrix}\lambda_{1}\\ \cdots\\ \lambda_{n}\\ \varphi\end{bmatrix}=\begin{bmatrix}\gamma_{01}\\ \cdots\\ \gamma_{0n}\\ 1\end{bmatrix} \tag{4.9}$$

where γ_{ij} is the semi-variogram between the i^{th} and j^{th} locations, or as

$$\underline{\Gamma}\underline{\lambda}=\underline{\gamma}_{0}. \tag{4.10}$$

The weighting vector is then solved by

$$\underline{\lambda} = \underline{\Gamma}^{-1}\underline{\gamma}_0 .$$

This can be expanded to

$$\underline{\lambda} = \left(\underline{\gamma}_0 + \underline{1}\frac{(1 - \underline{1}\underline{\Gamma}^{-1}\underline{\gamma}_0}{\underline{1}\underline{\Gamma}^{-1}\underline{\gamma}_0} \right)' \underline{\Gamma}^{-1} \tag{4.10a}$$

and

$$\varphi = -\frac{\left(1 - \underline{1}\underline{\Gamma}^{-1}\underline{\gamma}_0\right)}{\underline{1}\underline{\Gamma}^{-1}\underline{1}'} . \tag{4.10b}$$

Results (4.10a) and (4.10b) were obtained by means of matrix partitioning of (4.10) into the following blocks.

$$\begin{bmatrix} \underline{\Gamma} & \underline{1} \\ \underline{1}' & 0 \end{bmatrix} \begin{bmatrix} \underline{\lambda} \\ \varphi \end{bmatrix} = \begin{bmatrix} \underline{\gamma}_0 \\ 1 \end{bmatrix} . \tag{4.11}$$

The $S-OK$ system can also be expressed in terms of the covariance. Since the variogram and covariance are interchangeable, only intrinsic stationarity is required. The relationship between the variogram and the covariance (2.41) is used for this purpose.

The $S-OK$ system of (4.8), expressed in terms of covariances (*Goovaerts, 1997*) becomes

$$\begin{cases} \sum_{\alpha'=1}^{n} \lambda_{\alpha'} C(\underline{u}_\alpha - \underline{u}_{\alpha'}) + \varphi = C(\underline{u}_\alpha - \underline{u}_0) \qquad \alpha = 1,2,\cdots n \\ \sum_{\alpha'=1}^{n} \lambda_{\alpha'} = 1 \end{cases} . \tag{4.12}$$

The only difference between (4.8) and (4.12) is the use of the covariance functions, as well as the change in the sign of the Lagrange multiplier (*Goovaerts, 1997*).

The $S-OK$ system can also be written in terms of the correlation (correlogram) by utilizing the relationship between the covariance and the correlogram. The spatial ordinary kriging system expressed in terms of the correlogram is defined in (4.13). The choice of which system to use in terms of the variogram, covariance and correlogram depends on the researcher and which of the tools best describes the data.

$$\begin{cases} \sum_{\alpha'=1}^{n} \lambda_{\alpha'} \rho(\underline{u}_{\alpha} - \underline{u}_{\alpha'}) + \varphi = \rho(\underline{u}_{\alpha} - \underline{u}_{0}) \qquad \alpha = 1,2,\cdots n \\ \sum_{\alpha'=1}^{n} \lambda_{\alpha'} = 1 \end{cases} \tag{4.13}$$

Kriging can utilize the concept of predefined neighbourhoods that are selected based on the number of locations, as well as the distance of the locations from the target location similar to *IDW* (*Shepard, 1968*). This is especially useful in cases where the data are stationary only for certain neighbourhoods, but not for the whole dataset. Neighbourhood kriging is ordinary kriging where a specific neighbourhood is identified for which the variogram and kriging systems are established (*Switzer, 2002*).

In Section 2.6, the non-stationary data were split into trend and stationary residuals in order to comply with the stationary assumption needed for unbiased estimation. Kriging applied to residuals is called 'residual kriging' (*Goovaerts, 1997*).
The original data series is replaced with the residual values in each of the kriging equations discussed in the preceding sections without any loss of generality. The final interpolated value will then be the sum of the trend and the estimated residual by adapting equation (4.1).

$$\hat{Z}(\underline{u}_0) = m(\underline{u}) + \sum_{\alpha=1}^{n} \lambda_{\alpha} R(\underline{u}_{\alpha}) \tag{4.14}$$

One disadvantage of residual kriging is that the residuals are dependent on the identified trend and can therefore introduce additional bias to the data. Kriging with a trend model can also be investigated to identify the best predictor since the trend is included in the kriging system constraints (*Goovaerts, 1997, p143*).

Example 4-1

Example 4-1 is based on the dataset $S-COM$ used in Chapters 2 and 3. De-trended data from Example 2-15 and the subsequent omnidirectional semi-variograms defined in Example 2-17 and Example 3-1 will be used to illustrate the $S-OK$.

In order to illustrate the interpolation power of $S-OK$, 15 locations (15%) were randomly selected using the SURVEYSELECT procedure in SAS. The locations selected are provided in Table 4-2.

Table 4-2: Randomly selected missing locations.

$\underline{u}_{11}$=(20,10)	$\underline{u}_{14}$=(20,40)	$\underline{u}_{17}$=(20,70)	$\underline{u}_{18}$=(20,80)	$\underline{u}_{22}$=(30,20)
$\underline{u}_{23}$=(30,30)	$\underline{u}_{25}$=(30,50)	$\underline{u}_{36}$=(40,60)	$\underline{u}_{38}$=(40,80)	$\underline{u}_{59}$=(60,90)
$\underline{u}_{60}$=(60,100)	$\underline{u}_{69}$=(70,90)	$\underline{u}_{80}$=(80,100)	$\underline{u}_{90}$=(90,100)	$\underline{u}_{100}$=(100,100)

The identified locations are removed from the primary data in the complete de-trended dataset to create the set $MDS-COM$. This dataset will be used for the kriging system.

The residual omnidirectional semi-variogram model for the semi-variogram of Z_1, defined in Example 3-1 is

$$\gamma(\underline{h}_s)=(\frac{3\|\underline{h}_s\|}{60}-0.5\left(\frac{\|\underline{h}_s\|^3}{27000}\right))$$

In practice, this model will be estimated from the incomplete dataset.The next step is to determine the equations for the $S-OK$ system that ensure unbiased weights, and to interpolate the missing values in the primary dataset.

The interpolate value for location $\underline{u}_{11}$ can be expressed by using (4.14) and (4.2) as $\hat{Z}(\underline{u}_{11})=m(\underline{u})+\sum_{\alpha=1}^{85}\lambda_\alpha R(\underline{u}_\alpha)$ and $\sum_{\alpha=1}^{85}\lambda_\alpha=1$ respectively. The $S-OK$ system (4.9) is expanded as follows for the missing location

$$\sum_{\alpha'=1}^{85} \lambda_{\alpha'} \gamma(\underline{u}_{\alpha} - \underline{u}_{\alpha'}) - \varphi = \gamma(\underline{u}_{\alpha} - \underline{u}_{11}) \quad \forall \quad \alpha = 1,..85 .$$

An example of the expansion where $\alpha = 1$ is given as

$$\sum_{\alpha'=1}^{85} \lambda_{\alpha'} \gamma(\underline{u}_{1} - \underline{u}_{\alpha'}) - \varphi = \gamma(\underline{u}_{1} - \underline{u}_{11})$$

(1) $\lambda_1 \gamma(\underline{u}_1 - \underline{u}_1) + \lambda_2 \gamma(\underline{u}_1 - \underline{u}_2) + ... + \lambda_{85} \gamma(\underline{u}_1 - \underline{u}_{85}) - \varphi = \gamma(\underline{u}_1 - \underline{u}_{11})$

An equation as above is created for each of the 85 sampled locations.

(2) $\lambda_1 \gamma(\underline{u}_2 - \underline{u}_1) + \lambda_2 \gamma(\underline{u}_2 - \underline{u}_2) + ... + \lambda_{85} \gamma(\underline{u}_2 - \underline{u}_{85}) - \varphi = \gamma(\underline{u}_2 - \underline{u}_{11})$

(3) $\lambda_1 \gamma(\underline{u}_3 - \underline{u}_1) + \lambda_2 \gamma(\underline{u}_3 - \underline{u}_2) + ... + \lambda_{85} \gamma(\underline{u}_3 - \underline{u}_{85}) - \varphi = \gamma(\underline{u}_3 - \underline{u}_{11})$

… …

(85) $\lambda_1 \gamma(\underline{u}_{85} - \underline{u}_1) + \lambda_2 \gamma(\underline{u}_{85} - \underline{u}_2) + ... + \lambda_{85} \gamma(\underline{u}_1 - \underline{u}_{85}) - \varphi = \gamma(\underline{u}_{85} - \underline{u}_{11})$

(86) $\lambda_1 + \lambda_2 + ... + \lambda_{85} = 1$

These equations can be solved simultaneously to determine $\lambda_1, \lambda_2, ..., \lambda_{85}$ and φ, using (4.10a) and (4.10b). It is important to note that for each measurement that must be interpolated, a new set of weights and Lagrange multipliers must be calculated. The weights are also only calculated for those locations were there are no missing measurements.

The interpolated values, as well as the estimation variance (4.4c) for the missing primary measurements at the locations defined above are provided in Table 4-3. The difference between the original and interpolated measurements highlights the fact that bias is introduced bacause of a semi-variogram model that does not fit perfectly due to random and undefined random variation. The interpolated value is also affected by the number of neighboring locations that are also missing. The introduced bias is also reflected in the large estimation variance.

The researcher can decide at this point that he or she is comfortable with the results, or try to determine a different variogram that could perform better. The SAS code is

available in *Appendix B.15*.

Table 4-3: Interpolated measurements.

Location	**Original** Z_1	**Univariate estimate** Z_1	**Univariate** $\hat{\sigma}^2(\underline{u}_0)$
$\underline{u}_{11}$=(20,10)	99.24	99.09	0.45
$\underline{u}_{14}$=(20,40)	100.65	100.77	0.39
$\underline{u}_{17}$=(20,70)	102.20	102.22	0.43
$\underline{u}_{18}$=(20,80)	102.69	102.18	0.43
$\underline{u}_{22}$=(30,20)	101.02	101.27	0.42
$\underline{u}_{23}$=(30,30)	101.24	101.15	0.41
$\underline{u}_{25}$=(30,50)	101.90	101.64	0.38
$\underline{u}_{36}$=(40,60)	103.08	102.80	0.38
$\underline{u}_{38}$=(40,80)	101.65	101.85	0.38
$\underline{u}_{59}$=(60,90)	102.63	102.18	0.46
$\underline{u}_{60}$=(60,100)	101.54	102.49	0.49
$\underline{u}_{69}$=(70,90)	104.02	103.40	0.43
$\underline{u}_{80}$=(80,100)	104.10	103.09	0.54
$\underline{u}_{90}$=(90,100)	103.33	102.96	0.65
$\underline{u}_{100}$=(100,100)	103.82	102.60	0.67

CHAPTER 5

MULTIVARIATE SPATIAL INTERPOLATION

Chapter 4 provided a detailed discussion on how to interpolate spatially correlated data when measurements from only one attribute are available. An alternative method is the multivariate form of spatial co-kriging (CASE II in Table 2.1). Chapter 5 presents the background and the methodology used for the interpolation of multivariate spatially correlated data.

5.1 INTRODUCTION

Co-kriging originated from mining applications (*Cressie, 1993; Journel and Huijbregts, 1978*) and has since been utilized in soil sciences, biogeography, climatology and general environmental studies. The co-kriging methodology assumes that available attributes are correlated. The tools that incorporate the correlation structure between the different attributes into the spatial variation are the cross-variogram and cross-covariance functions (Section 2.5).

Matheron (*1971*), *Journel and Huijbreghts* (*1978*), *Myers* (*1984*), as well as *Aboufirassi and Marino* (*1984*) introduced the basic theory of co-kriging. Data sets very often contain the primary attribute under investigation, as well as additional information in the form of secondary attributes. These attributes can be spatially correlated to a certain degree and could possibly aid the interpolation or simulation of the primary attribute. Intuitively, it seems that the cross-correlated information between the primary and secondary attributes should help to improve the estimate and reduce the estimation error. Co-kriging was developed to derive estimates that exploit any possible correlated relationships.

The usefulness of secondary attributes in co-kriging depends on the completeness of the primary attribute and the strength of the correlation between the attributes. More emphasis is placed on additional secondary information if the percentage of missing

measurements in the primary attribute is very high compared with the percentage of missing measurements of the secondary attributes.

A good example, given in *Cressie* (*1991*), is mineral exploration to determine the feasibility of opening a copper mine. Ore samples are taken at $\underline{u}_1, \underline{u}_2, ..., \underline{u}_n$ locations and assessed. These samples contain certain percentages of copper, lead, zinc and negligible trace amounts of other minerals. In this example, copper is the primary attribute and the lead and zinc the secondary attributes. The spatial intra- and cross-correlation between the copper, lead and zinc can be used in co-kriging to interpolate any possible missing copper measurements.

Co-kriging incorporates more information and must adhere to stricter model assumptions to ensure a minimized interpolation error. The researcher must therefore prove that the correlation between the attributes exists and is strong enough to warrant this calculation-intensive method.

5.2 SPATIAL ORDINARY CO-KRIGING ($S-OCK$)

Co-kriging can be seen as a powerful extension of ordinary kriging. The system must satisfy the same constraints (minimization of the estimation error, providing an unbiased estimator that is true to the measurements) along with the additional constraints of permissible variogram (covariance) and cross-variogram (cross-covariance) models as stated in Sections 2.5 and 2.6, as well as Chapter 3. For the remaining part of the study, ordinary co-kriging will be referred to as co-kriging.

Similar to the spatial ordinary kriging predictor, the co-kriging predictor for $Z_1(\underline{u}_0)$ is defined as a linear combination of all the available attributes at all the measured location points. The estimator is defined, based on the variable set (2.3) and the interpolation function (2.8b), when the primary and secondary means are assumed to be constant.

The estimator for the primary attribute (*Journel and Huijbreghts, 1978; Isaaks and Srivastava, 1989; Goovaerts, 1997*) at position $\underline{u}_0$ is

$$\hat{Z}_1(\underline{u}_0) = \sum_{k=1}^{K} \sum_{\alpha=1}^{n} \lambda_{k\alpha} Z_k(\underline{u}_\alpha). \tag{5.1}$$

Equation (5.1) can be adjusted for the case where the secondary attributes were not measured at the same locations as the primary attribute as

$$\hat{Z}_1(\underline{u}_0) = \sum_{k=1}^{K} \sum_{\alpha_k=1}^{n_k} \lambda_{k\alpha_k} Z_k(\underline{u}_{\alpha_k})$$

where α_k and n_k represent the measured location of the k^{th} attribute, and the total number of locations measured for the k^{th} attribute. The value $\lambda_{k\alpha_k}$ represents the weighting coefficient for the k^{th} attribute at the location of k^{th} attribute.

For a dataset that consists of two attributes the interpolation value is defined as

$$\begin{aligned} \hat{Z}_1(\underline{u}_0) &= \sum_{k=1}^{2} \sum_{\alpha_k=1}^{n_k} \lambda_{k\alpha_k} Z_k(\underline{u}_{\alpha_k}) \\ &= \sum_{\alpha_1=1}^{n_1} \lambda_{1\alpha_1} Z_1(\underline{u}_{\alpha_1}) + \sum_{\alpha_2=1}^{n_2} \lambda_{2\alpha_2} Z_2(\underline{u}_{\alpha_2}) \end{aligned} \tag{5.1a}$$

The necessary and sufficient coefficients needed to ensure that the linear predictor is unbiased are

$$\sum_{\alpha_k=1}^{n_k} \lambda_{1\alpha_k} = 1 \text{ for } k = 1 \tag{5.2a}$$

for the primary attribute and

$$\sum_{\alpha_k=1}^{n_k} \lambda_{k\alpha_k} = 0 \text{ for } k = 2,3,\cdots K. \tag{5.2b}$$

for the secondary attributes. The constraints in (5.2a) and (5.2b) are enforced to prevent weights that can lead to unexpected results and minimal secondary influence from the secondary attributes.

The reason for the constraints defined in (5.2a) and (5.2b) can be illustrated by means of the primary and a single secondary attribute. The expected value of (5.1a) yields the equation

$$\begin{aligned} E[\hat{Z}(\underline{u}_0)] &= E\left[\sum_{\alpha_1=1}^{n_1}\lambda_{1\alpha_1}Z_1(\underline{u}_{\alpha_1}) + \sum_{\alpha_2=1}^{n_2}\lambda_{2\alpha_2}Z_2(\underline{u}_{\alpha_2})\right] \\ &= \sum_{\alpha_1=1}^{n_1}\lambda_{1\alpha_1}E[Z_1(\underline{u}_{\alpha_1})] + \sum_{\alpha_2=1}^{n_2}\lambda_{2\alpha_2}E[Z_2(\underline{u}_{\alpha_2})] \end{aligned} \tag{5.3}$$

Equation (5.3) illustrates that to ensure an unbiased estimator for the primary attribute, the sum of the weights must equal one (5.2a) and the sum of the weights for the secondary attributes must equal zero (5.2b).

The best linear unbiased estimator is then determined by minimizing the estimation variance

$$E\left(Z_1(\underline{u}_0) - \sum_{k=1}^{K}\sum_{\alpha_k=1}^{n_k}\lambda_{k\alpha_k}Z_k(\underline{u}_{\alpha_k})\right)^2 \tag{5.4}$$

which is subjected to (5.2a) and (5.2b). This spatial co-kriging variance (minimum mean squared prediction error) can be extended, without assuming stationarity, to

$$\sigma_k^2(\underline{u}_0) = C_{11}(0,0) - \sum_{k=1}^{K}\sum_{\alpha_k=1}^{n_k}\lambda_{k\alpha_k}C_{1k}(\underline{u}_0,\underline{u}_{\alpha_k}). \tag{5.5}$$

where $C_{1k}(\underline{u}_0,\underline{u}_{a_k})$ is the covariance of the primary attribute and the k^{th} attribute. Note that the problem is similar to the spatial ordinary kriging methodology, except that the additional constraint of (5.2b) requires that more Lagrange multipliers $(\varphi_1,\varphi_2,\cdots,\varphi_K)$ be included in the co-kriging system.

The spatial ordinary co-kriging system, expanded in terms of covariance matrices, is shown in (5.6). Linear algebra is used to solve the $\sum n_k + 2$ equations and $\sum n_k + 2$ variables defined by the system in (5.6) (*Journel and Huijbreghts, 1978; Isaaks and Srivastava, 1989; Goovaerts, 1997*).

$$\begin{cases} \sum_{k=1}^{K}\sum_{\alpha_k=1}^{n_k}\lambda_{k\alpha_k}C_{k'k}(\underline{u}_{\alpha_k},\underline{u}_{\alpha_{k'}})+\varphi_{k'}=C_{1k'}(\underline{u}_0,\underline{u}_{\alpha_{k'}}) & \alpha_{k'}=1,2,\cdots,n_{k'};k'=1,2,\cdots,K \\ \sum_{\alpha_k=1}^{n_k}\lambda_{1\alpha_k}=1 & k=1 \\ \sum_{\alpha_k=1}^{n_k}\lambda_{k\alpha_k}=0 & k=2,3,\cdots K \end{cases} \tag{5.6}$$

To obtain a better understanding of the equations, we look at the case where there is only two attributes $(K=2)$ (*Goovaerts, 1997*).

$$\begin{cases} \sum_{\alpha_1=1}^{n_1}\lambda_{1\alpha_1}C_{11}(\underline{u}_{\alpha_1},\underline{u}_{\alpha_1'})+\sum_{\alpha_2=1}^{n_2}\lambda_{2\alpha_2}C_{12}(\underline{u}_{\alpha_2},\underline{u}_{\alpha_2'})+\varphi_1=C_{11}(\underline{u}_{\alpha_1},\underline{u}_{\alpha_1'}) \\ \sum_{\alpha_1=1}^{n_1}\lambda_{1\alpha_1}C_{21}(\underline{u}_{\alpha_1},\underline{u}_{\alpha_1'})+\sum_{\alpha_2=1}^{n_2}\lambda_{2\alpha_2}C_{22}(\underline{u}_{\alpha_2},\underline{u}_{\alpha_2'})+\varphi_2=C_{12}(\underline{u}_{\alpha_2},\underline{u}_{\alpha'_2}) \\ \sum_{\alpha_1=1}^{n_1}\lambda_{1\alpha_1}=1 \\ \sum_{\alpha_2=1}^{n_2}\lambda_{k\alpha_2}=0 \quad k=2,3,\cdots K \end{cases} \tag{5.6a}$$

If the series adheres to the second-order stationarity assumption then

$$C_{kk'}(\underline{u}_\alpha-\underline{u}_{\alpha'})=\mathrm{cov}(Z_k(\underline{u}_\alpha),Z_{k'}(\underline{u}_{\alpha'})) \tag{5.7}$$

can be re-written as defined in (2.39b).

Equation (5.6) can also be written in terms of the cross-variograms (*Webster and Oliver, 2007*)

$$\begin{cases} \sum_{k=1}^{K}\sum_{\alpha_k=1}^{n_k}\lambda_{k\alpha_k}\gamma_{k'k}(\underline{u}_{\alpha_k}-\underline{u}_{\alpha_{k'}})-\varphi_{k'}=\gamma_{1k'}(\underline{u}_0-\underline{u}_{\alpha_{k'}}) & \alpha_{k'}=1,2,\cdots,n_k \quad k'=1,2,\cdots,K \\ \sum_{\alpha_k=1}^{n_k}\lambda_{1\alpha_k}=1 & k=1 \\ \sum_{\alpha_k=1}^{n_k}\lambda_{k\alpha_k}=0 & k=2,3,\cdots K \end{cases} \tag{5.8}$$

In most instances, the true mean is unknown, intrinsic stationarity is implied and (5.8) is the most commonly used system (*Cressie, 1993*).

The matrix notation for the above equations can be written as

$$G\underline{\lambda}=\underline{b} \tag{5.9}$$

where G, $\underline{\lambda}$ and $\underline{b}$ are defined as

$$G=\begin{bmatrix} \Gamma_{\alpha_1\alpha_1} & \Gamma_{\alpha_1\alpha_2} & \underline{1}_i & \underline{0}_i \\ \Gamma_{\alpha_2\alpha_1} & \Gamma_{\alpha_2\alpha_2} & \underline{0}_j & \underline{1}_j \\ (\underline{1}_i)' & (\underline{0}_j)' & 0 & 0 \\ (\underline{0}_i)' & (\underline{1}_j)' & 0 & 0 \end{bmatrix} \tag{5.10a}$$

$$\underline{\lambda}'=[\underline{\lambda}_1 \quad \underline{\lambda}_2 \quad \varphi_{\alpha_1} \quad \varphi_{\alpha_2}] \tag{5.10b}$$

$$\underline{b}'=[\underline{b}_{\alpha_1\alpha_1} \quad \underline{b}_{\alpha_1\alpha_2} \quad 1 \quad 0] \tag{5.10c}$$

Γ_{ij}, $\underline{\lambda}_k$ and $\underline{b}_{\alpha_k\alpha_{k'}}$ is defined respectively as

$$\Gamma_{\alpha_k\alpha_{k'}}=\begin{bmatrix} \gamma_{\alpha_k\alpha_{k'}}(\underline{u}_{\alpha_1}-\underline{u}_{\alpha_1}) & \gamma_{\alpha_k\alpha_{k'}}(\underline{u}_{\alpha_1}-\underline{u}_{\alpha_2}) & \cdots & \gamma_{\alpha_k\alpha_{k'}}(\underline{u}_{\alpha_1}-\underline{u}_{\alpha_{n_2}}) \\ \gamma_{\alpha_k\alpha_{k'}}(\underline{u}_{\alpha_2}-\underline{u}_{\alpha_1}) & \gamma_{\alpha_k\alpha_{k'}}(\underline{u}_{\alpha_2}-\underline{u}_{\alpha_2}) & \cdots & \gamma_{\alpha_k\alpha_{k'}}(\underline{u}_{\alpha_2}-\underline{u}_{\alpha_{n_2}}) \\ \vdots & \vdots & \cdots & \vdots \\ \gamma_{\alpha_k\alpha_{k'}}(\underline{u}_{\alpha_{n_1}}-\underline{u}_{\alpha_1}) & \gamma_{\alpha_k\alpha_{k'}}(\underline{u}_{\alpha_{n_1}}-\underline{u}_{\alpha_2}) & \cdots & \gamma_{\alpha_k\alpha_{k'}}(\underline{u}_{\alpha_{n_1}}-\underline{u}_{\alpha_{n_2}}) \end{bmatrix} \tag{5.10d}$$

$$\underline{\lambda}'_{\alpha_k}=[\lambda_{k\alpha_1} \quad \lambda_{k\alpha_2} \quad \ldots \quad \lambda_{k\alpha_{n_1}}] \tag{5.10e}$$

$$\underline{b}'_{\alpha_k\alpha_{k'}} = [\gamma_{\alpha_k\alpha_{k'}}(\underline{u}_{\alpha_1} - \underline{u}_{\alpha_0}) \quad \gamma_{\alpha_k\alpha_{k'}}(\underline{u}_{\alpha_2} - \underline{u}_{\alpha_0}) \quad \cdots \quad \gamma_{\alpha_k\alpha_{k'}}(\underline{u}_{\alpha_{n_2}} - \underline{u}_{\alpha_0})] \tag{5.10f}$$

The weights can then be solved by

$$\underline{\lambda} = G^{-1}\underline{b}. \tag{5.11}$$

The estimation variance (5.5) can also be written in matrix format as

$$\sigma_k^2(\underline{u}_0) = \underline{b}'\underline{\lambda}. \tag{5.12}$$

Co-kriging can also be performed in terms of residuals (similar to Section 4.2) by de-trending each data series for the different attributes.

Example 5-1

The objective of Example 5-1 is to demonstrate how the $S-OCK$ system is practically applied.

From Example 2-1 it is known that a negative correlation of 0.39 exists between the primary and secondary attributes.

The four residual omnidirectional semi-variograms fitted in Example 3-1 were used.

$$\gamma_{z_1}(\underline{h}_s) = \begin{cases} 1\left(\frac{3\|\underline{h}_s\|}{60} - 0.5\left(\frac{\|\underline{h}_s\|^3}{27000}\right. & \|\underline{h}_s\| \le 30 \\ 1 & \|\underline{h}_s\| > 30 \end{cases}$$

$$\gamma_{z_2}(\underline{h}_s) = \begin{cases} 2.6\left(\frac{3\|\underline{h}_s\|}{100} - 0.5\left(\frac{\|\underline{h}_s\|^3}{125000}\right. & \|\underline{h}_s\| \le 50 \\ 2.6 & \|\underline{h}_s\| > 50 \end{cases}$$

$$\gamma_{z_1z_2}(\underline{h}_s) = \gamma_{z_2z_1}(\underline{h}_s) \begin{cases} 0.04\left(\frac{3\|\underline{h}_s\|}{20} - 0.5\left(\frac{\|\underline{h}_s\|^3}{1000}\right. & \|\underline{h}_s\| \le 10 \\ -0.06 + 0.002649\|\underline{h}_s\| & \|\underline{h}_s\| > 10 \end{cases}$$

The interpolated value will be determined using (5.1a) where $n_1 = 85$ and $n_2 = 100$. The weights and Lagrange multipliers are determined by using (5.11) with the respective matrices defined as

$$G = \begin{bmatrix} \underset{(85\times85)}{\Gamma_{11}} & \underset{(85\times100)}{\Gamma_{12}} & \underset{(85\times1)}{\underline{1}} & \underset{(85\times1)}{\underline{0}} \\ \underset{(100\times85)}{\Gamma_{21}} & \underset{(100\times100)}{\Gamma_{22}} & \underset{(100\times1)}{\underline{0}} & \underset{(100\times1)}{\underline{1}'} \\ \underset{(1\times85)}{\underline{1}'} & \underset{(1\times100)}{\underline{0}'} & 0 & 0 \\ \underset{(1\times85)}{\underline{0}'} & \underset{(1\times100)}{\underline{1}'} & 0 & 0 \end{bmatrix}, \quad \underline{b} = \begin{bmatrix} \underset{(85\times1)}{\underline{b}_{11}} \\ \underset{(100\times1)}{\underline{b}_{12}} \\ 1 \\ 0 \end{bmatrix} \text{ and } \underline{\lambda} = \begin{bmatrix} \underset{(85\times1)}{\underline{\lambda}_1} \\ \underset{(100\times1)}{\underline{\lambda}_2} \\ \varphi_1 \\ \varphi_2 \end{bmatrix}$$

Table 5-1 provides the original measurements compared with the interpolated values. Compared with the interpolated measurements from Example 4-1, this particular co-kriging does not present substantially better estimates.

Table 5-1: Interpolated measurements

Location	**Original** Z_1	**Univariate Estimate** Z_1	**Univariate** $\hat{\sigma}^2(\underline{u}_0)$	**Bivariate Estimate** Z_1	**Bivariate** $\hat{\sigma}^2(\underline{u}_0)$
$\underline{u}_{11}$=(20,10)	99.24	99.09	0.45	99.28	0.45
$\underline{u}_{14}$=(20,40)	100.65	100.77	0.39	100.66	0.38
$\underline{u}_{17}$=(20,70)	102.20	102.22	0.43	102.16	0.42
$\underline{u}_{18}$=(20,80)	102.69	102.18	0.43	102.17	0.42
$\underline{u}_{22}$=(30,20)	101.02	101.27	0.42	101.35	0.41
$\underline{u}_{23}$=(30,30)	101.24	101.15	0.41	101.20	0.41
$\underline{u}_{25}$=(30,50)	101.90	101.64	0.38	101.56	0.38
$\underline{u}_{36}$=(40,60)	103.08	102.80	0.38	102.96	0.37
$\underline{u}_{38}$=(40,80)	101.65	101.85	0.38	101.83	0.37
$\underline{u}_{59}$=(60,90)	102.63	102.18	0.46	101.99	0.46
$\underline{u}_{60}$=(60,100)	101.54	102.49	0.49	102.48	0.48
$\underline{u}_{69}$=(70,90)	104.02	103.40	0.43	103.39	0.42
$\underline{u}_{80}$=(80,100)	104.10	103.09	0.54	102.89	0.54
$\underline{u}_{90}$=(90,100)	103.33	102.96	0.65	102.50	0.65
$\underline{u}_{100}$=(100,100)	103.82	102.60	0.67	102.14	0.68

Co-kriging did not increase the predictability of the estimates for this particular case study. The $S-OK$ will be preferred to $S-OCK$, since the same results are obtained with less computational effort.

The SAS code is available in *Appendix B.16*.

CHAPTER 6

UNIVARIATE SPATIAL-TEMPORAL INTERPOLATION

Chapters 4 and 5 described two interpolation techniques that utilize only the spatial correlation between the sampled locations. Chapter 6 follows the same structure as the previous two, beginning with background information, as well as a discussion on the methodology where temporal correlation is introduced to the ordinary kriging structure (CASE III from Table 2-1).

6.1 INTRODUCTION

Over the years, geostatistical spatial-temporal models have been developed and applied to spatial-temporal distributions, and specific stochastic spatial-temporal and smooth interpolated functions have been developed for attribute maps. *Kyriakidis and Journel* (*1999*) provide a detailed discussion and references of these models.

Standard time series models assume that the data were sampled over a regular time grid and that the temporal lag operator (h_t) is utilized to model the difference between the current and previous measurements along this specific time axis (*Weyl, 1952; Reichenbach, 1958; Journel, 1986; Kyriakidis and Journel, 1999*). This time lag operator, however, cannot easily be generalized to a spatial domain, which is very often sampled over an irregular grid. A spatial dependence factor can therefore not be included (*Cressie, 1993, p450*). Specific spatial time series models can be applied but is only relevant for a specific location.

Geostatistics provides a tool to analyze the space and time dependences simultaneously and is based on the spatial kriging techniques that were developed independently in the fields of geology, forestry and meteorology. Chapters 4 and 5 provide detailed discussions of types of spatial interpolation, namely spatial ordinary kriging ($S-OK$) and spatial ordinary co-kriging ($S-OCK$).

Both these methods proved to be effective interpolation and prediction tools, but it became apparent that certain fields of study measurements over time cannot be adequately described by spatial correlations only. Several fields of study consist of measurements made over time at different locations and where historical events can play a significant role. An example of this is deforestation that could alter rainfall patterns. Examples of fields of study where the dynamic processes involve spatial and temporal correlation are the environmental sciences, climate prediction, meteorology, hydrology and reservoir engineering.

The spatial-temporal variable set and interpolation function defined in Section 2.2 by (2.6), (2.7), (2.8c) and (2.8d) allows the researcher to view the data in terms of the $D \times T$ space-time framework. As previously indicated (Section 2.2), there is a fundamental difference between the spatial and the time co-ordinate axes. The spatial axis is characterized by the state of co-existence, often containing several dimensions and directions. The order of the data plays no significant role. The temporal axis is, however, characterized as a state of successive existence where the non-reversible ordering of data into past, present and future measurements in one dimension, is of great significance (*Weyl, 1952; Reichenbach, 1958; Journel, 1986; Kyriakidis and Journel, 1999*).

Section 6.2 will combine the spatial-temporal moments (Section 2.5) and their modelling structure, defined in Section 3.4, with the kriging systems, defined in Chapter 4, to create a spatial-temporal kriging system that adheres to the *BLUE* conditions of kriging.

6.2 SPATIAL-TEMPORAL KRIGING ($ST - OK$)

After a permissible variogram has been fitted to the data, the interpolation or simulation by means of spatial-temporal kriging can be executed. The kriging system and equations are, by definition, an extension of the spatial ordinary kriging system.

The underlying methodology of spatial-temporal kriging is the same as that of spatial ordinary kriging. All the assumptions and model restrictions for spatial ordinary

kriging are therefore also applicable to the spatial-temporal model. The kriging system equations in Section 4.2 are adjusted to compensate for the temporal dependency.

For notational purposes, assume that the spatial-temporal random variable $Z(\underline{u}_\alpha, t_\tau)$ is stationary. The measurement to be interpolated at a specific location and time is defined in (2.8c).

The spatial-temporal ordinary kriging estimator is given as

$$\hat{Z}(\underline{u}_0, t_0) = \sum_{\tau=1}^{T} \sum_{\alpha=1}^{n} \lambda_{\alpha\tau} Z(\underline{u}_\alpha, t_\tau) \tag{6.1}$$

where T and n represent the number of time instances and the number of spatial locations respectively (*Rouhani and Wackernagel, 1990; Kyriakidis and Journel, 1999*). As with spatial kriging, the estimator is subjected to the constraint

$$\sum_{\tau=1}^{T} \sum_{\alpha=1}^{n} \lambda_{\alpha\tau} = 1. \tag{6.2}$$

If, for example, there are three locations $(n=3)$ with four time $(T=4)$ points, then equation (6.1) will reduce to

$$\begin{aligned}\hat{Z}(\underline{u}_0, t_0) = {} & \lambda_{11} z(\underline{u}_1, t_1) + \lambda_{12} z(\underline{u}_1, t_2) + \lambda_{13} z(\underline{u}_1, t_3) + \lambda_{14} z(\underline{u}_1, t_4) + \\ & \lambda_{21} z(\underline{u}_2, t_1) + \lambda_{22} z(\underline{u}_2, t_2) + \lambda_{23} z(\underline{u}_2, t_3) + \lambda_{24} z(\underline{u}_1, t_4) + \\ & \lambda_{31} z(\underline{u}_3, t_1) + \lambda_{32} z(\underline{u}_3, t_2) + \lambda_{33} z(\underline{u}_3, t_3) + \lambda_{34} z(\underline{u}_3, t_4).\end{aligned}$$

The covariance (variogram) is therefore taken into account at each location and each time point. The $ST-OK$ system will be expressed only in terms of the covariance function for illustration purposes.

To ensure that (6.1) is a best linear unbiased estimate (*BLUE*), the weights $\lambda_{\alpha\tau}$ must sum to one (6.2). The expected error (6.3) must be equal to zero and the estimation variance (6.4) must be minimized (*Christakos and Hristopulos, 1998; Lui and Koike, 2007*).

$$E[\hat{Z}(\underline{u}_0,t_0)-Z(\underline{u}_0,t_0)]=0 \tag{6.3}$$

$$\begin{aligned}\sigma^2(\underline{u}_0,t_0) &= E\left[\left\{\hat{Z}(\underline{u}_0,t_0)-Z(\underline{u}_0,t_0)\right\}^2\right] \\ &= C_{11}(\underline{u}_\alpha-\underline{u}_{\alpha'},t_\tau-t_{\tau'})+\sum_{\tau=1}^{T}\sum_{\alpha=1}^{n}\lambda_{\alpha\tau}\sum_{\tau'=1}^{T}\sum_{\alpha'=1}^{n}\lambda_{\alpha'\tau'}C(\underline{u}_\alpha-\underline{u}_{\alpha'},t_\tau-t_{\tau'}) \\ &\quad -2\sum_{\tau=1}^{T}\sum_{\alpha=1}^{n}\lambda_{\alpha\tau}C(\underline{u}_\alpha-\underline{u}_{\alpha'},t_\tau-t_{\tau'})\end{aligned} \tag{6.4}$$

Similar to Section 4.2, the *BLUE* conditions are adhered to if the spatial-temporal kriging system is expressed as

$$\begin{cases}\displaystyle\sum_{\tau=1}^{T}\sum_{\alpha'=1}^{n}\lambda_{\alpha'\tau'}C(\underline{u}_{\alpha_k}-\underline{u}_{\alpha_{k'}};t_\tau-t_{\tau'})+\varphi=C(\underline{u}_0-\underline{u}_{\alpha_k};t_0-t_{\tau'}) \\ \qquad\qquad \alpha=1,2,\cdots n \quad \tau=1,2,\cdots T \\ \displaystyle\sum_{\tau=1}^{T}\sum_{\alpha'=1}^{n}\lambda_{\alpha_{k'}\tau'}=1\end{cases} \tag{6.5}$$

and is known as the spatial-temporal kriging system.

The matrix of the spatial-temporal kriging system can, under intrinsic stationarity, be expressed in terms of the semi-variograms (*Christakos and Hristopulos, 1998; Lui and Koike, 2007*).

The spatial-temporal ordinary kriging system is defined under the assumption that the spatial-temporal random variable $Z(\underline{u}_\alpha,t_\tau)$ is stationary. However, in almost all studies that involve time as a parameter, a trend or seasonal component can be identified that renders the stationarity assumption invalid. As discussed in Section 2.6 and (4.14), this problem is circumvented by removing the trend and utilizing the residual kriging methodology.

Example 6-1

In Example 6-1, the spatial-temporal ordinary kriging system was tested on variable Z_1 from a randomly selected subset of $ST-COM$. Similar to Example 4-1, 15% of the 3000 observations were randomly selected with the SAS procedure SURVEYSELECT and are considered to be missing. A sample of the 450 space-time locations will be provided in this example to demonstrate the efficiency of the investigated kriging system.

Table 6-1: Sample of 20 out of the 450 randomly selected space-time locations ($\underline{ut}$)

$\underline{ut}_{777}$=[(30,60),27]	$\underline{ut}_{779}$=[(30,60),29]	$\underline{ut}_{780}$=[(30,60),30]	$\underline{ut}_{782}$=[(30,70),2]
$\underline{ut}_{783}$=[(30,70),3]	$\underline{ut}_{1328}$=[(50,50),8]	$\underline{ut}_{1330}$=[(50,50),10]	$\underline{ut}_{1331}$=[(50,50),11]
$\underline{ut}_{1332}$=[(50,50),12]	$\underline{ut}_{1333}$=[(50,50),13]	$\underline{ut}_{1973}$=[(70,60),23]	$\underline{ut}_{1974}$=[(70,60)24,]
$\underline{ut}_{1975}$=[(70,60),25]	$\underline{ut}_{1976}$=[(70,60),26]	$\underline{ut}_{1980}$=[(70,60),30]	$\underline{ut}_{1986}$=[(70,70),6]
$\underline{ut}_{1988}$=[(70,70),8]	$\underline{ut}_{1989}$=[(70,70),9]	$\underline{ut}_{1991}$=[(70,70),11]	$\underline{ut}_{1993}$=[(70,70),13]

The residual product-sum spatial-temporal model $\gamma_{1,st}(\underline{h}_s, h_t)$ as per Example 3-2 is used.

The spatial-temporal kriging system can be expanded in a similar way, as explained in Example 4-1, but for the purpose of this example the unbiased weights and Lagrange multipliers were calculated using matrix multiplication.

Table 6-2 provides the original and interpolated measurements along with the estimation variance. The interpolated values are very close to the original measurements, which are reflected in the small variance. All 450 interpolated measurements follow the same trend as the sample. The SAS code is available in *Appendix B.17*.

Table 6-2: Interpolated values of the sample of missing locations

Location	**Original** Z_1	**Univariate estimate** Z_1	**Univariate** $\hat{\sigma}^2(\underline{u}_0)$
$\underline{ut}_{777}$=[(30,60),27]	100.63	99.91	0.10
$\underline{ut}_{779}$=[(30,60),29]	100.67	101.63	0.11
$\underline{ut}_{780}$=[(30,60),30]	101.11	100.31	0.07
$\underline{ut}_{782}$=[(30,70),2]	99.33	99.99	0.09
$\underline{ut}_{783}$=[(30,70),3]	99.32	98.08	0.07
$\underline{ut}_{1328}$=[(50,50),8]	105.84	105.55	0.05
$\underline{ut}_{1330}$=[(50,50),10]	97.44	97.27	0.06
$\underline{ut}_{1331}$=[(50,50),11]	100.90	100.68	0.05
$\underline{ut}_{1332}$=[(50,50),12]	99.98	100.81	0.06
$\underline{ut}_{1333}$=[(50,50),13]	100.34	100.86	0.07
$\underline{ut}_{1973}$=[(70,60),23]	102.60	101.20	0.09
$\underline{ut}_{1974}$=[(70,60)24,]	102.87	102.54	0.06
$\underline{ut}_{1975}$=[(70,60),25]	101.46	100.63	0.05
$\underline{ut}_{1976}$=[(70,60),26]	100.42	99.16	0.05
$\underline{ut}_{1980}$=[(70,60),30]	99.41	99.10	0.05
$\underline{ut}_{1986}$=[(70,70),6]	99.05	98.55	0.05
$\underline{ut}_{1988}$=[(70,70),8]	105.88	105.51	0.05
$\underline{ut}_{1989}$=[(70,70),9]	99.68	100.16	0.05
$\underline{ut}_{1991}$=[(70,70),11]	99.03	98.85	0.05
$\underline{ut}_{1993}$=[(70,70),13]	97.63	98.09	0.05

CHAPTER 7

MULTIVARIATE SPATIAL-TEMPORAL INTERPOLATION

The last interpolation technique discussed in this study is the spatial-temporal co-kriging model (CASE IV from Table 2-1). The model defined in this chapter combines the spatial-temporal structure with co-kriging, which is the multivariate ordinary kriging system. The formulas and kriging systems from Chapter 6 will be expanded to incorporate dependent secondary attributes.

7.1 INTRODUCTION

As discussed in Chapter 6, various studies consist of spatial-temporal correlated data that are observed at several locations over a specific time period. In Chapter 7 the univariate spatial-temporal model is extended to the multivariate form to increase the predictability of the kriging estimator by including additional spatial-temporal information.

The first attempt to construct spatial-temporal multivariate kriging systems can be found in *Rouhani and Wackernagel* (*1990*), where attention was given to long time series data collected at a few spatial locations. *Goovaerts and Sonnet* (*1993*) considered data as realizations of regionalized variables (set of observed $\underline{Z}$) at each observed time instance. This was followed by *Christakos and Hristopulos* (*1998*) that introduced a vectorial spatial-temporal random field, and *Kyriakidis and Journel* (*1999*) who provided a detailed discussion on spatial-temporal data, with some reference to spatial-temporal simple co-kriging.

In 2002, *De Iaco* et al. (*2002*) used principal component analysis to determine a space-time function for total air pollution index through the dual from of kriging (radial basis functions). *De Iaco* et al. (*2005*) extends the existing multivariate geostatistical techniques to incorporate both the spatial and temporal information. The

paper also points out that the generalized product-sum model (3.12a and 3.12b) can be utilized and provides more flexibility to the kriging system.

For the modelling of the spatial-temporal multivariate moments, the separable and non-separable models discussed in Section 3.4 can also be applied to the spatial-temporal cross-variograms and cross-covariances. The product-sum model (3.12a) and (3.12b) complements the spatial-temporal co-kriging system, since the temporal dependency is automatically incorporated into the variogram (covariance) and cross-variogram (cross-covariance).

7.2 SPATIAL-TEMPORAL ORDINARY CO-KRIGING $(ST-OCK)$

For illustration purposes, it is assumed that the second-order stationary variable is defined according to (2.7). As in Chapters 4 to 6, an unbiased estimator (*Rouhani and Hall, 1989; Rouhani and Wackernagel, 1990*; *Kyriakidis and Journel, 1999*; *Christakos and Hristopulos, 1998; De Iaco* et al., *2005; Lui and Koike, 2007*) of the primary attribute at location $\underline{u}_0$ and time point t_0 that minimizes the variance is defined as

$$\hat{Z}(\underline{u}_0, t_0) = \sum_{k=1}^{K} \sum_{\tau_k=1}^{T_k} \sum_{\alpha_k=1}^{n_k} \lambda_{k\alpha_k\tau_k} Z_k(\underline{u}_{\alpha_k}, t_{\tau_k}) . \tag{7.1}$$

were τ_k and α_k indicate the time point and location number of the k^{th} attribute.

The constraints (7.2a) and (7.2b) ensure an unbiased estimator.

$$\sum_{\tau_k=1}^{T_k} \sum_{\alpha_k=1}^{n_k} \lambda_{\alpha_k\tau_k} = 1 \text{ for } k = 1 \tag{7.2a}$$

and

$$\sum_{\tau_k=1}^{T_k} \sum_{\alpha_k=1}^{n_k} \lambda_{\alpha_k\tau_k} = 0 \text{ for } k = 2,3,\cdots K . \tag{7.2b}$$

The conditions (7.2a) and (7.2b) must be adhered to in order to ensure that the estimator (7.1) is unbiased (7.3) and has a minimum mean-squared prediction error (7.4) – *Rouhani and Wackernagel* (*1990*), *Kyriakidis and Journel* (*1999*), *Christakos and Hristopulos* (*1998*) and *Lui and Koike* (*2007*).

$$E[\hat{Z}_k(\underline{u}_0,t_0)-Z_k(\underline{u}_0,t_0)]=0$$

$$0=\sum_{k'=1}^{K}\sum_{\tau_{k'}=1}^{T_{k'}}\sum_{\alpha_{k'}=1}^{n_{k'}}\lambda_{k'\alpha_k\tau_{k'}}E[z_{k'}(\underline{u}_{\alpha_{k'}},t_{\alpha_{k'}})]-E[z_k(\underline{u}_0,t_0)] \tag{7.3}$$

$$\sigma^2=\sum_{k'=1}^{K}\sum_{\tau_{k'}=1}^{T_{k'}}\sum_{\alpha_{k'}=1}^{n_{k'}}\lambda_{k'\alpha_k\tau_{k'}}\sum_{\theta=1}^{K}\sum_{\omega_\theta=1}^{T_\theta}\sum_{\upsilon_\theta=1}^{n_\theta}\lambda_{\theta\alpha_\theta\tau_\theta}C_{k\theta}(\underline{u}_{\alpha_k}-\underline{u}_{\alpha_{k'}},t_{\tau_k}-t_{\tau_{k'}})$$

$$-2\sum_{k'=1}^{K}\sum_{\tau_{k'}=1}^{T_{k'}}\sum_{\alpha_{k'}=1}^{n_{k'}}\lambda_{k'\alpha_k\tau_{k'}}C_{k'k}(\underline{u}_{\alpha_k}-\underline{u}_{\alpha_{k'}},t_{\tau_k}-t_{\tau_{k'}}) \tag{7.4}$$

$$+C_{kk}(\underline{u}_{\alpha_k}-\underline{u}_{\alpha_{k'}},t_{\tau_k}-t_{\tau_{k'}})$$

For two attributes (7.1) reduces to

$$\hat{Z}(\underline{u}_0,t_0)=\sum_{k=1}^{2}\sum_{\tau_k=1}^{T_k}\sum_{\alpha_k=1}^{n_k}\lambda_{k\alpha_k\tau_k}Z_k(\underline{u}_{\alpha_k},t_{\tau_k})$$

$$=\sum_{\tau_1=1}^{T_1}\sum_{\alpha_1=1}^{n_1}\lambda_{1\alpha_1\tau_1}Z_1(\underline{u}_{\alpha_1},t_{\tau_1})+\sum_{\tau_2=1}^{T_2}\sum_{\alpha_2=1}^{n_2}\lambda_{2\alpha_2\tau_2}Z_2(\underline{u}_{\alpha_2},t_{\tau_2}) \tag{7.5}$$

with

$$\sum_{\tau_1=1}^{T_1}\sum_{\alpha_1=1}^{n_1}\lambda_{\alpha_1\tau_1}=1 \tag{7.5a}$$

and

$$\sum_{\tau_2=1}^{T_2}\sum_{\alpha_2=1}^{n_2}\lambda_{\alpha_2\tau_2}=0\,. \tag{7.5b}$$

The parameters in (7.5) are defined as

- T_1, T_2 the number of temporal measurements collected for Z_1 and Z_2
- n_1, n_2 the number of spatial measurements collected for Z_1 and Z_2
- τ_1, τ_2 represent the temporal parameter for Z_1 and Z_2
- α_1, α_2 represent the spatial parameter for Z_1 and Z_2.

The spatial-temporal co-kriging system (*Rouhani and Wackernagel, 1990*; *Kyriakidis and Journel, 1999*; *Christakos and Hristopulos, 1998; Lui and Koike, 2007*) is then defined as

$$\begin{cases} \sum_{k=1}^{T} \sum_{\tau_k=1}^{T_k} \sum_{\alpha_k=1}^{n_k} \lambda_{k\alpha_k\tau_k} C_{k'k}(\underline{u}_{\alpha_k} - \underline{u}_{\alpha_{k'}}; t_{\tau_k} - t_{\tau_{k'}}) + \varphi_{k'} = C_{1k'}(\underline{u}_0 - \underline{u}_{\alpha_{k'}}; t_0 - t_{\tau_{k'}}) \\ \qquad\qquad \alpha_{k'} = 1,2,...,n_k \quad \tau_{k'} = 1,2,...,T_k \quad k = 1,2,...,T \\ \sum_{\tau_1=1}^{T_1} \sum_{\alpha_1=1}^{n_1} \lambda_{\alpha_1\tau_1} = 1 \\ \sum_{\tau_k=1}^{T_k} \sum_{\alpha_k=1}^{n_k} \lambda_{\alpha_k\tau_k} = 0 \end{cases} \tag{7.6}$$

The auto- and cross-covariances in the spatial-temporal co-kriging system (7.6) can be replaced with the auto- and cross semi-variograms (*Rouhani and Wackernagel, 1990*; *Kyriakidis and Journel, 1999*; *Christakos and Hristopulos, 1998; Lui and Koike, 2007*).

Example 7-1

Example 7-1 attempts to establish the spatial-temporal cokriging system, based on the residual product-sum semi-variogram models defined in Example 3-2. The 450 missing observations, as defined in Example 6-1 were investigated.

At certain missing locations ($\underline{u}_{1332}$, $\underline{u}_{1973}$ and $\underline{u}_{1980}$) the interpolated values differ significantly from the original values. For this case study, $ST-OK$ performs better than the $ST-OCK$ methodology. Factors that introduced the additional bias include

the small negative correlation between attributes, analysis with residuals, poor cross semi-variogram model fitting and the inherent bias introduced by the product-sum model. Information from the secondary attribute is also not fully utilized since a small percentage of the primary information is missing. The $ST-OK$ system is preferred over the $ST-OCK$ system for this set of data.

Table 7-1: Interpolated values of the sample of missing locations ($\underline{ut}$)

Location	**Original** Z_1	**Univariate estimate** Z_1	**Univariate** $\hat{\sigma}^2(\underline{u}_0)$	**Bivariate estimate** Z_2	**Bivariate** $\hat{\sigma}^2(\underline{u}_0)$
$\underline{ut}_{777}$=[(30,60),27]	100.63	99.91	0.10	101.35	0.06
$\underline{ut}_{779}$=[(30,60),29]	100.67	101.63	0.11	70.52	0.08
$\underline{ut}_{780}$=[(30,60),30]	101.11	100.31	0.07	87.76	0.12
$\underline{ut}_{782}$=[(30,70),2]	99.33	99.99	0.09	94.22	0.06
$\underline{ut}_{783}$=[(30,70),3]	99.32	98.08	0.07	93.83	0.07
$\underline{ut}_{1328}$=[(50,50),8]	105.84	105.55	0.05	112.29	0.03
$\underline{ut}_{1330}$=[(50,50),10]	97.44	97.27	0.06	92.62	0.07
$\underline{ut}_{1331}$=[(50,50),11]	100.90	100.68	0.05	96.47	0.10
$\underline{ut}_{1332}$=[(50,50),12]	99.98	100.81	0.06	109.49	0.10
$\underline{ut}_{1333}$=[(50,50),13]	100.34	100.86	0.07	90.25	0.06
$\underline{ut}_{1973}$=[(70,60),23]	102.60	101.20	0.09	111.73	0.07
$\underline{ut}_{1974}$=[(70,60)24,]	102.87	102.54	0.06	98.25	0.10
$\underline{ut}_{1975}$=[(70,60),25]	101.46	100.63	0.05	96.63	0.13
$\underline{ut}_{1976}$=[(70,60),26]	100.42	99.16	0.05	94.59	0.12
$\underline{ut}_{1980}$=[(70,60),30]	99.41	99.10	0.05	110.21	0.08
$\underline{ut}_{1986}$=[(70,70),6]	99.05	98.55	0.05	98.66	0.06
$\underline{ut}_{1988}$=[(70,70),8]	105.88	105.51	0.05	93.96	0.06
$\underline{ut}_{1989}$=[(70,70),9]	99.68	100.16	0.05	100.06	0.05
$\underline{ut}_{1991}$=[(70,70),11]	99.03	98.85	0.05	102.38	0.04
$\underline{ut}_{1993}$=[(70,70),13]	97.63	98.09	0.05	105.80	0.05

CHAPTER 8

PRACTICAL APPLICATION

Chapter 8 provides a practical application of spatial and spatial-temporal kriging. The data investigated are three-dimensional (latitude, longitude and elevation), with the two attributes primarily spatially dependent on the elevation. The purpose of this chapter is to illustrate how spatial kriging and cokriging compare with their spatial-temporal counterparts when analysing a dataset that exhibits both space and time dependencies.

8.1 DATA

To illustrate the practical application of univariate and multivariate spatial and spatial-temporal kriging, a meteorological dataset was identified and analysed. A set of 23 meteorological stations was selected from a set of 112 stations situated across Central Oregon (USA) for the time period 1 January 2000 to 31 December 2004. The data were extracted from the dataset created by Luke Spadevecchia (*Spadevecchia and Williams, 2009*) as part of his PhD thesis on investigating and quantifying error in spatial implementations of ecosystem models. Spatial-temporal models were developed for the average daily temperatures and daily precipitation measurements. The main focus of the thesis, however,was to investigate any possible interpolation bias that is introduced owing to additional spatial factors.

The study area consists of the 23 stations that fall within an area of 100×100 km in the Central Cascades region of Oregon, USA (Figure 8-1). All analyses will be performed on the daily maximum ($T_{\max}$) and minimum ($T_{\min}$) temperatures, in degree Celsius, at each station. The data, expressed as SI units, were downloaded from the website (http://www.geos.ed.ac.uk/homes/s0198247/). The station coordinates were provided in DMS, Decimal Degree and UTM zone 10 metres (WGS84 datum).

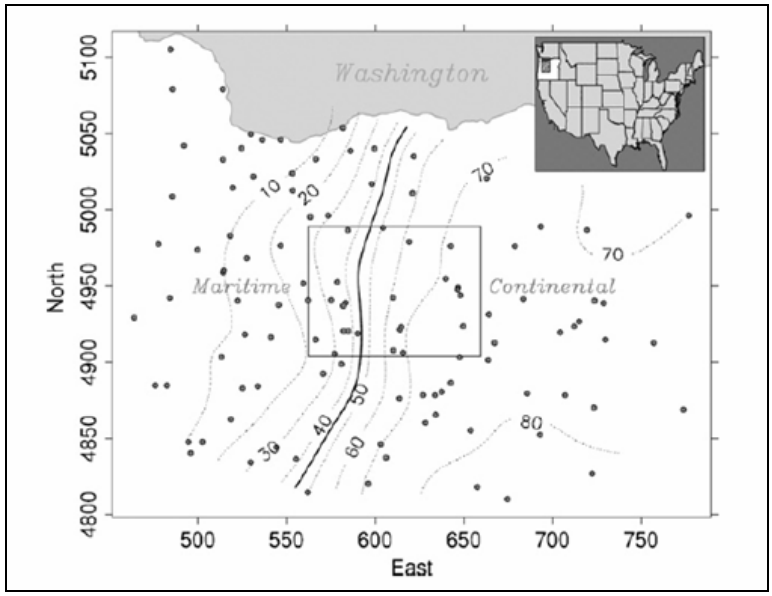

Figure 8-1: Location of the meteorological stations used in the study. The rectangular outline indicates the 100×100km detailed region of interest. (*Spadevecchia and Williams, 2009*).

UTM (Universal Transverse Mercator System) coordinates provide constant distance relationships in terms of the x-coordinate (Eastings) and the y-coordinate (Northings). Distances between the stations are calculated using the standard Euclidean distance formula for Cartesian coordinate systems and these coordinates are therefore used in the analysis of the data. All stations falling in the Easting interval [562.6186, 659.6186] and the Northing interval [4903.722, 4988.722] were extracted and analysed. For the purpose of this study, elevation is introduced as the z-coordinate.

8.2 ANALYSES

In this section, the data preparation, non-spatial and spatial exploratory methods, variogram analysis and interpolation, using the four kriging methodologies, will be investigated. The stations to be investigated are indicated in Table 8-1.

Table 8-1: The 23 meteorological stations in Central Oregon to be investigated.

SID	Latitude (Degrees)	Longitude (Degrees)	Easting (km)	Northing (km)
2	44.68	-121.15	646.88	4949.07
7	44.30	-122.03	577.11	4905.65
33	44.63	-121.13	648.06	4943.91
34	44.67	-121.15	646.65	4947.59
35	44.60	-121.95	583.33	4939.05
43	44.73	-121.23	639.89	4954.85
51	44.43	-121.97	582.24	4920.52
54	44.30	-121.55	615.67	4906.22
64	44.72	-122.01	578.78	4952.54
72	44.32	-121.62	610.38	4907.88
77	44.52	-121.49	649.83	4923.61
78	44.96	-121.49	619.17	4979.15
82	44.63	-121.61	610.20	4942.51
84	44.93	-121.19	642.67	4976.27
90	45.03	-121.93	584.49	4986.56
102	45.04	-121.67	604.51	4988.22
105	44.58	-121.97	582.03	4937.18
106	44.43	-121.93	584.89	4920.56
107	44.42	-121.87	590.23	4918.78
108	44.38	-122.17	566.38	4914.79
109	44.62	-122.05	575.37	4940.81
111	44.44	-121.57	614.06	4921.43
112	44.45	-121.56	614.79	4923.14

Data Preparation

The analysis route followed in Examples 4-1 to 7-1 was initially considered. A single day was identified for the spatial analyses over the 23 stations; ignoring the rest of the available data. These results were to be compared with the spatial-temporal results which included all the available information.

Closer inspection revealed that 23 observations over a 100×100 grid are not enough to illustrate the underlying statistical and spatial properties. Results from the spatial and non-spatial exploratory analyses are as follows:

- Spatial exploratory analysis indicated that the data are not normally distributed and there exists a correlation of less than 5% between the two attributes
- Erroneous contour maps are produced owing to the large sections that have to be interpolated
- Symbol, greyscale and indicator maps are too sparsely populated to make deductions in terms of trends in the data
- There is not enough information to warrant moving window statistics or the development of spatial continuity graphs
- The h-scatter plots, variograms and the test for stationarity gave the impression that these observations occurr at random

If no additional data were available, it would be recommended to either obtain supplementary information by performing additional sampling to obtain a better populated grid, or to use alternative interpolation techniques.

Since the spatial analysis of a single time series as described above proved to be impractical, and more information is available, the researcher decided to include much of the given information in the geostatistical analyses and variogram development. Generic variograms were subsequently developed and used in the interpolation of a missing station measurement when considering a single time series. For this study, station 34 will be interpolated individually for each of the 31 days in July 2002.

Referring to *Spadevecchia and Williams* (*2009*), analyses of the 112 meteorological stations indicated that the elevation best describes the large-scale spatial pattern of the temperature variables $T_{\max}$ and $T_{\min}$. *Spadevecchia and Williams* (*2009*) provided a detailed description of this relationship as well as the seasonal-trend models (Table 8-2) that are not only highly significant but also adequately describe the behaviour of the data. Figure 8-2 provides a graphical description of the average observed and detrended temperature by day of the year.

Table 8-2: Temporal trends of the meteorological attributes (*Spadevecchia and Williams, 2009*).

Month	T_{min}		T_{max}	
	Intercept	**Elevation**	**Intercept**	**Elevation**
January	2.3	-0.005	8.8	-0.004
February	2.4	-0.005	11.4	-0.005
March	3.6	-0.005	13.8	-0.004
April	5.0	-0.005	17	-0.004
May	7.6	-0.004	20.2	-0.003
June	10.3	-0.004	24.4	-0.002
July	12.0	-0.003	28.1	-0.001
August	11.9	-0.003	28	-0.001
September	10.1	-0.004	24.8	-0.002
October	7.0	-0.005	18.3	-0.003
November	3.4	-0.005	11.6	-0.004
December	2.8	-0.005	8.6	-0.004

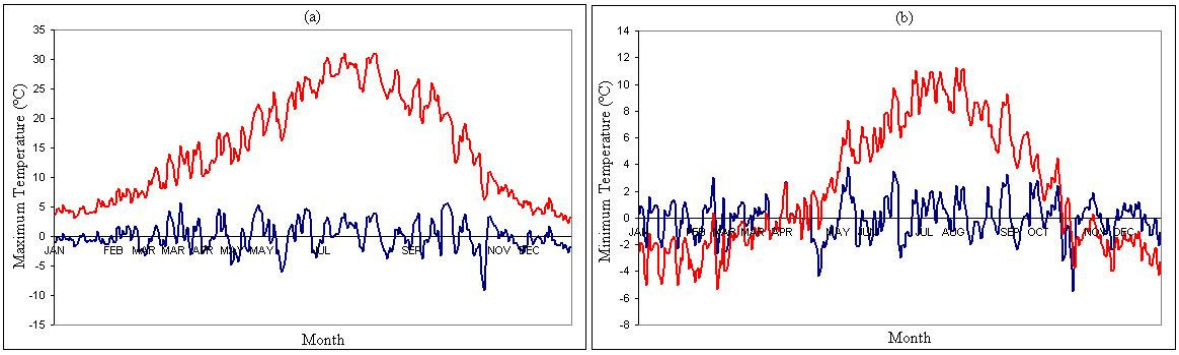

Figure 8-2: Average observed (red) and detrended (blue) temperatures by day of the year for the 23 stations: (a) for T_{max} and (b) for T_{min}.

Non-Spatial Exploratory Methods

The daily maximum temperature (T_{max}) is chosen as the primary attribute (Z_1) and the daily minimum temperature (T_{min}) as the secondary attribute (Z_2) for the purpose

of this example. The Kolmogorov-Smirnoff statistics, as well as Figure 8-3 confirm the normality of both the detrended attributes. Table 8-3 provides the non-spatial statistical breakdown of the two detrended attributes. A positive correlation (Figure 8-4) of 37.18% exists between the two attributes. The Q-Q plot (Figure 8-5) indicates that the underlying distributions of the primary and secondary variables are similar; in this case Gaussian.

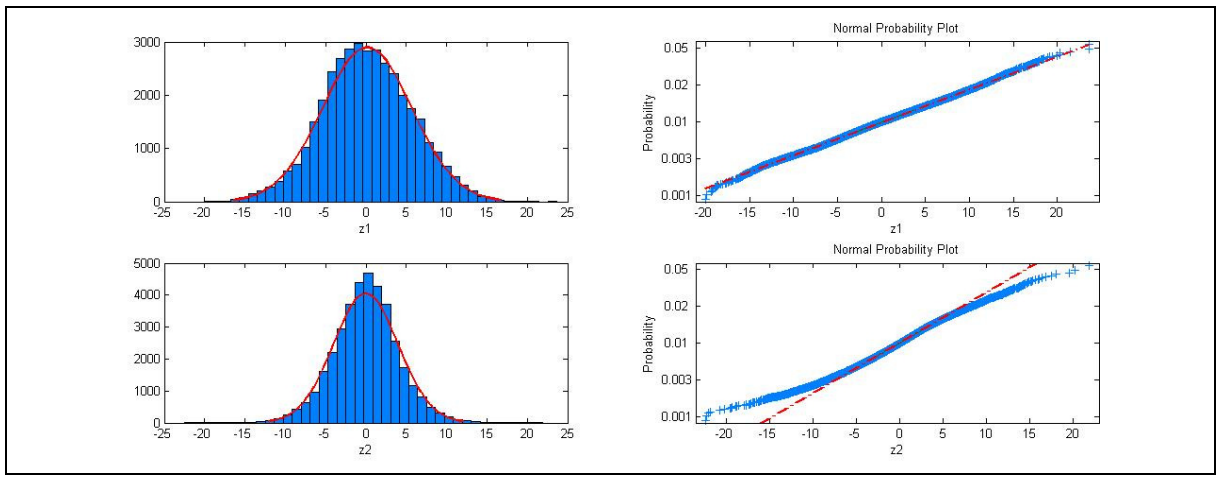

Figure 8-3: Histogram and normality plots for the primary attribute $T_{\max}$ (top) and the secondary attribute $T_{\min}$ (bottom).

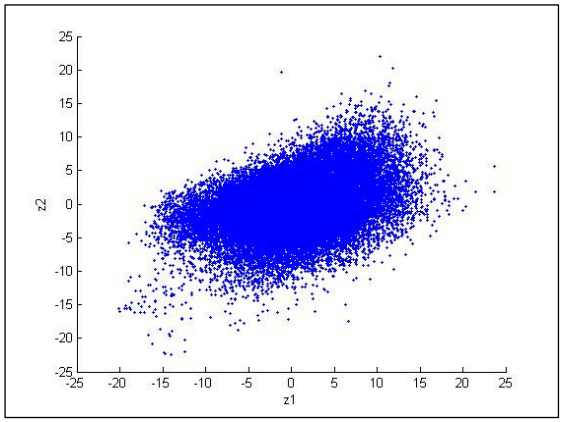

Figure 8-4: Scatter plot representing the correlation between the attributes.

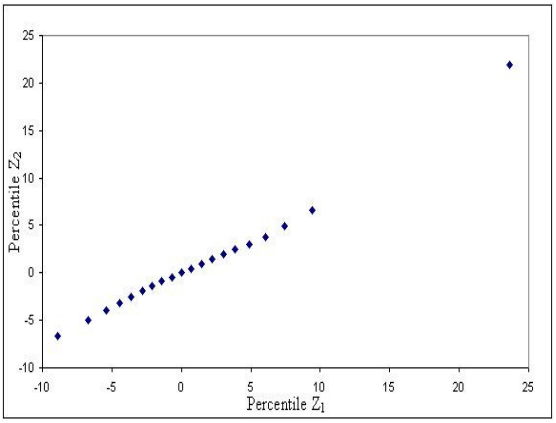

Figure 8-5: Q-Q plot of the primary (Z_1) and secondary attributes (Z_2).

Table 8-3: Non-spatial exploratory statistics of primary and secondary attributes.

Statistic	Z_1	Z_2
Mean	0.09	-0.007
Standard deviation	5.56	4.039
Maximum	23.66	21.94
Minimum	-20.06	-22.48
Kolmogorov-Smirnoff p-value	<0.010	<0.010

Spatial Exploratory Methods

The second step is to investigate the spatial properties of the given dataset. All the observed data are considered in the spatial analyses since the time-series aspect forms a critical part of the data structure. However, owing to the numerous measurements at each station, techniques such as data postings, contour maps and symbol maps became impossible to plot and were therefore ignored. The spatial techniques of moving windows statistics and spatial continuity graphs were also ignored as there are only 23 stations within the grid investigated; any sub-setting of so few stations would lead to erroneous results.

h-Scatter Plots

The h-scatter and cross h-scatter plots were created by using categorized distance and direction matrices. The distances and angles between the stations were calculated and categorized, e.g. distances that fall in the interval $[0\,\text{km}, 1\,\text{km})$ were assigned to group 1. A total of 100 distance groups and 4 angle groups were created. These groups were used to identify any possible anisotropy via the h-scatter plots as well as in the creation of the variograms.

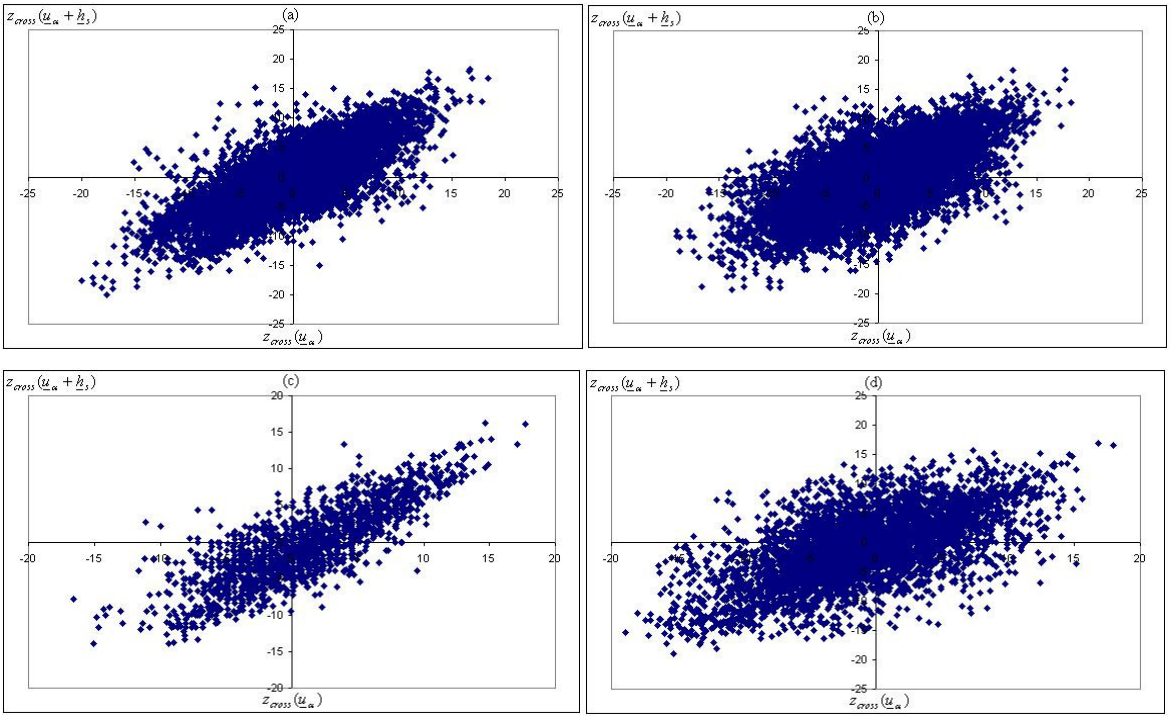

Figure 8-6: *h*-scatter plot of Z_1 at the lag distance group 36 and angle groups 1 (a), 2 (b), 3 (c) and 4 (d).

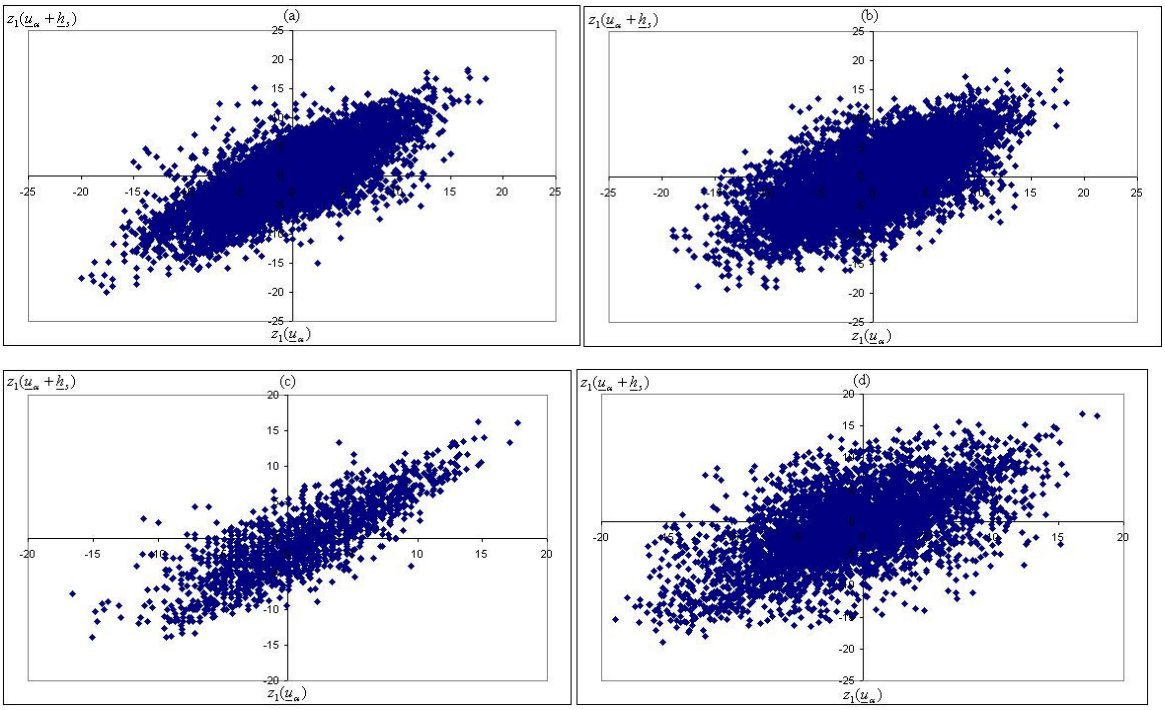

Figure 8-7: *h*-scatter plot of the cross attribute at the lag distance group 36 at angle group 1 (a), 2 (b), 3 (c) and 4 (d).

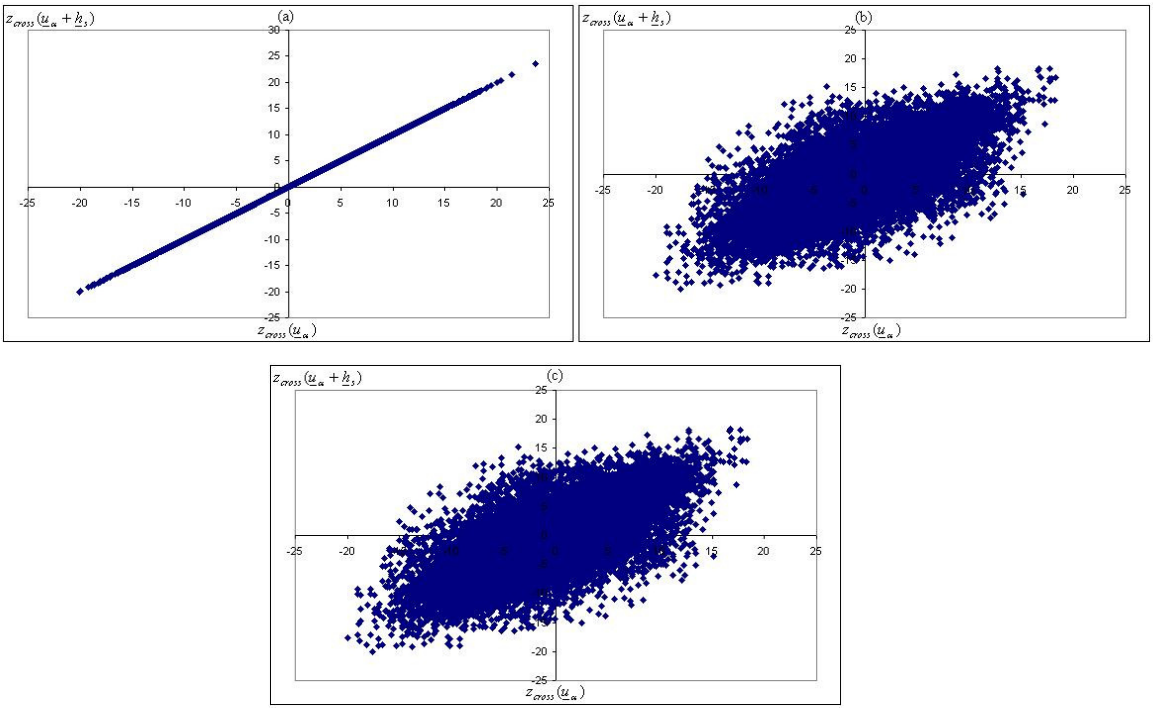

Figure 8-8: *h*-scatter plot of Z_1 at the lag distance groups 1 (a), 2 (b) and 50 (c).

The h-scatter plots for the primary and secondary attributes, as well as and the cross h-scatter plots were plotted per lag and angle. These graphs exhibit the same trend in each of the four directions, indicating that the data are isotropic. Figure 8-6 is an example of the primary h-scatter plots at distance group 36 for the four different angles. The same pattern is exhibited by all the distance and angle groups for the primary, secondary and cross attributes (Figure 8-7). Figure 8-8 represents the decreasing pattern followed by the primary, secondary and cross attributes at increasing distances when the angle between stations is not included.

Variograms

Stationarity is the last data property to be investigated to ensure optimal interpolation through the use of variograms. Intrinsic stationarity was confirmed by applying (2.40) to both the primary and secondary attributes. The approach followed in Example 2-14 was used to confirm second-order stationarity, yielding a graph of the variogram and covariance (Figure 8-9). The two models follow the same trend in opposite directions - confirming second-order stationarity of the primary and secondary data.

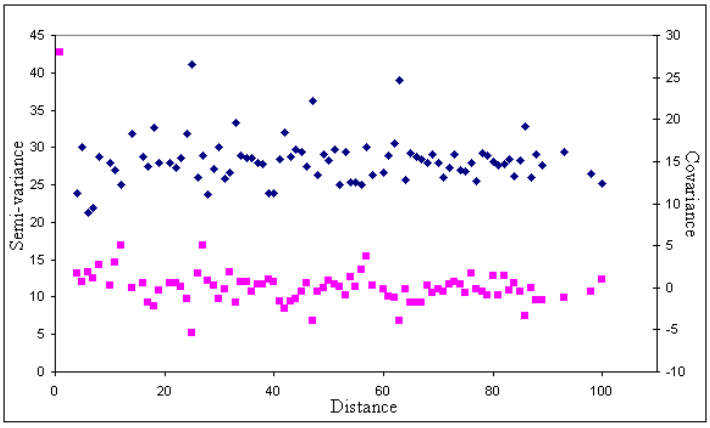

Figure 8-9: Semi-variance (top) and covariance (bottom) of selected data.

The omnidirectional semi-variograms were subsequently developed for the univariate and multivariate spatial analysis, as well as the semi-variograms needed for the product-sum methodology for spatial-temporal kriging and cokriging. Each model was calculated by using the weighted least squares (WLS) methodology, by means of the NLIN procedure in SAS, with suggested initial parameters (as identified from the semi-variogram graphs) and the standard error (defined as $\sigma = \sqrt{2\gamma}$ in *Houlding, 2000*) as the weights. These weights provide the best linear unbiased estimates of the parameters.

Spatial Semi-Variogram

The spatial univariate and multivariate semi-variogram models were developed by calculating the semi-variogram points for both the detrended attributes (Figure 8-10). The three models are provided in Table 8-4, as well as the *p*-value of the F-test for lack of regression model fit.

As seen from Table 8-4, at least the models for Z_1 and Z_2 are valid for a confidence limit of 10%, however Z_{cross} is not. The Rational quadratic model for the cross semi-variogram provided the best results compared with the Gaussian, Exponential and Spherical models, and was therefore chosen, since the semi-variogram points have outliers that influence the fit of the model (Figure 8-10c). The models provided in Table 8-4 will be used in the spatial kriging and cokriging procedures, keeping in mind that this poor model fit for Z_{cross} could lead to questionable cokriging results.

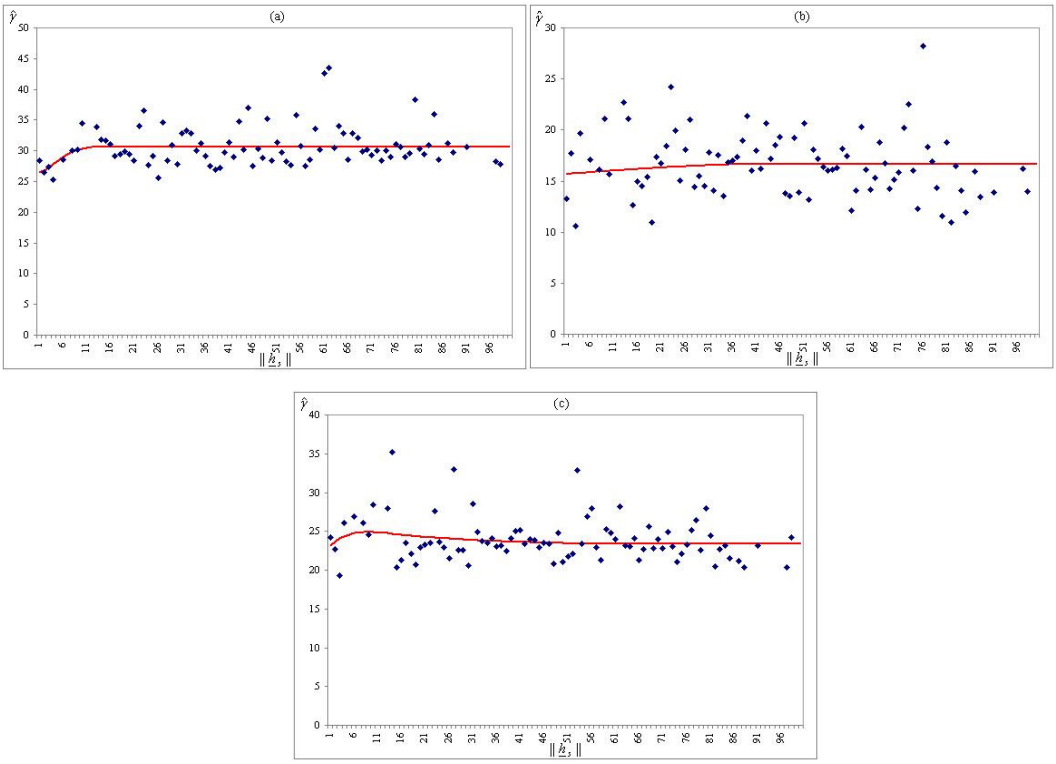

Figure 8-10: Semi-variogram scatter plot and fitted model for Z_1 (a), Z_2 (b) and Z_{cross} (c).

Table 8-4: Estimated model parameters calculated using *WLS* .

Attribute	$Z_1 = T_{\max}$	$Z_2 = T_{\min}$	Z_{cross}
Model type	Gaussian	Spherical	Rational quadratic
c_0	26.3143	15.6492	22.7199
c_e	4.3393	1.0123	4.3671
q	6.2081	43.6717	8.7091
Model fit (Pr<F)	0.0377	0.0921	0.2086

Spatial-Temporal Semi-Variogram

The product-sum model (3.18) was utilized to determine the semi-variogram for both the univariate and multivariate spatial-temporal analyses. The semi-variogram points and models for $\gamma(\| \underline{h}_s \|,0)$ are provided in Figure 8-11, with the resulting model parameters in Table 8-5. The cross semi-variogram model $\gamma(\| \underline{h}_s \|,0)$ should be rejected based on the lack-of fit test at a significance level of 10%. However, visual

inspection indicates that the model follows the same general trend of the data, except for a few outliers. Therefore the model will be used, keeping in mind the less than favourable statistical fit.

The pure temporal semi-variogram scatter plots and models were calculated and plotted, as seen in Figure 8-12 for the primary, secondary and cross attributes, with all three models (Table 8-6) accepted based on a 10% level of significance. The parameter k (3.17) was calculated for Z_1, Z_2 and Z_{cross} as 0.12, 0.17 and 0.01 respectively.

Table 8-5: Estimated parameters for $\gamma_{st}(\| \underline{h}_s \|,0)$.

Attribute	$Z_1 = T_{\max}$	$Z_2 = T_{\min}$	Z_{cross}
Model type	Exponential	Exponential	Spherical
c_0	0.3334	-1.6169	14.6706
c_e	11.8809	9.2893	0.9566
q	31.7101	3.9734	47.1138
Model fit (Pr<F)	<0.0001	<0.0001	0.3031

Table 8-6: Estimated parameters for $\gamma_{st}(0, \underline{h}_t)$.

Attribute	$Z_1 = T_{\max}$	$Z_2 = T_{\min}$	Z_{cross}
Model type	Exponential	Exponential	Exponential
c_0	-1.7695	1.3081	15.132
c_e	30.2834	12.1552	9.4246
q	2.221	2.8133	2.4106
Model fit (Pr<F)	<0.0001	<0.0001	<0.0001

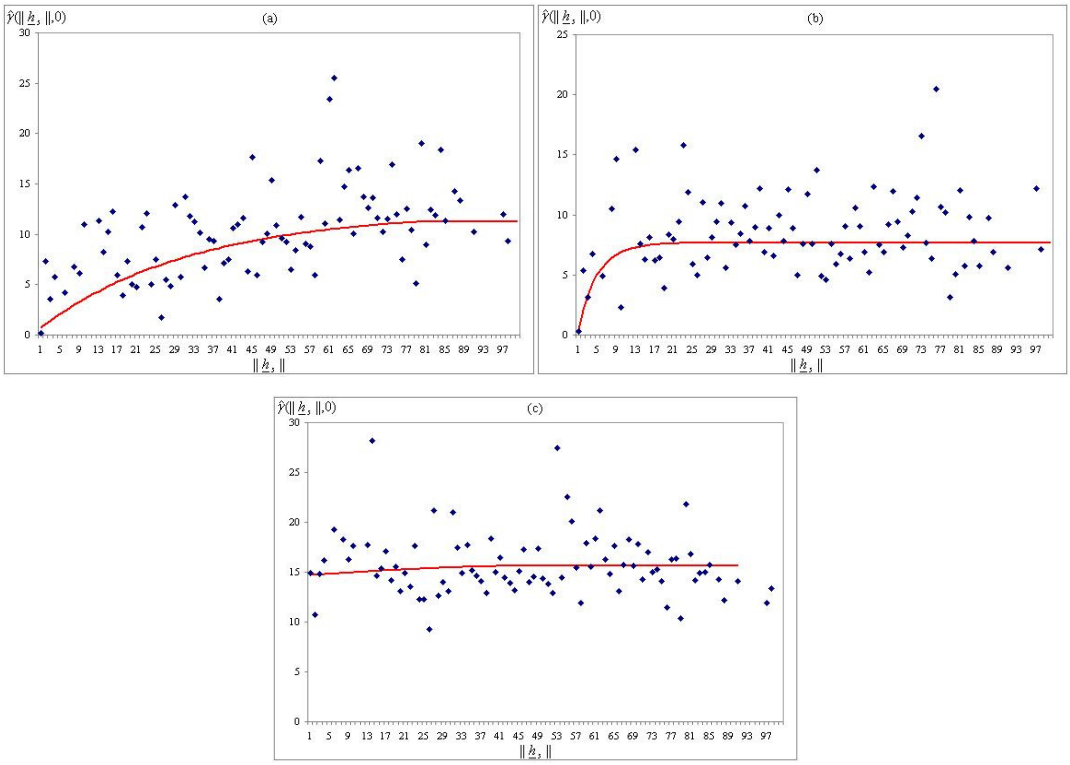

Figure 8-11: $\gamma(\| \underline{h}_s \|,0)$ and fitted model for Z_1 (a), Z_2 (b) and Z_{cross} (c).

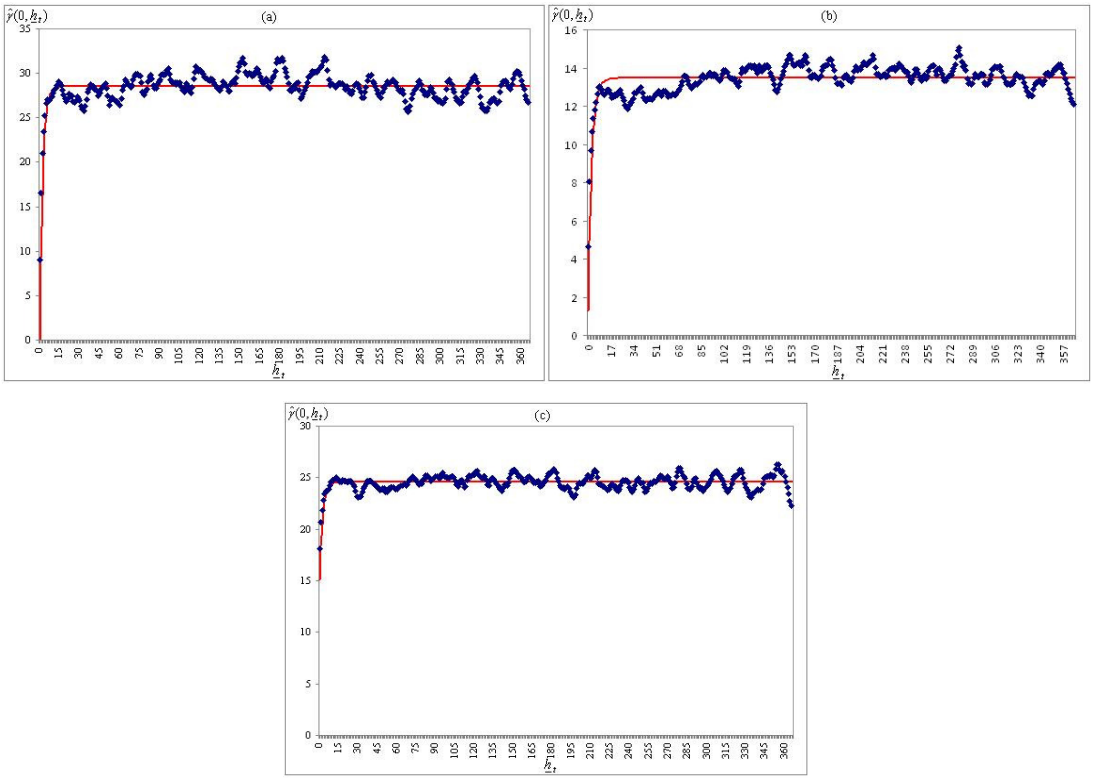

Figure 8-12: $\gamma_{st}(0,\underline{h}_t)$ fitted model for Z_1 (a), Z_2 (b) and Z_{cross} (c).

Kriging

The final step in the analytical process is the interpolation of selected missing values based on the methodologies as discussed in Chapters 4 to 7.

Spatial Kriging

The spatial semi-variograms, as proved in Table 8-4, were used to interpolate the maximum temperature ($T_{\max} = Z_1$) at station 34 for the 31 days of July 2002, by means of univariate and multivariate kriging. As seen from Examples 4-1 and 5-1, any form of spatial kriging can only provide a single interpolated value per location regardless of the possible number of observed measurements. Therefore, station 34 was interpolated for each of the 31 days using the developed general semi-variograms and observed measurements for each specific day. Table 8-7 provides the calculated interpolated and variance values, as per spatial kriging and cokriging, as well as the observed daily maximum temperature.

The kriging and cokriging processes provided conflicting interpolated measurements, with both methodologies having very high interpolation variances. The univariate estimates differ from the observed measurements by ‘n range of $\pm\ 7^{\circ}C$. The cokriging estimates are completely wrong. Closer inspection to the cokriging estimates indicated that all the requirements for optimal interpolation are met (e.g. stationarity, weight restrictions etc). Future investigations into the cause for this severe deviation from the observed measurements in the multivariate case are recommended.

Based on the results in Table 8-7, it can therefore be assumed that spatial kriging is not the best interpolation tool to be used in this scenario. The next step is to determine whether the introduction of the time component could improve the accuracy of the interpolated values.

Table 8-7: Interpolated values using the spatial kriging methodologies.

Day	**Original** Z_1	**Univ. est** Z_1	**Univ.** $\hat{\sigma}_2(\underline{u}_0)$	**Multiv. est.** Z_1	**Multiv.** $\hat{\sigma}_2(\underline{u}_0)$
1	25.56	25.78	26.54	-239.79	29.09
2	26.67	30.03	26.54	-218.96	29.09
3	30.56	24.82	26.54	-163.34	29.09
4	24.44	22.71	26.54	-155.26	29.09
5	22.22	26.55	26.54	-142.63	29.09
6	27.22	30.98	26.54	-341.58	29.09
7	31.67	32.06	26.54	-333.96	29.09
8	32.22	25.23	26.54	-98.62	29.09
9	25.56	31.91	26.54	-137.44	29.09
10	32.22	37.11	26.54	-91.47	29.09
11	38.33	38.82	26.54	-81.50	29.09
12	40	40.00	26.54	-288.68	29.09
13	41.11	37.81	26.54	-369.78	29.09
14	37.22	29.30	26.54	-184.96	29.09
15	28.89	32.39	26.54	-70.70	29.09
16	33.33	33.22	26.54	-208.32	29.09
17	33.89	32.33	26.54	-159.85	29.09
18	33.89	31.69	26.54	-103.89	29.09
19	32.78	27.53	26.54	-146.25	29.09
20	29.44	32.29	26.54	-263.47	29.09
21	32.22	33.41	26.54	-324.25	29.09
22	33.33	34.51	26.54	-274.29	29.09
23	34.01	33.85	26.54	-132.95	29.09
24	33.89	34.80	26.54	-84.85	29.09
25	35.56	31.43	26.54	-75.56	29.09
26	31.11	28.17	26.54	-59.01	29.09
27	31.11	28.33	26.54	-218.73	29.09
28	29.44	29.45	26.54	-350.78	29.09
29	30	31.41	26.54	-156.30	29.09
30	32.78	31.26	26.54	-0.40	29.09
31	31.67	26.89	26.54	18.50	29.09

Spatial-Temporal Kriging

To illustrate the effectiveness of the spatial-temporal kriging methodology, the month of July 2002 of station 34 was selected to be interpolated (i.e. 31 days), using the product-sum variograms as defined in Tables 8-5 and 8-6. Owing to operating system restrictions (Chapter 9) only the information of the stations that fall within a 30 km radius of station 34, as well as data six months prior and after the missing month was used. The information from stations 43, 84, 34, 3, 33 and 77 for the period 1 January 2002 to 31 January 2003 was used.

The kriging results for both the kriging and cokriging methodologies are provided in Table 8-8. Figure 8-13 shows that the interpolated values for both the univariate and multivariate methodologies have the same pattern. This pattern mirrors that of the observed values with an apparent lag of one day. Since both the kriging and cokriging methodologies can be used, it is proposed that the univariate methodology be used as it requires less computation.

Spatial-temporal kriging and cokriging proved its effectiveness and suitability based on the temperature dataset as described in Section 8.1. The time-dependency factor must, therefore, be included to provide a meaningful result that is comparable to neighbouring measurements in both space and time.

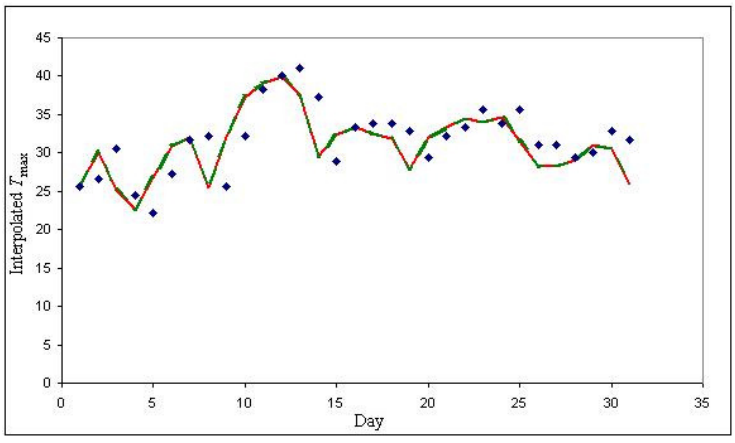

Figure 8-13: Univariate (red) and multivariate (green) interpolated values compared with observed values (blue).

Table 8-8: Interpolated values using the spatial-temporal kriging methodologies.

Day	Original Z_1	Univ. est Z_1	Univ. $\hat{\sigma}_2(\underline{u}_0)$	Multiv. est. Z_1	Multiv. $\hat{\sigma}_2(\underline{u}_0)$
1	25.56	25.72	0.43	25.72	0.43
2	26.67	29.98	1.16	30.00	1.16
3	30.56	25.17	1.46	25.18	1.46
4	24.44	22.71	1.59	22.72	1.59
5	22.22	26.70	1.64	26.71	1.64
6	27.22	30.94	1.66	30.95	1.66
7	31.67	31.98	1.67	31.99	1.67
8	32.22	25.40	1.68	25.40	1.68
9	25.56	31.98	1.68	31.99	1.68
10	32.22	37.35	1.68	37.37	1.68
11	38.33	39.05	1.68	39.07	1.68
12	40	39.96	1.68	39.98	1.68
13	41.11	37.67	1.68	37.67	1.68
14	37.22	29.57	1.68	29.58	1.68
15	28.89	32.40	1.68	32.42	1.68
16	33.33	33.34	1.68	33.35	1.68
17	33.89	32.54	1.68	32.55	1.68
18	33.89	31.88	1.68	31.90	1.69
19	32.78	27.84	1.68	27.85	1.68
20	29.44	31.98	1.68	32.00	1.68
21	32.22	33.29	1.68	33.30	1.68
21	32.22	33.29	1.68	33.30	1.68
22	33.33	34.56	1.68	34.57	1.68
23	34.01	1.68	34.01	1.68	
24	33.89	34.61	1.68	34.63	1.68
25	35.56	31.46	1.67	31.47	1.67
26	31.11	28.17	1.66	28.18	1.66
27	31.11	28.25	1.64	28.26	1.64
28	29.44	29.07	1.59	29.08	1.59
29	30	31.01	1.46	31.01	1.46
30	32.78	30.55	1.16	30.55	1.16
31	31.67	26.01	0.43	26.01	0.43

CHAPTER 9

CONCLUSION

Chapters 2 to 8 discussed the theory of geostatistics and kriging as an interpolation tool. The effectiveness, advantages and disadvantages of the methodology were illustrated through the use of examples, and are summarized below.

Advantages

The examples from Chapters 2 and 3 illustrated the different techniques that geostatistics uses in order to describe spatially and spatial-temporal dependent data. The additional descriptive statistics, such as the different spatial maps and modelling of the moments provide the researcher with the necessary information of the underlying data structures, thus enabling him/her to choose the best interpolation or simulation technique.

The kriging methodology relies on the data measurements and a continuous model of the variation, which take lag effects into account (variogram) and not simply an arbitrary distance between the locations, as in the case of *IDW* . The effect of missing measurements in neighbouring locations has a smaller influence on the final interpolated value.

The models of the moments account for possible anisotropy, nugget effects and short ranges that can have a significant effect on the variance structure of the data. A major advantage of kriging is the requirement of optimal interpolation by minimizing the variance of the estimation error, thus ensuring that the best possible estimate is obtained.

In theory, the introduction of highly correlated secondary attributes can greatly enhance the interpolation power of kriging by means of co-kriging. In Examples 6-1 and 7-1 the correlation between the attributes was not strong enough, resulting in the secondary attribute not providing additional value to the estimation process. The

multivariate spatial-temporal practical example in Chapter 8 also provided results equivalent to the univariate kriging methodology. Information from the secondary attribute is also not fully utilized since small percentages of the primary information in each example are missing.

Spatial-temporal ordinary kriging and co-kriging have all the advantages and disadvantages of ordinary kriging and co-kriging. An additional advantage is the inclusion of the temporal and the spatial-temporal dependence to the variance structure, allowing the variance to change over time.

Disadvantages

As with any form of data analysis, geostatistics depends heavily on the quantity and quality of the data. Too few measurements can produce a skewed perception of the data and can lead to incorrect assumptions. If the data are highly skewed or only a few measurements are available, the kriging systems become more complex and the results unstable.

To ensure unique solutions for the kriging systems, the underlying restrictions of stationarity, conditional weights and minimized estimation variance must be strictly adhered to. This may require additional transformations that can introduce additional bias to the data.

Additional disadvantages of kriging and co-kriging include the degree of subjectivity introduced by employing user-defined spatial-lag measurements, as well as the selection of appropriate and permissible models for the variograms. These selections make kriging a more time-consuming technique compared with less complex interpolation tools, such as *IDW* . Therefore it is essential that the data and underlying methodology is understood.

Spatial-temporal geostatistics is inherently more complex because of the inclusion of the temporal dependence structure. The most difficult part of this kriging methodology is the fitting of spatial-temporal variograms (Section 3.4), making it more labour intensive.

Challenges in Geostatistics

Real-time data often require complex transformations in terms of normality, stationarity, anisotropy or irregularly spaced measurements. Additional field-specific knowledge, such as, for instance, the existence of a dam wall between two river-flow gauging stations is necessary to ensure realistic estimates. To illustrate the different concepts of descriptive statistics, moment modelling and interpolation of missing measurements, a spatial-temporal dataset that would require the least number of transformations was generated (Section 2.3).

The development of geostatistics was driven by the need to address the complex problems in the mining sector. Even though the original methodologies were developed by D.G Krige, a mining engineer, and G. Matheron, who was proficient in mathematics, physics and probability theory, a wide variety of notations exists in the literature. One of the challenges in drafting this dissertation was to remove some of the confusion in the notation by combining the different styles and to define a standard notation for the core of univariate and multivariate spatial and spatial-temporal kriging systems.

Extensive research has been done over the years on the modelling of variograms (covariance) for spatial stationary, isotropic and non-isotropic data, as well as the modelling of spatial-temporal variation. Recent advances have been made to create kriging methodologies for non-stationary data, such as defining a non-stationary covariance structure (e.g. *Paciorek and Schervish, 2006*). More in-depth studies to define kriging structures that do not require any stationarity assumptions are needed in both the spatial and spatial-temporal dependency structures.

The different methodologies used in geostatistics were and are being developed mainly by mathematicians and statisticians, but are primarily used by natural scientists, some of whom do not have the necessary background to correctly interpret and apply the theory. In many instances the available software (Section 2.7) is used as a ‘black box’ where data are analyzed without a clear understanding of the underlying methodology. A definite need exists for the intensive training of mathematicians, statisticians, physicists and other natural scientists in geostatistics and, especially,

kriging since it is becoming a popular interpolation technique in both the natural and financial sciences.

Operating system restrictions proved to be problematic during the spatial-temporal analyses of the practical dataset (Chapter 8). Initially all the information stored in the 23 stations over the four years was used, however both the SAS, Matlab and Fortran applications consistently ran out of memory when dealing with large square matrices (arrays). Although these systems do allow for additional memory to be assigned to the matrix (array) calculations, there exists a limit on the total workspace that can be assigned (e.g. http://www.mathworks.com/support/tech-notes/1100/1100.html). This problem forced the researcher, in this case, to reduce the total number of observations used in the final analyses. Further study is necessary to identify methodologies to overcome this problem.

Final remarks

In this dissertation the concept of geostatistics was defined and discussed in terms of the principle descriptive statistics, interpolation techniques and the advantages and disadvantages. Based on the results from this introductory theoretical study and practical applications on a simulated dataset, it can be concluded that geostatistics and, especially, kriging can be a very powerful tool when it is used in conjunction with experience and a comprehensive understanding of the methodology and data.

REFERENCES

Aboufirassi, M., Marino, M.A. (1984) Cokriging of aquifer transmissivities from field measurements of transmissivity and specific capacity. *Mathematical Geology.* 16 (1), pp19–35.

Banerjee, S., Carlin, B.P., Gelfand, A.E. (2004) Hierarchical modelling and analysis for spatial data. Chapman and Hall/CRC.

Brockwell, P.J., Davies, R.A. (1987) Time series: Theory and methods. Springer-Verlag.

Christakos, G. (1984) On the problem of permissible covariance and variogram models. *Water Resources Research*, Vol20, Issue 2. pp251–265.

Christakos, G. (1992) Random Field models in earth sciences*:* Academic Press, San Diego, CA, 474pp.

Christakos, G., Hristopulos, D.T. (1998) Spatiotemporal environmental health modelling: A tractatus stochasticus: Kluwer Academic Publ., Boston.

Clark, I. (1979) Practical geostatistics, Applied Science Publisher, London

Clark, I., Harper, W.V. (2000) Practical geostatistics, Geostokos (Ecosse) Limited, Scotland.

Cressie, N.A.C. (1985) Fitting variogram models by weighted least squares. *Mathematical Geology*, 17(5), pp563-586

Cressie, N.A.C. (1991). Statistics for Spatial Data, Wiley Series in Probability and Mathematical Statistics.

Cressie, N.A.C. (1993) Statistics for spatial data. John Wiley & Sons, New York, rev ed.

Cressie, N.A.C., Huang, H.-C. (1999) Classes of nonseparable, spatio-temporal stationary covariance functions. *Journal of the American Statistical Association*, 94, pp1330–1340.

De Cesare, L., Myers, D., Posa, D. (1996) Spatial-temporal modeling of SO_2 in Milan district. In Baafi, E.Y., Schofield, N.A. (eds), *Geostatistics Wollongong'96*. Kluwer Academic Publishers, Dordrecht, vol. 2, pp1031–1042.

De Cesare, L., Myers, D.E., Posa, D. (2001a) Product-sum covariance for space-time modeling : an enviromental application. *Envirometrics*, 12, pp11–23.

De Cesare, L., Myers, D.E., Posa, D. (2001b) Estimating and modeling space-time correlation structures. *Statistics and Probability Letters*, 51, pp9–14.

De Cesare, L., Myers, D.E., Posa, D. (2002) FORTRAN programs for space-time modeling. *Computers & Geosciences* 28, pp205–212.

De Iaco, S., Myers, D.E., Posa., D. (2001) Space-time analysis using a general product-sum model. *Statistics & Probability Letters* 52, p21–28.

De Iaco, S., Myers, D.E., Posa., D. (2002) Space-time variograms and a functional form for total air pollution measurements. *Computational Statistics and Data Analysis*, 41, pp311–328.

De Iaco, S., Myers, D.E., Posa, D. (2003) The linear coregionalizatoin model and the product-sum space-time variogram. *Mathematical Geology*, vol. 35, no.1.

De Iaco, S., Palma, M., Posa, D. (2005). Modeling and prediction of multivariate space-time random fields. *Computational Statistics and Data Analysis*, 48, pp525–547.

Deutsch, C.V. (2002) Geostatistical reservoir modeling. Oxford University Press.

Deutsch, C.V., Journel, A.G. (1998) GSLIB. Geostatistical software library and user′s guide, Oxford University Press, New York, NY, pp369.

Diablo Valley College http://voyager.dvc.edu/~twieden/meteorology/contouring/contouring. html

Dimitrakopoulos, R., Luo, X. (1993) Spatiotemporal modeling: Covariances and ordinary kriging systems. *Geostatistics for the Next Century*. Kluwer Academic Publishers , Dordrecht, pp88–93.

Dimitrakopoulos, R., Luo, X. (1997) Joint space-time modelling in the presence of trends. *Geostatistics-Wolongong '97*. E Baafi & N Scofield (cds), Kluwer Academic Publ, Dordrecht, pp138–149.

Gaetan, C., Guyon, X. (2009) Spatial statistics and modelling. Springer Series in Statistics, Springer – online version.

Gneiting, T. (2001) Nonseparable, stationary covariance functions for space-time data. NRCSE Technical Report Series, NRCSE-TRS No 063, May 23.

Gilgen, H. (2006) Univariate time series in geosciences: Theory and examples. Springer-Verlag.

Gómez-Hernández., J.J (1996) Geostatistics and hydrology: An overview, geographical information, Second Joint European Conference and Exhibition on Geographical Information, Barcelona, Spain.

Goovaerts, P. (1993) Spatial orthogonality of the principal components computed from coregionalized variables. *Mathematical Geology*, 25(3), pp281–302.

Goovaerts, P. (1997) Geostatistics for natural resources evaluation. Applied Geostatistics Series,Oxford University Press.

Goovaerts, P., Sonnet, P. (1993) Study of spatial and temporal variations of hydrogeochemical variables using factorial kriging analysis. In A. Soares, ed., Geostatistics Tróia '92, vol 2: Kluwer Academic Publ., Dordrecht, pp745–756.

Houlding, S., 2000. Practical Geostatistics – modelling and spatial analysis. Kindle edition.

Isaaks, E.H., Srivastava, R.M. (1989) An introduction to applied geostatistics. Oxford University Press (New York).

Jian, X., Olea, R.A., Yu, Y.S. (1996) Semivariogram modelling by weighted least squares. *Computers and Geosciences*, 22(4), pp387-397.

Journel, A.G. (1986) Geostatistics: Models and Tools for the Earth Sciences. *Mathematical Geology*. vol 18, no1.

Journel A.G., Huijbregts C.J. (1978) Mining Geostatistics, Academic Press (London)

Kolmogorov, A.N. (1941) Interpolated and extrapolated stationary random sequences), Izevestya Akademiya Nauk, SSSR, *Seriya Mathematicheskaya*, 5, pp3-14.

Krige, D.G. (1951) A statistical approach to some basic mine valuation problems on the Witwatersrand. *Journal of the Chemical, Metallurgical and Mining Society of South Africa.* 52 (6): pp119–139

Kyriakidis, P.C., Journel, A.G. (1999) Geostatistical space-time models: A review. *Mathematical Geology*, vol 31, no 6, pp651–684.

Lui, C., Koike, K. (2007) Extending multivariate space-time geostatistics for environmental data analysis. *Mathematical Geology*, 39, pp289–305.

Ma, C. (2003) Spatio-temporal stationary covariance models. *Journal of Multivariate Analysis*, 86, pp97–107.

Matern, B. (1986) (English version), Spatial variation, Springer, New York.

Matheron, G. (1962) Traité de géostatistique appliquée, tome I. Memoires du Bureaude Recherches Geologiques et Minières, 14, Editions Technip, Paris

Matheron, G. (1963) Principles of geostatistics. *Economic Geology*, 58, pp1246–1266.

Matheron, G. (1971) The theory of regionalized variables and its applications. Cahiers du Centre de Morphologic Mathématique, Ecole, des Mines de Paris, 5, Fontainebleau, France.

Myers, D.E. (1984) Cokriging: Methods and alternatives. In: P. S. Glaeser (ed.) The Role of Data in Scientific Progress. Elsvier Scientific Progress. Elsvier Science, New York. pp425–428.

Myers, D., Journel, A.G. (1990) Variogram with zonal anisotropies and non-invertiable kriging systems. *Mathematical Geology*, 22, pp779–785.

Nielsen, D.R., Wendroth, O. (2003) Spatial and temporal Statistics. GeoEcology textbook.

Paciorek, C.J., Schervish, M.J. (2006) Spatial modelling using a new class of nonstationary covariance functions. *Environmetrics*, 17(5), pp483–506.

Pardo-Igúzquiza, E. (1999) VARFIT: a Fortran-77 program for fitting variogram models by weighted least squares. *Computers and Geosciences*, 25, pp251-261.

Reichenbach, H. (1958) The philosophy of space and time. Dover. New York.

Rodriguez-Iturbe, I., Mejia, J.M. (1974) The design of rainfall networks in time and space. *Water Resources Research*, 10, pp713–729.

Rouhani, S., Hall, T.J. (1989) Space-time kriging of groundwater data. Armstrong. M. (ed.) Geostatistics. Kluwer Academic Publishers, Dordrecht, vol2. pp639–651.

Rouhani, S., Wackernagel, H. (1990) Multivariate geostatistical approach to Space-time data analysis, *Water Resources Research*., 26(4): pp585–591.

Schabenberger O., Gotway, C.A. (2000) Statistical methods for spatial data analysis. Chapman & Hall/CRC.

Shepard D. (1968) A two dimensional interpolation function for irregular spaced data, Proc 1968 ACM Nat Conf, pp517–524.

Spadavecchia, L., Williams, M., 2009, Can spatio-temporal geostatistical methods improve high resolution regionalisation of meteorological variables. *Agricultural and Forest Meteorology* 149, pp 1105-1117

Stein, A., Van der Meer, F., Gorte, B. (1999) Spatial statistics for remote sensing. Kluwer Academic Publishers.

Switzer, P. (2002) Encyclopedia of envirometrics, Vol 4, Abdel H. El-Shaarawi and Walter W. Piegorsch (eds). John Wiley & Sons, Ltd.

Wackernagel, H. (1995) Multivariate geostatistics. Springer-Verlag (Berlin), 256pp.

Webster, R., Oliver, M.A. (2007) Geostatistics for enviromental scientists. Wiley, Statistics in Practice.

Weyl, H. (1952) Space-time matter. Dover, New York.

Zhang, Y. (2007) Introduction to geoststatistics – Course notes. Dept of Geology and Geophysics. University of Wyoming. Draft date Novermber 8.

APPENDIX A

CONTENTS 147

APPENDIX A.1

SEMI-POSITIVE DEFINITE CONDITION FOR THE COVARIANCE FUNCTION

(*Wackernagel, 1995*)

A function is positive semi-definite if the inequality (3.2) holds for any second-order stationarity set of $Z(\underline{u}_1), Z(\underline{u}_2), ..., Z(\underline{u}_n)$ with $E(Z(\underline{u}_\alpha)) = \mu \ \ \forall \ \ \underline{u}_\alpha \in D$ where $\underline{\lambda}$ is any vector of arbitrary weights $(\lambda_1, \lambda_2, ..., \lambda_n)$

$$\sum_{\alpha=1}^{n}\sum_{\alpha'=1}^{n}\lambda_\alpha\lambda_{\alpha'}C(\underline{u}_\alpha - \underline{u}_{\alpha'}) \geq 0 \tag{3.2}$$

Assume L is the linear combination of the observed values and the associated weights.

$$L = \sum_{\alpha=1}^{n}\lambda_\alpha Z(\underline{u}_\alpha) \tag{A.1-1}$$

And the variance of L is defined as

$$\begin{aligned}
\text{var}(L) &= \text{var}\left[\sum_{\alpha=1}^{n}\lambda_\alpha Z(\underline{u}_\alpha)\right] \\
&= E\left\{\left[\sum_{\alpha=1}^{n}\lambda_\alpha\left[Z(\underline{u}_\alpha) - \mu\right]\right]^2\right\} \\
&= E\left\{\left[\sum_{\alpha=1}^{n}\lambda_\alpha\left(Z(\underline{u}_\alpha) - \mu\right)\right]\left[\sum_{\alpha'=1}^{n}\lambda_{\alpha'}\left(Z(\underline{u}_{\alpha'}) - \mu\right)\right]\right\} \\
&= \sum_{\alpha=1}^{n}\sum_{\alpha'=1}^{n}\lambda_\alpha\lambda_{\alpha'}E\left\{\left[Z(\underline{u}_\alpha) - \mu\right]\left[Z(\underline{u}_{\alpha'}) - \mu\right]\right\} \\
&= \sum_{a=1}^{n}\sum_{a'=1}^{n}\lambda_a\lambda_{a'}C(Z(\underline{u}_a), Z(\underline{u}_{a'}))
\end{aligned} \tag{A.1-2}$$

$$\sum_{a=1}^{n}\sum_{a'=1}^{n}\lambda_a\lambda_{a'}C(Z(\underline{u}_a),Z(\underline{u}_{a'})) = \sum_{a=1}^{n}\sum_{a'=1}^{n}\lambda_a\lambda_{a'}C(\underline{h}_s) \text{ under the stationarity assumption.}$$

$$= \sum_{a=1}^{n}\sum_{j=1}^{n}\lambda_\alpha\lambda_{\alpha'}C(\underline{u}_\alpha - \underline{u}_{\alpha'}).$$

Since a variance can only be equal to zero or larger than zero results in (3.2) to be true.

$$\sum_{a=1}^{n}\sum_{j=1}^{n}\lambda_\alpha\lambda_{\alpha'}C(\underline{u}_\alpha - \underline{u}_{\alpha'}) \geq 0$$

APPENDIX A.2

CONDITIONAL NEGATIVE CONDITION FOR THE VARIOGRAM

(*Wackernagel, 1995*)

The model to be fitted to the variogram must comply with the conditional negative definite condition defined as

$$-\sum_{\alpha=1}^{n}\sum_{\alpha'=1}^{n}\lambda_\alpha\lambda_{\alpha'}\gamma(\underline{u}_\alpha-\underline{u}_{\alpha'})\geq 0 \tag{3.3}$$

for all $\lambda_\alpha \quad (\alpha=1,2,\cdots,n)\in\Re$ and

$$\sum_{\alpha=1}^{n}\lambda_\alpha=0 \tag{3.3a}$$

when intrinsic stationarity is applicable.

The semi-variogram, under instrinsic stationarity, can be expressed as

$$\begin{aligned}\gamma(Z(\underline{u}_\alpha),Z(\underline{u}_{\alpha'}))&=\frac{1}{2}\operatorname{var}[Z(u_\alpha)-Z(u_{\alpha'})]\\&=\frac{1}{2}E\left[Z(\underline{u}_\alpha)-Z(\underline{u}_{\alpha'})\right]^2\\&=\frac{1}{2}\operatorname{var}\left[Z(\underline{u}_\alpha)\right]+\frac{1}{2}\operatorname{var}\left[Z(\underline{u}_{\alpha'})\right]-C(Z(\underline{u}_\alpha),Z(\underline{u}_{\alpha'}))\end{aligned} \tag{A.2-1}$$

and can be re-written as

$$C(Z(\underline{u}_\alpha),Z(\underline{u}_{\alpha'}))=\frac{1}{2}\operatorname{var}\left[Z(\underline{u}_\alpha)\right]+\frac{1}{2}\operatorname{var}\left[Z(\underline{u}_{\alpha'})\right]-\gamma(Z(\underline{u}_\alpha),Z(\underline{u}_{\alpha'})) \tag{A.2-2}$$

Utilizing (A.1-2)

$$\sum_{\alpha=1}^{n}\sum_{\alpha'=1}^{n}\lambda_\alpha\lambda_{\alpha'}C(\underline{u}_\alpha,\underline{u}_{\alpha'})\geq 0$$

$$= \sum_{\alpha=1}^{n}\sum_{\alpha'=1}^{n}\lambda_\alpha\lambda_{\alpha'}\left\{\frac{1}{2}\,\mathrm{var}\left[Z(\underline{u}_\alpha)\right]+\frac{1}{2}\,\mathrm{var}\left[Z(\underline{u}_{\alpha'})\right]-\gamma(Z(\underline{u}_\alpha),Z(\underline{u}_{\alpha'}))\right\}$$

$$= \frac{1}{2}\sum_{\alpha'=1}^{n}\lambda_{\alpha'}\sum_{\alpha=1}^{n}\lambda_\alpha\,\mathrm{var}\left[Z(\underline{u}_\alpha)\right]+\frac{1}{2}\sum_{\alpha=1}^{n}\lambda_\alpha\sum_{\alpha'=1}^{n}\lambda_{\alpha'}\,\mathrm{var}\left[Z(\underline{u}_{\alpha'})\right]-\sum_{\alpha=1}^{n}\sum_{\alpha'=1}^{n}\lambda_\alpha\lambda_{\alpha'}\gamma(Z(u_\alpha),Z(u_{\alpha'}))$$

The first two terms are equal to zero as a result of condition (3.3a). This results in

$$-\sum_{\alpha=1}^{n}\sum_{\alpha'=1}^{n}\lambda_\alpha\lambda_{\alpha'}\gamma(Z(u_\alpha),Z(u_{\alpha'}))\geq 0 \qquad \text{(A.2-3)}$$

Applying the intrinsic stationarity condition to (A.2-3)

$$-\sum_{\alpha=1}^{n}\sum_{\alpha'=1}^{n}\lambda_\alpha\lambda_{\alpha'}\gamma(\underline{h}_s)\geq 0$$

and

$$-\sum_{\alpha=1}^{n}\sum_{\alpha'=1}^{n}\lambda_\alpha\lambda_{\alpha'}\gamma(\underline{u}_\alpha-u_{\alpha'})\geq 0$$

APPENDIX A.3

DERIVE PRODUCT-SUM MODEL COEFFICIENTS

(*De Iaco* et al., *2001*)

Assuming that the property exhibited in (3.13) holds, it follows that

$$\gamma_{st}(\underline{h}_s,0)=[k_2+k_1C_t(0)]\gamma_s(\underline{h}_s)=k_s\gamma_s(\underline{h}_s) \tag{3.13a}$$

and

$$\gamma_{st}(\underline{0},h_t)=[k_3+k_1C_s(\underline{0})]\gamma_t(h_t)=k_t\gamma_t(h_t) \tag{3.13b}$$

with k_s and k_t defined as the proportionality coefficients between $\gamma_{st}(\underline{h}_s,0)$ and $\gamma_{st}(\underline{0},h_t)$, and the spatial and temporal semi-variograms $\gamma_s(\underline{h}_s)$ and $\gamma_t(h_t)$ respectively.

The coefficients k_1, k_2 and k_3 can be written in terms of the sills and the parameters k_s and k_t, which allows the practitioner to model $\gamma_s(\underline{h}_s)$ and $\gamma_t(h_t)$ in terms of $\gamma_{st}(\underline{h}_s,0)$ and $\gamma_{st}(\underline{0},h_t)$. The parameters k_s and k_t can be combined into a single parameter k (3.17).

Combining

$$k_s=k_2+k_1C_t(0) \tag{3.14a}$$

and

$$k_t=k_3+k_1C_s(\underline{0}) \tag{3.14b}$$

with

$$C_{st}(\underline{0},0)=k_1C_s(\underline{0})C_t(0)+k_2C_s(\underline{0})+k_3C_t(0) \tag{3.16}$$

obtained from (3.13a), allows k_1, k_2 and k_3 to be solved in terms of the covariance sill values as seen in (3.15a), (3.15b) and (3.15c).

$$k_1 = \frac{k_s C_s(\underline{0}) + k_t C_t(0) - C_{st}(\underline{0},0)}{C_s(\underline{0}) C_t(0)} \tag{3.15a}$$

$$k_2 = \frac{C_{st}(\underline{0},0) - k_t C_t(0)}{C_s(\underline{0})} \tag{3.15b}$$

$$k_3 = \frac{C_{st}(\underline{0},0) - k_s C_s(\underline{0})}{C_t(0)} \tag{3.15c}$$

If $k_1 > 0$, $k_2 \geq 0$ and $k_3 \geq 0$ (Theorem1, Corollary 1 and 2 in *Appendix A.4*) the positive-definiteness is assured for any class of covariance models as it is related to the sill values.

Finally a single parameter is derived using Theorem 2 (*Appendix A.4).*

$$k = \frac{k_1}{k_s k_t} = \frac{k_s C_s(\underline{0}) + k_t C_t(0) - C(\underline{0},0)}{k_s C_s(\underline{0}) k_t C_t(0)} \tag{3.17}$$

The process of estimating $\gamma_{st}(\underline{h}_s,0)$ and $\gamma_{st}(\underline{0},h_t)$ yields the estimates for $k_s C_s(\underline{0})$ and $k_t C_t(0)$, requiring that ultimately only k needs to be estimated. Theorem 2, Corollary 1 and 2 (*Appendix A.4*) provide the necessary and sufficient conditions to ensure permissibility of γ_{st}.

APPENDIX A.4

SEPARABLE MODEL THEOREMS

(*De Iaco* et al., *2001*)

Theorem 1

For the following models assumptions

- $Z(\underline{u}_\alpha, t_\tau)$ is a second-order stationary spatial-temporal random field
- The spatial-temporal covariance is continuous in the space-time structure and represented by equation (3.12a)
- The semi-variogram is defined as in (3.18)
- The parameter k is defined by equation (3.17).

Then $k_1 > 0,\ \ k_2 \geq 0,\ \ k_3 \geq 0$ if, and only if, k holds to the following inequality

$$0 < k \leq \frac{1}{\max\{sill(\gamma(\underline{h}_s, 0)); sill(\gamma(\underline{0}, h_t))\}} \tag{A.4-1}$$

Proof

Given the assumptions, it follows that

$$k_s = k_2 + k_1 C_t(0) > 0 \tag{3.14a}$$

$$k_t = k_3 + k_1 C_s(\underline{0}) > 0 \tag{3.14b}$$

resulting in $k > 0$. The assumption satisfies the following inequalities

$$k_1 = \frac{k_s C_s(\underline{0}) + k_t C_t(0) - C(\underline{0},0)}{C_s(\underline{0}) C_t(0)} > 0 \Rightarrow\ C(\underline{0},0) < k_s C_s(\underline{0}) + k_t C_t(0)$$

$$k_2 = \frac{C(\underline{0},0) - k_t C_t(0)}{C_s(\underline{0})} \geq 0 \ \ \Rightarrow\ \ C(\underline{0},0) \geq k_t C_t(0)$$

$$k_3 = \frac{C(\underline{0},0) - k_s C_s(\underline{0})}{C_s(\underline{0})} \geq 0 \quad \Rightarrow \quad C(\underline{0},0) \geq k_s C_s(\underline{0})$$

If

$$C(\underline{0},0) \geq \max\{k_s C_s(\underline{0}); k_t C_t(0)\}$$

then the last two equalities are satisfied simultaneously.

For

$$C(\underline{0},0) < k_s C_s(\underline{0}) + k_t C_t(0)$$

and

$$C(\underline{0},0) \geq \max\{k_s C_s(\underline{0}); k_t C_t(0)\}$$

to be true, k is defined to be less than or equal to

$$\left(\max\{k_s C_s(\underline{0}); k_t C_t(0)\}\right)^{-1}$$

hence

$$k \in \left]0; \left(\max\{k_s C_s(\underline{0}); k_t C_t(0)\}\right)^{-1}\right]$$

Conversely, if k holds to the inequality

$$0 < k \leq \frac{1}{\max\{sill(\gamma(\underline{h}_s,0)); sill(\gamma(\underline{0},h_t))\}}$$

then

$$\gamma_{st}(\underline{h}_s,h_t) = \gamma_{st}(\underline{h}_s,0) + \gamma_{st}(\underline{0},h_t) - k\gamma_{st}(\underline{h}_s,0)\gamma_{st}(\underline{0},h_t) \qquad (3.18)$$

is a permissible variogram derived from a permissible covariance model i.e.

$$k = \frac{(sill\gamma(\underline{h}_s,0) + sill\gamma(\underline{0},h_t) - sill\gamma(\underline{h}_s,h_t))}{(sill\gamma(\underline{h}_s,0)sill\gamma(\underline{0},h_t))}$$

$$\equiv$$

$$C(\underline{h}_s,h_t) = k_1 C_s(\underline{h}_s)C_t(h_t) + k_2 C_s(\underline{h}_s) + k_3 C_t(h_t)$$

Therefore the bounds on k along with the inequalities

$$C(\underline{0},0) < k_s C_s(\underline{0}) + k_t C_t(0)$$

$$C(\underline{0},0) < k_s C_s(\underline{0}) + k_t C_t(0)$$

and $C(\underline{0},0) \geq \max\{k_s C_s(\underline{0}); k_t C_t(0)\}$ implies $k_1 > 0$, $k_2 \geq 0$ and $k_3 \geq 0$.

Corollary 1

If either $\gamma(\underline{h}_s,0)$ or $\gamma(\underline{0},h_t)$ is unbounded, then there exists no k that satisfies

$$0 < k \leq \frac{1}{\max\{sill(\gamma(\underline{h}_s,0)); sill(\gamma(\underline{0},h_t))\}} \qquad \text{(A.4-1)}$$

such that

$$\gamma_{st}(\underline{h}_s,h_t) = \gamma_{st}(\underline{h}_s,0) + \gamma_{st}(\underline{0},h_t) - k\gamma_{st}(\underline{h}_s,0)\gamma_{st}(\underline{0},h_t) \qquad (3.17)$$

is a valid, permissible spatial-temporal semi-variogram.

Proof

This follows from Theorem 1.

Corollary 2

If either $\gamma(\underline{h}_s,0)$ or $\gamma(\underline{0},h_t)$ is unbounded, then (3.12b) is not a valid model for any choice of k_1, k_2 and k_3.

Proof

This is implied by Corollary 1.

Theorem 2

Let $Z(\underline{u}_\alpha, t_\tau)$ represent the second-order stationary spatial-temporal random variable, with the continuous spatial-temporal covariance C_{st} expressed as in (3.12a). By utilizing equations (3.13a) and (3.13b), the following equations are true.

$$\lim_{h_s \to \infty} \lim_{h_t \to \infty} \gamma_{st}(\underline{h}_s, h_t) = C_{st}(\underline{0},0) \tag{A.4-2}$$

$$\lim_{h_s \to \infty} \gamma_{st}(\underline{h}_s,0) = k_s C_s(\underline{0}) \tag{A.4-3}$$

$$\lim_{h_t \to \infty} \gamma_{st}(\underline{0}, \underline{h}_t) = k_t C_t(0) \tag{A.4-4}$$

Proof

Proof of (A.4-2)

(A.4-2) is derived by substituting the continuity of C_{st}

$$\lim_{h_s \to \infty} \lim_{h_t \to \infty} C_{st}(\underline{h}_s, h_t) = 0 \tag{A.4-5}$$

into the equation that defines the relationship between the semi-variogram and covariance (3.19a).

Proof of (A.4-3)

Using the implicit relation of the product-sum model

$$C_{st}(\underline{h}_s,0) = [k_2 + k_1 C_t(0)] C_s(\underline{h}_s) + k_3 C_t(0) \tag{A.4-5}$$

It follows that

$$\lim_{h_s \to \infty} C_{st}(\underline{h}_s,0) = k_3 C_t(0)$$

By applying (3.15c) yields

$$\lim_{h_s \to \infty} \gamma_{st}(\underline{h}_s,0) = C_{st}(\underline{0},0) - \lim_{h_s \to \infty} C_{st}(\underline{h}_s,0) = k_s C_s(\underline{0})$$

Proof of (A.4-4)

Equation A.4-4 is proven in a similar fashion by noting that

$$C_{st}(\underline{0},h_t) = [k_3 + k_1 C_s(\underline{0})]C_t(h_t) + k_2 C_s(\underline{0})$$

and applying (3.15b)

$$\lim_{h_t\to\infty} \gamma_{st}(\underline{0},h_t) = C_{st}(\underline{0},0) - \lim_{h_t\to\infty} C_{st}(\underline{0},h_t) = k_t C_t(0)$$

Equations (3.12b), (3.13a) and (3.13b) are used to simplify $\gamma_{st}(\underline{h}_s,h_t)$ to

$$\gamma_{st}(\underline{h}_s,h_t) = \gamma_{st}(\underline{h}_s,0) + \gamma_{st}(\underline{0},\underline{h}_t) - k\gamma_{st}(\underline{h}_s,0)\gamma_{st}(\underline{0},h_t) \qquad (3.18)$$

where (3.15a) leads to

$$k = \frac{k_s C_s(\underline{0}) + k_t C_t(0) - C_{st}(\underline{0},0)}{k_s C_s(\underline{0}) k_t C_t(0)} = \frac{k_1}{k_s k_t}$$

APPENDIX A.5

ORDINARY KRIGING WEIGHTING CONDITION

(*Isaaks and Srivastava, 1989*)

The estimated value of the missing observation is defined by (4.1). The difference between the estimate and the true value is expressed as

$$\tilde{R}(\underline{u}_0) = \hat{Z}(\underline{u}_0) - Z(\underline{u}_0) \tag{A.5-1}$$

Substituting (4.1) into (A.5-1) yields

$$\tilde{R}(\underline{u}_0) = \sum_{\alpha=1}^{n} \lambda_a Z(\underline{u}_\alpha) - Z(\underline{u}_0) \tag{A.5-2}$$

Equation (A.5-2) is completely expressed in terms of the original $n+1$ random variables. By taking the expected value, equation (A.5-2) changes to

$$\begin{aligned} E[\tilde{R}(\underline{u}_0)] &= E[\sum_{\alpha=1}^{n} \lambda_\alpha Z(\underline{u}_\alpha) - Z(\underline{u}_0)] \\ &= \sum_{\alpha=1}^{n} \lambda_\alpha E[Z(\underline{u}_\alpha)] - E[Z(\underline{u}_0)] \end{aligned} \tag{A.5-3}$$

with $E[\tilde{R}(\underline{u}_0)]$ also known as the bias. As the data are assumed to be stationarity, (A.5-3) can be expressed as

$$E[\tilde{R}(\underline{u}_0)] = \sum_{\alpha=1}^{n} \lambda_\alpha E[Z(\underline{u}_\alpha)] - E[Z(\underline{u}_\alpha)] \tag{A.5-4}$$

To ensure an unbiased estimator, the bias is set to zero, which yields the condition of (4.2).

$$E[\tilde{R}(\underline{u}_0)] = 0 = \sum_{\alpha=1}^{n} \lambda_\alpha E[Z(\underline{u}_\alpha)] - E[Z(\underline{u}_\alpha)]$$

$$\sum_{\alpha=1}^{n} \lambda_\alpha E[Z(\underline{u}_\alpha)] = E[Z(\underline{u}_\alpha)]$$

$$\sum_{\alpha=1}^{n} \lambda_\alpha = 1$$

APPENDIX A.6

LAGRANGE MULTIPLIER

Lagrange multipliers are useful when the researcher wants to determine the minimum or maximum of a function $f(x, y, z)$ that is subject to the constraint $g(x, y, z) = k$. This constraint can be an equation that describes the boundary of the region. To better explain the multiplier, we revert to general notation.

Translated to the kriging equations, λ_α is chosen such that the mean square error is minimized under the constraint that $\sum \lambda_\alpha = 1$.

The general problem can be expressed as

$$\min f(\lambda_\alpha) \text{ for } \alpha = 1,...,n \tag{A.6-1}$$

That is subjected to certain constraints

$$g_k(\lambda_\alpha) = b_k \text{ for } k = 1,..,p \tag{A.6-2}$$

Equations (A.6-1) and (A.6-2) represent a constrained optimization problem that can be solved with the aid of Lagrange multipliers.

The steps to determine the Lagrange multipliers are

1. The Lagrangian is defined in terms of the weights and the multipliers (A.6-3)

$$L(\lambda_1,\lambda_2,\cdots,\lambda_n,,\varphi_1,\varphi_2,\cdots,\varphi_p)$$
$$= f(\lambda_1,\lambda_2,\cdots,\lambda_n) + 2\varphi_1\{g_1(\lambda_1,\lambda_2,\cdots,\lambda_n) - b_1\} + \cdots + 2\varphi_p\{g_p(\lambda_1,\lambda_2,\cdots,\lambda_n) - b_p\}$$

The constant 2 is used for convenience.

2. The derivatives of L with respect to $\lambda_1, \lambda_2,..., \lambda_n$ and $\varphi_1, \varphi_2,..., \varphi_p$ are taken and

set to zero, as seen in equations (A.6-4) and (A.6-5)

$$\frac{\partial f}{\partial \lambda_i} + 2\varphi_1 \frac{\partial g_1}{\partial \lambda_i} + ... + 2\varphi_p \frac{\partial g_p}{\partial \lambda_i} = 0 \quad \text{with } i = 1,2,...,n \tag{A.6-4}$$

$$g_k = b_k \text{ with } k = 1,2,..., p \tag{A.6-5}$$

3. The $n \times p$ equations defined in (A.6-4) and (A.6-5) are solved.

The method of Lagrange multipliers therefore achieve the objective of ordinary kriging as set out in equations 4.8, 4.12 and 4.13.

More general examples on the functionality of the Lagrange multiplier can be found on the website http://tutorial.math.lamar.edu/Classes/CalcIII/LagrangeMultipliers.aspx

APPENDIX B

SAS PROGRAMS

CONTENTS

APPENDIX B.1

SIMULATED DATA

```
DEFINE THE 100x100 GRID
DATA lib.grid;
INPUT i x y @@;
CARDS;
1     10    10    2     10    20    3     10    30    4     10    40
. . .
97    100   70    98    100   80    99    100   90    100   100   100;
RUN;

PROC IML;
USE grid;
READ all INTO x; xmat=x[,2:3];

START eucdist(xmat,rowname,DMAT);
m=nrow(xmat);
DMAT=j(m,m,0);

DO j=1 TO m BY 1;
DO k=1 TO m BY 1;
DMAT[k,j] =((xmat[k,]-xmat[j,])*(xmat[k,]-xmat[j,])`)##0.5;
END;
END;
FINISH eucdist;
CALL eucdist(xmat,rowname,DMAT);

rmat=exp((-1/50)*dmat);
GENERATING SIGMA MATRICES FOR THE VMA(4) TIME SERIES
sigmaA={ 1.0  0.5, 0.5   0.9};
theta1={ 0.9 -0.1,-0.1  -0.4};      theta2={ 0.4  0.0, 0.9   0.4};
theta3={ 0.6  0.3, 0.6  -0.1};      theta4={-0.6 -0.7,-0.75  0.6};
teta=theta1//theta2//theta3//theta4;
gamma0=sigmaA + theta1*sigmaA*theta1` + theta2*sigmaA*theta2` +
       theta3*sigmaA*theta3` + theta4*sigmaA*theta4`;
gamma1=theta1*sigmaA + theta2*sigmaA*theta1` + theta3*sigmaA*theta2`
       + theta4*sigmaA*theta3`;
gamma2=theta2*sigmaA + theta3*sigmaA*theta1` + theta4*sigmaA*theta2`;
gamma3=theta3*sigmaA + theta4*sigmaA*theta1`;

gamma4=theta4*sigmaA;
THE REST OF THE SIGMA'S ARE EQUAL TO ZERO
gammaL ={0 0,0 0};
gamma_mat=
gamma0||gamma1||gamma2||gamma3||gamma4||(gammaL`*j(25*2,2,1)`);

2n x 2n TOEPLITZ MATRIX
      sigmaAT=toeplitz(gamma_mat);
      sigma=rmat@sigmaAT;

GENERATE X~N(mean, sigmaATS)
      z=rannor(j(nrow(sigma),1,0));
      v=half(sigma);
      xvec=v`*z+100;
CREATE lib.rmat          FROM rmat;          APPEND FROM rmat;
CREATE lib.sigmaAT       FROM sigmaAT;       APPEND FROM sigmaAT;
CREATE lib.sigma         FROM sigma;         APPEND FROM sigma;
CREATE lib.Xvec          FROM Xvec;          APPEND FROM Xvec;
```

```
QUIT;

PROC IML;
USE lib.xvec ; READ all INTO xvec;
USE grid;      READ all INTO xmat;

time={1,2,3,4,5,6,7,8,9,10,11,12,13,14,15,16,17,18,19,20,21,22,23,24,
      25,26,27,28,29,30};
t1=j(nrow(time),1,1);

SPLIT DATA INTO THE STATION
OBS 1 TO 30 IS STATION1 (ATT1) AND OBS 31-60 IS THE STATION (ATT2)
JOIN TIME OBSERVATIONS, COORDINATES AND STATION NAME
e.g.
tS1A1=
time||Xvec[1:30,]||(xmat[1,1]*t1)||(xmat[1,2]*t1)||(xmat[1,3]*t1);

CREATE tS1A1 FROM tS1A1; APPEND FROM tS1A1;
QUIT;

%MACRO rename(station,att);
data lib.ts&station.a&att;
set  ts&station.a&att;
time=col1;
z&att.=col2;
station=col3;
x=col4 ;
y=col5;
drop col1-col5;
run;
%MEND;
e.g.
%rename(1,1);%rename(1,2);%rename(2,1);%rename(2,2);%rename(3,1);

DATA lib.st_comz1;
SET
lib.ts1a1 lib.ts2a1 lib.ts3a1 lib.ts4a1 lib.ts5a1 lib.ts6a1 lib.ts7a1
. . .
lib.ts98a1  lib.ts99a1 lib.ts100a1;
RUN;

DATA lib.st_comz2;
SET
lib.ts1a2 lib.ts2a2 lib.ts3a2 lib.ts4a2 lib.ts5a2 lib.ts6a2 lib.ts7a2
. . .
lib.ts98a2 lib.ts99a2 lib.ts100a2;
RUN;

PROC SORT DATA = lib.st_comz1; BY time station; RUN;
PROC SORT DATA = lib.st_comz2; BY time station; RUN;

SPATIAL-TEMPORAL DATA SET OF 100 LOCATIONS AND 30 TIME OBSERVATIONS
DATA lib.ST_COM;
MERGE lib.st_comz1 lib.st_comz2;
BY time station;
RUN;
SPATIAL-TEMPORAL DATA SET OF 100 LOCATIONS AND 1 TIME OBSERVATIONS
DATA lib.S_COM;
SET lib.ST_COM;
IF time=1;
RUN;
```

APPENDIX B.2

EXAMPLE 2-1

```
DESCRIPTIVE STATISTICS – SPATIAL DATA
HISTOGRAM & CORRELATION
PROC UNIVARIATE DATA = orig.S_COM;
HISTOGRAM/NORMAL;
VAR z1;
OUTPUT OUT = lib.s_com_z1
CV=COEFVAR
KURTOSIS=KURTOSIS
MAX=MAX
MEAN=MEAN
MIN=MIN
MODE=MODE
N=NUMBEROBS
RANGE=RANGE
SKEWNESS=SKEWNESS
STD=STD
VAR=VAR
Q1=Q1
MEDIAN=MEDIAN
Q3=Q3
QRANGE=QRANGE
STD_QRANGE=STD_QRANGE
P10=P10 P90=P90 P95=P95 P99=P99
NORMAL=NORMALTEST;
RUN;
THE SAME PROCEDURE IS FOLLOWED FOR Z2

DETERMINE THE CORRELATION BETWEEN Z1&Z2
ODS GRAPHICS ON;
PROC CORR DATA=orig.s_com nomiss plots=matrix(histogram);
VAR z1 z2;
RUN;
ODS GRAPHICS OFF;
```

APPENDIX B.3

EXAMPLE 2-3

```
CONTOUR MAPPING
PROC SQL;
CREATE TABLE create TABLE s_com
AS SELECT y,x,z1
FROM lib.s_com;
QUIT;

PROC GCONTOUR DATA = lib.s_com;
PLOT y*x=z1/LEVELS=97.74 TO 105.22 BY 0.5 SMOOTH;
run;

PROC GCONTOUR DATA = lib.s_com;
PLOT y*x=z2/LEVELS=95.55 TO 103.75 BY 0.5 SMOOTH;
run;
```

APPENDIX B.4

EXAMPLE 2-5

```
DESCRIPTIVE STATISTICS - SPATIAL DATA
MOVING WINDOWS STATISTICS
```

```
DUMP OUT SPECIFIC WINDOWS
```

```
DATA lib.window1 lib.window2 lib.window3 lib.window4 lib.window5
     lib.window6 lib.window7 lib.window8 lib.window9;
SET  orig.s_com;
IF station in (1,2,3,4,11,12,13,14,21,22,23,24,31,32,33,34)THEN
OUTPUT lib.window1;
IF station in (4,5,6,7,14,15,16,17,24,25,26,27,34,35,36,37) THEN
OUTPUT lib.window2;
IF station in (7,8,9,10,17,18,19,20,27,28,29,30,37,38,39,40) THEN
OUTPUT lib.window3;
IF station in (31,32,33,34, 41,42,43,44, 51,52,53,54,61,62,63,64)
THEN OUTPUT lib.window4;
IF station in (34,35,36,37,44,45,46,47,54,55,56,57,64,65,66,67) THEN
OUTPUT lib.window5;
IF station in (37,38,39,40,47,48,49,50, 57,58,59,60,67,68,69,70) THEN
OUTPUT lib.window6;
IF station in (61,62,63,64,71,72,73,74,81,82,83,84,91,92,93,94) THEN
OUTPUT lib.window7;
IF station in (64,65,66,67, 74,75,76,77,84,85,86,87, 94,95,96,97)
THEN OUTPUT lib.window8;
IF station in (67,68,69,70,77,78,79,80,87,88,89,90,97,98,99,100) THEN
OUTPUT lib.window9;
RUN;
```

```
SUMMARY STATISTICS OF THE MOVING WINDOWS
```

```
%MACRO mws2(window,in,var);
proc univariate data = lib.&window normaltest;
histogram/normal;
var &var;
output out=sum_&in.&var MEAN=MEAN STD=STD;
run;

data  sum_&in.&var._2;
set sum_&in.&var;
format att $4.;
att="&in";
mean=MEAN;
std=STD;
keep  att mean std;
run;
%MEND;

%mws2(window1,w1,z1);%mws2(window2,w2,z1);%mws2(window3,w3,z1);
%mws2(window4,w4,z1);%mws2(window5,w5,z1);%mws2(window6,w6,z1);
%mws2(window7,w7,z1);%mws2(window8,w8,z1);%mws2(window9,w9,z1);

DATA window_z1;
SET sum_w1z1_2    sum_w2z1_2  sum_w3z1_2  sum_w4z1_2  sum_w5z1_2
    sum_w6z1_2    sum_w7z1_2  sum_w8z1_2  sum_w9z1_2;
RUN;

PROC SQL;
CREATE TABLE lib.window_z1
```

```
AS SELECT att, mean, std
FROM window_z1;
QUIT;
```

SUMMARY STATISTICS

```
%MACRO mws(name,out) ;
ODS GRAPHICS ON;
   PROC CORR DATA=lib.&name out=&out
                        nomiss
                        plots=matrix(histogram);
      VAR z1 z2;
   RUN;
ODS GRAPHICS OFF;
%MEND;

%mws(window1,ws1);%mws(window2,ws2);%mws(window3,ws3);
%mws(window4,ws4);%mws(window5,ws5);%mws(window6,ws6);
%mws(window7,ws7);%mws(window8,ws8);%mws(window9,ws9);
```

THE EXACT SAME CODE IS USED FOR Z2

The SAME PROCEDURES ARE FOLLOWED FOR THE 4 GROUP MOVING WINDOWS

APPENDIX B.5

EXAMPLE 2-8

```
H-SCATTER PLOT - Z1
%MACRO z(station, att);
data ts&station.a&att;
set orig.ts&station.a&att;
IF time=1;
col&station=z&att;
KEEP time col&station;
RUN;
%MEND;

CREATE DATA SETS PER STATION PER ATTRIBUTE

%z(1,1);%z(1,2);
%z(2,1);%z(2,2);
. . .
%z(100,1);%z(100,2);

%MACRO hscatter(s1,s2,col1,col2,m,d);
data &s1._&s2._&m._&d;
merge &s1  &s2;
by time;
run;

data &s1._&s2._&m._&d;
set &s1._&s2._&m._&d;
c1=COL&col1;
c2=COL&col2;
drop COL&col1 COL&col2;
run;
%MEND;

CREATE TABLES THATCONTAINS THE DATA FOR EACH DIRECTION AND LAG
DISTANCES (0m TO 50m APART)
i.e. In the horizontal distance at 10 meters apart, create the table
that contain the observation for:
station 1 vs station 11
station 2 vs station 21
station 3 vs station 31
station 4 vs station 41 etc.
e.g
Z1 - HORIZONTAL 10M
%hscatter(ts1a1,ts11a1,1,11,10,0);
%hscatter(ts11a1,ts21a1,11,21,10,0);
. . .
%hscatter(ts80a1,ts90a1,80,90,10,0);
%hscatter(ts90a1,ts100a1,90,100,10,0);

DATA lib.H10mz1;SET
ts1a1_ts11a1_10_0       ts11a1_ts21a1_10_0
. . .
ts80a1_ts90a1_10_0      ts90a1_ts100a1_10_0
;RUN;


TO
Z1 - DIAGONAL 50M
```

```
%hscatter(ts5a1,ts60a1,5,60,50,45);
%hscatter(ts4a1,ts59a1,4,59,50,45);
. . .
%hscatter(ts42a1,ts97a1,42,97,50,45);
%hscatter(ts41a1,ts96a1,41,96,50,45);

DATA lib.D50mz1;SET
ts5a1_ts60a1_50_45      ts4a1_ts59a1_50_45
. . .
ts42a1_ts97a1_50_45     ts41a1_ts96a1_50_45
;RUN;
```

IDENTICAL CODE FOR Z2

APPENDIX B.6

EXAMPLE 2-9

```
CROSS H-SCATTERPLOTS
%MACRO z(station, att);
data ts&station.a&att;
set orig.ts&station.a&att;
IF time=1;
col&station=z&att;
KEEP time col&station;
RUN;
%MEND;
CREATE DATA SETS PER STATION PER ATTRIBUTE
%z(1,1);%z(1,2);
. . .
%z(100,1);%z(100,2);

%MACRO hscatter(s1,s2,col1,col2,m,d);
data &s1._&s2._&m._&d;
merge &s1  &s2;
by time;
run;

data &s1._&s2._&m._&d;
set &s1._&s2._&m._&d;
c1=COL&col1;
c2=COL&col2;
drop COL&col1 COL&col2;
run;
%MEND;
THE SAME PROCEDURE IS FOLLOWED AS WITH Z1 EXCEPT THAT ATTRIBUTE 1
FROM Z1 IS COMPARED TO ATTRIBUTE 2 FROM Z2 AND VISA VERSA
e.g.
Z1Z2 - HORIZONTAL 10M
%hscatter(ts1a1,ts11a2,1,11,10,0);
%hscatter(ts11a1,ts21a2,11,21,10,0);
. . .
%hscatter(ts80a1,ts90a2,80,90,10,0);
%hscatter(ts90a1,ts100a2,90,100,10,0);

data lib.H10mz1z2;set
ts1a1_ts11a2_10_0       ts11a1_ts21a2_10_0
. . .
ts80a1_ts90a2_10_0      ts90a1_ts100a2_10_0
;run;

TO

Z1Z2 - DIAGONAL 50M

IDENTICAL CODE FOR Z2Z1 (CHANGE a1 AND a2 AROUND)
```

APPENDIX B.7

EXAMPLE 2-10

```
%MACRO z(station, att);
data ts&station.a&att;
set orig.ds_com;
time=1;
if station=&station;
col&station._&att=dz&att;
KEEP time col&station._&att ;
RUN;
%MEND;
%z(1,1);%z(1,2);
. . .
%z(100,1);%z(100,2);
```

```
CREATE DATA SETS PER STATION PER ATTRIBUTE
```

```
%MACRO hscatter(a,b,m,d);
data stat&a._stat&b._&m._&d._a1;
merge ts&a.a1
      ts&b.a1;
by time;
run;

data stat&a._stat&b._&m._&d._a1;
set stat&a._stat&b._&m._&d._a1;
c1c2=(COL&a._1-COL&b._1)*(COL&a._1-COL&b._1);
drop  COL&a._1 COL&b._1 ;
run;
%MEND;
```

```
DUMP THE DATA OUT IN THE CORRECT FORMAT FOR VARIOGRAM ESTIMATES
```

```
0M
```

```
%hscatter(1,1,0,0);      %hscatter(2,2,0,0);
. . .
%hscatter(99,99,0,0);    %hscatter(100,100,0,0);

DATA lib.h0a1; SET
stat1_stat1_0_0_a1     stat2_stat2_0_0_a1
. . .
stat99_stat99_0_0_a1   stat100_stat100_0_0_a1
;RUN;
```

```
HORIZONTAL STEP 1
```

```
%hscatter(1,11,10,0);    %hscatter(11,1,10,0);
. . .
%hscatter(90,100,10,0); %hscatter(100,90,10,0);
DATA lib.h10a1; SET
stat1_stat11_10_0_a1    stat11_stat1_10_0_a1
. . .
stat90_stat100_10_0_a1 stat100_stat90_10_0_a1
;RUN;
```

```
DIAGONAL STEP 5
```

```
%hscatter(1,56,50,45);   %hscatter(56,1,50,45);
. . .
%hscatter(45,100,50,45);%hscatter(100,45,50,45);
```

```
DATA lib.d50a1; SET
stat1_stat56_50_45_a1   stat56_stat1_50_45_a1
. . .
stat45_stat100_50_45_a1 stat100_stat45_50_45_a1
;RUN;

READ DATA INTO IML
PROC IML;
USE lib.h10a1;  READ all INTO h10a1;
USE lib.h20a1;  READ all INTO h20a1;
. . .
USE lib.d50a1;  READ all INTO d50a1;

DETERMINE THE GAMMA VALUES
HORIZONTAL
gh0a1=0;
h10a1_sum=sum(h10a1[,2]);
. . .
h50a1_sum=sum(h50a1[,2]);

h10a1_n=nrow(h10a1);
. . .
h50a1_n=nrow(h50a1);

gh10a1=h10a1_sum/(2*h10a1_n);
. . .
gh50a1=h50a1_sum/(2*h50a1_n);
VERTICAL
gv0a1=0;
v10a1_sum=sum(v10a1[,2]);
. . .
v50a1_sum=sum(v50a1[,2]);

v10a1_n=nrow(v10a1);
. . .
v50a1_n=nrow(v50a1);

gv10a1=v10a1_sum/(2*v10a1_n);
. . .
gv50a1=v50a1_sum/(2*v50a1_n);
DIAGONAL
gd0a1=0;
d10a1_sum=sum(d10a1[,2]); d10a1_n=nrow(d10a1);
. . .
d50a1_sum=sum(d50a1[,2]); d50a1_n=nrow(d50a1);

gd10a1=d10a1_sum/(2*d10a1_n);
. . .
gd50a1=d50a1_sum/(2*d50a1_n);

A1=(gh0a1//. .//gh50a1)||(gv0a1//. .//gv50a1)||(gd0a1//..//gd50a1);
A2=(gh0a2//. .//gh50a2)||(gv0a2//. .//gv50a2)||(gd0a2//..//gd50a2);
A1A2=(gh0a1a2//..gh50a1a2)||(gv0a1a2//..gv50a1a2)||(gd0a1a2//..gd50a1
a2);
A2A1=(gh0a2a1//..gh50a2a1)||(gv0a2a1//..gv50a2a1)||(gd0a2a1//..gd50a2
a1);
CREATE lib.A1_DIR FROM A1; APPEND FROM A1;
QUIT;
```

APPENDIX B.8

EXAMPLE 2-11

```
%MACRO z(station, att);
data ts&station.a&att;
set orig.ds_com;
time=1;
if station=&station;
col&station._&att=dz&att;
KEEP time col&station._&att ;
RUN;
%MEND;
%z(1,1);%z(1,2);
. . .
%z(100,1);%z(100,2);

%MACRO hscatter(a,b,m,d);
data stat&a._stat&b._&m._&d._a1a2;
merge ts&a.a1  ts&a.a2  ts&b.a1   ts&b.a2;
by time;
run;

data stat&a._stat&b._&m._&d._a1a2;
set stat&a._stat&b._&m._&d._a1a2;
c1c2=(COL&a._1-COL&b._1)*(COL&a._2-COL&b._2);
drop  COL&a._1 COL&b._1 COL&a._2 COL&b._2;
run;%MEND;
```

THE MACRO STATEMENTS ARE THE SAME AS APPENDIX B.7.

```
PROC IML;
USE lib.h0a1a2;  READ all INTO h0a1a2;
USE lib.h10a1a2;  READ all INTO h10a1a2;
. . .
USE lib.d40a2a1;  READ all INTO d40a2a1;
USE lib.d50a2a1;  READ all INTO d50a2a1;

gh0a1a2=0;
h10a1a2_sum=sum(h10a1a2[,2]);
h10a1a2_n=nrow(h10a1a2);
gh10a1a2=h10a1a2_sum/(2*h10a1a2_n);

      TO

d50a1a2_sum=sum(d50a1a2[,2]);
d50a1a2_n=nrow(d50a1a2);
gd50a1a2=d50a1a2_sum/(2*d50a1a2_n);
```

CODE FOR Z2Z1 IS SIMILAR

```
A1  =(gh0a1//..//gh50a1)||(gv0a1//..//gv50a1)||(gd0a1//..//gd50a1);
A2  =(gh0a2//..//gh50a2)||(gv0a2//..//gv50a2)||(gd0a2//..//gd50a2);
A1A2=(gh0a1a2//.//gh50a1a2)||(gv0a1a2//.//gv50a1a2)||
     (gd0a1a2//.//gd50a1a2);
A2A1=(gh0a2a1//..//gh50a2a1)||(gv0a2a1//..//gv50a2a1)||(gd0a2a1//..//
      gd50a2a1);
CREATE lib.A1_DIR FROM A1; APPEND FROM A1;
. . .
CREATE lib.A2A1_DIR     FROM A2A1;  APPEND FROM A2A1;
QUIT;
```

APPENDIX B.9

EXAMPLE 2-12

```
%MACRO z(station, att);
data ts&station.a&att;
set orig.comz&att;
if station=&station;
col&station._&att=z&att;
KEEP time col&station._&att ;
RUN;
%MEND;
%z(1,1);%z(1,2);
. . .
%z(100,1);%z(100,2);

%MACRO hscatter(a,b,m,d);
data stat&a._stat&b._&m._&d._a1;
merge ts&a.a1        ts&b.a1;
by time;
run;

data stat&a._stat&b._&m._&d._a1;
set stat&a._stat&b._&m._&d._a1;

l0=(COL&a._1-COL&b._1)*(COL&a._1-COL&b._1);
l1=(COL&a._1-lag1(COL&b._1))*(COL&a._1-lag1(COL&b._1));
. . .
l15=(COL&a._1-lag15(COL&b._1))*(COL&a._1-lag15(COL&b._1));
drop  COL&a._1 COL&b._1 ;
run;
%MEND;
```

```
THE MACRO STATEMENTS ARE THE SAME AS APPENDIX B.7.
```

```
PROC IML;
USE lib.h0a1;   READ all INTO h0a1;
. . .
USE lib.d50a1;  READ all INTO d50a1;

*0m;
*t0; sum_0t0=sum(h0a1[,2]); n_0t0=-0*(nrow(h0a1)/30)+nrow(h0a1);
*t1; sum_0t1=sum(h0a1[,3]); n_0t1=-1*(nrow(h0a1)/30)+nrow(h0a1);
. . .
*t15;sum_0t15=sum(h0a1[,17]);n_0t15=-15*(nrow(h0a1)/30)+nrow(h0a1);

g0t0 =sum_0t0/(2*n_0t0);    g0t1 =sum_0t1/(2*n_0t1);
. . .
g0t14=sum_0t14/(2*n_0t14);  g0t15=sum_0t15/(2*n_0t15);

G0Ta1=g0t0//. . . //g0t15;
```

```
THE SAME CODE IS APPLICABLE FOR :
Horizontal, Vertical and Diagonal at 10m, 20m, 30m, 40m, 50m,
```

```
A1horizontal= G0Ta1||Gh10Ta1||Gh20Ta1||Gh30Ta1||Gh40Ta1||Gh50Ta1;
A1vertical  = G0Ta1||Gv10Ta1||Gv20Ta1||Gv30Ta1||Gv40Ta1||Gv50Ta1;
A1diagonal  = G0Ta1||Gd10Ta1||Gd20Ta1||Gd30Ta1||Gd40Ta1||Gd50Ta1;
CREATE lib.A1_HOR FROM A1horizontal; APPEND FROM A1horizontal;
CREATE lib.A1_VER FROM A1horizontal; APPEND FROM A1horizontal;
CREATE lib.A1_DIA FROM A1horizontal; APPEND FROM A1horizontal;
QUIT;
```

APPENDIX B.10

EXAMPLE 2-13

```
%MACRO z(station, att);
data ts&station.a&att;
set orig.comz&att;
if station=&station;
col&station._&att=z&att;
KEEP time col&station._&att ;
RUN;
%MEND;

%z(1,1); %z(1,2);
…
%z(100,1);%z(100,2);

%MACRO hscatter(a,b,m,d);
data stat&a._stat&b._&m._&d._a1a2;
merge ts&a.a1
      ts&a.a2
      ts&b.a1
      ts&b.a2;
by time;
run;

data stat&a._stat&b._&m._&d._a1a2;
set stat&a._stat&b._&m._&d._a1a2;
l0=(COL&a._1-COL&b._1)*(COL&a._2-COL&b._2);
l1=(COL&a._1-lag1(COL&b._1))*(COL&a._2-lag1(COL&b._2));
l2=(COL&a._1-lag2(COL&b._1))*(COL&a._2-lag2(COL&b._2));
l3=(COL&a._1-lag3(COL&b._1))*(COL&a._2-lag3(COL&b._2));
l4=(COL&a._1-lag4(COL&b._1))*(COL&a._2-lag4(COL&b._2));
l5=(COL&a._1-lag5(COL&b._1))*(COL&a._2-lag5(COL&b._2));
l6=(COL&a._1-lag6(COL&b._1))*(COL&a._2-lag6(COL&b._2));
l7=(COL&a._1-lag7(COL&b._1))*(COL&a._2-lag7(COL&b._2));
l8=(COL&a._1-lag8(COL&b._1))*(COL&a._2-lag8(COL&b._2));
l9=(COL&a._1-lag9(COL&b._1))*(COL&a._2-lag9(COL&b._2));
l10=(COL&a._1-lag10(COL&b._1))*(COL&a._2-lag10(COL&b._2));
l11=(COL&a._1-lag11(COL&b._1))*(COL&a._2-lag11(COL&b._2));
l12=(COL&a._1-lag12(COL&b._1))*(COL&a._2-lag12(COL&b._2));
l13=(COL&a._1-lag13(COL&b._1))*(COL&a._2-lag13(COL&b._2));
l14=(COL&a._1-lag14(COL&b._1))*(COL&a._2-lag14(COL&b._2));
l15=(COL&a._1-lag15(COL&b._1))*(COL&a._2-lag15(COL&b._2));

drop  COL&a._1 COL&b._1 COL&a._2 COL&b._2;
run;
%MEND;
```

THE MACRO STATEMENTS ARE THE SAME AS APPENDIX B.7.

THE IML PROCEDURE IS SIMILAR TO THE IML STATEMENT FOR APPENDIX B.9.

APPENDIX B.11

EXAMPLE 2-15

```
DETRENDING SPATIAL DATA
proc sql;
create table s_comz1
as select station,x,y,z1
from orig.s_com;
quit;

proc reg data=s_comz1;
model z1 = x y /selection=stepwise;
output out=gmoutz1 predicted=predz1 residual=Residualz1;
run;
quit;

proc sql;
create table s_comz2
as select station,x,y,z2
from orig.s_com;
quit;

proc reg data=s_comz2;
model z2 = x y /selection=stepwise;
output out=gmoutz2 predicted=predz2 residual=Residualz2;
run;
quit;

data lib.ds_comz1;
set  s_comz1;
tz1=  98.76752+0.01453*x+0.04187*y;
dz1=z1-tz1;
run;

data lib.ds_comz2;
set  s_comz2;
tz2=  102.96153-0.03689*x-0.01880*y;
dz2=z2-tz2;
run;

proc sort data = lib.ds_comz2; by station x y; run;
proc sort data = lib.ds_comz1; by station x y; run;

data lib.ds_com;
merge lib.ds_comz1 lib.ds_comz2;
by station  x y;
run;
```

```
DETRENDING SPATIAL-TEMPORAL DATA
PROC SQL;
CREATE TABLE st_comz1
AS SELECT station, time, z1
FROM orig.st_comz1;
QUIT;
proc sort data = st_comz1; by station time; run;
```

```
ASSIGN ARBITRARY DATES FOR DETRENDING PURPOSES

data  st_comz1;
set st_comz1;
```

```
format date date9.;
     if time = 1  then date = '01SEP2009'd;
else if time = 2  then date = '02SEP2009'd;
. . .
else if time = 30 then date = '30SEP2009'd;
run;

proc timeseries data=st_comz1 outdecomp=decomp1 ;
by station;
decomp TCC/mode=add ;
id date interval=day accumulate=total;
var z1;
run;

data decomp1;
set decomp1;
keep station  date tcc;
proc sort;  by station date;  run;

proc sort data =  st_comz1;  by station date;  run;

data st_comz1;
merge st_comz1 decomp1;
by station date;
run;

data lib.comz1;
set st_comz1;
if tcc ne . then z = tcc;
else z=z1;
tz1=z1-z;
run;

PROC SQL;
CREATE TABLE st_comz2
AS SELECT station, time, z2
FROM orig.st_comz2;
QUIT;
```

DE-TREND Z2 IN THE SAME MANNER

APPENDIX B.12

EXAMPLE 2-17

```
THE CODE USED IN APPENDIX B.7 AND APPENDIX B.8 IS APPLIED TO THE DE-
TRENDED SPATIAL DATA.
```

```
CODE FOR OMNIDIRECTIONAL SEMI-VARIOGRAM
```

```
PROC IML;
USE lib.h10a1;  READ all INTO h10a1;
. . .
USE lib.d50a1;  READ all INTO d50a1;

M10a1=h10a1//v10a1//d10a1;
. . .
M50a1=h50a1//v50a1//d50a1;

M10a1_sum=sum(M10a1[,2]);
. . .
M50a1_sum=sum(M50a1[,2]);

M10a1_n=nrow(M10a1);
. . .
M50a1_n=nrow(M50a1);

g_M10a1=M10a1_sum/(2*M10a1_n);
. . .
g_M50a1=M50a1_sum/(2*M50a1_n);

A1=0//g_M10a1//g_M20a1//g_M30a1//g_M40a1//g_M50a1;
A2=0//g_M10a2//g_M20a2//g_M30a2//g_M40a2//g_M50a2;

CREATE lib.A1_OMN FROM A1; APPEND FROM A1;
QUIT;
```

APPENDIX B.13

EXAMPLE 3-1

```
DATA grid;
INPUT i x y @@;
CARDS;
1   10 10
2   10 20
. . .
99   100 90
100 100 100
;RUN;

PROC IML;
USE grid;    READ all INTO x; xmat=x[,2:3];

START eucdist(xmat,rowname,DMAT);
m=nrow(xmat);
DMAT=j(m,m,0);

DO j=1 TO m BY 1;
DO k=1 TO m BY 1;
DMAT[k,j] =((xmat[k,]-xmat[j,])*(xmat[k,]-xmat[j,])`)##0.5;
END;
END;

FINISH eucdist;
CALL eucdist(xmat,rowname,DMAT);

DETERMINE THE VARIOGRAM MATRIX USING DMAT
START rho(dmat,rowname,rhoMAT);
m=nrow(dmat);
rhoMAT=j(m,m,0);

DO j=1 TO m BY 1;
DO k=1 TO m BY 1;
if dmat[j,k]<=10 THEN
      rhoMAT[k,j]=-0.04*((3*dmat[j,k])/20)+0.02
      *(dmat[j,k]*dmat[j,k]*dmat[j,k])/1000;
ELSE  rhoMAT[k,j] =-0.06+0.002649*dmat[j,k];
END;
END;

FINISH rho;
CALL rho(dmat,rowname,rhoMAT);
g=inv(rhoMAT) ;
g1=eigval(rhoMAT);

sum1=g1*g1`;
sum2=rhoMAT*sum1`;


sum3=sum(sum2);
QUIT;
```

APPENDIX B.14

EXAMPLE 3-2

```
*GAMMA(Hs,0);
%MACRO z(station, att);
data ts&station.a&att;
set orig.comz&att;
if station=&station;
col&station._&att=z;
KEEP time col&station._&att ;
RUN;
%MEND;
%z(1,1); %z(1,2);
...
%z(100,1);%z(100,2);


%MACRO hscatter(a,b,m,d);
data stat&a._stat&b._&m._&d._a1;
merge ts&a.a1
      ts&b.a1;
by time;
run;

data stat&a._stat&b._&m._&d._a1;
set stat&a._stat&b._&m._&d._a1;
c1c2=(COL&a._1-COL&b._1)*(COL&a._1-COL&b._1);
drop  COL&a._1 COL&b._1 ;
run;
%MEND;
```

```
THE MACRO STATEMENTS ARE THE SAME AS APPENDIX B.7.
```

```
PROC IML;
```

```
Z1
USE lib.h10a1;  READ all INTO h10a1;
USE lib.h20a1;  READ all INTO h20a1;
. . .
USE lib.d40a1;  READ all INTO d40a1;
USE lib.d50a1;  READ all INTO d50a1;

M10a1=h10a1//v10a1//d10a1;
. . .
M50a1=h50a1//v50a1//d50a1;

M10a1_sum=sum(M10a1[,2]);
. . .
M50a1_sum=sum(M50a1[,2]);

M10a1_n=nrow(M10a1);
. . .
M50a1_n=nrow(M50a1);

g_M10a1=M10a1_sum/(2*M10a1_n);
. . .
g_M50a1=M50a1_sum/(2*M50a1_n);
```

```
THE SAME CODE IS USED FOR Z2, Z1Z2 & Z2Z1
A1   =0//g_M10a1//g_M20a1//g_M30a1//g_M40a1//g_M50a1;
A2   =0//g_M10a2//g_M20a2//g_M30a2//g_M40a2//g_M50a2;
A1A2 =0//g_M10a1a2//g_M20a1a2//g_M30a1a2//g_M40a1a2//g_M50a1a2;
```

```
A2A1 =0//g_M10a2a1//g_M20a2a1//g_M30a2a1//g_M40a2a1//g_M50a2a1;
CREATE lib.A1_OMN       FROM A1;    APPEND FROM A1;
CREATE lib.A2_OMN       FROM A2;    APPEND FROM A2;
CREATE lib.A1A2_OMN     FROM A1A2;  APPEND FROM A1A2;
CREATE lib.A2A1_OMN     FROM A2A1;  APPEND FROM A2A1;
QUIT;
```

GAMMA(0,Ht)

```
%MACRO hscatter(a,b,m,d);
data stat&a._stat&b._&m._&d._a1;
merge ts&a.a1
      ts&b.a1;
by time;
run;

data stat&a._stat&b._&m._&d._a1;
set stat&a._stat&b._&m._&d._a1;

l0=(COL&a._1-COL&b._1)*(COL&a._1-COL&b._1);
l1=(COL&a._1-lag1(COL&b._1))*(COL&a._1-lag1(COL&b._1));
. . .
l15=(COL&a._1-lag15(COL&b._1))*(COL&a._1-lag15(COL&b._1));
drop  COL&a._1 COL&b._1 ;
run;
%MEND;
%hscatter(1,1,0,0);
. . .
%hscatter(99,99,0,0);
%hscatter(100,100,0,0);

DATA lib.h0a1; SET
stat1_stat1_0_0_a1    stat2_stat2_0_0_a1
. . .
stat99_stat99_0_0_a1  stat100_stat100_0_0_a1 ;
RUN;

PROC IML;
USE lib.h0a1;  READ all INTO h0a1;
*0m;
*t0; sum_0t0=sum(h0a1[,2])  ; n_0t0=-0*(nrow(h0a1)/30)  +nrow(h0a1);
*t1; sum_0t1=sum(h0a1[,3])  ; n_0t1=-1*(nrow(h0a1)/30)  +nrow(h0a1);
. . .
*t14;sum_0t14=sum(h0a1[,16]);n_0t14=-14*(nrow(h0a1)/30)+nrow(h0a1);
*t15;sum_0t15=sum(h0a1[,17]);n_0t15=-15*(nrow(h0a1)/30)+nrow(h0a1);

g0t0 =sum_0t0 /(2*n_0t0);     g0t1 =sum_0t1 /(2*n_0t1);
. . .
g0t14=sum_0t14/(2*n_0t14);    g0t15=sum_0t15/(2*n_0t15);

G0Ta1=g0t0//. . . //g0t15;
CREATE lib.A1_H0  FROM G0Ta1; APPEND FROM G0Ta1;
QUIT;
```

SAME PROCEDURE FOR H0A2, H0A1A2 AND H0A2A1

APPENDIX B.15

EXAMPLE 4-1

```
SELECT 15% RANDOM MISSING STATIONS
DATA locations;
INPUT i x y @@;
CARDS;
1      10     10
2      10     20
...
99     100    90
100    100    100
;RUN;

PROC SURVEYSELECT DATA=locations  METHOD = srs
OUT = Ms_com
N = 15
SEED = 0;
ID i;
RUN;

DATA lib.missingloc;
INPUT i x y @@;
CARDS;
11     20     10     14     20     40     17     20     70
18     20     80     22     30     20     23     30     30
25     30     50     36     40     60     38     40     80
59     60     90     60     60     100    69     70     90
80     80     100    90     90     100    100    100    100
;RUN;

DATA lib.MS_COM;
SET orig.ds_com;
IF station in (11,14,17,18,22,23,25,36,38,59,60,69,80,90,100) THEN
DELETE;
run;

DATA z1;
SET orig.ds_comz1;
IF station in (11,14,17,18,22,23,25,36,38,59,60,69,80,90,100) THEN
DELETE;
KEEP station x y z1 tz1 dz1;
RUN;

DATA lib.grid;
INPUT i x y @@;
CARDS;
1      10     10
2      10     20
...
99     100    90
100    100    100
;RUN;
quit;

PROC IML;
USE lib.grid;      READ all INTO x; xmat=x[,2:3];

START eucdist(xmat,rowname,DMAT);
m=nrow(xmat);
```

```
DMAT=j(m,m,0);
DO j=1 TO m BY 1;
DO k=1 TO m BY 1;
DMAT[k,j] =((xmat[k,]-xmat[j,])*(xmat[k,]-xmat[j,])`)##0.5;
END;
END;
FINISH eucdist;

CALL eucdist(xmat,rowname,DMAT);
```

DETERMINE THE VARIOGRAM MATRIX USING DMAT

```
START rho(dmat,rowname,rhoMAT);
m=nrow(dmat);
rhoMAT=j(m,m,0);
DO j=1 TO m BY 1;
DO k=1 TO m BY 1;
IF dmat[j,k]<=30 then
      rhoMAT[k,j] = 1*(((3*dmat[j,k])/60)
      -0.5*((dmat[j,k]*dmat[j,k]*dmat[j,k])/27000));
ELSE  rhoMAT[k,j] = 1;
END;
END;
FINISH rho;

CALL rho(dmat,rowname,rhoMAT);

m1     = rhoMAT[,1:10]||. . . ||rhoMAT[,91:99];
rhoMATm= m1[1:10,]//. . . //m1[91:99,];
matrix = rhoMAT[1:10,]//. . . //rhoMAT[91:99,];
```

CALCULATE LAMDA AND PHI

```
START par(dmat,rhoMATm,rhoMAT,col,rowname,gam0,lamda1,lamda,phi);
m=nrow(rhoMATm);
lamda1=j(m,1,0);
lamda=j(m,1,0);
phi=j(1,1,0);
gam0=j(m,1,0);
one=j(1,m,1);
onep  =one`;
gam0  =
rhoMAT[1:10,col]//. . . //rhoMAT[91:99,col];

lamda1=
gam0+onep*((1-(one*inv(rhoMATm)*gam0))/(one*inv(rhoMATm)*gam0));
lamda =lamda1`*inv(rhoMATm);
phi=-1*(1-one*inv(rhoMATm)*gam0)/(one*inv(rhoMATm)*onep);
FINISH par;

CALL par(dmat,rhoMATm,rhoMAT,11,rowname ,gam0,lamda1,lamda11,phi11);
CALL par(dmat,rhoMATm,rhoMAT,14,rowname ,gam0,lamda1,lamda14 ,phi14);
. . .
CALL par(dmat,rhoMATm,rhoMAT,90,rowname ,gam0,lamda1,amda90 ,phi90);
CALL
par(dmat,rhoMATm,rhoMAT,100,rowname,gam0,lamda1,lamda100,phi100);

LAMDA = lamda11//. . . //lamda100;
PHI   = phi11//. . . //phi100;
```

TEST LAMDA

```
sum11 =sum(lamda11`);   sum14 =sum(lamda14`);
. . .
```

```
sum90 =sum(lamda90`);  sum100=sum(lamda100`);

sum=sum11//. . . //sum100;
```

```
DETERMINE THE INTERPOLATED VALUE
USE z1;     READ all INTO z1;
START system(z1,lamda,phi,row,rowname,LR);
LR = lamda*(z1[,6]+z1[,5]);
FINISH system;

CALL system(z1,lamda11 ,phi11,11,rowname,LR11);
CALL system(z1,lamda14 ,phi14,14,rowname,LR14);
. . .
CALL system(z1,lamda90 ,phi90,90,rowname,LR90);
CALL system(z1,lamda100,phi100,100,rowname,LR100);

INT = LR11//. . . //LR100;
```

```
CALCULATE THE ESTIMATED KRIGING VARIANCE
START var(matrix,lamda,rhoMAT,gam0,col,rowname,sigma);
gam0=matrix[,col];
sigma=gam0`*lamda`;
FINISH var;

CALL var(matrix,lamda11, rhoMAT,gam0,11,rowname,sigma_11 );
CALL var(matrix,lamda14, rhoMAT,gam0,14,rowname,sigma_14 );
. . .
CALL var(matrix,lamda90, rhoMAT,gam0,90,rowname,sigma_90 );
CALL var(matrix,lamda100,rhoMAT,gam0,100,rowname,sigma_100);

sigma=sigma_11//. . . //sigma_100;
CREATE lib.rhoMAT       FROM rhoMAT;       APPEND FROM rhoMAT;
CREATE lib.Interpolated FROM INT;          APPEND FROM INT;
CREATE lib.lamda        FROM lamda;        APPEND FROM lamda;
CREATE lib.phi          FROM phi;          APPEND FROM phi;
CREATE lib.sigma        FROM sigma;        APPEND FROM sigma;
QUIT;
```

APPENDIX B.16

EXAMPLE 5-1

```
DATA z1a;
SET orig.ds_comz1;
IF station in (11,14,17,18,22,23,25,36,38,59,60,69,80,90,100) THEN
DELETE;
KEEP station x y z1 tz1 dz1;
RUN;

DATA z2a;
SET orig.ds_comz2;
KEEP station x y z2 tz2 dz2;
RUN;
PROC SQL;
CREATE TABLE z1 AS SELECT
station,x,y,z1,tz1,dz1
FROM z1a;
QUIT;
PROC SQL;
CREATE TABLE z2 AS SELECT
station,x,y,z2,tz2,dz2
FROM z2a;
QUIT;

DATA lib.grid;
INPUT i x y @@;
CARDS;
1      10     10
2      10     20
...
99     100    90
100    100    100
;RUN;

PROC IML;
USE lib.grid;      READ all INTO x; xmat=x[,2:3];

START eucdist(xmat,rowname,DMAT);
m=nrow(xmat);
DMAT=j(m,m,0);

DO j=1 TO m BY 1;
DO k=1 TO m BY 1;
DMAT[k,j] =((xmat[k,]-xmat[j,])*(xmat[k,]-xmat[j,])`)##0.5;
END;
END;
FINISH eucdist;
CALL eucdist(xmat,rowname,DMAT);

DETERMINE THE Z1 VARIOGRAM MATRIX USING DMAT
START rho1(dmat,rowname,rho1MAT);
m=nrow(dmat);
rho1MAT=j(m,m,0);

DO j=1 TO m BY 1;
DO k=1 TO m BY 1;
IF dmat[j,k]<=30 THEN
      rho1MAT[k,j] = 1*(((3*dmat[j,k])/60)
      -0.5*((dmat[j,k]*dmat[j,k]*dmat[j,k])/27000));
```

```
ELSE  rho1MAT[k,j] = 1;
END;
END;
FINISH rho1;
CALL rho1(dmat,rowname,rho1MAT);

m1 =  rho1MAT[,1:10]||. . . ||rho1MAT[,91:99];

rho11 is a 85*85 matrix
rho11= m1[1:10,]//. . . //m1[91:99,];

DETERMINE THE Z2 VARIOGRAM MATRIX BY USING DMAT
START rho2(dmat,rowname,rho2MAT);
m=nrow(dmat);
rho2MAT=j(m,m,0);

DO j=1 TO m BY 1;
DO k=1 TO m BY 1;
IF dmat[j,k]<=50 THEN
      rho2MAT[k,j] = 2.6*(((3*dmat[j,k])/100)
      -0.5*((dmat[j,k]*dmat[j,k]*dmat[j,k])/125000));
ELSE  rho2MAT[k,j] = 2.6;
END;
END;
FINISH rho2;

CALL rho2(dmat,rowname,rho2MAT);
rho22 is a 100*100 matrix
rho22     =  rho2MAT;

DETERMINE THE Z1Z2 VARIOGRAM MATRIX USING DMAT
START rho12(dmat,rowname,rho12MAT);
m=nrow(dmat);
n=ncol(dmat);
rho12MAT=j(m,n,0);

DO j=1 TO m BY 1;
DO k=1 TO n BY 1;
IF dmat[j,k]<=10 THEN
      rho12MAT[k,j]=-0.04*((3*dmat[j,k])/20)
                    +0.02*(dmat[j,k]*dmat[j,k]*dmat[j,k])/1000;
ELSE
      rho12MAT[k,j] =-0.06+0.002649*dmat[j,k];
END;
END;
FINISH rho12;

CALL rho12(dmat,rowname,rho12MAT);
rho12 is a 85*100 matrix
rho12=rho12MAT[1:10,]//. . . //rho12MAT[91:99,];

DETERMINE THE Z2Z1 VARIOGRAM MATRIX USING DMAT

START rho21(dmat,rowname,rho21MAT);
m=nrow(dmat);
n=ncol(dmat);
rho21MAT=j(m,n,0);

DO j=1 TO m BY 1;
DO k=1 TO n BY 1;
IF dmat[j,k]<=10 THEN
```

```
rho21MAT[k,j]=-0.04*((3*dmat[j,k])/20)
              +0.02*(dmat[j,k]*dmat[j,k]*dmat[j,k])/1000;
ELSE rho21MAT[k,j] =-0.06+0.002649*dmat[j,k];
END;
END;
FINISH rho21;

CALL rho21(dmat,rowname,rho21MAT);
rho21 is a 100*85 matrix
rho21=rho21MAT[,1:10]||. . . ||rho21MAT[,91:99];

DEFINE G
RHO=(rho11||rho12)//(rho21||rho22);

ONE11=j(nrow(rho11),1,1);
ONE22=j(nrow(rho22),1,1);
ZERO11=j(nrow(rho11),1,0);
ZERO22=j(nrow(rho22),1,0);

NUL=j(1,2,0);

A1=ONE11//ZERO22;
A2=ZERO11//ONE22;

G=(RHO||A1||A2)//(ONE11`||ZERO22`||NUL)//(ZERO11`||ONE22`||NUL);

DEFINE B
E=j(1,1,1);
N=j(1,1,0);

REMOVE THOSE THAT ARE MISSING
B11=rho1MAT[1:10,11]//. . . .//rho12MAT[,11]//E//N;
B14=rho1MAT[1:10,14]//. . . //rho12MAT[,14]//E//N;
. . .
B90 =rho1MAT[1:10,90]//. . . //rho12MAT[,90] //E//N;
B100=rho1MAT[1:10,100]//. . . //rho12MAT[,100] //E//N;

CALCULATE LAMDA AND PHI
START par(G,rowname,B,lamda);
m=nrow(B);
lamda=j(m,1,0);
lamda = inv(G)*B;
FINISH par;

CALL par(G,rowname,B11 ,lamda11);  CALL par(G,rowname,B14 ,lamda14);
. . .
CALL par(G,rowname,B90 ,lamda90);  CALL par(G,rowname,B100,lamda100);

LAMDA1=lamda11[1:85,]||. . . ||lamda100[1:85,];
LAMDA2=lamda11[86:185,]||. . . ||lamda100[86:185,];
PHI1  =lamda11[186,]||. . . ||lamda100[186,];
PHI2  =lamda11[187,]||. . . ||lamda100[187,];

TEST LAMDA
sum11_1 =sum(lamda11[1:85,]);  SUM11_2   =sum(lamda11[86:185,]);
. . .
sum100_1=sum(lamda100[1:85,]); SUM100_2  =sum(lamda100[86:185,]);

sum1=sum11_1//. . . //sum100_1;
sum2=sum11_2//. . . //sum100_2;
```

```
DETERMINE THE INTERPOLATED VALUE
USE z1;      READ all INTO z1;
USE z2;      READ all INTO z2;

START system(z1,z2,lamdaz1,lamdaz2,rowname,LR);
LR = lamdaz1`*(z1[,6]+z1[,5]) + lamdaz2`*(z2[,6]+z2[,5]) ;
FINISH system;

CALL system(z1,z2,lamda11[1:85,] ,lamda11[86:185,],rowname,LR11);
CALL system(z1,z2,lamda14[1:85,] ,lamda14[86:185,],rowname,LR14);
. . .
CALL system(z1,z2,lamda90[1:85,] ,lamda90[86:185,],rowname,LR90);
CALL system(z1,z2,lamda100[1:85,],lamda100[86:185,],rowname,LR100);

INT =LR11//LR14//LR17//LR18//LR22//LR23//LR25//LR36//LR38//LR59//LR60
     //LR69//LR80//LR90//LR100;
```

```
CALCULATE THE ESTIMATED KRIGING VARIANCE
START var(B,lamda,rowname,sigma);
sigma=B`*lamda;
FINISH var;

CALL var(B11 ,lamda11 ,rowname,sigma_11 );
CALL var(B14 ,lamda14 ,rowname,sigma_14 );
. . .
CALL var(B90 ,lamda90 ,rowname,sigma_90 );
CALL var(B100,lamda100,rowname,sigma_100);

sigma=
sigma_11//sigma_14//sigma_17//sigma_18//sigma_22//sigma_23//sigma_25/
/sigma_36//sigma_38//sigma_59//sigma_60//sigma_69//sigma_80//sigma_90
//sigma_100;

CREATE lib.rho11        FROM rho11;  APPEND FROM rho11;
CREATE lib.rho12        FROM rho12;  APPEND FROM rho12;
CREATE lib.rho21        FROM rho21;  APPEND FROM rho21;
CREATE lib.rho22        FROM rho22;  APPEND FROM rho22;
CREATE lib.Interpolated FROM INT;    APPEND FROM INT;
CREATE lib.lamda1       FROM lamda1; APPEND FROM lamda1;
CREATE lib.lamda2       FROM lamda2; APPEND FROM lamda2;
CREATE lib.phi1         FROM phi1;   APPEND FROM phi1;
CREATE lib.phi2         FROM phi2;   APPEND FROM phi2;
CREATE lib.sigma        FROM sigma;  APPEND FROM sigma;
QUIT;
```

APPENDIX B.17

EXAMPLE 6-1

```
OPTION COMPRESS = yes;

proc sort data = orig.st_com; by x y time; run;

DATA locations;
INPUT i x y t @@;
CARDS;
1      10     10     1
2      10     10     2
3      10     10     3
..
30     10     10     30
31     10     20     1
...
3000   100    100    30
;RUN;

PROC SURVEYSELECT DATA=locations
METHOD = srs
OUT = Ms_com
N = 450
SEED = 0;
ID i;
RUN;

DATA lib.missingloc;
set MS_com;
RUN;

EDELETE THE RANDOMLY SELECTED VALUES FROM THE STATION
DATA z1;
SET lib.comz1;
     if x=10 and y=10 and time=3 then delete;
else if x=10 and y=10 and time=4 then delete;
. . .
else if x=100 and y=100 and time=21 then delete;
else if x=100 and y=100 and time=29 then delete;
KEEP station x y time z1 muz1 dz1;
RUN;

DATA lib.spacegrid;
INPUT   i x y  @@;
CARDS;
1      10     10
2      10     10
3      10     10
..
3000   100    100
;RUN;
PROC SORT DATA = lib.spacegrid;
BY i;
RUN;

DATA lib.timegrid;
INPUT i time @@;
CARDS;
1      1
```

```
...
29     29
30     30
...
3000   30
;RUN;
PROC SORT DATA = lib.timegrid;
BY i;
RUN;

PROC IML;
USE lib.spacegrid;    READ all INTO x;   xmat=x[,2:3];
USE lib.timegrid;     READ all INTO y;   timemat=y[,2];

SPACE DISTANCE MATRIX BETWEEN STATIONS
START eucdist1(xmat,rowname,DMAT);
m=nrow(xmat);
DMAT=j(m,m,0);

DO j=1 TO m BY 1;
DO k=1 TO m BY 1;
DMAT[k,j] =((xmat[k,]-xmat[j,])*(xmat[k,]-xmat[j,])`)##0.5;
END;
END;

FINISH eucdist1;
CALL eucdist1(xmat,rowname,DMAT);

TIME DISTANCE MATRIX BETWEEN STATIONS
START eucdist2(timemat,rowname,TMAT);
m=nrow(timemat);
TMAT=j(m,m,0);

DO j=1 TO m BY 1;
DO k=1 TO m BY 1;
TMAT[k,j] =((timemat[k,]-timemat[j,])*(timemat[k,]-
timemat[j,])`)##0.5;
END;
END;

FINISH eucdist2;
CALL eucdist2(timemat,rowname,TMAT);

DETERMINE THE VARIOGRAM MATRIX USING DMAT
START rho(dmat,tmat,rowname,rhoMAT);
m=nrow(dmat);
rhoMAT=j(m,m,0);

DO j=1 TO m BY 1;
DO k=1 TO m BY 1;
IF dmat[j,k] <= 50 THEN
rhoMAT[k,j] = 1*(((3*dmat[j,k])/100)
            - 0.5*((dmat[j,k]*dmat[j,k]*dmat[j,k])/125000))
            + 1.27*(1-exp(-(tmat[j,k])/5))
            - 0.74*(1*(((3*dmat[j,k])/100)
            - 0.5*((dmat[j,k]*dmat[j,k]*dmat[j,k])/125000)))
            *(1.27*(1-exp(-(tmat[j,k])/5)));
ELSE
rhoMAT[k,j] = 1
            + 1.27*(1-exp(-(tmat[j,k])/5))
            - 0.74*(1)*(1.27*(1-exp(-(tmat[j,k])/5)));
```

```
END;
END;

FINISH rho;
CALL rho(dmat,tmat,rowname,rhoMAT);

REMOVE THE ROWS AND COLUMNS THAT ARE MISSING
m1= rhoMAT[,1:2]||rhoMAT[,5:7]||rhoMAT[,9:14]||rhoMAT[,16:18]||
. . .
rhoMAT[,2979]||rhoMAT[,2981:2990]||rhoMAT[,2992:2998]||rhoMAT[,3000];

rhoMATm=m1[1:2,]//m1[5:7,]//m1[9:14,]//m1[16:18,]//m1[20:31,]//
. . .
m1[2967:2977,]//m1[2979,]//m1[2981:2990,]//m1[2992:2998,]//m1[3000,];

matrix=rhoMAT[1:2,]//rhoMAT[5:7,]//rhoMAT[9:14,]//rhoMAT[16:18,]//
. . .
rhoMAT[2979,]//rhoMAT[2981:2990,]//rhoMAT[2992:2998,]//rhoMAT[3000,];

rhoMATmI=inv(rhoMATm);

CREATE lib.rhoMATmI   FROM rhoMATmI;     APPEND FROM rhoMATmI;
CREATE lib.matrix     FROM matrix;       APPEND FROM matrix;
CREATE lib.rhoMAT     FROM rhoMAT;       APPEND FROM rhoMAT;
CREATE lib.rhoMATm    FROM rhoMATm;      APPEND FROM rhoMATm;
QUIT;

PROC IML;
USE lib.rhoMATmI; READ all INTO rhoMATmI;
USE lib.matrix;        READ all INTO matrix;
USE lib.rhoMAT;        READ all INTO rhoMAT;

CALCULATE LAMDA AND PHI ONLY FOR THE SELECTED STATIONS IN THE EXAMPLE
START par2(rhoMATmI,matrix,col,rowname,gam0,lamda1,lamda,phi);
      m=nrow(rhoMATmI);

      lamda1 =j(m,1,0);
      lamda  =j(m,1,0);
      phi    =j(1,1,0);
      gam0   =j(m,1,0);
      one    =j(1,m,1);
      onep  =one`;
      gam0  =matrix[,col];
      lamda1=gam0+onep*((1-(one*rhoMATmI*gam0))/(one*rhoMATmI*gam0));
      lamda =lamda1`*rhoMATmI;
      phi=-1*(1-(one*rhoMATmI*gam0))/(one*rhoMATmI*onep);
FINISH par2;

CALL par2(rhoMATmI,matrix,777,rowname,gam0,lamda1,lamda777,phi777);
. . .
CALL
par2(rhoMATmI,matrix,1993,rowname,gam0,lamda1,lamda1993,phi1993);

lamda=lamda777//. . . //lamda1993;
phi=phi777//. . . //phi1993;

DETERMINE THE INTERPOLATED VALUE
USE z1;     READ all INTO z1;

START system(z1,lamda,phi,row,rowname,LR);
LR = lamda*(z1[,6]+z1[,7]);
```

```
FINISH system;

CALL system(z1,lamda777,phi777,777,rowname,LR777);
CALL system(z1,lamda779,phi779,779,rowname,LR779);
CALL system(z1,lamda780,phi780,780,rowname,LR780);
. . .
CALL system(z1,lamda1991,phi1991,1991,rowname,LR1991);
CALL system(z1,lamda1993,phi1993,1993,rowname,LR1993);

INT=
LR777//. . . //LR1993;

CALCULATE THE ESTIMATED KRIGING VARIANCE
START var3(lamda,matrix,gam0,col,rowname,sigma);
gam0  =matrix[,col];
sigma=gam0`*lamda`;
FINISH var3;

CALL var3(lamda777,matrix,gam0,777,rowname,sigma_777);
CALL var3(lamda779,matrix,gam0,779,rowname,sigma_779);
. . .
CALL var3(lamda1991,matrix,gam0,1991,rowname,sigma_1991);
CALL var3(lamda1993,matrix,gam0,1993,rowname,sigma_1993);

SIGMA_1=
sigma_777//. . . //sigma_1993;

CREATE lib.Interpolated FROM INT;     APPEND FROM INT;
CREATE lib.lamda        FROM lamda;   APPEND FROM lamda;
CREATE lib.phi          FROM phi;     APPEND FROM phi;
CREATE lib.sigma        FROM sigma;   APPEND FROM sigma;

QUIT;
```

APPENDIX B.18

EXAMPLE 7-1

```
USE Z1 AND Z2 DETERMINE IN APPENDIX B.17
PROC IML;
USE lib.spacegrid;  READ all INTO x;      xmat=x[,2:3];
USE lib.timegrid;   READ all INTO y;      timemat=y[,2];

SPACE DISTANCE MATRIX BETWEEN STATIONS
START eucdist1(xmat,rowname,DMAT);
m=nrow(xmat);
DMAT=j(m,m,0);

DO j=1 TO m BY 1;
DO k=1 TO m BY 1;
DMAT[k,j] =((xmat[k,]-xmat[j,])*(xmat[k,]-xmat[j,])`)##0.5;
END;
END;
FINISH eucdist1;
CALL eucdist1(xmat,rowname,DMAT);

TIME DISTANCE MATRIX BETWEEN STATIONS
START eucdist2(timemat,rowname,TMAT);
m=nrow(timemat);
TMAT=j(m,m,0);

DO j=1 TO m BY 1;
DO k=1 TO m BY 1;
TMAT[k,j]
        =((timemat[k,]-timemat[j,])*(timemat[k,]-timemat[j,])`)##0.5;
END;
END;
FINISH eucdist2;
CALL eucdist2(timemat,rowname,TMAT);

DETERMINE THE Z1 VARIOGRAM USING DMAT & TMAT
START rho1(dmat,tmat,rowname,rho1MAT);
m=nrow(dmat);
rho1MAT=j(m,m,0);

DO j=1 TO m BY 1;
DO k=1 TO m BY 1;
IF dmat[j,k] <= 50 THEN
rho1MAT[k,j] = 1*(((3*dmat[j,k])/100)-
                 0.5*((dmat[j,k]*dmat[j,k]*dmat[j,k])/125000))
               + 1.27*(1-exp(-(tmat[j,k])/5))
               - 0.74*(1*(((3*dmat[j,k])/100)
               - 0.5*((dmat[j,k]*dmat[j,k]*dmat[j,k])/125000)))
               * (1.27*(1-exp(-(tmat[j,k])/5)));
ELSE
rho1MAT[k,j] = 1
               + 1.27*(1-exp(-(tmat[j,k])/5))
               - 0.74*(1)*(1.27*(1-exp(-(tmat[j,k])/5)));
END;
END;
FINISH rho1;
CALL rho1(dmat,tmat,rowname,rho1MAT);

REMOVE THE COLUMNS THAT ARE MISSING
```

```
m1=rho1MAT[,1:2]||rho1MAT[,5:7]||rho1MAT[,9:14]||rho1MAT[,16:18]||
. . .
rho1MAT[,2981:2990]||rho1MAT[,2992:2998]||rho1MAT[,3000];
```

```
Rho11 IS A 2550 x 2550 MATRIX
rho11=m1[1:2,]//m1[5:7,]//m1[9:14,]//m1[16:18,]//m1[20:31,]//m1[33,]
. . .
m1[2967:2977,]//m1[2979,]//m1[2981:2990,]//m1[2992:2998,]//m1[3000,];

CREATE lib.rho11              FROM rho11;     APPEND FROM rho11;
CREATE lib.rho1MAT            FROM rho1MAT;   APPEND FROM rho1MAT;
```

```
DETERMINE THE Z2 VARIOGRAM MATRIX USING DMAT & TMAT
START rho2(dmat,tmat,rowname,rho2MAT);
m=nrow(dmat);
rho2MAT=j(m,m,0);

DO j=1 TO m BY 1;
DO k=1 TO m BY 1;

IF DMAT[k,j]<=50 & TMAT[j,k] <=5 then
rho2MAT[k,j] = 1*(((3*dmat[j,k])/100)-
               0.5*((dmat[j,k]*dmat[j,k]*dmat[j,k])/125000))
              +1.70*(((3*dmat[j,k])/16)-
               0.5*((tmat[j,k]*tmat[j,k]*tmat[j,k])/512))
              -0.50*(1*(((3*dmat[j,k])/100)-
               0.5*((dmat[j,k]*dmat[j,k]*dmat[j,k])/125000)))
               *(1.70*(((3*dmat[j,k])/16)-
               0.5*((tmat[j,k]*tmat[j,k]*tmat[j,k])/512)));

ELSE IF DMAT[k,j]>50 & TMAT[j,k] <=5  then
rho2MAT[k,j] = 1
            + 1.70*(((3*dmat[j,k])/16)-
              0.5*((tmat[j,k]*tmat[j,k]*tmat[j,k])/512))
            - 0.50*(1)*(1.70*(((3*dmat[j,k])/16)-
              0.5*((tmat[j,k]*tmat[j,k]*tmat[j,k])/512)));

ELSE IF DMAT[k,j]<=50 & TMAT[j,k]>5 then
rho2MAT[k,j] = 1*(((3*dmat[j,k])/100)-
               0.5*((dmat[j,k]*dmat[j,k]*dmat[j,k])/125000))
             + 1.70
             - 0.50*(1*(((3*dmat[j,k])/100)-
               0.5*((dmat[j,k]*dmat[j,k]*dmat[j,k])/125000)))*(1.70);

ELSE IF DMAT[k,j]>50 & TMAT[j,k]>5  then
rho2MAT[k,j] = 1
            + 1.70
            - 0.50*(1)*(1.70);

END;
END;
FINISH rho2;
CALL rho2(dmat,tmat,rowname,rho2MAT);
```

```
rho22 IS A 3000*3000 MATRIX
rho22     =  rho2MAT;
CREATE lib.rho22              FROM rho22;    APPEND FROM rho22;
```

```
DETERMINE THE Z1Z2 SEMI-VARIOGRAM MATRIX BY USING DMAT & TMAT
START rho12(dmat,tmat,rowname,rho12MAT);
m=nrow(dmat);
```

```
n=ncol(dmat);
rho12MAT=j(m,n,0);

DO j=1 TO m BY 1;
DO k=1 TO n BY 1;
IF TMAT[j,k] <=10 then
rho12MAT[k,j] = -0.20*(1-exp((dmat[j,k]*dmat[j,k])/1681))
                -0.17*(((3*dmat[j,k])/20)
                -0.5*((tmat[j,k]*tmat[j,k]*tmat[j,k])/1000))
                -0.03*( -0.20*(1-exp((dmat[j,k]*dmat[j,k])/1681)))*
                (-0.17*(((3*dmat[j,k])/20)0.5*(tmat[j,k]**3)/1000)));
ELSE
rho12MAT[k,j] = -0.20*(1-exp((dmat[j,k]*dmat[j,k])/1681))
                -0.17
                -0.03*(-0.20*(1-exp((dmat[j,k]*dmat[j,k])/1681)))
                *(- 0.17);
END;
END;
FINISH rho12;
CALL rho12(dmat,tmat,rowname,rho12MAT);
/* rho12 IS A 2250*3000 MATRIX */
rho12  =
rho12MAT[1:2,]//rho12MAT[5:7,]//rho12MAT[9:14,]//rho12MAT[16:18,]//
. . .
rho12MAT[2981:2990,]//rho12MAT[2992:2998,]//rho12MAT[3000,];

CREATE lib.rho12MAT           FROM rho12MAT; APPEND FROM rho12MAT;
CREATE lib.rho12              FROM rho12;    APPEND FROM rho12;
```

```
DETERMINE THE Z2Z1 SEMI-VARIOGRAM MATRIX BY USING DMAT & TMAT
START rho21(dmat,tmat,rowname,rho21MAT);
m=nrow(dmat);
n=ncol(dmat);
rho21MAT=j(m,n,0);

DO j=1 TO m BY 1;
DO k=1 TO n BY 1;
IF TMAT[j,k] <=10 THEN
rho21MAT[k,j] = - 0.20*(1-exp((dmat[j,k]*dmat[j,k])/1681))
                - 0.17*(((3*dmat[j,k])/20)-
                  0.5*((tmat[j,k]*tmat[j,k]*tmat[j,k])/1000))
                - 0.03*( -0.20*(1-
                  exp((dmat[j,k]*dmat[j,k])/1681)))
                *(- 0.17*(((3*dmat[j,k])/20)-
                  0.5*((tmat[j,k]*tmat[j,k]*tmat[j,k])/1000)));
ELSE
rho21MAT[k,j] = -0.20*(1-exp((dmat[j,k]*dmat[j,k])/1681))
                - 0.17
                - 0.03*(-0.20*(1-exp((dmat[j,k]*dmat[j,k])/1681)))
                *(- 0.17)      ;
END;
END;
FINISH rho21;

CALL rho21(dmat,tmat,rowname,rho21MAT);
```

```
rho21 IS A 3000*2550 MATRIX
rho21=
rho21MAT[,1:2]||rho21MAT[,5:7]||rho21MAT[,9:14]||rho21MAT[,16:18]||
. . .
rho21MAT[,2981:2990]||rho21MAT[,2992:2998]||rho21MAT[,3000];
```

```
CREATE lib.rho21              FROM rho21;    APPEND FROM rho21;
```

```
DEFINE G
RHO=(rho11||rho12)//(rho21||rho22);
ONE11=j(nrow(rho11),1,1);
ONE22=j(nrow(rho22),1,1);
ZERO11=j(nrow(rho11),1,0);
ZERO22=j(nrow(rho22),1,0);

NUL=j(1,2,0);

A1=ONE11//ZERO22;
A2=ZERO11//ONE22;

A4=ONE11`||ZERO22`||NUL ;
A5=ZERO11`||ONE22`||NUL ;

A3=A1||A2;
A6=A4//A5;

G1=RHO||A3;
G=G1//A6;
Ginv=inv(G);

CREATE lib.RHO  FROM RHO;     APPEND FROM RHO;
CREATE lib.G1   FROM G1;      APPEND FROM G1;
CREATE lib.Ginv FROM Ginv;    APPEND FROM Ginv;
CREATE lib.G    FROM G;       APPEND FROM G;
```

```
DEFINE B;
START Bcol(rho12MAT,rho1MAT,col,rowname,Bcol);
m=2550+3000+2;
n=1;
Bcol=j(m,n,0);
E=j(1,1,1);
N=j(1,1,0);
Bcol=rho1MAT[1:2,col]//rho1MAT[5:7,col]//rho1MAT[9:14,col]//
. . .
rho1MAT[2992:2998,col]//rho1MAT[3000,col]//rho12MAT[,col]//E//N;
FINISH Bcol;

CALL Bcol(rho12MAT,rho1MAT,777,rowname,B777);
. . .
CALL Bcol(rho12MAT,rho1MAT,1993,rowname,B1993);

B=B777||. . . ||B1993;
```

```
CALCULATE LAMDA AND PHI
USE lib.Ginv;     READ all INTO Ginv;

START par(Ginv,rowname,B,lamda);
m=nrow(B);
lamda=j(m,1,0);
lamda = Ginv*B;
FINISH par;

CALL par(Ginv,rowname,B777,lamda777);
. . .
CALL par(Ginv,rowname,B1993,lamda1993);

LAMDA_1=lamda777[1:2550,]||. . . ||lamda1993[1:2550,];
```

```
LAMDA_2=lamda777[2551:5550,]||. . .||lamda1993[2551:5550,];
PHI_1  =lamda777[5551,]||. . .||lamda1993[5551,];
PHI_2  =lamda777[5552,]||. . .||lamda1993[5552,];

CREATE lib.lamda_1     FROM lamda_1; APPEND FROM lamda_1;
CREATE lib.lamda_2     FROM lamda_2; APPEND FROM lamda_2;
CREATE lib.phi_1       FROM phi_1;   APPEND FROM phi_1;
CREATE lib.phi_2       FROM phi_2;   APPEND FROM phi_2;
```

DETERMINE THE INTERPOLATED VALUE

```
USE z1;     READ all INTO z1;
USE z2;     READ all INTO z2;

START system2(z1,z2,lamdaz1,lamdaz2,rowname,LR);
      LR = lamdaz1`*(z1[,6]+z1[,7]) + lamdaz2`*(z2[,6]+z2[,7]) ;
FINISH system2;

CALL
system2(z1,z2,lamda777[1:2550,],lamda777[2551:5550,],rowname,LR777);
. . .
CALL
system2(z1,z2,lamda1993[1:2550,],lamda1993[2551:5550,],rowname,LR1993
);

INT = LR777//. . . //LR1993;
```

CALCULATE THE ESTIMATED KRIGING VARIANCE

```
START var(B,lamda,rowname,sigma);
sigma=B`*lamda;
FINISH var;

CALL var(B777,lamda777,rowname,sigma_777);
. . .
CALL var(B1993,lamda1993,rowname,sigma_1993);

sigma=sigma_777//. . . //sigma_1993;

CREATE lib.Interpolated FROM INT;   APPEND FROM INT;
CREATE lib.sigma        FROM sigma; APPEND FROM sigma;
CREATE lib.B            FROM B;     APPEND FROM B;
QUIT;
```

SUMMARY

INTERPOLATION IN STATIONARY SPATIAL AND SPATIAL-TEMPORAL DATASETS

by

ANSIE SMIT

Supervisor:	**Dr. H. Boraine**
Department:	**Statistics**
Degree:	**MSc (Course Work) Mathematical Statistics**

In the early 1950s the study on how to determine true ore-grade distributions in the mining sector, sparked the development of a series of statistical tools that specifically allows for spatial and subsequently spatial-temporal dependence. These statistics are commonly referred to as geostatistics, and has since been incorporated in several fields of study characterized by this dependence.

Basic descriptive statistics and mapping tools for geostatistics are defined and illustrated by means of a simulated dataset. The moments are modelled according to predefined conditions and model structures to describe the spatial and spatial-temporal variance in the data. These variograms and covariance structures are subsequently utilized in the least square procedure, namely kriging. At present, kriging is most commonly used in geostatistics for the interpolation and simulation of spatial or spatial-temporal data. The univariate and multivariate spatial and spatial-temporal kriging techniques are tested on the simulated dataset, to demonstrate how interpolation weights are determined according to the lag distances and underlying variance structure. The strength, weaknesses and inherent complexities of the methodologies are highlighted.